Research Topics

Toward carbon neutrality: Spatial planning and sustainable utilization of natural resource

Edited by
Jingying Fu, Jingli Fan, Ayman Elshkaki, Xian Zhang and Monica Salvia

Published in
Frontiers in Environmental Science
Frontiers in Energy Research

ISSN 1664-8714
ISBN 978-2-83251-514-3
DOI 10.3389/978-2-83251-514-3

About Frontiers

Frontiers is more than just an open access publisher of scholarly articles: it is a pioneering approach to the world of academia, radically improving the way scholarly research is managed. The grand vision of Frontiers is a world where all people have an equal opportunity to seek, share and generate knowledge. Frontiers provides immediate and permanent online open access to all its publications, but this alone is not enough to realize our grand goals.

Frontiers journal series

The Frontiers journal series is a multi-tier and interdisciplinary set of open-access, online journals, promising a paradigm shift from the current review, selection and dissemination processes in academic publishing. All Frontiers journals are driven by researchers for researchers; therefore, they constitute a service to the scholarly community. At the same time, the *Frontiers journal series* operates on a revolutionary invention, the tiered publishing system, initially addressing specific communities of scholars, and gradually climbing up to broader public understanding, thus serving the interests of the lay society, too.

Dedication to quality

Each Frontiers article is a landmark of the highest quality, thanks to genuinely collaborative interactions between authors and review editors, who include some of the world's best academicians. Research must be certified by peers before entering a stream of knowledge that may eventually reach the public - and shape society; therefore, Frontiers only applies the most rigorous and unbiased reviews. Frontiers revolutionizes research publishing by freely delivering the most outstanding research, evaluated with no bias from both the academic and social point of view. By applying the most advanced information technologies, Frontiers is catapulting scholarly publishing into a new generation.

What are Frontiers Research Topics?

Frontiers Research Topics are very popular trademarks of the *Frontiers journals series*: they are collections of at least ten articles, all centered on a particular subject. With their unique mix of varied contributions from Original Research to Review Articles, Frontiers Research Topics unify the most influential researchers, the latest key findings and historical advances in a hot research area.

Find out more on how to host your own Frontiers Research Topic or contribute to one as an author by contacting the Frontiers editorial office: frontiersin.org/about/contact

Toward carbon neutrality: Spatial planning and sustainable utilization of natural resource

Topic editors
Jingying Fu — Institute of Geographic Sciences and Natural Resources Research, Chinese Academy of Sciences (CAS), China
Jingli Fan — China University of Mining and Technology, Beijing, China
Ayman Elshkaki — Key Laboratory of Resource Utilization and Environmental Restoration, Institute of Geographic Sciences and Natural Resources Research, Chinese Academy of Sciences (CAS), China
Xian Zhang — Ministry of Science and Technology (China), China
Monica Salvia — Institute of Methodologies for Environmental Analysis, Department of Earth System Sciences and Technologies for the Environment, National Research Council (CNR), Italy

Citation
Fu, J., Fan, J., Elshkaki, A., Zhang, X., Salvia, M., eds. (2023). *Toward carbon neutrality: Spatial planning and sustainable utilization of natural resource*. Lausanne: Frontiers Media SA. doi: 10.3389/978-2-83251-514-3

Table of contents

frontiers | Frontiers in Environmental Science

TYPE Editorial
PUBLISHED 17 January 2023
DOI 10.3389/fenvs.2023.1127814

OPEN ACCESS

EDITED AND REVIEWED BY
Haikun Wang,
Nanjing University, China

*CORRESPONDENCE
Jingying Fu,
fujy@igsnrr.ac.cn

SPECIALTY SECTION
This article was submitted to Environmental Economics and Management,
a section of the journal
Frontiers in Environmental Science

RECEIVED 20 December 2022
ACCEPTED 09 January 2023
PUBLISHED 17 January 2023

CITATION
Fu J, Elshkaki A, Salvia M, Zhang X and Fan J (2023), Editorial: Toward carbon neutrality: Spatial planning and sustainable utilization of natural resource.
Front. Environ. Sci. 11:1127814.
doi: 10.3389/fenvs.2023.1127814

Editorial: Toward carbon neutrality: Spatial planning and sustainable utilization of natural resource

Jingying Fu[1,2,3]*, Ayman Elshkaki[1,2], Monica Salvia[4], Xian Zhang[5] and Jingli Fan[6]

[1]Institute of Geographic Sciences and Natural Resources Research, Chinese Academy of Sciences (CAS), Beijing, China, [2]College of Resources and Environment, University of Chinese Academy of Sciences (UCAS), Beijing, China, [3]Key Laboratory of Coupling Process and Effect of Natural Resources Elements, Ministry of Natural Resources, Beijing, China, [4]Institute of Methodologies for Environmental Analysis, National Research Council (CNR), Tito Scalo (PZ), Italy, [5]Ministry of Science and Technology (China), Beijing, China, [6]School of Energy and Mining Engineering, China University of Mining and Technology, Beijing, China

KEYWORDS

carbon neutrality and emission peak, natural resources, geographic information system–GIS, renewable energy, mining, carbon emission (CE)

Editorial on the Research Topic
Toward carbon neutrality: Spatial planning and sustainable utilization of natural resource

Carbon peak and carbon neutralization are the new development strategies adopted by human society to cope with global warming. Territorial space and natural resources are the basic carrier and key medium of carbon peak and carbon neutrality achievement. The approaches and strategies for the sustainable utilization of natural resources and spatial planning to achieve carbon neutral are deemed to be worth investigating.

This Research Topic on "*Toward Carbon Neutrality: Spatial Planning and Sustainable Utilization of Natural Resource*" mainly focuses on the methods and strategies in achieving decarbonization by sustainable utilization of natural resources and spatial planning from the geography perspective. There are 45 authors and 11 papers that have contributed to this Research Topic.

Ye et al. employed the natural resources capitalization (NRC) as the ecological civilization policy to investigate whether the implementation of NRC has contributed to the carbon emissions reduction with a difference-in-differences (DID) method. The study showed that different variables of carbon emissions in four pilot cities can be effectively affected by the implementation of NRC. This research provides a timely and necessary study that the NRC policy could be a contributing factor to carbon emissions reduction.

The study by Zhao et al. presents that growing energy plants on marginal lands, not only helps to alleviate the energy crisis, but also reduces soil erosion and improves marginal soil quality without interfering with food production. The study assessed the potential of marginal land and analyzes the impact of environmental variables for Jerusalem artichoke (Helianthus tuberosus L.) in Shaanxi Province, China. The study shows that the dominant land type used for the growth of Jerusalem artichoke was moderately dense grassland.

Xinmin et al. investigated the relationship between energy use greenization, CO_2 emission, and economic growth in China. The analysis was carried out using Cobb–Douglas production function model and data from 2000 to 2018. Energy use greenization and CO_2 emissions were used either as dependent or independent variables and several factors were used as independent variables to examine the causality of income including capital, labor, energy use, GDP, direct foreign investment, trade openness, oil prices, financial development, and urbanization. The study shows that energy use greenization reduces carbon dioxide emissions and promotes sustainable economic growth at the same time. The contribution rate of energy use greenization to economic growth shows an inverted U-shaped trend while carbon emissions have a relatively large contribution rate to green energy use and economic growth. The authors emphasized that China should maintain economic growth and employment stability in the process of energy use greenization and should promote the transformation of the traditional energy production industry (such as coal and oil industries) to mechanization and intelligence, transit from simple resource mining to deep processing, and eliminate the backward production capacity.

Li et al. constructed a carbon emission model for coal production enterprises. The main innovation of this study lies in the comprehensive analysis of the carbon emission sources of relevant enterprises from six aspects, including fuel combustion, torch burning, CH_4 and CO_2 dissipation, net purchased electricity and heat implication, coal gangue storage and utilization, and coal transportation. Moreover, the source–sink relationship method is proposed when the CH_4 and CO_2 dissipation is calculated.

Hou et al. analysed the lifecycle water footprint of the renewable energy industry in a typical arid region in north-western China. The water consumption of power generation enterprises was estimated based on current scenarios and three future scenarios. The study provides evidence on the significant pressure (in terms of high-water consumption) that the local renewable energy industry can exert on water resources in areas such as north-western China, which are plagued by long-term water scarcity. This leads to a limitation of the potential increase in installed solar energy capacity in this country, despite its rich solar energy resources, highlighting the need to adopt strategic planning to evaluate possible future upgrades in installed capacity.

Sun et al. explored the path of urban energy reform and low-carbon development for the industrial energy system in the city of Suzhou, which is an energy-dependent city in China that is dominated using coal for energy consumption mainly in the industrial sector. The authors have implemented a Long-term Energy Alternative Planning System (LEAP)-Suzhou model based on the LEAP model to explore the energy system optimization and emission reduction path of Suzhou city to 2050. The study shows that energy consumption is expected to be reduced by 37.9%, 37.4%, and 74.8%, respectively in the industrial structure optimization scenario, energy structure optimization scenario, and energy transformation optimization scenario by 2050 compared to the baseline scenario, which is expected to consume 259,954 million tons of standard coal and to emit 677.6 Mt of carbon emission by 2050.

The study by Mouzas et al. focuses on sustainable mobility and criteria that are broadly applicable to different urban environments. The proposes model is based on an index of intermodal walkability to rank the pedestrian mobility of a car-oriented urban environment. The index, based on an open-source geospatial analysis toolbox, is tested on a case study of the municipality of Nicosia (Cyprus). The study shows that pedestrian transportation can be ranked in terms of walkability from the point of private car delivery and that fossil fuel use and primary electricity generation can be reduced by focusing urban sustainable mobility planning on areas with negative scores on the proposed intermodal walkability index.

Sun et al. used the Tapio decoupling model to measure the relationship between China's economic development and mining carbon emissions from 2001 to 2018 and analyze the overall industry and its subdivisions. In addition, the authors identified the factors driving carbon emissions with the use of an improved Kaya identity and LMDI decomposition models. The study shows that all mining divisions, except oil and natural gas mining industries, have a strong decoupling and become stable with a continuous positive trend. In addition, the economic factor and energy intensity effects are the key factors in increasing and restraining carbon emissions, respectively.

The study by Yang et al. investigated the impacts of the low-carbon city pilot policy and fiscal pressure on carbon productivity based on data for 282 cities in China over the period 2005 to 2017. The staggered difference-in-differences (DID) model was used to identify the causal relationship among the low-carbon city pilot policy, fiscal pressure, and carbon productivity. The study shows that this pilot policy can significantly improve carbon productivity and that the improvement effect presents a dynamic and persistent feature.

The study by Xi et al. discusses the relevant evaluation principles and technical key points of constructing pumped storage power stations using abandoned mines (PSPSuM) in the Yellow River basin, and carries out feasibility assessment preliminarily from the perspective of multidisciplinary integration. The study shows that 91 PSPSuM can be built in this area, with a total installed capacity of 15,830 MW, comprehensively considering the aspects of spatial size, spatial structure, and space stability.

Lin et al. have built a simulation system of urban carbon emission based on system dynamics from four perspectives of population, economy, water resources and energy. It is aiming at building a method system for carbon peak path that is universally applicable to resource-based cities from a systematic perspective. The total carbon emissions of the whole industry in Taiyuan increased slightly every year from 2005 to 2021. The study shows that the comprehensive scenario had the best coordination benefit for the coupling system, which will reduce CO_2 by 17.14 million tons, water consumption by 158 million m^3, energy consumption by 5.58 million tons of standard coal and economic growth by 175.21 billion yuan in 2029.

Overall, the goal of this Research Topic has been achieved thanks to the contribution of the 45 authors. The Research Topic includes, but are not limited to: 1) the national space governance and carbon neutrality, especially in China and Cyprus. 2) assessments of natural resources for achieving carbon neutrality, especially in mining city. The editors think that this Research Topic will enrich the theory and technology and cases toward carbon neutrality.

Author contributions

JFu designed the whole editorial, summarized four articles and written the manuscript. AE concluded three articles and polished the

Editorial. MS summarized two articles, XZ and JFa summarized one article, respectively.

Conflict of interest

The authors declare that the research was conducted in the absence of any commercial or financial relationships that could be construed as a potential conflict of interest.

Publisher's note

All claims expressed in this article are solely those of the authors and do not necessarily represent those of their affiliated organizations, or those of the publisher, the editors and the reviewers. Any product that may be evaluated in this article, or claim that may be made by its manufacturer, is not guaranteed or endorsed by the publisher.

frontiers in Environmental Science

ORIGINAL RESEARCH
published: 04 February 2022
doi: 10.3389/fenvs.2022.831840

Can the Natural Resources Capitalization Contribute to the Achievement of Carbon Neutrality? A Pilot Experiment Evidence From China

Penghao Ye[1], Senmao Xia[2], Yu Xiong[3], Yanan Li[4,5] and Lei Chen[4]*

[1]School of Economics, Hainan Open Economy Research Institute, Hainan University, Haikou, China, [2]International Centre for Transformational Entrepreneurship and Center for Business in Society, Coventry University, Coventry, United Kingdom, [3]Surrey Business School, University of Surrey, Guildford, United Kingdom, [4]School of Business Administration, Zhongnan University of Economics and Law, Wuhan, China, [5]Research Center for Environment and Health, Zhongnan University of Economics and Law, Wuhan, China

There has been renewed interest in assessing the pilot scheme for compiling the natural resources capitalization (NRC). A growing body of evidence highlights the good effects that the policy of NRC has on the construction of ecological civilization. No known empirical research has focused on exploring relationships between the policy of NRC and carbon emissions reduction. This paper employs the NRC as the ecological civilization policy to investigate whether the implementation of NRC has contributed to the carbon emissions reduction with a difference-in-differences (DID) method. The results showed that different variables of carbon emissions in four pilot cities can be effectively affected by the implementation of NRC. There were significant negative correlations between the carbon emissions per GDP (Gross Domestic Product) and the policy for Hulun Buir, Huzhou and Loudi cities, and a significant increase of carbon sequestration was found in Yan'an city. This research provides a timely and necessary study that the NRC policy could be a contributing factor to carbon emissions reduction. As a result of these investigations, suggestions were identified for future research. Further research should be undertaken to investigate the collaborative effects of multi-policies on environmental issues.

Keywords: natural resources capitalization, carbon neutrality, natural resources management and policy, China, difference–In–differences

Edited by:
Jingying Fu,
Institute of Geographic Sciences and Natural Resources Research (CAS), China

Reviewed by:
Luigi Aldieri,
University of Salerno, Italy
Wan Yu Liu,
National Chung Hsing University, Taiwan

****Correspondence:***
Yanan Li
ynli@stu.zuel.edu.cn

Specialty section:
This article was submitted to Environmental Economics and Management, a section of the journal Frontiers in Environmental Science

Received: *09 December 2021*
Accepted: *17 January 2022*
Published: *04 February 2022*

Citation:
Ye P, Xia S, Xiong Y, Li Y and Chen L (2022) Can the Natural Resources Capitalization Contribute to the Achievement of Carbon Neutrality? A Pilot Experiment Evidence From China. Front. Environ. Sci. 10:831840. doi: 10.3389/fenvs.2022.831840

INTRODUCTION

Global climate change has become one of the biggest challenges to human development and poses a major threat to human society, which has attracted considerable attention, both scholarly and socially (Thomas et al., 2004; Davidson and Janssens, 2006; Meng et al., 2018). According to the report of the Intergovernmental Panel on Climate Change (IPCC) in October 2018, the world must control global warming within 1.5°C to avoid extreme climate disasters (IPCC, 2018). Only when the whole world achieves net-zero emission of greenhouse gases in the middle of the 21st century, can this goal be achieved (Yao et al., 2021). At present, more than 120 countries and regions around the world have put forward the goal of carbon neutrality. And among which, 60 countries have promised to achieve zero carbon emissions by 2050 or even earlier based on the report of the Secretariat of the United Nations Framework Convention on Climate Change (UNFCCC) in 2019 (UNFCCC, 2019).

China is the largest total carbon emitter in 2020 currently, accounting for 32% of the world (IEA, 2020). With China's rising carbon emissions in the world, both the carbon emission reduction pressure and responsibility are greater (Onyango et al., 2019). In 2015, China submitted its National Subsidy Contribution (NDC), promising to reduce CO_2 emissions per unit GDP by 60–65% compared with 2005 by 2030, and formally signed the Paris Agreement in 2016 (UNFCCC, 2016). At the general debate of the 75th session of the United Nations General Assembly on 22 September 2020, China made it clear that its carbon dioxide emissions will reach the peak before 2030 and strive to achieve carbon neutrality before 2060 (UN, 2020). On 18 December 2020, at the Central Economic Work Conference, carbon neutrality was listed as one of the eight key tasks of the country in 2021.

The issue of carbon neutrality, an important concept in the study of climate change, has received considerable critical attention (Zanchi et al., 2012; Ji et al., 2014). It is a systematic process that requires the cooperation of multiple departments to achieve this goal (Yue et al., 2021; Zhang et al., 2021). Recent research has reported that setting emission reduction targets is substantially delineating the boundaries of natural capital (or carbon assets) (Zhou et al., 2021). China's "14th Five-Year Plan", starting from 2021, allocates the national emission reduction target to various provinces and cities, where key carbon emission enterprises are deeply involved. A number of policies in China have been developed to achieve the peak carbon dioxide emissions and carbon neutralization (Wen et al., 2020; Soregaroli et al., 2021). One of the most important policies was capitalization of natural resources (NRC) (Fan et al., 2020). However, what remains unknown is how such policy and practice affect the carbon emissions. From an economic perspective, this is a process of defining property rights. The capitalization of natural resources is the basis for the definition of natural capital property rights. Therefore, in theory, the preparation of the capitalization of natural resources (NRC) is beneficial to the realization of carbon neutrality, but no known empirical research has focused on exploring relationships between pilot schemes for compiling capitalization of natural resources and carbon emissions.

In 2015, the General Office of the State Council issued the pilot scheme for compiling capitalization of natural resources, clearly pointed out that the pilot work should be carried out in Hulun Buir City of Inner Mongolia, Huzhou City of Zhejiang Province, Loudi City of Hunan Province, Chishui City of Guizhou Province and Yan'an City of Shaanxi Province (MNR, 2015). Natural resources capitalization is fundamental to promoting the effective use of natural resources and the construction of ecological civilization in China (Zhang et al., 2019b; Song et al., 2020a). There has been extensive research on the accounting of water resources, forest resources, land resources and other natural resources assets (Zhang et al., 2019a; Zhu et al., 2021). For example, the mining of mineral resources plays a key role in carbon emissions growth (Wang et al., 2017), and the capitalization of land resources has brought favorable changes in environmental loads, ecosystem services and growth models in several districts and counties (Fan et al., 2020; Fan et al., 2021). Recent research suggests that there is a positive relationship between natural resources management policy and environmental quality (Kurniawan et al., 2021). Therefore, questions have been raised about whether the NRC can achieve a win-win situation of eco-environmental protection and low-carbon emission reduction. The year 2015 can be regarded as the time point for the implementation of the scheme in China, which is a top-down process and lays a foundation for considering NRC as a "quasi-natural experiment", enabling us to apply a difference-in-differences (DID) identification strategy. This study will combine panel data to compare the changes in low-carbon emission reduction in pilot cities before and after the implementation of NRC. Further description of this method will be introduced in **Section 2.2**.

What we know about carbon neutrality is derived from research by Schlamadinger, which explores whether it is true carbon neutral in the whole life cycle when biomass energy replaces fossil fuels (Marland and Schlamadinger, 1997). Recently, considerable literature has grown up around the theme of carbon emissions. A key aspect of this field is CO_2 emission reduction technologies, including CO_2 capture and storage (CCS) (Xu et al., 2021), carbon sink (Pan et al., 2011), biochar (Papageorgiou et al., 2021; Wang et al., 2021) and carbon sequestration (Marland and Schlamadinger, 1997; Lal, 2004; Laudicina et al., 2021). There has also been a surge of interest in the effects of these numerous techniques (Bonan, 2008; Fuhrman et al., 2020). What's more, existing research recognizes the critical role played by the market that includes carbon tax (Soregaroli et al., 2021; Zhang et al., 2021) and carbon emissions trading scheme (Wang et al., 2019). Recent evidence suggests that there is a positive relationship between China's carbon emissions trading scheme (ETS) and companies' stock returns (Wen et al., 2020). Also, it has been observed that ETS could be a contributing factor to energy conservation and emission reduction (Zhou et al., 2019; Sun et al., 2020). To date, factors found to be influencing carbon emissions have been explored in several studies (Gao et al., 2020; Nie et al., 2020; Yi et al., 2020; Hao et al., 2021; Ling et al., 2021). An investigation regarding the Yangtze River Delta has examined that industrial transformation gradually dominated by the service and advanced manufacturing sectors are thought to contribute to slow growth in CO_2 emissions (Zhang S. et al., 2019). One study by Yang and Wang (2020) examined the effect of population aging on carbon emissions, and found that population aging has a negative coefficient on carbon emissions. In a study conducted by Lin and Zhu (2019), it was shown that renewable energy technological innovation (RETI) had a significant effect on CO_2 emissions. Hong et al. (2021) found that the low-carbon city pilot policy can effectively reduce the energy intensity. Emissions in cities were shown to vary in response to different local public expenditure, local public expenditure scale and public environmental expenditure (Cheng et al., 2021). Although there are several reports in the literature on carbon emissions and related factors over the past decade, few studies have been able to consider the important role played by NRC. This study provides a timely and necessary study of this policy and its effect on carbon emissions.

Theoretically, the impact of NRC on carbon emissions may exist in three different aspects. First of all, according to the Porter Hypothesis, environmental policies and regulations could stimulate technological innovation (Hu et al., 2020; Du et al., 2021). Specifically, the compliance pressure of NRC could motivate the pilot cities to increase investment in innovation and to improve technological progress, which may propel the improvement of the efficiency of resource and energy use with less greenhouse gas emission or more advanced carbon capture and storage technologies. Also, NRC could encourage key firms to improve the allocation of input factors, protect resources, and then promote eco-environmental protection and low-carbon production (Yang et al., 2017; Song et al., 2020b). For example, when natural resources such as forests have been priced, the exploitation cost for the enterprises will rise accordingly, this can relieve the depletion of natural wealth and urge the enterprises to promote their green productivities based on existing resources (Ogilvy, 2015; Sokil, 2018). These measures can indirectly affect the energy structure and industrial structure and finally achieve emission reduction targets. What's more, a key measure of NRC policy is compiling the natural resources balance sheet (NRBS) to intake the resources like land, forest and water into national assets, requiring the local to preserve them from devaluation and to make their value increase as far as possible, this may enable the expansion of the green plants and the carbon sequestration will increase since then (Song et al., 2019). As a consequence, the role played by NRC on climatic effects, with its influencing mechanism, is worth detecting.

On the basis of a batch of NRC pilot Chinese cities selected in 2015, the primary aim of this paper is to explore the relationship between NRC and carbon emissions, and a further interpretation of heterogeneous results will be discussed if the pilot cities showed differential results. In the pages that follow, the remaining issues will be addressed. **Section 2** introduces the study area, data, and the economic model employed for this study. The third part seeks to analyze the data gathered and addresses each of the research questions in turn. And the fourth section of this paper is concerned with discussion undertaken upon the various theoretical and empirical strands of the thesis. The final part draws together the key findings, making the implication of the findings to future research.

DATA AND METHOD

Study Area and Data

Data were gathered from multiple sources, including annual China City Statistical Yearbooks (CCSY) from 2004 to 2017, China Environmental Statistics Database (CESD) and published literature. The CCSY are informative publications published by the National Bureau of Statistics of the People's Republic of China, which comprehensively reflects the economic and social development of Chinese cities. There has been substantial research undertaken with the support of data from CCSY (Wang et al., 2019; Song et al., 2020b). The county-level CO_2 emissions and sequestration data in China during 2004–2017 were open data offered by Chen et al. (2020). It has been filled for partial missing data through forward and backward interpolation.

Balancing the growing demand and climate change is a key motivating factor for enacting the NRC in China, where the corresponding measurement index can be embodied with the following variables: CO_2 emission per unit GDP, CO_2 emission per capita and carbon sequestration amount. In summary, **Figure 1** provides a possible mechanism of action for NRC in the climatic environment.

The key point of NRC is the capitalization of natural resources including land, forest, water, etc. As **Figure 1** shows, the NRC policy requires the pilot cities to conduct the natural capitals accounting and to charge for the exploitation of the natural resources. This obligates the pilot cities to develop more elaborate and rational industrial and civilian use of natural resources, including transiting fossil energy to cleaner energy, afforesting marginal farmland, popularizing energy-saving equipment in buildings, and subsidizing electric vehicles. During this resource-protecting and energy-saving process, three positive results may come into being: CO_2 reduction per capita, CO_2 reduction per unit GDP, and promotion of carbon sequestration.

Some basic city-relevant information was obtained from the CCSY. Of our interest, we get the data of GDP and population. And the CESD provides carbon emissions of different cities. In particular, the treatment group analyzed in this study contains pilot regions except for Chishui as it is a county rather than a city of others. Thus, the implementation of the NRC policy on carbon emissions could be shown in **Figure 2**.

With respect to the control group, a number of criteria were considered when selecting the control cities as follows. First, those cities included in the control group should not be under the pilot scheme of NRC. Then, the cities in both the treatment group and control group should have homogeneous features that affect carbon emissions other than NRC. That is to say, the pilot and control cities should have similar GDP, amount of population, level of administration (rather than provincial cities), and surroundings or even the climate. This study will choose four representative control cities for each pilot city with the comprehensive consideration of homogeneity on the geographical position and city scale. What's more, to rule out the possibility of geographical difference, the cities out of the pilot province were not selected. Taken together, 16 representative control cities which matched the selection criteria were identified, and the detailed information of treatment and control groups is shown in **Table 1**.

Economic Model Specifications

Several methods currently exist for the assessment of environmental policy and action (Cheng et al., 2021; Lu et al., 2021; Wang and Qiu, 2021; Yang et al., 2021). Among which DID is one of the most widely-used tools, as the usefulness of this technique has been demonstrated in several notable research.

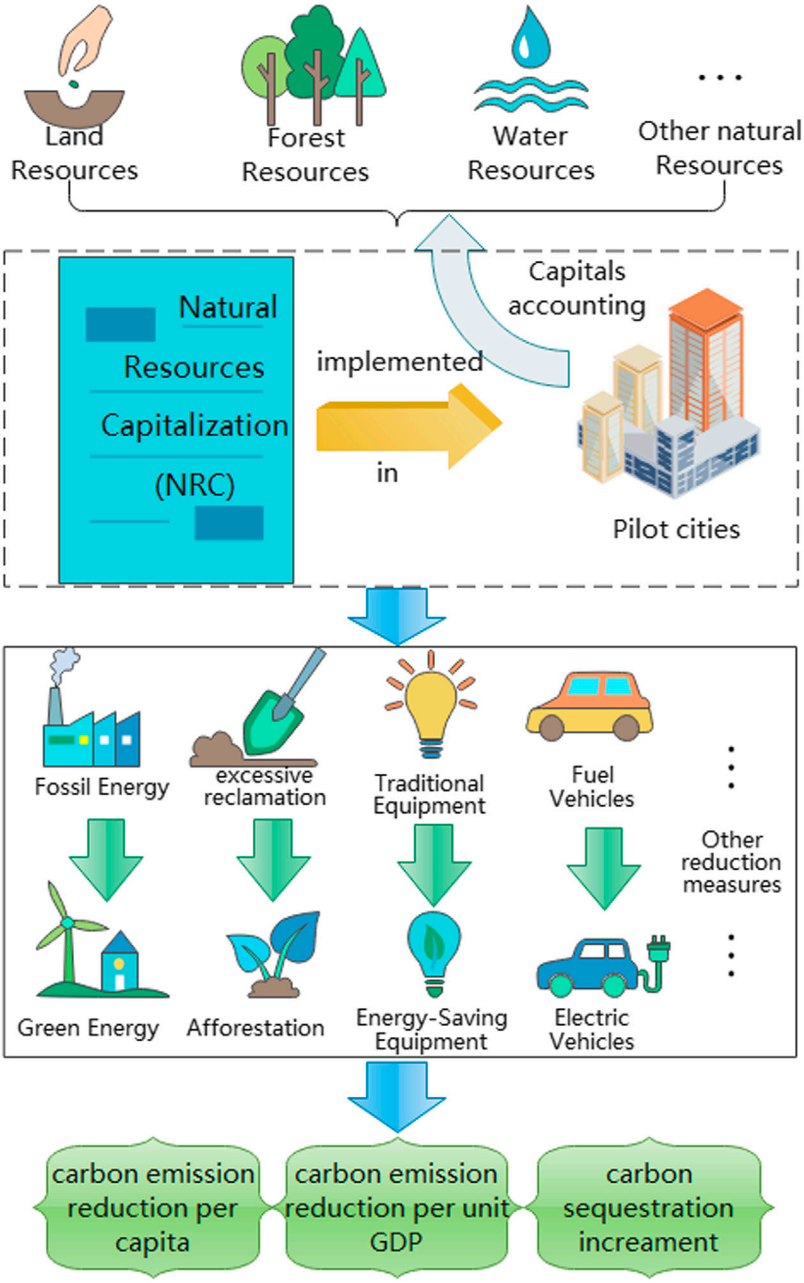

FIGURE 1 | Flowchart of NRC implementation analysis[1].

Samples were analyzed using DID that was detailed for effects of medical marijuana and recreational marijuana use (Pacula et al., 2015). Li et al. (2016) found that the flattening of the government hierarchy has a negative effect on economic performance with the Propensity Score Matching and DID (PSM-DID). Wen et al. (2020) argue that companies participating in the carbon market have higher carbon exposures when the conditions of the coefficient of carbon risk factor, a parameter of the DID model, is significantly positive. In recent years, DID is frequently utilized for the evaluation of environmental policy and action (Agüero and Beleche, 2014; Agüero and Beleche, 2017; He et al., 2020; Yang et al., 2020; Ye et al., 2020; Zhou et al., 2020). Therefore, the relationship between NRC and carbon emissions for this study was examined using DID. Data management and analysis were performed using Stata 16.0. Descriptive data were generated for all variables. Statistical significance levels were analyzed using analysis of variance and t-tests.

As **Table 2** shows, five variables are used to investigate the effect of the Natural Resource Balance Sheet (NRC), where the explained variables are the Carbon emission per unit of GDP, per

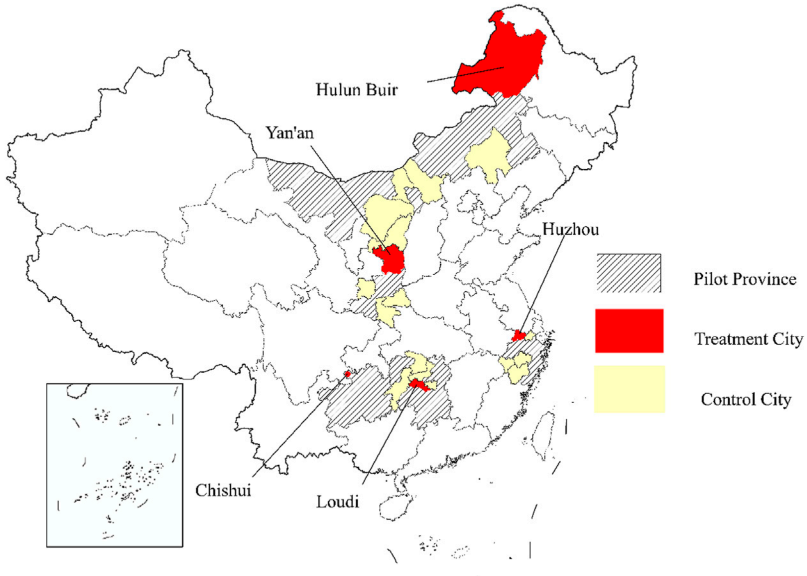

FIGURE 2 | Spatial distribution of NRC policy pilot areas in China.

TABLE 1 | A comparison between the treatment and the control groups.

City	Province	Group	GDP (billion CNY)	Population (million)	Administrative level
Hulun Buir	Inner Mongolia	Treatment	159.90	25.93	Prefecture-level
Ulan Qab		Control	91.38	27.39	Prefecture-level
Baotou		Control	372.19	22.39	Prefecture-level
Erdos		Control	422.61	15.73	Prefecture-level
Chifeng		Control	186.13	46.26	Prefecture-level
Huzhou	Zhejiang	Treatment	208.43	26.37	Prefecture-level
Lishui		Control	110.33	26.64	Prefecture-level
Jiaxing		Control	351.78	34.95	Prefecture-level
Quzhou		Control	114.61	25.64	Prefecture-level
Jinhua		Control	340.23	47.81	Prefecture-level
Loudi	Hunan	Treatment	129.17	44.77	Prefecture-level
Yiyang		Control	135.44	48.08	Prefecture-level
Huaihua		Control	127.32	51.80	Prefecture-level
Xiangtan		Control	170.31	28.93	Prefecture-level
Changde		Control	270.90	60.92	Prefecture-level
Yan'an	Shaanxi	Treatment	119.86	23.55	Prefecture-level
Yulin		Control	262.13	37.75	Prefecture-level
Baoji		Control	178.76	38.45	Prefecture-level
Ankang		Control	77.25	30.48	Prefecture-level
Shangluo		Control	62.18	25.10	Prefecture-level

Note: 1. The GDP and population data are in 2015 and were published by National Bureau of Statistics of China; 2. The administrative level in mainland China includes municipality, provincial city, prefecture city, and county-level city (from high to low); 3. Considering the enormous gap between the prefecture city and provincial city (e.g., The difference of the GDP and population between Zhejiang's provincial city and Huzhou in 2015 is 796.93 billion CNY and 45.99 million) the disparities inside the prefecture cities are much smaller and can be seen as homogeneous.

TABLE 2 | Critical variables and control variables.

Full name of the variable	Unit	Variable code	Function
CO_2 emission per unit of GDP	ton per thousand CNY	*CO_2PerGDP*	Explained variable
CO_2 emission per capita	10 ton per capita	*CO_2PerCapita*	Explained variable
Carbon sequestration	million ton	*Sequestration*	Explained variable
The time in and after the policy implementation year	–	*Post*	Explanatory variable
Policy of NRC	–	*NRC*	Explanatory variable

TABLE 3 | Descriptive statistics of variables.

	$CO_2PerGDP$	$CO_2PerCapita$	*Sequestration*
Full Sample			
Mean	0.347	1.166	55.010
Std. Dev	0.400	1.337	91.346
Min	0.067	0.076	5.609
Max	2.211	7.013	525.674
Number of Obs	280	280	280
Control Group			
Mean	0.225	0.923	35.648
Std. Dev	0.149	1.262	21.849
Min	0.067	0.076	5.609
Max	1.008	7.013	111.488
Number of Obs	224	224	224
Treatment Group			
Mean	0.832	2.138	132.457
Std. Dev	0.646	1.178	179.759
Min	0.108	0.625	9.371
Max	2.211	5.454	525.674
Number of Obs	56	56	56

capita, and the total carbon sequestration of the pilot cities. The pilot policy of NRC, indicated as *DID*, represents the key dummy variable whose significance we want to verify. Besides, two controlled variables, the output value of primary industry and retail sales are listed as they may affect the three explained variables under the conditions that they are not the pilot duties of NRC.

To verify the pilot scheme of NRC, Difference-In-Differences (DID) models are set as follows:

$$CO_2PerGDP_{it} = \alpha + \beta \cdot DID_{it} + \delta_i + \mu_t + \epsilon_{it} \quad (1)$$

$$CO_2PerCapita_{it} = \alpha + \beta \cdot DID_{it} + \delta_i + \mu_t + \epsilon_{it} \quad (2)$$

$$Sequestration_{it} = \alpha + \beta \cdot DID_{it} + \delta_i + \mu_t + \epsilon_{it} \quad (3)$$

$$DID_{it} = NRC_i \times Post_t \quad (4)$$

From the above, (1) (2) are the main DID models aimed at finding whether NRC policy can effectively lower the carbon emissions in terms of unit gross regional production ($CO_2PerGDP$) and per capita ($CO_2PerCapita$). (3) is a DID model to verify whether NRC can promote carbon sequestration (*Sequestration*), which is fixing the carbon dioxide from blowing into the atmosphere. i denotes the individual (city) and t represents the time (year). The second factor in (**Eqs 1–3**), $\beta \cdot DID_{it}$, is the key factor that indicates the effectiveness of the NRC pilot test, as the statistical significance and the value of the estimated coefficient β will indicate the impact degree and the impact direction by NRC. δ_i is the individual fixed effect, μ_t is the time fixed effect, and ε_{it} represents the residual errors. As (4) shows, DID_{it} is composed of two indicative variables, NRC_i and $Post_t$, which delegate the existence of NRC policy and the time before or after the year of NRC's implementation respectively. NRC_i equals 1 if city i belongs to the pilot city and equals 0 otherwise, $Post_t$ takes 1 if time $t \geq 2015$ and be zero when $t < 2015$, Hence, DID_{it} only takes 1 if the individuals are the four pilot cities in and after 2015.

TABLE 4 | Regression results of $CO_2PerGDP$.

	Hulun buir (1)	Huzhou (2)	Loudi (3)	Yan' an (4)
DID ($\hat{\beta}$ =)	−0.269***	−0.102***	−0.243***	−0.075
	(−3.25)	(0.034)	(−3.97)	(−0.88)
Constant ($\hat{\alpha}$ =)	0.472***	0.175***	0.494***	0.275***
	(30.32)	(27.44)	(0.012)	(17.09)
Time Fixed Effects	YES	YES	YES	YES
Region Fixed Effects	YES	YES	YES	YES
Observations	70	70	70	70
R-squared	0.141	0.124	0.198	0.012

*Note: ***, **, and * means the statistical significance is at the 1, 5, and 10% level. The values in the brackets are the* t *statistics of the regression.*

TABLE 5 | Regression results of $CO_2PerCapita$.

	Hulun buir (1)	Huzhou (2)	Loudi (3)	Yan'an (4)
DID ($\hat{\beta}$ =)	0.811	0.070	2.195***	0.522***
	(1.23)	(0.87)	(7.67)	(2.78)
Constant ($\hat{\alpha}$ =)	2.266***	0.709***	0.802***	0.734***
	(18.17)	(46.56)	(14.86)	(20.75)
Time Fixed Effects	YES	YES	YES	YES
Region Fixed Effects	YES	YES	YES	YES
Observations	70	70	70	70
R-squared	0.023	0.012	0.479	0.108

*Note: ***, **, and * means the statistical significance is at the 1, 5, and 10% level. The values in the brackets are the t statistics of the regression.*

TABLE 6 | Regression results of *Sequestration*.

	Hulun buir (1)	Huzhou (2)	Loudi (3)	Yan' an (4)
DID ($\hat{\beta}$ =)	4.964	0.271	0.518	8.895***
	(0.39)	(0.33)	(0.50)	(3.09)
Constant ($\hat{\alpha}$ =)	126.307***	21.414***	29.381***	42.311
	(53.11)	(139.15)	(151.76)	(77.95)
Time Fixed Effects	YES	YES	YES	YES
Region Fixed Effects	YES	YES	YES	YES
Observations	70	70	70	70
R-squared	0.002	0.002	0.004	0.130

*Note: ***, **, and * means the statistical significance is at the 1, 5, and 10% level. The values in the brackets are the t statistics of the regression.*

EMPIRICAL RESULTS

Descriptive Statistics

The sample data for pilot and non-pilot cities in this research are obtained from annual CCSY and CESD from 2004 to 2017.4 non-pilot cities are being treated as control groups for each pilot region, considering the complex nature of geographical factors. The number of observations for the control group is 4 times over than the treatment group. Simple statistical analyses of all variables, including CO_2 emissions per GDP, CO_2 per Capita and carbon sequestration, are set out in **Table 3**. Of all samples, we can see that the mean values of all variables in the treatment group were much higher than those in the control group. For instance, the mean of $CO_2PerGDP$ in the treatment group is about four times more than that in the control group; the mean of $CO_2PerCapita$ is over two times more than that in the control group; the mean of *Sequestration* is about four times as that in the control group.

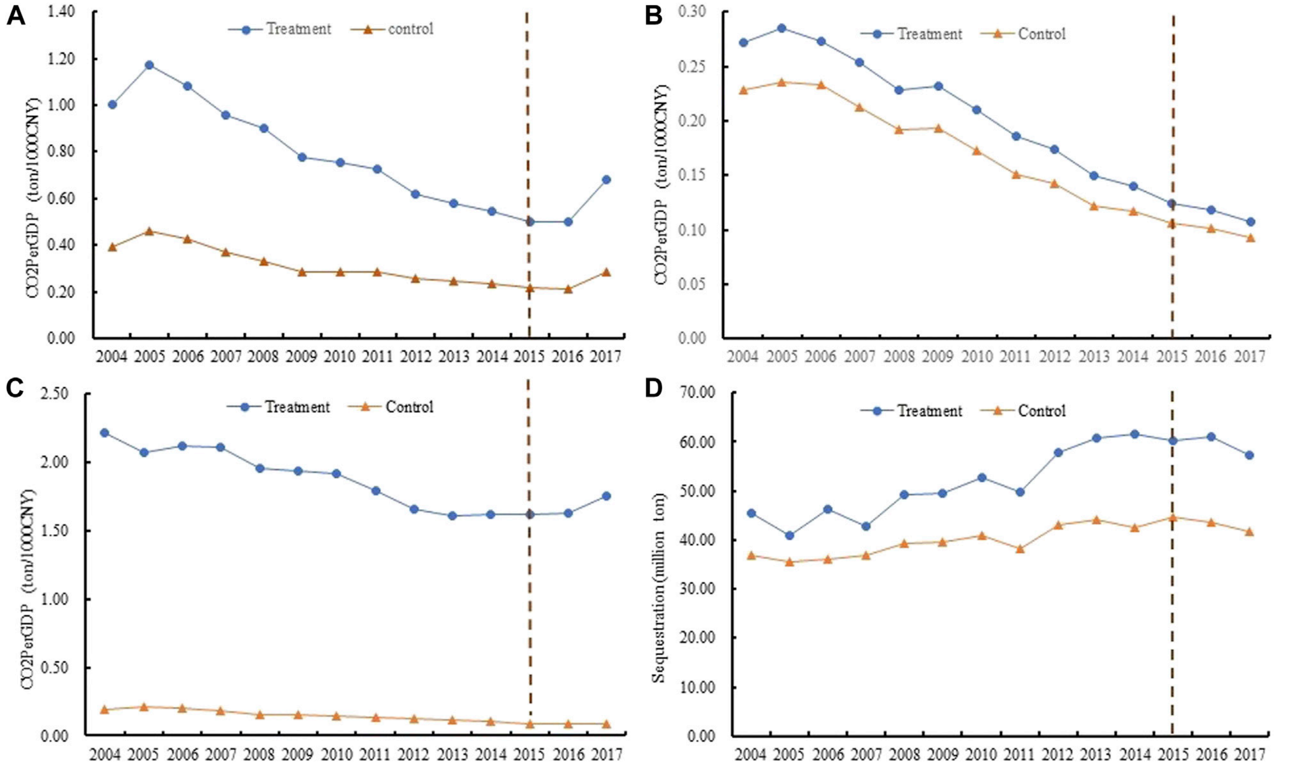

FIGURE 3 | Trends of average values of explained variables of the pilot and non-pilot cities over 2004–2017. Note: **(A)**, **(B)**, and **(C)** are the results of CO2PerGDP for Hulun Buir, Huzhou and Loudi cities, respectively. **(D)** displays the trend of Sequestration for Yan'an city.

Regression Results

The results obtained from the regression analysis of NRC pilot policy in 2015 on carbon emissions are presented in **Tables 4–6**. **Table 4** provides the overview of carbon emissions in terms of unit gross regional production in four treated cities. Columns (1) to (4) show the outcome of Hulun Buir, Huzhou, Loudi and Yan' an, respectively, which is the same as **Table 5**; **Table 6**. Apparently, there was a significant negative correlation between the pilot cities and $CO_2PerGDP$ at the $p = 0.01$ level, except for Yan'an city. The difference in carbon emissions in terms of unit gross regional production between the treatment and control groups in Hulun Buir, Huzhou, and Loudi were significant. The results indicated that, following each thousand increase in GDP, the CO_2 emissions decreases 0.269, 0.102, and 0.243 ton for these three pilot cities after NRC implementation than the control group. While no statistically significant correlation was observed between balanced control and treatment groups in Yan' an city.

The regression results of $CO_2PerCapita$ are displayed in **Table 4**. It is obvious that a significant difference was found between the NRC policy and carbon emissions in terms of per capita in Loudi and Yan'an cities. The values of $CO_2PerCapita$ in these two cities were distinctly higher than those in the control groups at the $p = 0.01$ level. Also, the coefficient estimates of DID for Hulun Buir and Huzhou cities reported in the table showed that there was no significant difference in both groups after the policy implementation.

The regression results of sequestration can be seen in **Table 6**. Of four pilot cities, surprisingly, only one coefficient evaluation of *DID* shows a significant increase of sequestration, suggesting that NRC policy in Yan' an city has brought significant improvement in carbon reduction at a 1% significant level. No significant increase in carbon sequestration was detected in Hulun Buir, Huzhou and Loudi cities, which means sequestration of these regions tends to be insignificantly affected by NRC policy.

Parallel Trend Analysis

This study took the form of "parallel trend analysis" to identify the premise condition of DID estimation. Specifically, it needs to be ensured that treatment and control groups have similar development trends without policy interference. **Figure 3** shows the change trends of the mean values for the variables including $CO_2PerGDP$ and Sequestration of the pilot and non-pilot cities. An inspection of the results in the figure reveals that they basically follow similar patterns before the implementation of pilot policy, although the results show a slight difference.

Robustness Checks

According to the analysis above, there were significant correlations between the implementation of NRC policy and different explained variables ($CO_2PerGDP$, $CO_2PerCapita$ and *Sequestration*), which contributes to the reduction of carbon emissions to a certain degree. The correlation between the implementation of the NRC policy and the reduction of

TABLE 7 | Counterfactual results for Baotou City.

	CO_2PerGDP	CO_2PerCapita	Sequestration
DID	−0.074	0.491	0.779
	−1.23	1.37	0.29
Constant	0.226***	0.916	35.638
	36.5	24.74	129.34
Observations	224	224	224
R-squared	0.007	0.009	0.000

*Note: ***, **, and * means the statistical significance is at the 1, 5, and 10% level. The values in the brackets are the t statistics of the regression.*

TABLE 8 | Counterfactual results for Jinhua City.

	CO_2PerGDP	CO_2PerCapita	Sequestration
DID	−0.068	0.117	−0.215
	−1.13	0.33	−0.08
Constant	0.226***	0.921	35.651
	36.47	24.77	129.37
Observations	224	224	224
R-squared	0.006	0.001	0.000

*Note: ***, **, and * means the statistical significance is at the 1, 5, and 10% level. The values in the brackets are the t statistics of the regression.*

TABLE 9 | Counterfactual results for Huaihua City.

	CO_2PerGDP	CO_2PerCapita	Sequestration
DID	−0.075	0.059	3.492
	−1.26	0.16	1.32
Constant	0.226***	0.922	35.602
	36.51	24.79	129.73
Observations	224	224	224
R-squared	0.008	0.000	0.008

*Note: ***, **, and * means the statistical significance is at the 1, 5, and 10% level. The values in the brackets are the t statistics of the regression.*

carbon emissions was verified using robustness checks. This study selected four randomized controlled cities as the assumed pilot cities to conduct the counterfactual tests. Hence, it could conceivably be hypothesized that these assumptive cities were implemented the NRC policy in 2015. If statistically significant results were still observed between explained variables and the policy of NRC, we can infer that the reduction of carbon emissions may be caused by other unobserved factors rather than NRC. The regression results from four cities of three explained variables are displayed in **Tables 7–10**.

Looking at **Tables 7–10**, it can be seen that no statistically significant correlation between the three explained variables for all four assumptive cities and the policy of NRC, which means NRC is the unique exogenous impact for the true pilot cities. Therefore, the counterfactual results validate the reliability of the empirical results in 3.2. On average, the policy of NRC was shown to have a positive effect on carbon emissions reduction from different indicators in this study. We can then conclude that the implementation of NRC makes the relevant pilot cities paid more attention to environmental protection, and utilization efficiency of natural resources, which contributed to the achievement of carbon neutrality.

TABLE 10 | Counterfactual results for Baoji City.

	CO_2PerGDP	CO_2PerCapita	Sequestration
DID	-0.079	0.118	3.511
	-1.32	0.33	1.34
Constant	0.227***	0.921	35.601
	36.53	24.77	129.74
Observations	224	224	224
R-squared	0.008	0.001	0.009

*Note: ***, **, and * means the statistical significance is at the 1, 5, and 10% level. The values in the brackets are the t statistics of the regression.*

TABLE 11 | A summarization of NRC on low-carbon transition in four cities.

	CO_2PerGDP	CO_2PerCapita	Sequestration
Hulun Buir	Positive effect	Noneffective	Noneffective
Huzhou	Positive effect	Noneffective	Noneffective
Loudi	Positive effect	Negative effect	Noneffective
Yan'an	Noneffective	Negative effect	Positive effect

DISCUSSION

The empirical results above have proven that the NRC policy can exert positive effects on the carbon emission reduction accompanied by economic growth. Three of four pilot cities in China achieved the reversion of high-carbon growth as NRC brought down the CO_2 emissions per unit of GDP, indicating that the public awareness of low-carbon development can be aroused by treating natural resources like social assets. Despite the carbon drop effect on the unit economy has not been significant in the fourth city, Yan'an, the effect on carbon sequestration is fairly fruitful in this pilot city, as its statistically significant coefficient on carbon sink is much larger. **Table 10** summarizes the distribution of the results on four pilot cities.

As **Table 11** displays, in each pilot city, NRC can only bring in one of three positive effects, this indicating a single environmental protection policy can only achieve limited mitigation, or even give rise to non-ideal effects such as per-capita carbon emission's increasing in Loudi and Yan'an cities.

The differentiated results among the four pilot cities may be due to their heterogeneous regional characteristics (Yu and Tsai, 2018; Tang and Dou, 2021). Compared with the other three cities, Yan'an has the lowest scale of the secondary industry, with only 18.0, 10.8 and 17.7% of the secondary industry's output value in Hunlun Buir, Huzhou and Loudi averagely from 2015 to 2017, this weakened its emission-reducing potential because the manufacturing industry is the main source of CO_2 emission.

As for the CO_2 emission per capita, economic activities may explain the negative effect on Loudi and Yan'an, the residents' retail spending in Loudi and Yan'an is 58.81 million and 81.24 million less than Huzhou's in the post NRC period averagely, indicating that the basic household needs occupied more family spending where energy-intensive products such as heating and refrigeration are essential (Liu et al., 2021).

Although Yan'an has not benefited from the first two effects, carbon sequestration has only been promoted significantly there after the execution of NRC. A reliable reason is that the barren soil in northwest China enables larger development space on the contrary, where Yan'an is a part of the large-scale tree planting action in northwest China guided by the Central government. The new forestation area reached 13.64 million-acre in 2018 compared to 2004, including the 7.18 million acres of farmland's returning (Zhang et al., 2018), and NRC could strengthen this process. Hence, more carbon sequestration could be created considering the larger land space in northwest regions.

Considering the distinguishing results above, a synergism of multiple green environment policies is necessary for realizing greater abatement. Fortunately, more countermeasures have come into effect since 2018, such as ultra-low emission of iron and steel industry, or building of energy storage facilities to serve the growing renewable energy. Further research should be undertaken to investigate the collaborative effects of multi-policies on environmental issues.

CONCLUSION AND POLICY RECOMMENDATIONS

This study has examined the relationship between the implementation of NRC and carbon emissions reduction. The following conclusions can be drawn from the present investigation. First, the findings clearly indicated, following the increase in each increase of one thousand GDP, that the impact on CO_2 emissions was statistically significant negative, about almost 0.269, 0.102, and 0.243 decreases in three pilot cities, which are Hulun Buir, Huzhou and Loudi, respectively. Second, the results of this study showed that there was a significant positive correlation between the policy of NRC and Sequestration in Yan'an City, although the indicator $CO_2PerGDP$ of that region appeared to be unaffected by this scheme. The evidence from these findings indicates that carbon emission reduction can be partially achieved through the implementation of NRC. All the results were tested successfully by robustness tests. Taken together, this study appears to provide the first comprehensive assessment of NRC on carbon emission reduction. These results have significant implications for the understanding of how NRC affects carbon emissions, which complement those of earlier studies.

In line with the findings, this study has a number of policy implications for future practice. On the one hand, carbon emission is considered not only a climate issue, but also an environmental factor. The policy of NRC has demonstrated to achieve a win-win situation between the construction of ecological civilization and climate mitigation. Therefore, it is an efficient way for the government to encourage enterprises to promote their green productivities based on existing resources, since the natural resources such as forests have been priced, the exploitation cost for the enterprises will rise accordingly. On the other hand, this information can be used to develop targeted inventions aimed at carbon emissions reduction with many other green environmental policies. The results have confirmed the important role played by NRC on carbon emissions reduction, although the effect of NRC is different in various pilot cities. Cities with higher natural resources should do their best to intake them into national assets, add their value as far as possible, and eventually expand the coverage scale of green plants and increase the carbon sequestration.

Despite these promising results, some limitations need to be noted regarding the present study. First, this analysis has only examined the role of NRC on carbon emissions reduction without considering the context of many other green environmental policies. Also, with relatively small samples, caution must be applied regarding the generalizability of these findings. Further studies, which take other variables into account, will need to be undertaken to develop a deeper understanding of the relationships between the collaborative effects of multi-policies on environmental issues and carbon emissions.

DATA AVAILABILITY STATEMENT

The original contributions presented in the study are included in the article/supplementary material, further inquiries can be directed to the corresponding author.

AUTHOR CONTRIBUTIONS

PY: Conceptualization, Methodology, Data curation, Formal analysis, writing-original draft, Project administration. SX: Conceptualization, Writing-review and editing. YX: Conceptualization, Supervision, Writing-review and editing. YL: Methodology, Formal analysis, Writing-original draft, Funding acquisition,. LC: Methodology, Writing-review and editing.

FUNDING

This work is supported by the China Scholarship Council (CSC 202107080008).

REFERENCES

Agüero, J. M., and Beleche, T. (2017). Health Shocks and Their Long-Lasting Impact on Health Behaviors: Evidence from the 2009 H1N1 Pandemic in Mexico. *J. Health Econ.* 54, 40–55.

Bonan, G. (2008). Fertilizing Change. *Nat. Geosci* 1 (10), 645–646. doi:10.1038/ngeo328

Chen, J., Gao, M., Cheng, S., Hou, W., Song, M., Liu, X., et al. (2020). County-level CO2 Emissions and Sequestration in China during 1997-2017. *Sci. Data* 7 (1), 391. doi:10.1038/s41597-020-00736-3

Cheng, S., Chen, Y., Meng, F., Chen, J., Liu, G., and Song, M. (2021). Impacts of Local Public Expenditure on CO_2 Emissions in Chinese Cities: A Spatial Cluster Decomposition Analysis. *Resour. Conservation Recycling* 164. doi:10.1016/j.resconrec.2020.105217

Davidson, E. A., and Janssens, I. A. (2006). Temperature Sensitivity of Soil Carbon Decomposition and Feedbacks to Climate Change. *Nature* 440 (7081), 165–173. doi:10.1038/nature04514

Du, K. R., Cheng, Y. Y., and Yao, X. (2021). Environmental Regulation, green Technology Innovation, and Industrial Structure Upgrading: The Road to the green Transformation of Chinese Cities. *Energ. Econ.* 98, 10. doi:10.1016/j.eneco.2021.105247

Fan, W., Chen, N., Li, X., Wei, H., and Wang, X. (2020). Empirical Research on the Process of Land Resource-Asset-Capitalization-A Case Study of Yanba, Jiangjin District, Chongqing. *Sustainability* 12 (3), 1236. doi:10.3390/su12031236

Fan, W., Chen, N., Yao, W., Meng, M., and Wang, X. (2021). Integrating Environmental Impact and Ecosystem Services in the Process of Land Resource Capitalization-A Case Study of Land Transfer in Fuping, Hebei. *Sustainability* 13 (5), 2837. doi:10.3390/su13052837

Fuhrman, J., McJeon, H., Patel, P., Doney, S. C., Shobe, W. M., and Clarens, A. F., (2020). Food-energy-water Implications of Negative Emissions Technologies in a +1.5 °C Future. *Nat. Clim. Chang.* 10(10), 920, 927-+.doi:10.1038/s41558-020-0876-z

Gao, Y., Li, M., Xue, J., and Liu, Y. (2020). Evaluation of Effectiveness of China's Carbon Emissions Trading Scheme in Carbon Mitigation. *Energ. Econ.* 90. doi:10.1016/j.eneco.2020.104872

Greenstone, M., and Hanna, R. (2014). Environmental Regulations, Air and Water Pollution, and Infant Mortality in India. *Am. Econ. Rev.* 104, 3038–3072. doi:10.1257/aer.104.10.3038

Hao, L. N., Umar, M., Khan, Z., and Ali, W. (2021). Green Growth and Low Carbon Emission in G7 Countries: How Critical the Network of Environmental Taxes, Renewable Energy and Human Capital Is. *Sci. Total Environ.* 752, 141853. doi:10.1016/j.scitotenv.2020.141853

He, G., Xie, Y., and Zhang, B. (2020). Expressways, GDP, and the Environment: The Case of China. *J. Dev. Econ.* 145, 102485. doi:10.1016/j.jdeveco.2020.102485

Hong, M., Chen, S., and Zhang, K. (2021). Impact of the "Low-Carbon City Pilot" Policy on Energy Intensity Based on the Empirical Evidence of Chinese Cities. *Front. Environ. Sci.* 9. doi:10.3389/fenvs.2021.717737

Hu, Y., Ren, S., Wang, Y., and Chen, X. (2020). Can Carbon Emission Trading Scheme Achieve Energy Conservation and Emission Reduction? Evidence from the Industrial Sector in China. *Energ. Econ.* 85. doi:10.1016/j.eneco.2019.104590

IEA (2020). *CO_2 Emissions from Fuel Combustion*. Paris: IEA.

IPCC (2018). Mitigation Pathways Compatible with 1.5 °C in the Context of Sustainable Development. Available at: https://www.ipcc.ch/sr15/chapter/chapter-2/.

Ji, H., Zhao, X., Qiao, Z., Jung, J., Zhu, Y., Lu, Y., et al. (2014). Capacitance of Carbon-Based Electrical Double-Layer Capacitors. *Nat. Commun.* 5, 3317. doi:10.1038/ncomms4317

Kurniawan, R., Sugiawan, Y., and Managi, S. (2021). Economic Growth - Environment Nexus: An Analysis Based on Natural Capital Component of Inclusive Wealth. *Ecol. Indic.* 120, 10. doi:10.1016/j.ecolind.2020.106982

Lal, R. (2004). Soil Carbon Sequestration Impacts on Global Climate Change and Food Security. *Science* 304 (5677), 1623–1627. doi:10.1126/science.1097396

Laudicina, V. A., Dazzi, C., Delgado, A., Barros, H., and Scalenghe, R. (2021). Relief and Calcium from gypsum as Key Factors for Net Inorganic Carbon Accumulation in Soils of a Semiarid Mediterranean Environment. *Geoderma* 398, 10. doi:10.1016/j.geoderma.2021.115115

Li, P., Lu, Y., and Wang, J. (2016). Does Flattening Government Improve Economic Performance? Evidence from China. *J. Dev. Econ.* 123, 18–37. doi:10.1016/j.jdeveco.2016.07.002

Lin, B., and Zhu, J. (2019). The Role of Renewable Energy Technological Innovation on Climate Change: Empirical Evidence from China. *Sci. Total Environ.* 659, 1505–1512. doi:10.1016/j.scitotenv.2018.12.449

Ling, Y. T., Xia, S. M., Cao, M. Q., He, K. R., Lim, M. K., Sukumar, A., et al. (2021). Carbon Emissions in China's thermal Electricity and Heating Industry: An Input-Output Structural Decomposition Analysis. *J. Clean. Prod.* 329. doi:10.1016/j.jclepro.2021.129608

Liu, J., Murshed, M., Chen, F., Shahbaz, M., Kirikkaleli, D., and Khan, Z. (2021). An Empirical Analysis of the Household Consumption-Induced Carbon Emissions in China. *Sustainable Prod. Consumption* 26, 943–957. doi:10.1016/j.spc.2021.01.006

Lu, Z., Feng, Q., Xiao, S., Xie, J., Zou, S., Yang, Q., et al. (2021). The Impacts of the Ecological Water Diversion Project on the Ecology-Hydrology-Economy Nexus in the Lower Reaches in an Inland River basin. *Resour. Conservation Recycling* 164. doi:10.1016/j.resconrec.2020.105154

Marland, G., and Schlamadinger, B. (1997). Forests for Carbon Sequestration or Fossil Fuel Substitution? A Sensitivity Analysis. *Biomass and Bioenergy* 13 (6), 389–397. doi:10.1016/s0961-9534(97)00027-5

Meng, J., Mi, Z., Guan, D., Li, J., Tao, S., Li, Y., et al. (2018). The Rise of South-South Trade and its Effect on Global CO2 Emissions. *Nat. Commun.* 9 (1), 1871. doi:10.1038/s41467-018-04337-y

MNR (2015). Pilot Scheme for Compiling Balance Sheets of Natural Resources. Available at: http://f.mnr.gov.cn/201702/t20170206_1436702.html.

Nie, J.-J., Shi, C.-L., Xiong, Y., Xia, S.-M., and Liang, J.-M. (2020). Downside of a Carbon Tax for Environment: Impact of Information Sharing. *Adv. Clim. Change Res.* 11 (2), 92–101. doi:10.1016/j.accre.2020.06.006

Ogilvy, S. (2015). Developing the Ecological Balance Sheet for Agricultural Sustainability. *Sustainability Account. Manage. Pol. J.* 6 (2), 110–137. doi:10.1108/sampj-07-2014-0040

Onyango, V., Gazzola, P., and Wood, G. (2019). The Effects of Recent Austerity on Environmental protection Decisions. *Meq* 30 (5), 1218–1234. doi:10.1108/meq-01-2019-0025

Pacula, R. L., Powell, D., Heaton, P., and Sevigny, E. L. (2015). Assessing the Effects of Medical Marijuana Laws on Marijuana Use: the Devil Is in the Details. *J. Pol. Anal. Manage.* 34 (1), 7–31. doi:10.1002/pam.21804

Pan, Y., Birdsey, R. A., Fang, J., Houghton, R., Kauppi, P. E., Kurz, W. A., et al. (2011). A Large and Persistent Carbon Sink in the World's Forests. *Science* 333 (6045), 988–993. doi:10.1126/science.1201609

Papageorgiou, A., Azzi, E. S., Enell, A., and Sundberg, C. (2021). Biochar Produced from wood Waste for Soil Remediation in Sweden: Carbon Sequestration and Other Environmental Impacts. *Sci. Total Environ.* 776, 13. doi:10.1016/j.scitotenv.2021.145953

Sokil, O. (2018). Taxonomy of Agricultural Enterprises' Sustainable Development Reporting. *Agric. Resour. Econ. Int. Sci. E-j* 4 (1), 120–135.

Song, M., Zhu, S., Wang, J., and Wang, S. (2019). China's Natural Resources Balance Sheet from the Perspective of Government Oversight: Based on the Analysis of Governance and Accounting Attributes. *J. Environ. Manage.* 248, 109232. doi:10.1016/j.jenvman.2019.07.003

Song, M., Ma, X., Shang, Y., and Zhao, X. (2020a). Influences of Land Resource Assets on Economic Growth and Fluctuation in China. *Resour. Pol.* 68. doi:10.1016/j.resourpol.2020.101779

Song, M., Zhao, X., and Shang, Y. (2020b). The Impact of Low-Carbon City Construction on Ecological Efficiency: Empirical Evidence from Quasi-Natural Experiments. *Resour. Conservation Recycling* 157. doi:10.1016/j.resconrec.2020.104777

Soregaroli, C., Ricci, E. C., Stranieri, S., Nayga, R. M., Capri, E., and Castellari, E. (2021). Carbon Footprint Information, Prices, and Restaurant Wine Choices by Customers: A Natural Field experiment. *Ecol. Econ.* 186. doi:10.1016/j.ecolecon.2021.107061

Sun, C., Zhan, Y., and Du, G. (2020). Can Value-Added Tax Incentives of New Energy Industry Increase Firm's Profitability? Evidence from Financial Data of China's Listed Companies. *Energ. Econ.* 86. doi:10.1016/j.eneco.2019.104654

Tang, C., and Dou, J. (2021). The Impact of Heterogeneous Environmental Regulations on Location Choices of Pollution-Intensive Firms in China. *Front. Environ. Sci.* 9. doi:10.3389/fenvs.2021.799449

Thomas, C. D., Cameron, A., Green, R. E., Bakkenes, M., Beaumont, L. J., Collingham, Y. C., et al. (2004). Extinction Risk from Climate Change. *Nature* 427 (6970), 145–148. doi:10.1038/nature02121

UN (2020). General Debate of the 75th Session of the General Assembly. Available at: https://www.un.org/en/delegate/general-debate-75th-session-general-assembly.

UNFCCC (2019). "Global Conference Aims to Link Climate Action, Sustainable Development Agendas More Closely," in The Conference of the Parties. Available at: https://unfccc.int/news/global-conference-aims-to-link-climate-action-sustainable-development-agendas-more-closely.

UNFCCC (2016). "The Paris Agreement," in The Conference of the Parties. Available at: https://unfccc.int/process-and-meetings/the-paris-agreement/the-paris-agreement.

Wang, C., Wang, F., Zhang, X., and Zhang, H. (2017). Influencing Mechanism of Energy-Related Carbon Emissions in Xinjiang Based on the Input-Output and Structural Decomposition Analysis. *J. Geogr. Sci.* 27 (3), 365–384. doi:10.1007/s11442-017-1382-8

Wang, H., Chen, Z., Wu, X., and Nie, X. (2019). Can a Carbon Trading System Promote the Transformation of a Low-Carbon Economy under the Framework of the porter Hypothesis? -Empirical Analysis Based on the PSM-DID Method. *Energy Policy* 129, 930–938. doi:10.1016/j.enpol.2019.03.007

Wang, L., Gao, C. C., Yang, K., Sheng, Y. Q., Xu, J., Zhao, Y. X., et al. (2021). Effects of Biochar Aging in the Soil on its Mechanical Property and Performance for Soil CO2 and N2O Emissions. *Sci. Total Environ.* 782, 10. doi:10.1016/j.scitotenv.2021.146824

Wang, Z., and Qiu, S. (2021). Can "Energy Saving and Emission Reduction" Demonstration City Selection Actually Contribute to Pollution Abatement in China. *Sust. Prod. Consumption* 27, 1882–1902. doi:10.1016/j.spc.2021.04.030

Wen, F., Wu, N., and Gong, X. (2020). China's Carbon Emissions Trading and Stock Returns. *Energ. Econ.* 86. doi:10.1016/j.eneco.2019.104627

Xu, M., Zhang, X., Shen, S., Wei, S. J., and Fan, J. L. (2021). Assessment of Potential, Cost, and Environmental Benefits of CCS-EWR Technology for Coal-Fired Power Plants in Yellow River Basin of China. *J. Environ. Manage.* 292, 11. doi:10.1016/j.jenvman.2021.112717

Yang, M., Yang, L., Sun, M., and Wang, Y. (2020). Economic Impact of More Stringent Environmental Standard in China: Evidence from a Regional Policy Experimentation in Pulp and Paper Industry. *Resour. Conservation Recycling* 158, 104831. doi:10.1016/j.resconrec.2020.104831

Yang, T., and Wang, Q. (2020). The Nonlinear Effect of Population Aging on Carbon Emission-Empirical Analysis of Ten Selected Provinces in China. *Sci. Total Environ.* 740, 140057. doi:10.1016/j.scitotenv.2020.140057

Yang, T., Zhu, Y., Li, Y., and Zhou, B. (2021). Achieving Win-Win Policy Outcomes for Water Resource Management and Economic Development: The Experience of Chinese Cities. *Sust. Prod. Consumption* 27, 873–888. doi:10.1016/j.spc.2021.02.006

Yang, Z., Fan, M., Shao, S., and Yang, L. (2017). Does Carbon Intensity Constraint Policy Improve Industrial green Production Performance in China? A Quasi-DID Analysis. *Energ. Econ.* 68, 271–282. doi:10.1016/j.eneco.2017.10.009

Yao, S. Y., Yu, X. Y., Yan, S., and Wen, S. Y. (2021). Heterogeneous Emission Trading Schemes and green Innovation. *Energy Policy* 155, 13. doi:10.1016/j.enpol.2021.112367

Ye, P., Xia, S., Xiong, Y., Liu, C., Li, F., Liang, J., et al. (2020). Did an Ultra-low Emissions Policy on Coal-Fueled Thermal Power Reduce the Harmful Emissions? Evidence from Three Typical Air Pollutants Abatement in China. *Ijerph* 17, 8555. doi:10.3390/ijerph17228555

Yi, L., Bai, N., Yang, L., Li, Z., and Wang, F. (2020). Evaluation on the Effectiveness of China's Pilot Carbon Market Policy. *J. Clean. Prod.* 246. doi:10.1016/j.jclepro.2019.119039

Yu, H.-C., and Tsai, B.-Y. (2018). Environmental Policy and Sustainable Development: An Empirical Study on Carbon Reduction Among Chinese Enterprises. *Corp Soc. Resp Env Ma* 25 (5), 1019–1026. doi:10.1002/csr.1499

Yue, X. G., Liao, Y. Y., Zheng, S. Y., Shao, X. F., and Gao, J. (2021). The Role of green Innovation and Tourism towards Carbon Neutrality in Thailand: Evidence from Bootstrap ADRL Approach. *J. Environ. Manage.* 292, 9. doi:10.1016/j.jenvman.2021.112778

Zanchi, G., Pena, N., and Bird, N. (2012). Is Woody Bioenergy Carbon Neutral? A Comparative Assessment of Emissions from Consumption of Woody Bioenergy and Fossil Fuel. *Glob. Change Biol. Bioenergy* 4 (6), 761–772. doi:10.1111/j.1757-1707.2011.01149.x

Zhang, J., Fu, J., Liu, C., Qu, Z., Li, Y., Li, F., et al. (2019a). Evaluating Water Resource Assets Based on Fuzzy Comprehensive Evaluation Model: A Case Study of Wuhan City, China. *Sustainability* 11 (17). doi:10.3390/su11174627

Zhang, J., Li, Y., Liu, C., Qu, Z., Li, F., Yang, Z., et al. (2019b). Application of Set Pair Analysis in a Comprehensive Evaluation of Water Resource Assets: A Case Study of Wuhan City, China. *Water* 11 (8). doi:10.3390/w11081718

Zhang, S., Li, H., Zhang, Q., Tian, X., and Shi, F. (2019). Uncovering the Impacts of Industrial Transformation on Low-Carbon Development in the Yangtze River Delta. *Resour. Conservation Recycling* 150. doi:10.1016/j.resconrec.2019.104442

Zhang, Y. F., Shi, X. P., Qian, X. Y., Chen, S., and Nie, R. (2021). Macroeconomic Effect of Energy Transition to Carbon Neutrality: Evidence from China's Coal Capacity Cut Policy. *Energy Policy* 155, 15. doi:10.1016/j.enpol.2021.112374

Zhang, Z., Ma, R., and Yang, Y. (2018). *Shaanxi Yan'an: Ecological Civilization Creates Gold & Silver Mountains*. Guangming Daily. Oct.26.2018 https://epaper.gmw.cn/gmrb/html/2018-10/26/nw.D110000gmrb_20181026_2-03.htm.

Zhou, B., Zhang, C., Song, H., and Wang, Q. (2019). How Does Emission Trading Reduce China's Carbon Intensity? an Exploration Using a Decomposition and Difference-In-Differences Approach. *Sci. Total Environ.* 676, 514–523. doi:10.1016/j.scitotenv.2019.04.303

Zhou, D., Liang, X., Zhou, Y., and Tang, K. (2020). Does Emission Trading Boost Carbon Productivity? Evidence from China's Pilot Emission Trading Scheme. *Ijerph* 17, 5522. doi:10.3390/ijerph17155522

Zhou, W., Shen, L., Zhong, S., and Yuan, G. (2021). System Margin and Path Research of Ecological Product Value Implementation. *Resour. Industries* 001. (In Chinese).

Zhu, D. L., Duan, W. J., Zhang, H., and Du, T. (2021). Natural Resource Balance Sheet Compilation: a Land Resource Asset Accounting Case. *J. Chin. Governance* 6 (4), 515–536. doi:10.1080/23812346.2021.1891721

Conflict of Interest: The authors declare that the research was conducted in the absence of any commercial or financial relationships that could be construed as a potential conflict of interest.

Publisher's Note: All claims expressed in this article are solely those of the authors and do not necessarily represent those of their affiliated organizations, or those of the publisher, the editors and the reviewers. Any product that may be evaluated in this article, or claim that may be made by its manufacturer, is not guaranteed or endorsed by the publisher.

frontiers in Environmental Science

ORIGINAL RESEARCH
published: 11 February 2022
doi: 10.3389/fenvs.2022.837947

Evaluation of Marginal Land Potential and Analysis of Environmental Variables of Jerusalem Artichoke in Shaanxi Province, China

Danyun Zhao[1], *Fang Yin*[1]*, *Tariq Ashraf*[2], *Zheng Yuan*[3] *and Linxiao Ye*[4]

[1]*Shaanxi Key Laboratory of Land Consolidation, School of Land Engineering, Chang'an University, Xi'an, China,* [2]*School of Earth Science and Resources, Chang'an University, Xi'an, China,* [3]*China Center for Resources Satellite Data, Beijing, China,* [4]*Qinba Ecological Protection Center, Hanzhong, China*

Based on the maximum entropy modeling (Maxent) and ArcGIS tool, this study assessed the potential of marginal land and analyzed the impact of environmental variables for Jerusalem artichoke (*Helianthus tuberosus* L.) in Shaanxi Province, China. The results showed that the dominant land type used for the growth of Jerusalem artichoke was moderately dense grassland. Additionally, significant environmental variables of Jerusalem artichoke and their suitable range in Shaanxi Province were average slope (SLP, 0–5°C), average soil depth (DPT, 1.50–1.60 m), max temperature of the warmest month (Bio5, 30–31°C), annual mean temperature (Bio1, 16.5–18.0°C), precipitation of the wettest quarter (Bio16, 0.01–0.02 m), July solar radiation (SR7, 1.66–1.67 × 10^7 W/m^2), precipitation seasonality (Bio15, 50–60%), precipitation of the driest quarter (Bio17, 0–0.005 m), and isothermality (Bio3, 265–275). Furthermore, the suitable area was mainly distributed in southern (mainly Hanzhong, Ankang, and Shangluo) and northern (mainly Yan'an and Yulin) parts of Shaanxi Province, covering around 8.81 × 10^{10} m^2 and accounting for 42.8% of the total area of the Shaanxi Province. This study can provide a reference for the rational planting of Jerusalem artichoke in Shaanxi Province.

Keywords: marginal land resources, energy plant, Maxent model, environmental variables, habitat suitability, Shaanxi Province

OPEN ACCESS

Edited by:
Ayman Elshkaki,
Institute of Geographic Sciences and Natural Resources Research (CAS), China

Reviewed by:
Manoj Kumar Jhariya,
Sant Gahira Guru Vishwavidyalaya, India
Lal Singh,
National Environmental Engineering Research Institute (CSIR), India

***Correspondence:**
Fang Yin
yinf@chd.edu.cn

Specialty section:
This article was submitted to Environmental Economics and Management, a section of the journal Frontiers in Environmental Science

Received: *17 December 2021*
Accepted: *17 January 2022*
Published: *11 February 2022*

Citation:
Zhao D, Yin F, Ashraf T, Yuan Z and Ye L (2022) Evaluation of Marginal Land Potential and Analysis of Environmental Variables of Jerusalem Artichoke in Shaanxi Province, China. Front. Environ. Sci. 10:837947. doi: 10.3389/fenvs.2022.837947

1 INTRODUCTION

Climate change has garnered huge attention worldwide, and rising greenhouse gas emissions are the primary drivers of climate change (such as carbon dioxide and methane) (Jhariya et al., 2019; Jhariya et al., 2021a; Jhariya et al., 2021c). The massive usage of fossil fuels has led to a rapid increase in greenhouse gas emissions (Foster, 2019; Jhariya et al., 2019). The United Nations Framework Convention on Climate Change (UNFCCC) was conducted to control carbon dioxide and other greenhouse gas emissions (Jhariya et al., 2019). Replacing or reducing the usage of fossil fuels with renewable energy is an effective way to reduce carbon emission (Maddalwar et al., 2021; Zhang B. et al., 2021). As one of the largest consumers of fossil energy and carbon emitter globally (Mi et al., 2017; Shi et al., 2022), the Chinese government actively responded to international carbon neutral actions (Nie et al., 2022), and it urgently needs to explore economical and environmentally friendly renewable energy sources to achieve carbon emission reduction targets.

Bioenergy, as one of the renewable energy sources (RES), is affianced with renewability, cleanliness (Li X. et al., 2020), and ecological friendliness (Paul et al., 2020) and has proven to be the most promising renewable resource in the future (Bauer et al., 2020; Cao et al., 2022). On the one hand, China has a vast potential for bioenergy production (Zhao and Liu, 2014). On the other hand, energy plant growth necessitates substantial land resources (Xue et al., 2020), putting land for energy plants in direct or indirect competition with land for food crops (Leppäkoski et al., 2021; Jhariya et al., 2021a). One feasible approach is growing energy plants on marginal lands (Jiang et al., 2018; Mehmood et al., 2019), which not only helps to alleviate the energy crisis (Liu et al., 2015) but also reduces soil erosion and improves marginal soil quality without interfering with food production (Bogucka and Jankowski, 2020; Qaseem and Wu, 2020). Besides, the marginal land resources have huge development potential in China. Xu et al. (2013) estimated that suitable marginal land for planting energy plants was approximately 17.6×10^{11} m^2, accounting for 1.82% of the total area of China.

Ideal energy crops for marginal lands were occupied with a long growing season, well-developed canopy, and fewer reproductive structures (Jones et al., 2015). After 2007, the grains and green grain crops as raw materials for biomass energy were banned in China (Xue et al., 2016; Qaseem and Wu, 2021), so the non-food biomass feedstock is the first choice of bioenergy production in China (Qaseem and Wu, 2021). FAO experts have dubbed Jerusalem artichoke (*Helianthus tuberosus L.*) a "21st-century human livestock crop" because of its high tolerance to environmental challenges such as soil salinity, drought, and plant diseases (Long et al., 2016; Krivorotova and Sereikaite, 2018), making it ideal for marginal lands. Moreover, with rapid growth and low production cost (such as fewer pesticides input, fertilizers, and water) (Bogucka et al., 2021), as well as high biomass (Bogucka and Jankowski, 2020), Jerusalem artichoke is regarded as one of the most promising bioenergy raw material sources (Epie et al., 2018).

Assessing the distribution of energy plants and habitat suitability is a prerequisite for their rational planting and development. Many models are being used to predict the species geographic distributions, such as the generalized linear model (GLM), boosted regression trees (BRT), support vector machine (SVM), multifactor-integrated assessment method (Fukuda et al., 2013; Yin et al., 2018; Jiang et al., 2019; Ghareghan et al., 2020), and maximum entropy modeling (Maxent). In comparison, Maxent is a widely recognized model used in geographical distribution of species (Phillips et al., 2006; Li J. et al., 2020) due to its good performance, especially in cases where species' distribution information is incomplete (Li J. et al., 2020; Zhang J.-M. et al., 2021). Most of the existing literature used the Maxent model to predict the potential distribution of energy plants (Wen et al., 2016; Li et al., 2021; Cao et al., 2022). But these studies lack further analysis of species suitability on the marginal land.

Shaanxi Province is one of the target areas for the development of bioenergy (Council, 2018). According to the investigation, Jerusalem artichoke has been widely planted in Yan'an and Shangluo. However, large-scale rational planting that is essential for the development of bioenergy has not been realized, and the marginal land resources suitable for Jerusalem artichoke planting are ambiguous. This study adopts the Maxent model and ArcGIS tools to assess the potential of marginal land suitable for Jerusalem artichoke and to analyze the impact of environmental variables for Jerusalem artichoke in Shaanxi Province. The main objectives of this study are as follows: 1) to determine the distribution of Jerusalem artichoke in Shaanxi Province; 2) to identify the most critical environmental variables for Jerusalem artichoke and determine their effects on the spread of Jerusalem artichoke; and 3) to access the potential marginal land resources suitable for planting Jerusalem artichoke in Shaanxi Province, and the habitat suitability of Jerusalem artichoke. For the first time, the Maxent model is used with ArcGIS tools to assess Jerusalem artichoke's marginal land resource potential in Shaanxi Province. It can provide a reference for the rational planting of Jerusalem artichoke and can contribute to relevant policy-making in Shaanxi Province.

2 MATERIALS AND METHODS

2.1 Study Area

Shaanxi Province is located in the northwestern part of China (105°29′E-111°15′E and 31°42′N-39°35′N). The area is 2.06×10^{11} m^2, where the Loess Plateau accounts for 40% of the whole land area of Shaanxi Province. The topography is low in the middle and high in the south and north. The northern part is the Loess Plateau, most of which belongs to the warm temperate monsoon climate, and the northern part of Shaanxi along the Great Wall belongs to the middle temperate monsoon climate; the precipitation varies from 0.40 to 0.60 m. The central part is the Guanzhong Plain, which belongs to the warm temperate monsoon climate, and the rainfall ranges from 0.50 to 0.70 m. The southern part is the Qinling Mountains, which belong to the north subtropical monsoon climate, and the precipitation varies from 0.70 to 0.90 m. Shaanxi Province spans from subtropical, warm temperate, and temperate zones from south to north, with significant climate differences.

2.2 Marginal Land

The marginal land is highly variable due to its various definitions (Richards et al., 2014; Jiang et al., 2018). Generally, the land unsuitable for food production, ambiguous lower quality land, and economically marginal land (Shortall, 2013) are considered marginal land. According to the method of Yin et al. (2018), this study selected seven types of land (including shrubland (SHL), sparse forest land (SFL), dense grassland (DG), moderately dense grassland (MDG), sparsely dense grassland (SDG), saline land (SAL), and bare land (BL)) as marginal land based on the land use data in 2018 (Xu et al., 2018). Eventually, the total area of marginal land in Shaanxi

Province is 1.07×10^{11} m^2, accounting for 51.9% of the total area of Shaanxi Province.

2.3 Datasets

2.3.1 Occurrence Data

In this study, the occurrence data were mainly obtained by retrieving the specimen database, consulting the data and field investigation. Specimen databases include the public repository of the Global Biodiversity Information Facility (https://www.gbif.org/) and the platform of teaching specimen standardization and resource sharing (http://mnh.scu.edu.cn/). A Garmin global positioning system receiver (accuracy 5 m) was used for detecting positions in the field survey. Google Earth software was used to fill in the missing geographic coordinates in the acquired data. A total of 28 Jerusalem artichoke sites were selected. The Krasovsky 1940 Albers projected coordinate system was used, and the data were stored in the csv format.

2.3.2 Environmental Variables

Natural conditions (such as soil quality, precipitation, topography, accumulated temperature, and solar radiation) significantly impact the growth of Jerusalem artichoke (Zorić et al., 2016). Therefore, 35 environmental variables affecting Jerusalem artichoke were chosen, including climate (19 variables), solar radiation (12 variables), soil conditions (2 variables), and terrain (2 variables) (**Supplementary Appendix A**).

The following is an overview of the data and its source.

Meteorology: The CHELSA version 1.2 (http://chelsa-climate.org/) climate dataset for earth land surface areas was adopted in this study, which is licensed under a Creative Commons Attribution 4.0 International License. It has high resolution (30 arc-second resolution). It included monthly and annual mean temperature and precipitation patterns incorporated with topological climate (such as orographic rainfall and wind fields) from 1979 to 2013.

Topography: The ASTER Digital Elevation Model (DEM) version 3 and slope version 3 datasets with 30 m resolution were obtained from the National Earth System Science Data Center, National Science and Technology Infrastructure of China (http://www.geodata.cn).

Solar radiation: The monthly Global-Extra Terrestrial Solar Radiation data (12 months, 30 arc-second resolution) was derived from the Consortium for Spatial Information (https://cgiarcsi.community/). The unit of the extraterrestrial solar radiation is W/m^2.

Soil: The National Secondary Soil Survey dataset was used in the analysis. Soil depth and organic matter content were used in the study, and an ordinary kriging interpolation algorithm obtained China's spatial continuous soil data.

Land use: The dataset was collected from the Data Center for Resources and Environmental Sciences, Chinese Academy of Sciences (RESDC) (http://www.resdc.cn).

After unifying the projected coordinate system (Krasovsky 1940 Albers), all environmental layers were trimmed and resampled to the exact geographic boundaries with a pixel size (about 100 m × 100 m) and recorded in an ASCII grid (.asc) format.

2.4 Modeling

The Maxent model, based on statistics and machine learning, is a popular software for predicting species distribution (Phillips et al., 2006), and it is available for free (https://biodiversityinformatics.amnh.org/open_source/maxent/). A model was built to forecast species distribution based on environmental layers for a group of grid cells and a collection of observed species sample locations (Phillips et al., 2004). The model's appropriateness was represented by the function of its environment variables in each grid cell. The higher the value of the function of a particular grid cell, the more suitable the conditions are for the species. The model was a probability distribution of all grid cells, and the selected distribution is the one with maximum entropy (Merow et al., 2013).

The percent contribution and the jackknife test are common indicators to evaluate the importance of environmental predictors in the model (Zhang J.-M. et al., 2021). The percent contribution is only heuristically defined as a function of the particular path of the optimal solution of the Maxent model (Phillips, 2017). The jackknife test creates a model in three ways: (a) removing one variable at a time and relying on the remaining variables; (b) each variable is used individually; and (c) using all variables (Charrua et al., 2020). The response curves depict the Maxent model, which was generated by using only the provided variables (Phillips, 2017), which showed the quantitative relationship between environmental variables and predicted sustainability (Yi et al., 2016; Zhang et al., 2019).

2.4.1 Selection of Environmental Variables

A preliminary Maxent model screened the variables that substantially impacted Jerusalem artichoke. As mentioned in Section 2.4.3, keeping the same settings, 28 occurrence points data of Jerusalem artichoke and 35 environmental variables were imported in the Maxent model. Then the environmental variables with a percent contribution greater than 1.5 as important variables on Jerusalem artichoke were chosen. 15 environmental variables (mentioned in bold letters in **Supplementary Appendix A**) with substantial impacts on the distribution of Jerusalem artichoke were selected by preliminary Maxent model, including average slope (SLP), digital elevation model (DEM), soil depth (DPT), May solar radiation (SR5), July solar radiation (SR7), mean temperature of the wettest quarter (Bio8), mean temperature of coldest quarter (Bio11), annual mean temperature (Bio1), max temperature of the warmest month (Bio5), min temperature of the coldest month (Bio6), precipitation of the wettest quarter (Bio16), precipitation of the driest quarter (Bio17), precipitation seasonality (Bio15), isothermality (Bio3), and organic matter (OM). Besides, highly correlated environmental variables demonstrated interference with the result of the Maxent model (Sillero and Barbosa, 2020); as a result, Pearson's correlation analysis was used to screen these 15 environmental factors, with 0.8 chosen as the correlation threshold (**Supplementary Appendix B**) (Yang et al.,

TABLE 1 | Statistics of nine significant environmental variables for modeling the habitat suitability distribution of Jerusalem artichoke.

Code	Variable	Unit	Min	Max	Mean	STD
Bio1	Annual mean temperature	°C	–3.00	17.0	10.4	2.47
Bio3	Isothermality	—	244	287	269	7.72
Bio5	Maximum temperature of warmest month	°C	13.0	31.7	27.5	2.26
Bio15	Precipitation seasonality	%	54	119	81.6	12.4
Bio16	Precipitation of wettest quarter	m	0.188	0.942	0.387	0.106
Bio17	Precipitation of driest quarter	m	0.005	0.058	0.017	0.008
DPT	Soil depth	m	0.976	1.58	1.27	0.12
SR7	The July solar radiation	W/m^2	1.66×10^7	1.67×10^7	1.67×10^7	1.41×10^4
SLP	Average slope	°	0	74.6	17.7	11.4

[a]STD, standard deviation.

2013), and nine significant environmental variables were selected for further study, including SLP, DPT, Bio5, Bio1, Bio16, SR7, Bio15, Bio17, and Bio3, and their descriptive statistics results are shown in **Table 1**.

2.4.2 Importing Data

In Maxent, 28 occurrence point data of Jerusalem artichoke and nine significant environmental variables were imported.

2.4.3 Parameter Setting

The replicates option was set to 10. The feature type of response curve selected was "hinge features," and the items checked "create response curves" and "do jackknife to measure variable importance." The bootstrap verification method was utilized, with 25% of random presence points reserved in each study phase. The rest of the parameters were left at their default settings.

2.4.4 Model Evaluation

The area under the receiver operating characteristic (AUC) curve is used to evaluate the model's accuracy. In general, the higher the AUC value, the stronger the correlation between the relevant environmental variables and the predicted geographical distribution of species, and the greater the accuracy of the model prediction results. The performance of the model is classified into five cases according to the value of AUC (Miguel et al., 2005): (1) fail model (AUC<0.5); (2) poor model (0.5 ≤ AUC<0.7); (3) fair model (0.7 ≤ AUC<0.8); (4) good model (0.8 ≤ AUC<0.9); and (5) excellent model (0.9 ≤ AUC<1).

2.4.5 Output Data

The output format of Maxent was set to the default output ("cloglog") that is the easiest way to conceptualize and give estimate values between 0 and 1 of the probability of presence.

2.4.6 Results Processing

By superimposing Shaanxi Province marginal land data on the Maxent result, the distribution of marginal land suitable for Jerusalem artichoke was eventually produced. To conceptualize the results according to Kumar (2012), the probability of existence ranged from 0 to 1 was reclassified and divided into four classes in ArcGIS 10.2: (1) unsuitable area (<0.08); (2) moderate potential area (0.08–0.28); (3) good potential area (0.28–0.58); and (4) high potential area (>0.58).

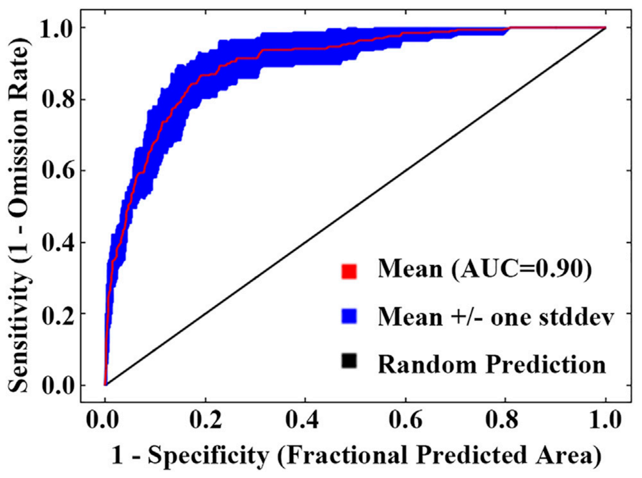

FIGURE 1 | ROC curves with error bars and average AUC across models (the red curve shows the mean of AUC of the Maxent model, the blue margins indicated the mean of +/– one standard deviation of the Maxent model, and the black line shows the random prediction calculated in 10 replicates respectively).

3 RESULTS

3.1 Modeling Precision

Because the results of the same species distribution predicted by this model somewhat varied each time (Cullen, 2017), the average results of 10 model runs were used in this study. The mean standard deviation of the model after 10 replicates was 0.08. The AUC values of all models performed well in the training data, ranging from 0.86 to 0.94 with a mean of 0.90. While in the test data, the AUC values ranged from 0.65 to 0.94 with a mean of 0.79. The area under the receiver operating characteristic curves with error bars and the average AUC across models (**Figure 1**) show an excellent model. The mean results of the model after 10 replicates calculations are used to ensure the reliability of the model results. Therefore, the model successfully predicted the distribution of Jerusalem artichoke in theory.

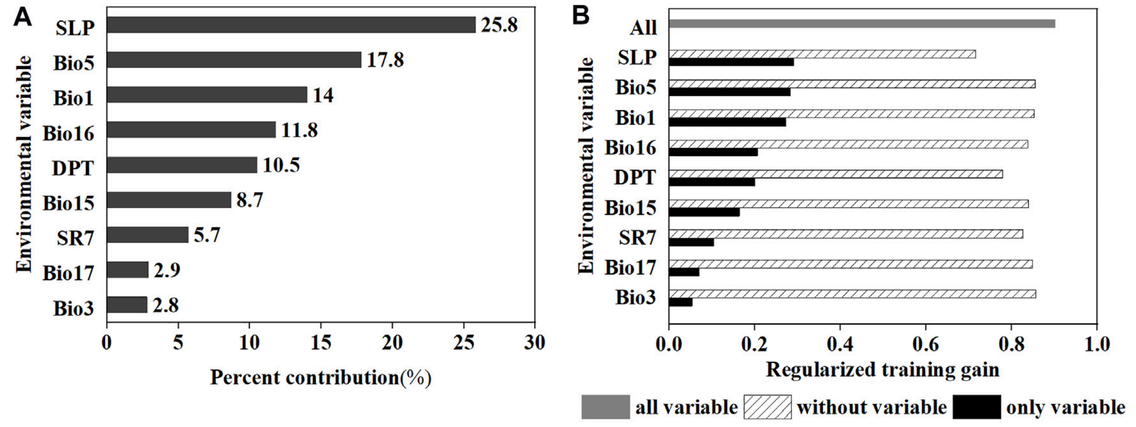

FIGURE 2 | Evaluation of the significant environmental predictors: **(A)** the estimates of percent contributions of the environmental variables to the Maxent model; **(B)** jackknife test evaluating the significant environmental variables on the distribution of Jerusalem artichoke.

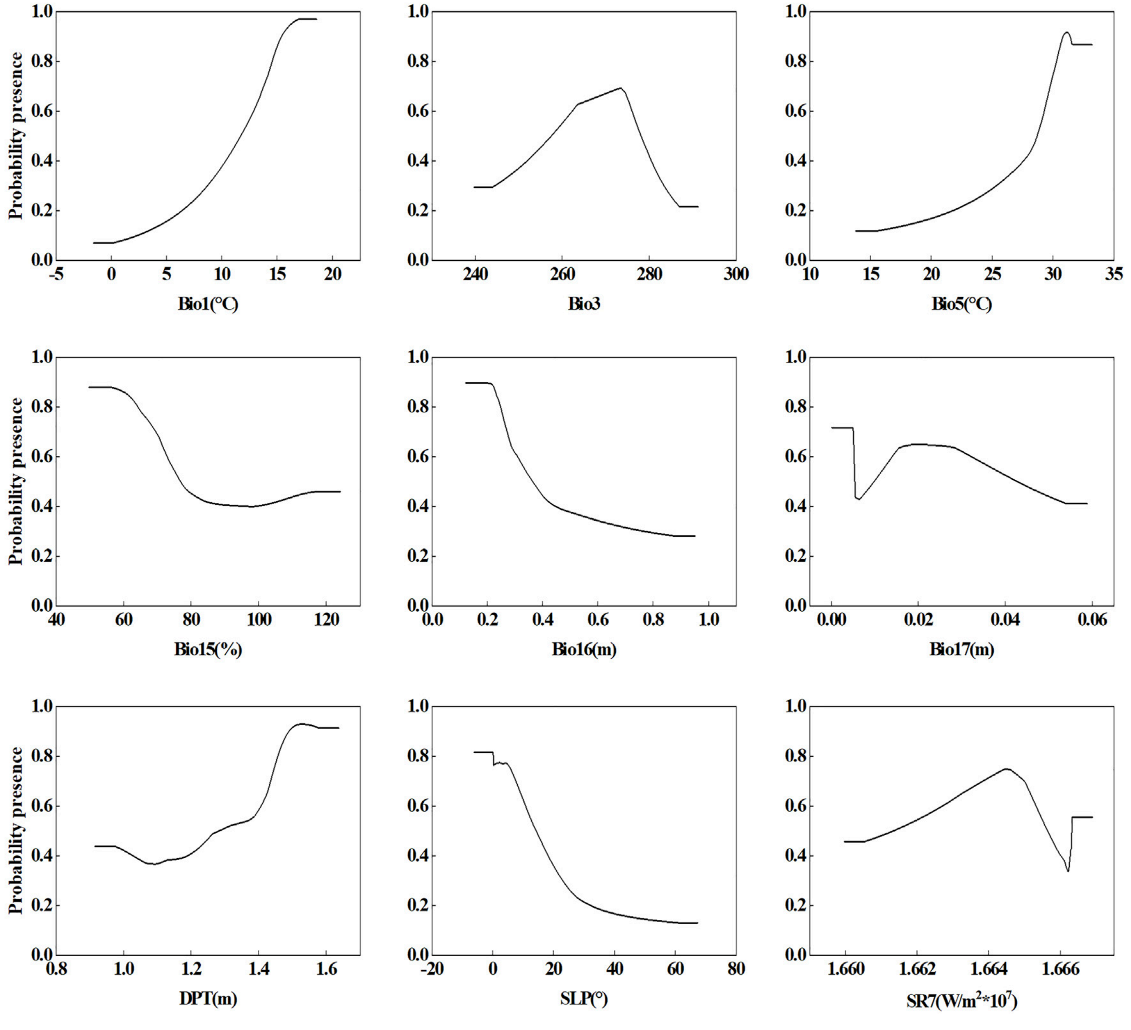

FIGURE 3 | The mean response curves of the 9 significant environment variables of the Maxent model calculated in 10 replicates.

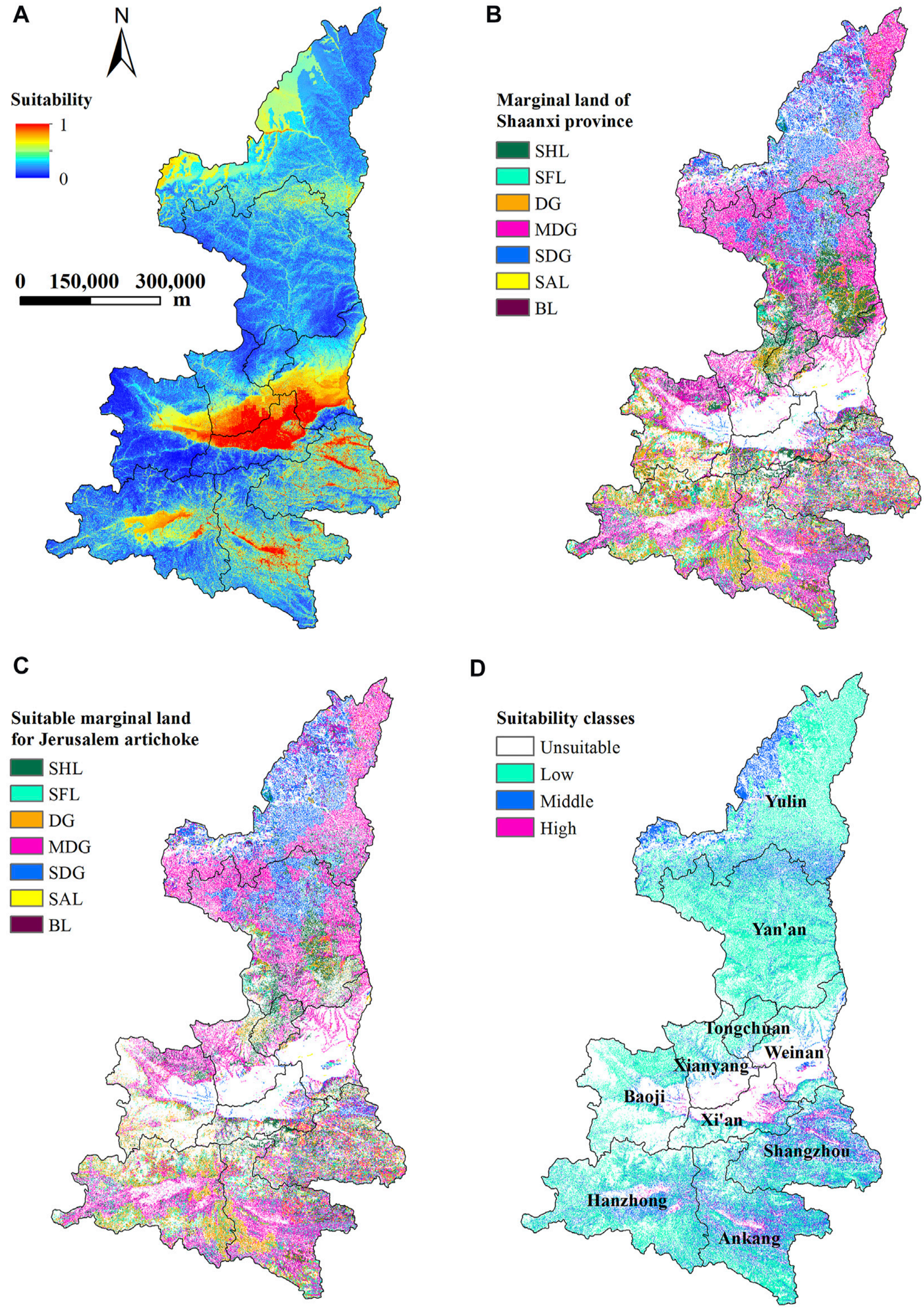

FIGURE 4 | The area suitable for planting Jerusalem artichoke in Shaanxi Province: **(A)** spatial distribution of the pre-diction of the Maxent model (different colors indicate the prediction probability of different suitable conditions, and the red color (the value close to 1) means more suitable for planting, and the blue color (the value close to 0) means less suitable for planting of Jerusalem artichoke); **(B)** spatial distribution of marginal land of Shaanxi Province (SHL: shrubland, SFL: sparse forest land, DG: dense grassland, MDG: moderate dense grassland, SDG: sparse dense grassland, SAL: saline land, BL: bare land); **(C)** spatial distribution of marginal land suitable for Jerusalem artichoke in Shaanxi Province; **(D)** spatial distribution of classification results of marginal land suitable for Jerusalem artichoke in Shaanxi Province.

TABLE 2 | Statistical results of marginal land suitable for growing Jerusalem artichoke in each city of Shaanxi Province with the unit 1.00×10^8 m^2.

		Shrubland	Sparse forest land	Dense grassland	Moderately dense grassland	Sparsely dense grassland	Saline land	Bare land	Total	
Guanzhong plain	Xi'an	5.45	2.09	5.96	6.81	3.67	0.00	0.01	24.00	111.05
	Baoji	5.59	3.29	8.89	24.19	1.35	0.00	0.01	43.32	
	Xianyang	3.14	0.83	2.31	13.46	0.71	0.00	0.05	20.49	
	Weinan	3.16	1.07	2.64	14.06	1.84	0.42	0.03	23.24	
Southern Shaanxi	Hanzhong	9.33	23.61	45.22	47.76	0.09	0.00	0.04	126.04	368.47
	Ankang	11.36	26.15	30.51	63.18	1.25	0.00	0.03	132.48	
	Shangluo	12.65	21.25	30.28	37.03	8.71	0.00	0.01	109.95	
Northern Shaanxi	Tongchuan	6.47	0.67	2.53	5.16	0.05	0.00	0.00	14.89	401.05
	Yan'an	38.74	12.99	14.20	94.31	33.44	0.00	0.26	193.94	
	Yulin	10.33	7.46	3.07	94.21	75.15	0.94	1.07	192.23	
Total		106.22	99.41	145.62	400.18	126.25	1.37	1.51	880.57	

3.2 Response of Significant Environmental Variables to Jerusalem Artichoke Species Distribution

Percentage contributions of the variables in the Maxent model are shown in **Figure 2A** with a descending order of SLP, DPT, Bio5, Bio1, Bio16, SR7, Bio15, Bio17, and Bio3. **Figure 2B** illustrates the jackknife test of regularized training gain of variable importance, which shows the variables SLP, Bio5, Bio1, Bio16, DPT, Bio15, SR7, Bio17, and Bio3 in a descending order. SLP and DPT were the most potent predictors of Jerusalem artichoke distribution since SLP and DPT variables contained more information than other factors. The training gain was dramatically reduced when the SLP and DPT variables were excluded. When Bio3 and Bio17 were employed in isolation, they had a minor influence on calculating the spread of Jerusalem artichoke (**Figure 2B**).

Figure 3 depicts the response curves of the nine significant environmental variables on the distribution of Jerusalem artichoke. It also indicates that the Jerusalem artichoke–favored areas in Shaanxi Province are places where the annual mean temperature (Bio1) is 16.5–18.0°C, the isothermality (Bio3) is 265–275, the max temperature of the warmest month (Bio5) is 30–31°C, the precipitation seasonality (Bio15) is 50–60%, the precipitation of wettest quarter (Bio16) is 0.01–0.02 m, the precipitation of the driest quarter (Bio17) is 0–0.005 m, the soil depth (DPT) is 1.50–1.60 m, the average slope (SLP) is 0–5°, and the July solar radiation (SR7) is 1.66–1.67 × 10^7 W/m^2.

3.3 Species Distribution and Habitat Suitability on Marginal Land

The prediction of the Maxent model is shown in **Figure 4A**, which indicates that the suitable areas for growing Jerusalem artichoke in the Guanzhong Plain (Xianyang, Baoji, Weinan, and Hanzhong) and the Southern Shaanxi (mainly Ankang and Shangluo). Superimposing **Figure 4A** and the marginal land of Shaanxi Province (**Figure 4B**) in ArcGIS 10.2 yielded the suitable marginal land for growing Jerusalem artichoke (**Figure 4C**), which revealed that moderately dense grassland was the dominating land type used for growing Jerusalem artichoke. The classification result of marginal land is shown in **Figure 4D**, which indicates that the areas suitable for Jerusalem artichoke are mainly in northern and southern parts of Shaanxi Province.

The results of the statistics in **Figure 4C** are shown in **Table 2**. The results show that the suitable area of shrubland, sparse forest land, dense grassland, moderately dense grassland, sparsely dense grassland, saline land, and bare land are 1.06×10^{10} m^2, 9.94×10^9 m^2, 1.46×10^{10} m^2, 4.00×10^{10} m^2, 1.26×10^{10} m^2, 1.37×10^8 m^2, and 1.51×10^8 m^2, respectively. Accounting for 99.7% of the total appropriate area in the southern (Hanzhong, Ankang, and Shangluo) and northern (Yan'an and Yulin) regions of Shaanxi Province, shrubland, sparse forest land, and dense, sparsely dense, and moderately dense grasslands are best for cultivating Jerusalem artichokes.

The results of the statistics in **Figure 4D** indicated that incompetent, moderate potential, good potential, and high potential areas for growing Jerusalem artichoke are approximately 1.89×10^{10} m^2, 6.29×10^{10} m^2, 2.19×10^{10} m^2, and 3.19×10^{10} m^2, respectively (**Table 3**). The total suitable area (moderate potential, good potential, and high potential) for growing Jerusalem artichoke in Shaanxi Province is approximately 8.81×10^{10} m^2, with the southern (Hanzhong, Ankang, and Shangluo) and northern (Yan'an and Yulin) regions accounting for 42.8% of the total area of Shaanxi Province.

4 DISCUSSION

4.1 Reliability of the Model

Studies have shown that soil, topography, and solar radiation are also important factors affecting the growth of Jerusalem artichoke (Zorić et al., 2016). Unlike previous studies that were limited to the effects of climatic factors on species distribution (Zhang et al., 2020; Tarnian et al., 2021), this study considered the effects of soil

TABLE 3 | Statistical results of classification of marginal lands suitable for planting Jerusalem artichoke in Shaanxi Province with the unit 1.00×10^8 m^2.

		Marginal land				Total of suitable area	Non-marginal land	Total	
		Unsuitable	Suitable area						
			Moderate	Good	High				
Guanzhong plain	Xi'an	8.69	12.91	5.98	5.11	24.00	67.13	99.82	523.50
	Baoji	42.99	38.10	4.76	0.46	43.32	102.78	189.09	
	Xianyang	8.21	15.57	4.45	0.47	20.49	76.03	104.74	
	Weinan	7.00	14.77	6.24	2.23	23.24	99.61	129.85	
Southern Shaanxi	Hanzhong	33.84	93.90	30.46	1.69	126.04	115.91	275.79	695.75
	Ankang	6.27	78.81	43.77	9.90	132.48	87.82	226.57	
	Shangluo	4.75	57.20	41.16	11.59	109.95	78.69	193.38	
Northern Shaanxi	Tongchuan	5.96	13.58	1.30	0.00	14.89	18.07	38.92	837.40
	Yan'an	53.82	167.98	25.86	0.10	193.94	121.20	368.96	
	Yulin	17.38	136.42	55.45	0.36	192.23	219.92	429.53	
Total		188.92	629.24	219.44	31.89	880.57	987.17	2056.65	

depth, topography, land use, and solar radiation on the distribution of Jerusalem artichoke. This multifactorial pattern explained and predicted species distribution better than a temperature-based pattern, and it was more in line with plant growth needs.

Furthermore, the preliminary Maxent model (**Supplementary Appendix A**) revealed that not all environmental variables substantially impact Jerusalem artichoke growth. A previous research has shown that modeling with strongly correlated variables might give unexpected results (Sillero and Barbosa, 2020). Moreover, compared with the multifactor-integrated assessment method, the Maxent model can obtain the contribution of environmental factors for species and respond to the impact of each environmental factor on the species. To improve the calculation efficiency of the model, this study screened 15 environmental variables that have a significant effect on the distribution of Jerusalem artichoke in combination with the percent contribution of the preliminary Maxent model, and then selected nine important environmental factors by Pearson's correlation analysis, excluding covariance among environmental variables. Then to make the model more resilient, the mean results from running the Maxent model 10 times are used, and each model has good accuracy.

Meanwhile, the distribution of Jerusalem artichoke in this study is consistent with previous research (Xu et al., 2013). The total area suitable for the growth of Jerusalem artichoke in this study is approximately 8.81×10^{10} m^2, which is less than 11.0×10^{10} m^2 given in Liu's study (Liu, 2011) owing to differences in research methods, environmental factors selection, classification criteria, and land use data. The results of the model, as stated previously, are credible.

4.2 Argumentation of the Response Results of Environmental Variables

Because of differences in evaluation methods, the jackknife and percent contribution results had minor differences in terms of variable orders. Still, the variables that significantly affected the Jerusalem artichoke were consistent, confirming that SLP and DPT were the main environmental variables affecting the distribution of Jerusalem artichoke. They were also compatible with the percent contribution of the preliminary model (**Supplementary Appendix A**). These findings revealed that topography and soil conditions were the most relevant variables for the Jerusalem artichoke species being modeled.

Furthermore, Jerusalem artichoke is a long day plant that requires a short photoperiod to flower, grows best at 18–26°C (Zhuang et al., 2011), needs abundant rainfall (>0.15 m) (Swanton et al., 1992), and it can survive in both flat and mountainous areas (Wang et al., 2019). The results of this study are compatible with these conditions. Moreover, the findings demonstrated that seasonality significantly impacted Jerusalem artichoke growth, consistent with earlier studies (Zorić et al., 2016; Krivorotova and Sereikaite, 2018).

4.3 Practical Implications of the Study

According to studies, Jerusalem artichoke has a huge potential for energy plant development in the arid and semi-arid areas in the western part of China (Liu et al., 2011). Simultaneously, the development and utilization of Jerusalem artichoke are of great practical significance to assist rural communities in overcoming poverty (Nie et al., 2022). According to the investigation, most marginal land areas are underutilized, and large-scale rational planting has yet to be realized. Jerusalem artichoke only grows sporadically on roadsides and wastelands in some regions. Thus, this study selected the Jerusalem artichoke as an energy plant and researched its potential on marginal lands that can guide the rational planting of Jerusalem artichoke, which is in line with the practical requirements.

Furthermore, the area suited for Jerusalem artichoke differed from **Figure 4A**, owing to the perfect environmental conditions for cultivating Jerusalem artichoke in Xi'an, Baoji, Xianyang, and Weinan. As shown in **Figure 4D**, the marginal land ideal for the growth of Jerusalem artichoke in Guanzhong only accounted for

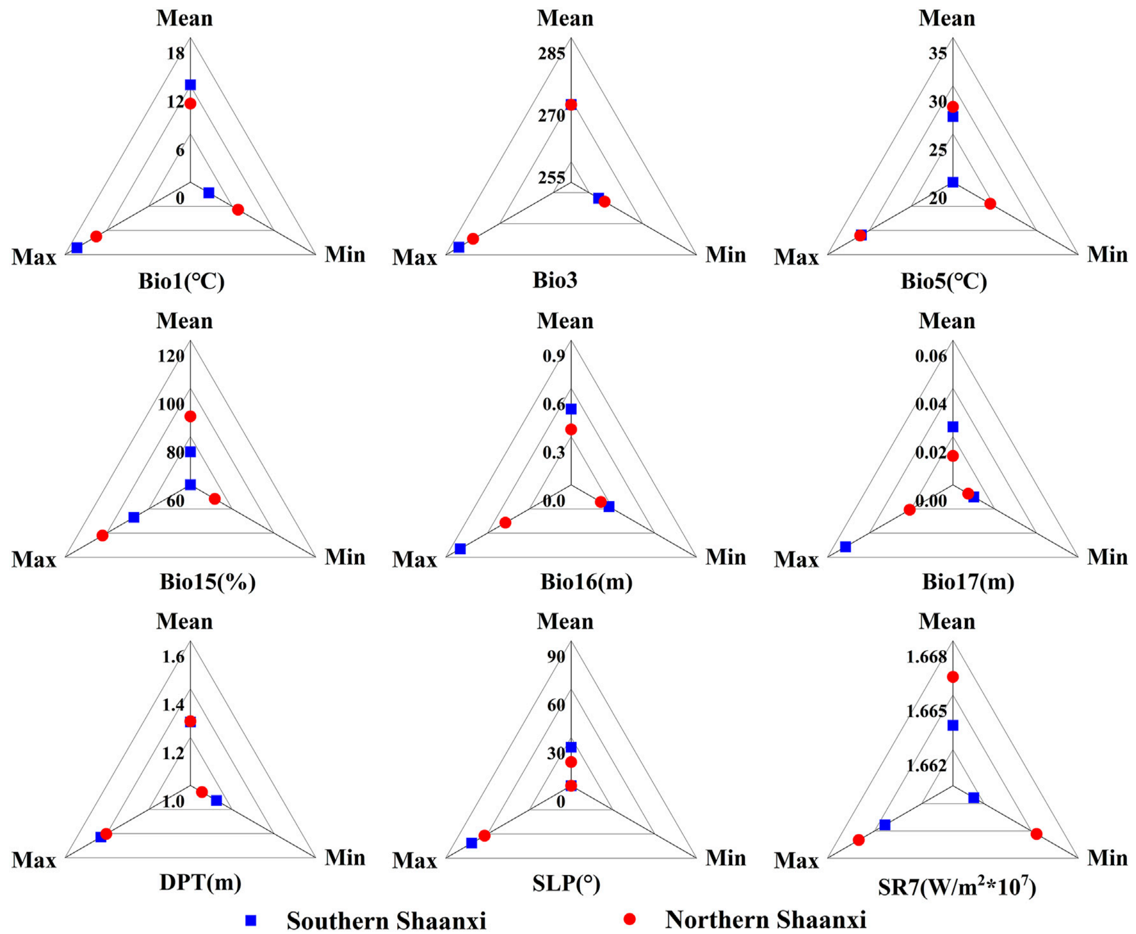

FIGURE 5 | Mean, maximum and minimum values of 9 significant environment variables in Southern and Northern Shaanxi.

5.40% of Shaanxi Province, indicating that industrialization and urbanization significantly impact the distribution of Jerusalem artichoke species. Furthermore, when the Guanzhong Plain (Xi'an, Baoji, Xianyang, and Weinan) was excluded, the results in **Figure 4D** showed that the area suitable for planting Jerusalem artichoke in Northern Shaanxi was greater than that in Southern Shaanxi. But, the good potential and high potential locations more ideal for producing Jerusalem artichoke in Northern Shaanxi were less than those in Southern Shaanxi. The differences between Southern and Northern Shaanxi in terms of nine environmental variables are shown in **Figure 5**, and this result shows significant differences between Southern and Northern Shaanxi at Bio1, Bio15, Bio16, Bio17, and SR7. Thus, these environmental variables make Southern Shaanxi more suitable for planting Jerusalem artichoke than Northern Shaanxi in terms of quality. It can be seen that temperature, precipitation, and solar radiation are important factors affecting the classification of Jerusalem artichoke suitability. Thus, this study's findings have greater practical implications and can guide smart Jerusalem artichoke planning.

5 CONCLUSION

This study used the Maxent model and ArcGIS tool to predict the distribution of Jerusalem artichoke on the marginal land in Shaanxi Province. Not only was the potential distribution of Jerusalem artichoke determined but also the main influencing factors and regional differences affecting the distribution of Jerusalem artichoke in Shaanxi Province were also discussed. Finally, the marginal land resource potential and habitat suitability classification for planting Jerusalem artichoke were evaluated:

a) The significant environmental variables affecting Jerusalem artichoke were SLP, DPT, Bio5, Bio1, Bio16, SR7, Bio15, Bio17, and Bio3. The suitable ranges of these environmental variables were 0–5°C, 1.50–1.60 m, 30–31°C, 16.5–18.0°C, 0.01–0.02 m, 1.66–1.67 × 10^7 W/m^2, 50–60%, 0–0.005 m, and 265–275, respectively. Additionally, the percent contribution and the jackknife test results showed that SLP and DPT were the strongest predictors affecting the distribution of Jerusalem artichoke species. In other words, the variables of topography and soil conditions have the most critical impact on species distribution.

(b) Shrubland, sparse forest land, dense grassland, moderately dense grassland, and sparsely dense grassland were the peripheral land use types more favorable for growing Jerusalem artichoke, accounting for 99.7% of the total suitable area for growing Jerusalem artichoke. Among them, moderately dense grassland was the dominant land use type for the growth of Jerusalem artichoke.

(c) The total area of Shaanxi Province suitable for cultivating Jerusalem artichoke was roughly 8.81×10^{10} m^2, accounting for 42.7% of the total area of Shaanxi Province. The area suitable for planting Jerusalem artichoke in Northern Shaanxi was more than Southern Shaanxi in terms of quantity. But, Hanzhong, Ankang, Shangluo, Yan'an, and Yulin areas of Southern Shaanxi were ideal for planting Jerusalem artichoke than Northern Shaanxi in terms of quality.

DATA AVAILABILITY STATEMENT

The raw data supporting the conclusion of this article will be made available by the authors, without undue reservation.

AUTHOR CONTRIBUTIONS

FY contributed to conceptualization. DZ, TA, and LY helped with data curation. FY and DZ performed formal analysis. DZ, ZY, and LY assisted with investigation. DZ and FY framed the methodology. FY contributed to project administration. DZ, FY, and LY helped with resources. DZ assisted with software. FY contributed to supervision. DZ assisted with writing—original draft. TA and FY helped with writing—review and editing.

FUNDING

The research was funded by the National Natural Science Foundation of China (42071258), Fund Project of Shaanxi Key Laboratory of Land Consolidation (2018-ZY04), and the Special Fund for Basic Scientific Research of Central Colleges (Nos. 300102270204, 300102278303, and 300102280401), Chang'an University, China.

SUPPLEMENTARY MATERIAL

The Supplementary Material for this article can be found online at: https://www.frontiersin.org/articles/10.3389/fenvs.2022.837947/full#supplementary-material

REFERENCES

Bauer, N., Klein, D., Humpenöder, F., Kriegler, E., Luderer, G., Popp, A., et al. (2020). Bio-energy and CO2 Emission Reductions: an Integrated Land-Use and Energy Sector Perspective. *Climatic Change* 163 (3), 1675–1693. doi:10.1007/s10584-020-02895-z

Bogucka, B., and Jankowski, K. (2020). Jerusalem Artichoke: Quality Response to Potassium Fertilization and Irrigation in Poland. *Agronomy* 10 (10), 1518. doi:10.3390/agronomy10101518

Bogucka, B., Pszczółkowska, A., Okorski, A., and Jankowski, K. (2021). The Effects of Potassium Fertilization and Irrigation on the Yield and Health Status of Jerusalem Artichoke (Helianthus Tuberosus L.). *Agronomy* 11 (2), 234. doi:10.3390/agronomy11020234

Cao, B., Bai, C., Zhang, M., Lu, Y., Gao, P., Yang, J., et al. (2022). Future Landscape of Renewable Fuel Resources: Current and Future Conservation and Utilization of Main Biofuel Crops in China. *Sci. Total Environ.* 806, 150946. doi:10.1016/j.scitotenv.2021.150946

Charrua, A. B., Bandeira, S. O., Catarino, S., Cabral, P., and Romeiras, M. M. (2020). Assessment of the Vulnerability of Coastal Mangrove Ecosystems in Mozambique. *Ocean Coastal Manag.* 189, 105145. doi:10.1016/j.ocecoaman.2020.105145

Council, S. (2018). The State Council Issued a Notice on the Three-Year Action Plan to Win the Blue Sky Defense War, Issued by the State Council. Available at: http://www.gov.cn/zhengce/content/2018-07/03/content_5303158.htm (Accessed October 3, 2021).

Cullen, R. (2017). Evaluating Renewable Energy Policies. *Aust. J. Agric. Resour. Econ.* 61 (1), 1–18. doi:10.1111/1467-8489.12175

Epie, K. E., Santanen, A., Makela, P. S. A., and Stoddard, F. L. (2018). Fertilizer and Intercropped Legumes as Nitrogen Source for Jerusalem Artichoke (Helianthus Tuberosus L.) Tops for Bioenergy. *Agric. Food Sci.* 27 (3), 199–205. doi:10.23986/afsci.70110

Foster, G. (2019). Low-Carbon Futures for Bioethylene in the United States. *Energies* 12 (10), 1958. doi:10.3390/en12101958

Fukuda, S., De Baets, B., Waegeman, W., Verwaeren, J., and Mouton, A. M. (2013). Habitat Prediction and Knowledge Extraction for Spawning European grayling (*Thymallus thymallus* L.) Using a Broad Range of Species Distribution Models. *Environ. Model. Softw.* 47 (-), 1–6. doi:10.1016/j.envsoft.2013.04.005

Ghareghan, F., Ghanbarian, G., Pourghasemi, H. R., and Safaeian, R. (2020). Prediction of Habitat Suitability of Morina Persica L. Species Using Artificial Intelligence Techniques. *Ecol. Indicators* 112, 106096. doi:10.1016/j.ecolind.2020.106096

Jhariya, M., Banerjee, A., Meena, R., Kumar, S., and Raj, A. (2021c). *Sustainable Intensification for Agroecosystem Services and Management*. Springer Nature Singapore.

Jhariya, M., Banerjee, A., Meena, R., and Yadav, D. (2019). *Sustainable Agriculture, Forest and Environmental Management*. Springer Nature Singapore.

Jhariya, M., Meena, R., and Banerjee, A. (2021a). *Ecological Intensification of Natural Resources for Sustainable Agriculture*. Springer Nature Singapore.

Jiang, D., Wang, Q., Ding, F., Fu, J., and Hao, M. (2019). Potential Marginal Land Resources of Cassava Worldwide: A Data-Driven Analysis. *Renew. Sust. Energ. Rev.* 104 (APR), 167–173. doi:10.1016/j.rser.2019.01.024

Jiang, W., Jacobson, M. G., and Langholtz, M. H. (2018). A Sustainability Framework for Assessing Studies about Marginal Lands for Planting Perennial Energy Crops. *Biofuels, Bioprod. Bioref.* 13 (1), 228–240. doi:10.1002/bbb.1948

Jones, M. B., Finnan, J., and Hodkinson, T. R. (2015). Morphological and Physiological Traits for Higher Biomass Production in Perennial Rhizomatous Grasses Grown on Marginal Land. *GCB Bioenergy* 7 (2), 375–385. doi:10.1111/gcbb.12203

Krivorotova, T., and Sereikaite, J. (2018). Correlation between Fructan Exohydrolase Activity and the Quality of Helianthus Tuberosus L. Tubers. *Agronomy* 8 (9), 184. doi:10.3390/agronomy8090184

Kumar, P. (2012). Assessment of Impact of Climate Change on Rhododendrons in Sikkim Himalayas Using Maxent Modelling: Limitations and Challenges. *Biodivers Conserv* 21 (5), 1251–1266. doi:10.1007/s10531-012-0279-1

Liu, L. (2011). *The Potential and Impacts of Biofuel Development for the Five Provinces in Southwest China*. Beijing: dissertation, University of Chinese Academy of Sciences.

Leppäkoski, L., Marttila, M. P., Uusitalo, V., Levänen, J., Halonen, V., and Mikkilä, M. H. (2021). Assessing the Carbon Footprint of Biochar from Willow Grown on Marginal Lands in Finland. *Sustainability* 13 (18), 10097. doi:10.3390/su131810097

Li, J., Fan, G., and He, Y. (2020a). Predicting the Current and Future Distribution of Three Coptis Herbs in China under Climate Change Conditions, Using the MaxEnt Model and Chemical Analysis. *Sci. Total Environ.* 698, 134141. doi:10.1016/j.scitotenv.2019.134141

Li, X., Cen, N., Liu, L., Chen, Y., Yang, X., Yu, K., et al. (2020b). Collagen Peptide Provides *Saccharomyces cerevisiae* with Robust Stress Tolerance for Enhanced Bioethanol Production. *ACS Appl. Mater. Inter.* 12 (48), 53879–53890. doi:10.1021/acsami.0c18919

Li, Y., Shao, W., and Jiang, J. (2021). Predicting the Potential Global Distribution of Sapindus Mukorossi under Climate Change Based on MaxEnt Modelling. *Environ. Sci. Pollut. Res.* 18. doi:10.1007/s11356-021-17294-9

Liu, Z., Han, L., Yosef, S., and Guang, h. (2011). Genetic Variation and Yield Performance of Jerusalem Artichoke Germplasm Collected in China. *Agricultural Sciences in China*. doi:10.1016/s1671-2927(11)60049-7

Liu, Z. X., Steinberger, Y., Chen, X., Wang, J. S., and Xie, G. H. (2015). Chemical Composition and Potential Ethanol Yield of Jerusalem Artichoke in a Semi-arid Region of China. *Ital. J. Agron.* 10 (1), 34. doi:10.4081/ija.2015.603

Long, X., Shao, H., Liu, L., Liu, L., and Liu, Z. (2016). Jerusalem Artichoke: A Sustainable Biomass Feedstock for Biorefinery. *Renew. Sust. Energ. Rev.* 54, 1382–1388. doi:10.1016/j.rser.2015.10.063

Maddalwar, S., Kumar Nayak, K., Kumar, M., and Singh, L. (2021). Plant Microbial Fuel Cell: Opportunities, Challenges, and Prospects. *Bioresour. Tech.* 341, 125772. doi:10.1016/j.biortech.2021.125772

Mehmood, M. A., Ahmad, M. S., Liu, Q., Liu, C.-G., Tahir, M. H., Aloqbi, A. A., et al. (2019). Helianthus Tuberosus as a Promising Feedstock for Bioenergy and Chemicals Appraised through Pyrolysis, Kinetics, and TG-FTIR-MS Based Study. *Energ. Convers. Manag.* 194, 37–45. doi:10.1016/j.enconman.2019.04.076

Merow, C., Smith, M. J., and Silander, J. A. (2013). A Practical Guide to MaxEnt for Modeling Species' Distributions: what it Does, and Why Inputs and Settings Matter. *Ecography* 36 (10), 1058–1069. doi:10.1111/j.1600-0587.2013.07872.x

Mi, Z., Meng, J., Guan, D., Shan, Y., Song, M., Wei, Y.-M., et al. (2017). Chinese CO2 Emission Flows Have Reversed since the Global Financial Crisis. *Nat. Commun.* 8, 10. doi:10.1038/s41467-017-01820-w

Miguel, B. A., Pearson, Richard. G., Thuiller, Wilfried., and Erhard, Markus. (2005). Validation of Species-Climate Impact Models under Climate Change. *Glob. Change Biol.* 11 (9). doi:10.1111/j.1365-2486.2005.001000.x

Nie, Y., Li, J., Wang, C., Huang, G., Fu, J., Chang, S., et al. (2022). A fine-resolution Estimation of the Biomass Resource Potential across China from 2020 to 2100. *Resour. Conservation Recycling* 176, 105944. doi:10.1016/j.resconrec.2021.105944

Paul, S., Bhagobaty, R. K., Nihalani, M. C., and Joshi, S. R. (2020). Characterization of Oleaginous Endophytic Fungi of Biodiesel Plants as Potential Biofuel Minifactories. *Biomass and Bioenergy* 142, 105750. doi:10.1016/j.biombioe.2020.105750

Phillips, S. J. (2017). A Brief Tutorial on Maxent. Available at: http://biodiversityinformatics.amnh.org/open_source/maxent/(Accessed October 5, 2021).

Phillips, S. J., Dudík and Schapire, R. E. (2004). *A Maximum Entropy Approach to Species Distribution Modeling*, Proceedings of the twenty-first international conference on Machine learning, Banff, Alberta, July 4–8, 2004. Machine learning. doi:10.1145/1015330.1015412

Phillips, S. J., Anderson, R. P., and Schapire, R. E. (2006). Maximum Entropy Modeling of Species Geographic Distributions. *Ecol. Model.* 190 (3-4), 231–259. doi:10.1016/j.ecolmodel.2005.03.026

Qaseem, M. F., and Wu, A.-M. (2020). Marginal Lands for Bioenergy in China; an Outlook in Status, Potential and Management. *GCB Bioenergy* 13 (1), 21–44. doi:10.1111/gcbb.12770

Qaseem, M. F., and Wu, A.-M. (2021). Marginal Lands for Bioenergy in China; an Outlook in Status, Potential and Management. *GCB Bioenergy* 13 (1), 21–44. doi:10.1111/gcbb.12770

Richards, B. K., Stoof, C. R., Cary, I. J., and Woodbury, P. B. (2014). Reporting on Marginal Lands for Bioenergy Feedstock Production: a Modest Proposal. *Bioenerg. Res.* 7 (3), 1060–1062. doi:10.1007/s12155-014-9408-x

Shi, H., Chai, J., Lu, Q., Zheng, J., and Wang, S. (2022). The Impact of China's Low-Carbon Transition on Economy, Society and Energy in 2030 Based on CO2 Emissions Drivers. *Energy* 239, 122336. doi:10.1016/j.energy.2021.122336

Shortall, O. K. (2013). "Marginal Land" for Energy Crops: Exploring Definitions and Embedded Assumptions. *Energy Policy* 62, 19–27. doi:10.1016/j.enpol.2013.07.048

Sillero, N., and Barbosa, A. M. (2020). Common Mistakes in Ecological Niche Models. *Int. J. Geographical Inf. Sci.* 35 (2), 213–226. doi:10.1080/13658816.2020.1798968

Swanton, C. J., Clements, D. R., Moore, M. J., and Cavers, P. B. (1992). The Biology of Canadian Weeds. 101. Helianthus Tuberosus L. *Can. J. Plant Sci.* 72 (72), 1367–1382.

Tarnian, F., Kumar, S., Azarnivand, H., Chahouki, M. A. Z., and Mossivand, A. M. (2021). Assessing the Effects of Climate Change on the Distribution of Daphne Mucronata in Iran. *Environ. Monit. Assess.* 193 (9), 1–19. doi:10.1007/s10661-021-09311-8

Wang, L., Sun, X., Tan, L., and Yi, L. I. (2019). Study on Accumulation and Dynamic Changes of Three Carbohydrates in Jerusalem Artichoke in Natural Habitats. *Agricultutural Blotechnology* 8 (3), 7.

Wen, J., Song, J., Xie, C., Zhang, Q., Zeng, F., and Zhang, Y. (2016). Identification of Potential Distribution Areas for Energy Plant Jatropha Curcas L. Using the Maxent Entropy Model. *Plant Sci. J.* 34 (6), 849–856.

Xu, X., Li, S., Fu, Y., and Zhuang, D. (2013). An Analysis of the Geographic Distribution of Energy Crops and Their Potential for Bioenergy Production. *Biomass and Bioenergy* 59, 325–335. doi:10.1016/j.biombioe.2013.08.036

Xu, X., Liu, J., Zhang, S., Li, R., Yan, C., and Wu, S. (2018). *China Multi-Period Land Use Land Cover Remote Sensing Monitoring Data Set(CNLUCC)*. Beijing: Data Registration and Publishing System of the Resource and Environmental Science Data Center of the Chinese Academy of Sciences. [DB/OL].

Xue, S., Guo, M., Iqbal, Y., Liao, J., Yang, S., Xiao, L., et al. (2020). Mapping Current Distribution and Genetic Diversity of the Native Miscanthus Lutarioriparius across China. *Renew. Sust. Energ. Rev.* 134, 110386. doi:10.1016/j.rser.2020.110386

Xue, S., Lewandowski, I., Wang, X., and Yi, Z. (2016). Assessment of the Production Potentials of Miscanthus on Marginal Land in China. *Renew. Sust. Energ. Rev.* 54, 932–943. doi:10.1016/j.rser.2015.10.040

Yang, X., Kushwaha, S. P. S., Saran, S., Xu, J., and Roy, P. S. (2013). Maxent Modeling for Predicting the Potential Distribution of Medicinal Plant, Justicia Adhatoda L. In Lesser Himalayan Foothills. *Ecol. Eng.* 51, 83–87. doi:10.1016/j.ecoleng.2012.12.004

Yi, Y. J., Cheng, X., Yang, Z. F., and Zhang, S. H. (2016). Maxent Modeling for Predicting the Potential Distribution of Endangered Medicinal Plant (*H. riparia* Lour) in Yunnan, China. *Ecol. Eng.* 92, 260–269. doi:10.1016/j.ecoleng.2016.04.010

Yin, F., Yang, X., Wang, H., Liu, L., Meng, X., and Li, S. (2018). Evaluation of the Potential Land for Biofuel Plant Development in the Shaanxi Province, China. *Geol. J.* 53, 332–341. doi:10.1002/gj.3120

Zhang, B., Yang, J., and Cao, Y. (2021a). Assessing Potential Bioenergy Production on Urban Marginal Land in 20 Major Cities of China by the Use of Multi-View High-Resolution Remote Sensing Data. *Sustainability* 13 (13), 7291. doi:10.3390/su13137291

Zhang, J. M., Song, M. L., Li, Z. J., Peng, X. Y., Su, S., Li, B., et al. (2021b). Effects of Climate Change on the Distribution of Akebia Quinata. *Front. Ecol. Evol.* 9, 11. doi:10.3389/fevo.2021.752682

Zhang, K., Zhang, Y., Jia, D., and Tao, J. (2020). Species Distribution Modeling of Sassafras Tzumu and Implications for Forest Management. *Sustainability* 12 (10), 4132. doi:10.3390/su12104132

Zhang, L., Jing, Z., Li, Z., Liu, Y., and Fang, S. (2019). Predictive Modeling of Suitable Habitats for Cinnamomum Camphora (L.) Presl Using Maxent Model under Climate Change in China. *Ijerph* 16 (17), 3185. doi:10.3390/ijerph16173185

Zhao, X., and Liu, P. (2014). Focus on Bioenergy Industry Development and Energy Security in China. *Renew. Sust. Energ. Rev.* 32, 302–312. doi:10.1016/j.rser.2014.01.011

Zhuang, D., Jiang, D., Liu, L., and Huang, Y. (2011). Assessment of Bioenergy Potential on Marginal Land in China. *Renew. Sust. Energ. Rev.* 15 (2), 1050–1056. doi:10.1016/j.rser.2010.11.041

Zorić, M., Terzić, S., Sikora, V., Brdar-Jokanović, M., and Vassilev, D. (2016). Effect of Environmental Variables on Performance of Jerusalem Artichoke (Helianthus Tuberosus L.) Cultivars in a Long Term Trial: a Statistical Approach. *Euphytica* 213 (1). doi:10.1007/s10681-016-1819-7

Conflict of Interest: The authors declare that the research was conducted in the absence of any commercial or financial relationships that could be construed as a potential conflict of interest.

Publisher's Note: All claims expressed in this article are solely those of the authors and do not necessarily represent those of their affiliated organizations, or those of the publisher, the editors, and the reviewers. Any product that may be evaluated in this article, or claim that may be made by its manufacturer, is not guaranteed or endorsed by the publisher.

frontiers | Frontiers in Environmental Science

ORIGINAL RESEARCH
published: 10 May 2022
doi: 10.3389/fenvs.2022.905471

Carbon Emission Peak Paths Under Different Scenarios Based on the LEAP Model—A Case Study of Suzhou, China

Wenjie Sun[1†], Yi Zhao[1†], Zeng Li[2,3]*, Yitong Yin[1] and Chenglong Cao[1]

[1]College of Geoscience and Surveying Engineering, China University of Mining and Technology, Beijing, China, [2]Key Laboratory of City Cluster Environmental Safety and Green Development, Ministry of Education, Institute of Environmental and Ecological Engineering, Guangdong University of Technology, Guangzhou, China, [3]State Key Laboratory of Resources and Environmental Information System, Institute of Geographical Sciences and Natural Resources Research, Beijing, China

OPEN ACCESS

Edited by:
Jingying Fu,
Institute of Geographic Sciences and Natural Resources Research (CAS), China

Reviewed by:
Xun Zhang,
Beijing Technology and Business University, China
Yonghui Huang,
China University of Petroleum, China

***Correspondence:**
Zeng Li
lizeng4000423@gdut.edu.cn

†These authors have contributed equally to this work

Specialty section:
This article was submitted to Environmental Economics and Management, a section of the journal Frontiers in Environmental Science

Received: 27 March 2022
Accepted: 27 April 2022
Published: 10 May 2022

Citation:
Sun W, Zhao Y, Li Z, Yin Y and Cao C (2022) Carbon Emission Peak Paths Under Different Scenarios Based on the LEAP Model—A Case Study of Suzhou, China.
Front. Environ. Sci. 10:905471.
doi: 10.3389/fenvs.2022.905471

Environmental pollution caused by energy consumption is a global problem. Optimization of the energy system will contribute to the sustainable development of city, especially of the industrial cities. Based on the Long-term Energy Alternative Planning System (LEAP) model, the LEAP-Suzhou model was established to explore the energy system optimization and emission reduction path of Suzhou to 2050. By accounting for current energy consumption and carbon emissions, the baseline scenario (BAU) was established. According to the different methods and intensities of energy transformation, an industrial structure optimization scenario (ISO), an energy structure optimization scenario (ESO), and an energy transformation optimization scenario (ETD) were created. Combined with the energy flow diagram, the energy structure and the direction of optimization were analyzed. The results showed that the baseline scenario will consume 259.954 million tons of standard coal by 2050, and the carbon emission will be 677.6 Mt. Compared with BAU, the ISO, ESO, and ETD scenarios will reduce energy consumption by 37.9%, 37.4%, and 74.8%, respectively, by 2050. ETD had the best carbon dioxide reduction, followed by ESO, and finally ISO. Among them, the carbon emission of ETD will reach its peak around 2030 and decrease to 73.8 Mt in 2050, resulting in the best emission reduction effect. This scenario is the best path for Suzhou to achieve the goal of "carbon peak and neutrality" and sustainable development. The LEAP-Suzhou model successfully explores the low carbon path of Suzhou, provides policy guidance for the optimization of energy transition and carbon neutrality of industrial cities, In the future, the energy structure should be further optimized in Suzhou, and advanced energy technologies should be introduced to improve energy efficiency, especially for the power generation sector, and the proportion of clean energy such as gas should be further expanded.

Keywords: energy planning, industrial city, LEAP model, carbon emission, scenario analysis

1 INTRODUCTION

Controlling carbon dioxide is the key to coping with climate change and reducing greenhouse gas emissions (Watts et al., 2015; Le et al., 2018). To this end, nearly 200 parties to the United Nations Framework Convention on Climate Change signed the Paris Agreement on Climate Change in 2015. The agreement, which harmonizes global action on climate change after 2020, sets a goal of achieving net zero emissions in the second half of the century. In order to implement the Paris Agreement (Liu et al., 2016), China included climate change targets in the outline of its 14th Five-Year Plan in 2020 (Chai et al., 2020). In September of the same year, the United Nations General Assembly pledged again to "strive for carbon peak by 2030 and carbon neutral by 2060" (Liu, 2021a). In addition, the roadmap for China's carbon peak and carbon neutral work was laid out after this assembly, which included accelerating the low-carbon and clean transformation of the energy system as an important step (Chu and Majumdar, 2012; He, 2014; Liu et al., 2022).

As we know, the consumption of fossil energy is only one factor causing greenhouse gas emissions such as carbon dioxide and affecting climate change and regional environmental quality (Li N. et al., 2021; Ponce and Khan, 2021). Urban areas account for only about 3% of the earth's land mass but consume more than 70% of global energy and contribute 75% of the global carbon emissions (Wu, 2019). Fossil energy consumption in Chinese cities accounts for 85% of the country's total energy consumption, and coal remained the most consumed among them at about 57.7% in 2020 (Zhang, 2021). Especially in industrial cities, economic development is mainly supported by industrial production, and fossil energy runs through the industrial chain of the entire city (Yang, 2021), consuming a lot of energy (Wang S. H. et al., 2021). As a result, typical energy balance and ecological pollution problems arise, resulting in the yearly increase in urban carbon emissions. Industrial cities are big energy consumers and carbon emission producers. Optimizing their energy systems is the key to exploring the path of energy innovation and emission reduction at the urban scale, and this plays a crucial role in the national and global response to climate change and carbon emission reduction (Liu et al., 2015). At present, countries and regions in the world are actively seeking effective ways of energy reform, and many studies on urban scale energy consumption at home and abroad have investigated the role of multi-factor energy consumption and carbon emissions in regional differences (Wang et al., 2020; Li Q. et al., 2021; Nuta et al., 2021). The input–output method is widely used in energy system research. For example, Xu et al. (2019) used multi-scale input–output analysis (MSIO) to analyze the carbon emissions of Tianjin in 2012 and estimate the carbon emissions caused by imported products. The results showed that carbon emissions in 2012 were 1.67 times those of 2007, and 6% of carbon emissions in 2012 came from imports. Structural decomposition analysis (SDA) is the most commonly used quantitative analysis method of energy consumption at present and is often combined with input–output analysis (IO). For example, based on the top-down IO-SDA model, Wang et al. (2013) analyzed the driving forces of carbon dioxide emission increment in Beijing from 1997 to 2010 from the perspectives of production and end demand. The results showed that the increase in carbon emissions in Beijing is mainly driven by the change in production structure and population growth. Stochastic Impacts by Regression on Population, Affluence, and Technology (STIRPAT) is an extendable stochastic environmental impact assessment model that evaluates the impact of different elements on carbon emissions. Based on the ICE-STIRPAT model, Shao et al. (2011) estimated the industrial carbon dioxide emissions in Shanghai from 1994 to 2009, summarized the characteristics of industrial carbon dioxide emissions, and proved that coal consumption is the largest source of carbon emissions in Shanghai. In addition, the LEAP model covers accounting and forecasting of energy systems, as well as accounting for air pollutants and carbon emissions. Hu et al. (2019) combined sustainable energy planning with economic analysis and took Shenzhen, China, as an example; they defined four scenarios to analyze the future forecast of energy production and consumption from 2015 to 2030 based on LEAP. Their work showed that the policy of energy efficiency improvement and energy structure upgrading in Shenzhen had a significant impact on its energy system.

The above studies on energy planning and carbon emissions at the city level mostly focused on a certain energy sector and lacked a detailed accounting and emission reduction path analysis of the whole energy system. From the perspective of time span, the forecast time was short, which cannot reflect the impact of emission reduction policies over a long period. From the perspective of research, input–output methods and their deformation and the STIRPAT model are often used, which are unable to produce detailed accounting and long-term energy system optimization prediction for the whole energy consumption sector. However, the Long-range Energy Alternatives Planning System (LEAP) is a bottom-up accounting tool for energy consumption and production. This model simulates the energy consumption system and has been widely used in industrial structure, carbon emission reduction, and carbon emission scenario prediction (Wang, 2016; Deng and Li, 2017). The LEAP model can effectively enable energy accounting and prediction from the country to the city and even smaller scales. It can cover whole consumption sectors of the energy system or study specific industry sectors. On a national scale, Nieves et al. (2019) studied energy consumption and GHG emissions in Colombia's multiple industries based on the LEAP model. Two scenarios were set up to demonstrate that energy consumption in Colombia will be concentrated in the transportation sector and carbon emissions will increase significantly in 2050. At the urban scale, Li et al. (2013) used the LEAP model to study the coordinated emission reduction of air pollutants and greenhouse gases in Beijing. The results showed that increasing energy conservation constraints and optimizing energy consumption structures can reduce the generation of pollutants and greenhouse gases under different emission reduction policies. LEAP can also facilitate research into specific industry sectors. Based on the LEAP model Hong et al. (2016) examined the effectiveness of the policies implemented by the South Korean government in the transportation sector and analyzed the ripple effects of the policies to 2050 from the energy and environmental aspects. The emission reduction effect of the transportation sector in this study was predicted by setting five emission scenarios, and policy suggestions were proposed for the transportation sector to achieve national emission reduction targets. In this paper, LEAP model is applied to analyze and study the current status of energy consumption, energy conversion and flow, and the multi-scenario long-term energy planning path of the whole consumption sectors in the city-scale energy system.

Suzhou is a megalopolis with a strong industrial character, and it is a central city in the Yangtze River Delta, playing an important role in the economic development of not only the Yangtze River Delta but the entire country (Liu et al., 2019; Sun et al., 2019; Xie and Sun, 2021). However, Suzhou is an energy-dependent city. Because of its geographical location, the local renewable energy resource endowment is limited, and its energy resource self-sufficiency rate is low. Raw coal and crude oil are required by other cities and provinces, which is significantly different from the energy structure of resource-based cities. Therefore, the structural contradiction of energy has become increasingly prominent (Liu et al., 2021b). Understanding the growth trend of energy consumption in Suzhou is an important path to controlling total energy consumption, reducing energy consumption intensity, and achieving green, low-carbon and sustainable development. In 2016, the "Report on Building Suzhou into a Model City of International Energy Reform and Development" was released, offering a solution for solving energy bottlenecks and other problems. This was China's first construction report in international energy reform and model city development. At present, research on the direction of Suzhou's energy system has made some progress. Wang Y. Z. et al. (2021) proposed a comprehensive evaluation system for industrial city energy transformation based on the interpretive structural model and analytic hierarchy process, analyzed the development process of urban energy transformation in Suzhou from 2013 to 2018, and offered suggestions for the subsequent development of energy transformation in Suzhou. Using the Wuzhong District of Suzhou as an example, Zhu et al. (2020) analyzed its urbanization characteristics from the viewpoints of historical geography, population development, economic industry, and so on, and explored the development path of energy reform under the new urbanization trend from multiple perspectives. Liao and Wu. (2013) analyzed carbon emissions from the energy consumption of industrial enterprises above scale in Suzhou and put forward suggestions for further adjustment of the industrial structure and improvement of energy conservation and emission reduction policies. At present, research on Suzhou's energy system is not comprehensive enough for the Research Department of Energy Transition and Low-carbon Development, which has failed to identify the connection among the various departments of the energy system and to offer an energy system development forecast. This research cannot establish a feasible optimization path for Suzhou energy system.

Thus, the LEAP-Suzhou model was established based on the LEAP model to explore the low-carbon optimization path of Suzhou's energy system, and a systematic and comprehensive accounting was conducted of the energy department and energy types in Suzhou. The high-consumption and high-pollution sectors were confirmed. Combined with the energy flow diagram, the energy flow situation of each department was considered to analyze the energy innovation and emission reduction potential of each department. In addition to the baseline scenario, this paper sets up three scenarios for different optimization methods and emission reduction intensity, so as to clarify the advantages of energy structure optimization on urban carbon emission reduction. A scenario analysis of the factors influencing energy consumption of city-scale was carried out. This paper explores the path of urban energy reform and low-carbon development. It provides guidance for the transformation of Suzhou industrial energy system. This study has important theoretical support for promoting urban low-carbon transformation and achieving carbon neutrality, and has practical significance for the global response to climate change.

2 STUDY AREA

Suzhou is an energy-dependent city, the main features are as follows: The main energy consumption sector is industry, the energy consumption structure is still dominated by coal, and electricity occupies an important position in the total energy. The problems of energy structural are becoming more serious. Coal accounts for a high proportion of energy consumption by enterprises above designated size, while oil and gas and other clean energy sources account for a low proportion. With the continuous and steady development of economy and society, the continuous improvement of people's living standard and the acceleration of urbanization, the energy consumption of construction, transportation and living will increase rapidly. The total energy consumption in Suzhou will keep a rapid growth momentum, which will bring great pressure to energy supply and economic development. Therefore, it is urgent for Suzhou to transform its industrial structure, optimize its energy structure and improve its technological level.

The total energy consumption in Suzhou shows an overall growth trend (**Figure 1**). The period from 2006 to 2011 saw rapid growth. Total energy consumption increased rapidly from 50.10 million tons of standard coal in 2006 to 76.84 million tons in 2011, with an average annual growth rate of 8.93%. The period from 2012 to 2016 was the period of adjustment growth. The total energy consumption in Suzhou increased slowly from 79.58 million tons of standard coal in 2012 to 84.27 million tons in 2016. In terms of energy types, the energy structure of Suzhou is characterized by coal as the main energy type, with natural gas, oil, electricity, and other as complementary types. The proportion of raw coal and coal in Suzhou's total energy consumption in has decreased yearly. In terms of the energy consumption sector, energy consumption in Suzhou is mainly concentrated in industry, which accounted for 80.57% in 2016. Although the industrial energy consumption continued to increase, the proportion of the total amount of the city decreased. The

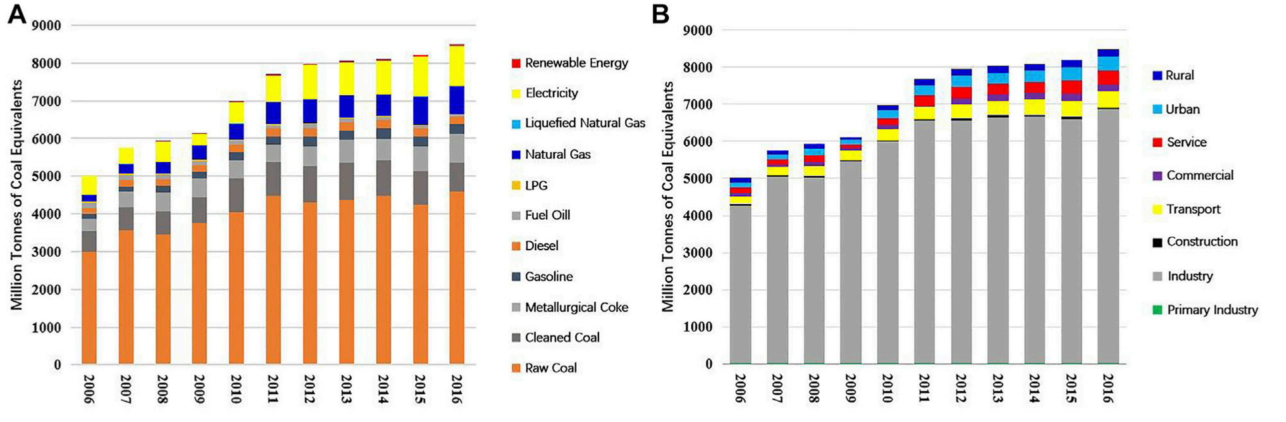

FIGURE 1 | Total energy consumption of **(A)** different energy types in Suzhou and **(B)** energy consumption sectors in Suzhou.

tracked sectors were the resident and transport sectors. Between them, the total resident energy consumption showed a growing trend, rising rapidly from 5.28% in 2006 to 6.76% in 2016. The share of energy consumption in the transportation sector increased from 3.91% in 2006 to 5.22% in 2016.

3 METHODOLOGY AND SCENARIO DEVELOPMENT

3.1 Method

The LEAP model is a static energy economic and environmental model developed by the Stockholm Environment Institute in Sweden. It takes energy demand, cost analysis, and environmental impact as the research objects, predicts the energy demand, economic cost, and environmental impacts of various sectors through a mathematical model, and conducts detailed economic benefit analyses of various energy schemes.

Taking Suzhou as the research object, this paper studied various types of energy consumption at the urban scale and the optimization path according to the pace of social and economic development. The energy demand of each department in Suzhou was analyzed from bottom to top by the energy supply side. Considering the actual energy resource situation in Suzhou under the constraints of the energy consumption revolution and emission reduction policies, different scenarios for adjusting the industrial structure and optimizing the energy structure were devised. At the same time, considering the development trends of various kinds of energy consumption in Suzhou under various scenarios, long-term energy consumption simulations in Suzhou for 2030, 2040, and 2050 were set up in order to achieve the goals of energy conservation, emission reduction, and consumption reduction. The overall framework is shown in **Figure 2**.

Relating to Suzhou's overall situation, the statistical data of GDP, population, urbanization, energy, and electricity were collected. The current environmental carrying capacity and energy consumption of Suzhou were analyzed, and existing characteristics and potential problems in the development were analyzed to lay a foundation for the establishment of the model. The LEAP-Suzhou model was constructed using the bottom-up method, and relevant studies and policy specifications were consulted to determine the sub-links covered by each stage of the energy industry chain. Based on the present situation and development of Suzhou, the structure and main modules of the model were constructed, and Suzhou industry was divided into primary, secondary, and tertiary industry. The demand sector was divided into seven sectors: agriculture, industry, construction, transportation, commercial, services, and residential. The industrial added value and energy consumption of each sector were counted, and energy intensity was calculated. Based on the relevant state policies of Jiangsu Province and Suzhou City, we set up four different scenarios for medium and long-term simulations of energy consumption. Taking 2015 as the base year, we analyzed the respective energy consumption situations of Suzhou in 2030, 2040 and 2050. According to the settings of the different scenarios, Suzhou's energy consumption situation from 2015 to 2050 was obtained. The appropriate scenario was then selected by comparing it with the constraint target. The scenario that was most conducive to the sustainable development of Suzhou was selected by comparing the results of each scenario, and the countermeasures suitable for the transformation of Suzhou's energy system were proposed.

3.2 Key Assumptions and Scenario Setting

3.2.1 Input Key Assumptions

The assessment model of each scenario in LEAP included four modules: setting of key parameters; energy demand module; energy transmission–distribution loss and energy processing–conversion process; and resource module (import and export analysis of primary and secondary energy). In LEAP, key assumptions, including population development scale data, GDP development status data, and urbanization rate, are described at the initial stage (**Table 1**).

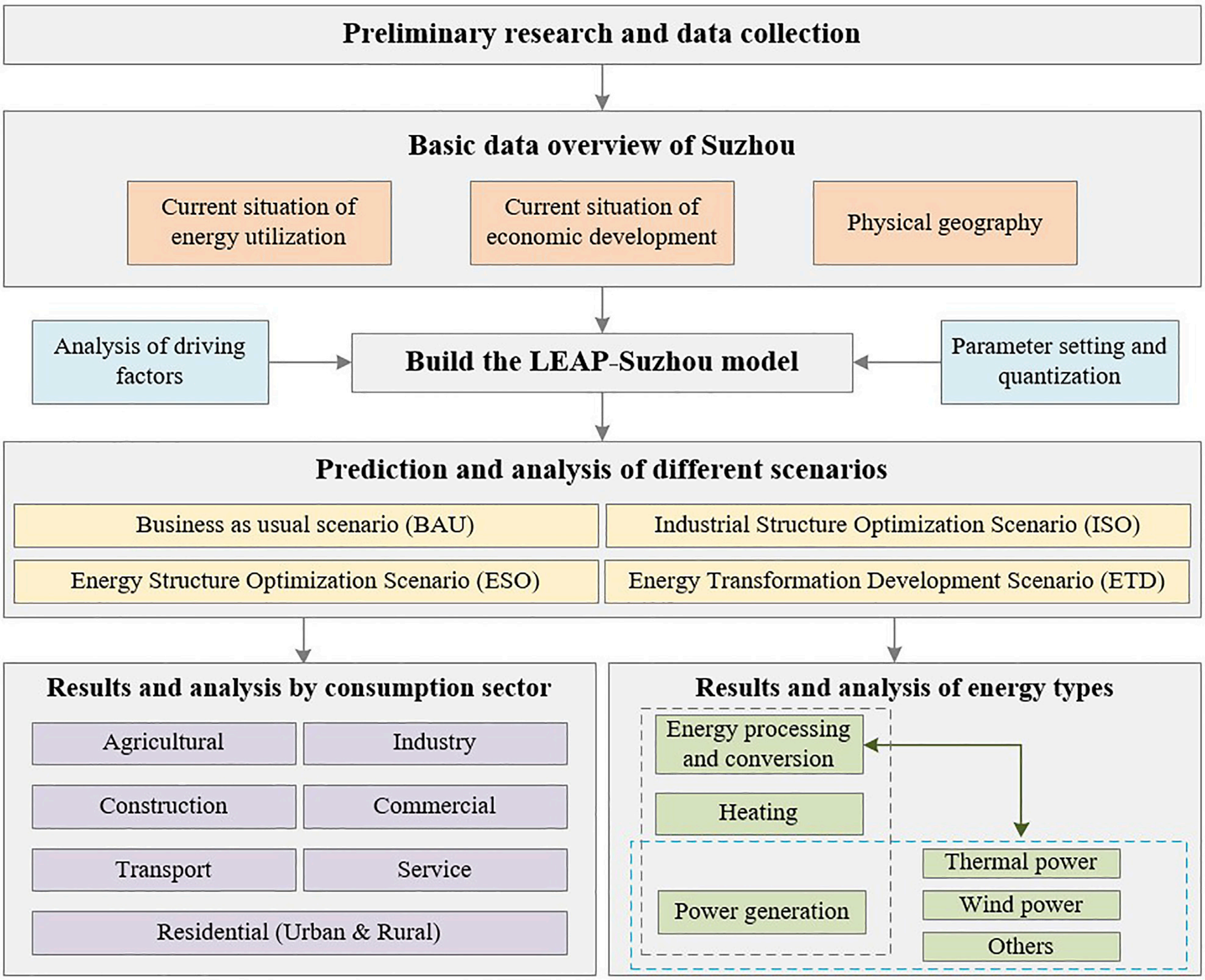

FIGURE 2 | Analysis framework of Energy consumption in Suzhou.

TABLE 1 | Basic assumptions of key macroeconomic indicators.

Key assumption	2015	2017	2020	2030	2040	2050
GDP (billion Yuan)[a]	1,420.41	1,565.96	1795.58	2,896.95	4,267.57	6,019.83
GDP growth rate (%)	—	5.5	5	4.00	3.5	3.5
Urbanization rate (%)[b]	73.59	78.08	80.00	85.00	90.00	95.00
Population (million)[c]	10.60	10.69	10.81	11.19	11.53	11.82
Urban population (million)	7.80	8.35	8.65	9.51	10.38	11.23
Rural population (million)	2.80	2.34	2.16	1.68	1.15	0.59

[a]*GDP was based on the 13th Five-Year Plan of Suzhou, meeting the normal economic development of Suzhou, and at the same time referring to policy planning and GDP development time series trend forecast.*

[b]*Urbanization wad forecast based on the urban planning of Suzhou and the forecast value of the trend development of time series.*

[c]*Population and related data were based on the population size of Suzhou, the natural growth rate and aging rate of Suzhou, through the past forecast of Jiangsu and Suzhou population growth trend.*

3.2.2 Design of Scenarios

This study analyzed the long-term energy consumption of Suzhou under different scenarios based on the LEAP-Suzhou model. There were many factors that needed to be considered in the selection and design of scenarios, such as GDP growth potential, population growth potential, energy technology status, energy policy, and urban development planning of Suzhou. Based on a reasonable conception of the future

TABLE 2 | Main strategies for scenario construction in various scenarios.

Scenario abbreviation	Assumptions	Energy supply	Energy demand
BAU		The industrial structure remains unchanged, and the processing and conversion sector develop according to the energy status in the base year	According to the 13th Five-Year Plan. Maintain the energy consumption structure. Adjust energy intensity
ISO	Adjust industrial structure based on BAU scenario	The conversion efficiency of the conversion department develops according to the energy status of the baseline scenario	The energy consumption structure is the same as the base year. Maintain primary industry, reduce secondary industry and develop tertiary industry
ESO	Adjust the industrial structure based on IOS scenarios	For the power generation and heating module, the proportion of natural gas consumption is increased, and the proportion of thermal power generation is reduced. The installed capacity of biomass, photovoltaic, and wind power is further increased	Based on ISO scenario, energy consumption per unit output value decreased, and energy consumption per unit GDP decreased by more than the provincial requirements. We will continue to increase the share of renewable energy
ETD	Integrate ISO and ESO scenarios to further optimize industrial structure	Increase the proportion of purchased electricity consumption. Further expand the proportion of electricity generated by gas. Focus on promoting the construction of urban and regional cogeneration units. Increase the proportion of clean energy in power generation	Drastically cut down on energy consumption sectors that are high energy consumption and high pollution. Develop energy-saving technologies to improve energy efficiency, increase the use of solar energy and clean coal. Further develop renewable energy sources

development of Suzhou and by setting the above related parameters and quantifying them individually, four future development scenarios of Suzhou were set (**Table 2**). All scenarios, namely, the Business As Usual scenario (BAU), Industrial Structure Optimization Scenario (ISO), Energy Structure Optimization Scenario (ESO), and Energy Transformation Development Scenario (ETD), needed to meet the economic and social development needs of Suzhou (GDP, population and urban development to ensure normal development).

1) Business as usual scenario

This study set the BAU scenario as the basis of the other three scenarios, that is, not interfering with the economic development of Suzhou, meeting the current economic needs and the development objectives of the planning outline. The other three scenarios were based on the BAU scenario, in which the optimization of industrial structure and energy consumption structure and the implementation of low-carbon technologies are carried out. The specific parameters were set as follows: Under the development conditions of the key parameters of population, GDP, and urbanization rate, the industrial structure will remain unchanged during 2021–2050. We used the same power and heat production structure as in the base year. The sectoral energy consumption structure will remain unchanged, and the energy intensity of all energy consumption sectors will be adjusted in accordance with the development requirements of the 13th Five-Year Plan. The reduction of energy intensity per unit GDP will meet provincial requirements, and the energy utilization efficiency and conversion efficiency of thermal power generation, heating and other processing and conversion sectors will be developed in accordance with the energy status in the base year.

TABLE 3 | References for the future development trend of industry proportion.

Energy consumption sector[a]	2015	2020	2030	2040	2050
Primary Industry	0.015	0.013	0.012	0.008	0.006
Secondary Industry	0.486	0.443	0.340	0.304	0.284
Industry	0.921	0.820	0.780	0.700	0.650
Construction	0.079	0.180	0.220	0.300	0.350
Tertiary Industry	0.499	0.544	0.649	0.684	0.709
Transport	0.068	0.180	0.150	0.120	0.080
Commercial	0.353	0.210	0.180	0.120	0.090
Service	0.579	0.610	0.670	0.760	0.830

[a]*The energy consumption sector was classified according to the Industrial Classification of National Economy; the forecast data were devised according to the* Suzhou Statistical Yearbook *and 13th Five-Year Plan.*

2) Industrial structure optimization scenario

Based on the BAU scenario, the energy consumption structure in the ISO scenario will maintain the base year level. Using the same electricity and heat production structure for the base year, the sectoral energy consumption structure will remain unchanged. Energy intensity and energy efficiency in all energy consumption sectors remain the same. The conversion efficiency of thermal power generation, heat supply, and other processing and conversion departments develop according to the baseline scenario energy status. This scenario focuses on developing the tertiary industry and constantly reducing the secondary industry. Industrial structure adjustment parameters are shown in **Table 3**.

3) Energy structure optimization scenario

Based on the ISO scenario, to achieve energy conservation and emission reduction goals, clean coal will be developed through the renewal and transformation of energy with new equipment, scientific and technological advances, the development of renewable energy technology, and reductions in the energy consumption per unit output value and per unit GDP of various industries. In this scenario, the power generation and heating module will increase the proportion of natural gas consumption and reduce the proportion of thermal power generation, and the installed capacity of biomass, photovoltaic, and wind power is further increased. With the future power supply requirements of Jiangsu province, the scale of thermal power generation will be stable, and gas power generation will gradually establish its dominant position in power generation, and the proportion will increase to 37% in 2050. The structure of terminal energy use will change. For example, alternative energy such as natural gas will be installed in the transport sector, and the proportion will increase by 10% every 10 years. In combination with Suzhou's energy resources, the proportion of renewable energy consumption will continue to increase. Details of parameter settings are recorded in **Supplementary Table S1**.

4) Energy transformation development scenario

The ETD scenario was based on the ISO and ESO scenarios to reduce the sectors with high energy consumption and high pollution. In it, advanced technologies will continue to improve energy efficiency, further develop renewable energy, and give industrial cities space to adjust their energy development. Especially in the power generation module, the share of coal-fired power generation will drop to 35% by 2050. The proportion of gas-fired power will be further increased to 48% by 2050. This scenario will promote key technologies for high-parameter supercritical (ultra-supercritical) power generation, integrated coal gasification combined cycle technology, and clean coal combustion technology, and develop distributed natural gas energy supply technology. At the same time, measures such as improving the utilization of solar energy, developing distributed photovoltaic power generation, and increasing the proportion of clean energy in power generation structures will be carried out. In this scenario, energy consumption declines the most. Details of the parameter settings are recorded in **Supplementary Material**.

3.3 Data Resource

The economic data of the base year were collected from the *Suzhou Statistical Yearbook* (2010–2016), including industrial output value and total GDP of each sector. The data of future scenarios were predicted according to the 13th Five-Year Plan of Suzhou Economic and Social Development. The population data came from the *Suzhou Statistical Yearbook* and the 13th Five-Year Plan for the Development of Population and Social Undertakings in Suzhou. Estimation of future population was based on historical growth trends (Ehrlich and Holdren, 1971). Among them, population growth considered the Chinese government's two-child policy. The year 2015, the most complete year for statistical data collection, was chosen as the base year. The period from 2021 to 2050 was the time range for scenario prediction. The energy price and technology cost referred to the *National Key Energy-saving and Low-carbon Technology Promotion Catalogue* and the *National Key Industries Cleaner Production Technical Guidance Catalogue* issued by China's Energy Statistics Bureau. The emission factors used in model construction came from the default IPCC fossil fuel emission factors of the LEAP model.

4 RESULT AND ANALYSIS

4.1 Energy Demand of Suzhou

As shown in **Figure 3**, under the BAU scenario, ISO scenario, and ESO scenario, Suzhou's total energy consumption rose continuously over time. The ETD scenario of energy transformation reached its peak around 2028 and then slowly declined, with the peak energy consumption of 82.31 million tons of standard coal.

The total energy demand in the BAU scenario increased from 75.40 million tons of standard coal in 2015 to 259.95 million tons in 2050, with an annual growth rate of 3.60%. The total energy demand in the ISO scenario increased from 75.40 million tons of standard coal in 2015 to 161.47 million tons in 2050, 98.48 million tons less than the BAU scenario, with an average annual growth rate of 2.25%. The total energy demand in the ESO scenario increased from 75.40 million tons of standard coal in 2015 to 162.74 million tons in 2050, with a decrease of 97.21 million tons compared with the BAU scenario and an annual growth rate of 2.22%. The total energy demand in the ETD scenario decreased from 75.40 million tons of standard coal in 2015 to 65.52 million tons in 2050, which was 194.44 million tons less than the BAU scenario. The ETD scenario was the only one of the four scenarios in which energy consumption decreased.

The energy use structure of the BAU scenario was basically unchanged from 2015. The consumption of coal accounted for the highest proportion, at 76.12% of the total energy consumption, natural gas was 10.57%, and electricity 5.34%. Under the policy change, the ratios of various fuel types in the four scenarios changed significantly (**Figure 4**). In the ISO scenario, coal dropped to 64.18% and electricity increased to 6.77%. In the ESO scenario, coal declined to 40.48%, electricity increased to 5.97%, and natural gas increased to 38.34% by 2050. In the ETD scenario, coal declined to 18.18%, electricity increased to 22.34%, and natural gas increased to 40.23% by 2050. It can be seen that, driven by various energy management policies, the proportions of raw coal and coke consumption continued decreasing, while those of electricity and natural gas continued rising (Zhu, 2006; Su et al., 2013; Zhang, 2018). Through the comparative analysis of the four scenarios, the total energy consumption under the BAU scenario, ISO scenario, and ESO scenario showed sharp yearly upward trends, which did not allow Suzhou to take the path of sustainable energy development and was not conducive to the construction of a green, low-carbon, environmental protection and energy-saving society in Suzhou. The ETD scenario reached its peak and appeared at an inflection point, which was suitable for Suzhou's path of energy transformation development.

As can be seen from the consumption levels of various sectors (**Figure 5**), in the BAU scenario, the secondary industry

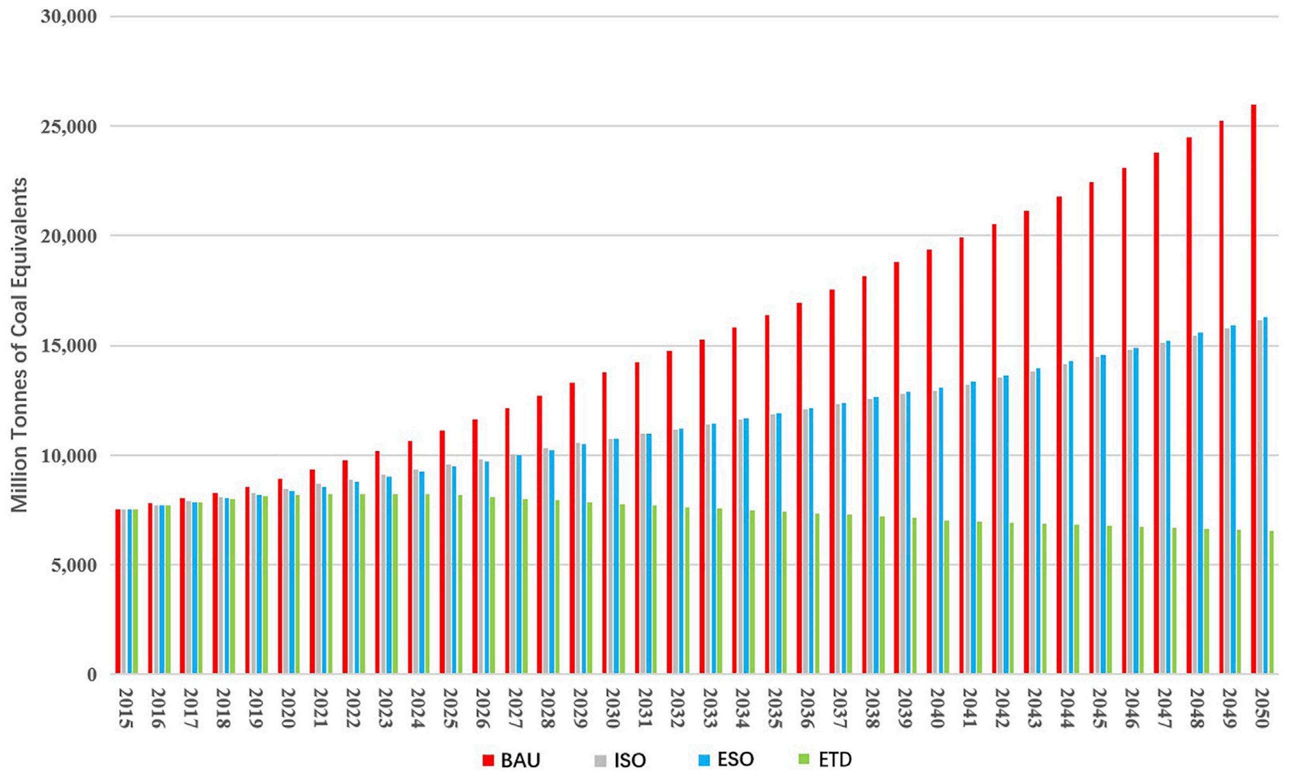

FIGURE 3 | Total energy demand trend of the different scenarios.

consumed the most energy, followed by the tertiary industry. With the development of the scenario, the energy consumption proportion of the industrial sector gradually rose, indicating that industry will always play a leading role in energy consumption. Under the BAU scenario, by 2050 the industrial energy consumption of Suzhou reached 22.996 million tons of standard coal, nearly four times that of 2015, and the industrial energy consumption accounted for 88.62%. In the ISO scenario, the tertiary industry developed rapidly and its proportion increased yearly, but the secondary industry still accounted for a large proportion of energy consumption, and the industrial sector still played a leading role. By 2050, the industrial sector consumption was 109.47 million tons of standard coal, accounting for 69.54% of the total energy consumption of all sectors. In the ESO scenario, industrial energy consumption still comprised the largest proportion, at 68.08% by 2050. The other services sector showed a clear upward trend, with an increase of 3.9919 million tons of standard coal compared to the BAU scenario. The transport sector was on the rise, from 4.06 million tons of standard coal in 2015 to 33.15 million tons in 2050. Under the ESO scenario, Suzhou's energy use structure gradually became environmental and clean energy grew rapidly, which provided positive policy suggestions for low-carbon development in Suzhou, but its total energy consumption still showed a long-term growth trend. Under the ETD scenario, the proportion of energy consumption in the industrial sector continued to decline by 2050, with the industrial sector accounting for 53.05%, down 23.07% compared with the base year. The proportion of energy consumption in the residential and service sectors continued to rise, while in the construction and commercial sectors it rose slowly and in agriculture declined slightly. In the ETD scenario, clean energy in Suzhou grew rapidly and energy use gradually became environmental, which provided positive policy suggestions for low-carbon development. This scenario was suitable for the low-carbon and environmentally friendly development of Suzhou.

4.2 Energy Supply of Suzhou

The energy demand of Suzhou's energy processing and conversion sectors under each scenario is shown in **Figure 6**. It can be seen that the long-term energy demand trend of the processing and conversion sectors was basically the same as the trend of energy demand. In BAU, ISO, and ESO scenarios, the transmission and distribution losses and the conversion rates of energy processing basically maintained long-term stability, and the energy consumption of the energy processing and conversion sectors increased yearly. However, the energy consumption in the ESO scenario was higher than that in the ISO scenario in the processing and conversion process. This was mainly due to energy consumption in the ESO scenario needing more power because of the limited technology level, and more initial fuel needed to be invested in the process of processing and conversion. In the ETD scenario, Suzhou adopted a series of positive policies and measures, adopted advanced technologies, reduced the loss

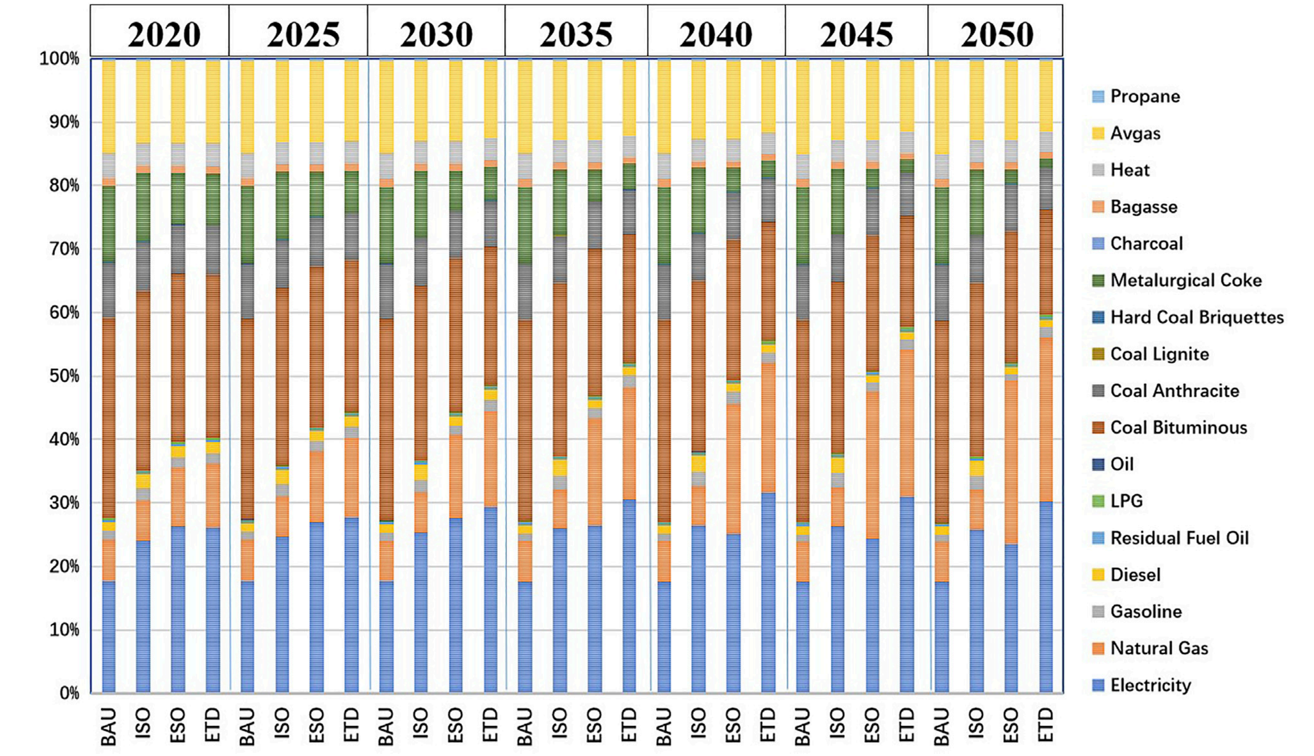

FIGURE 4 | Energy demand under the four scenarios in Tangshan.

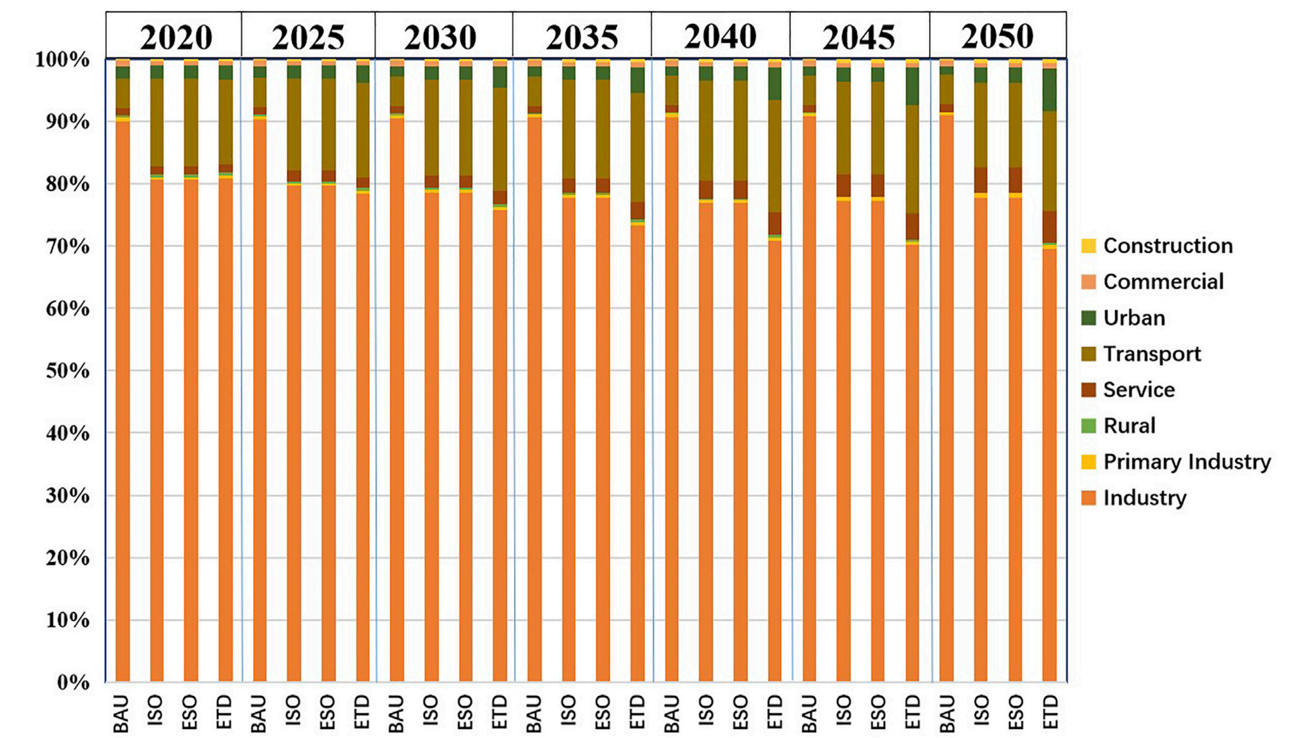

FIGURE 5 | The proportion of energy demand by sector.

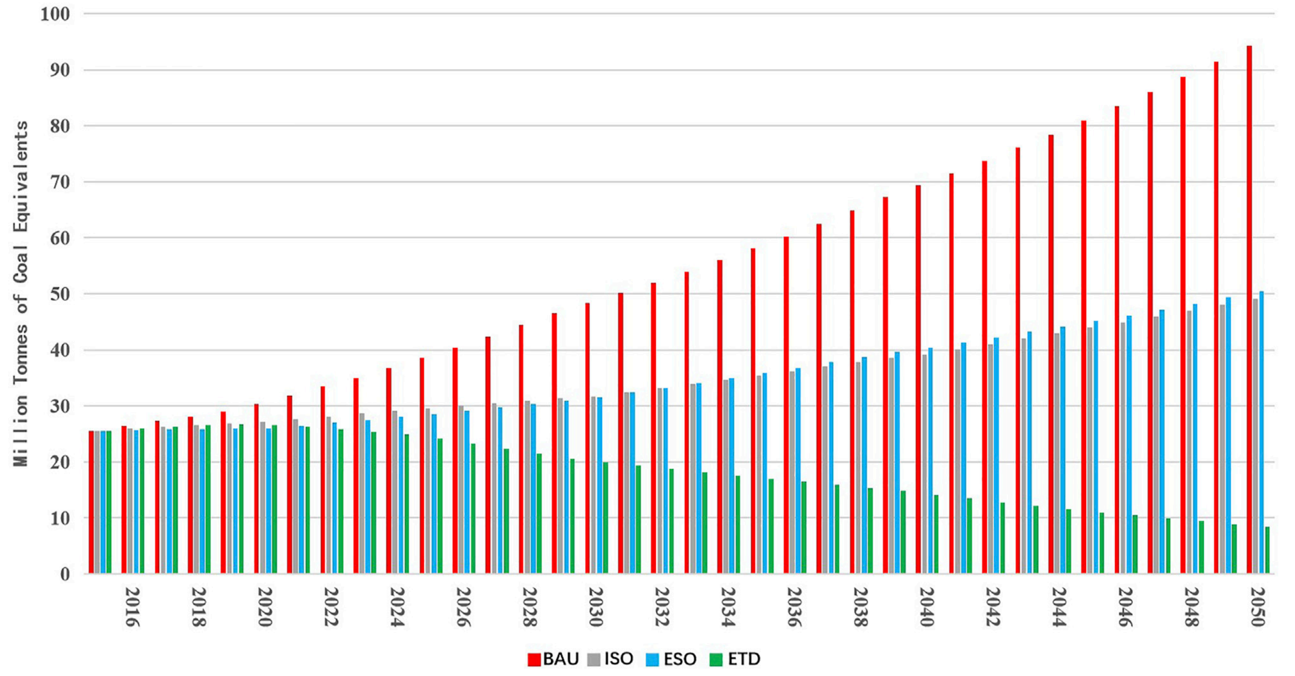

FIGURE 6 | Energy consumption in the different scenarios during the process of processing and conversion.

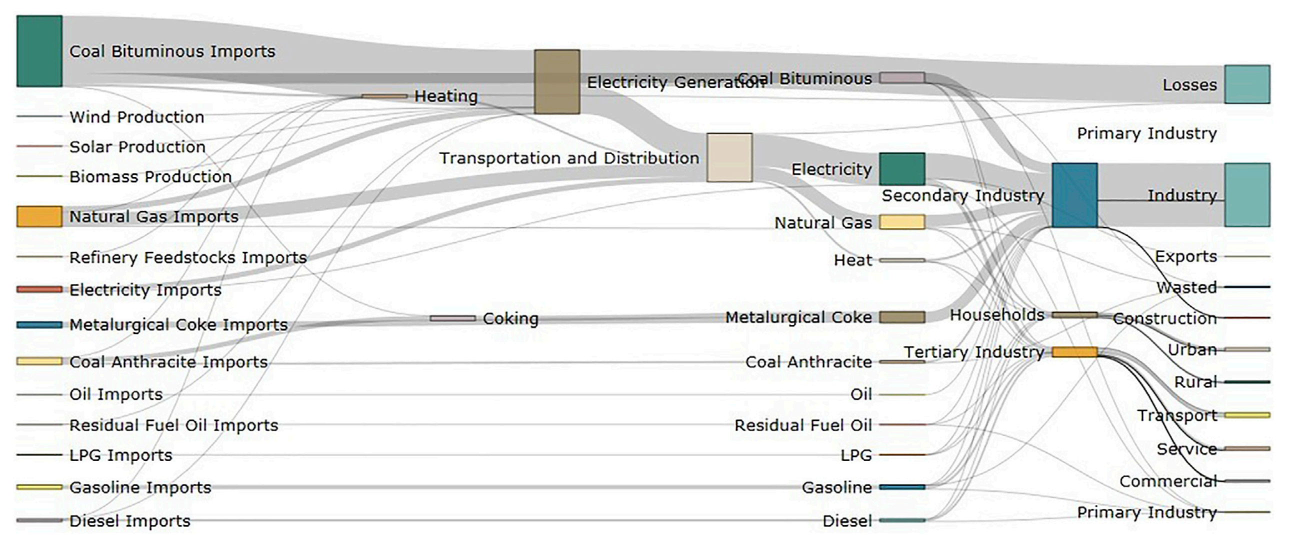

FIGURE 7 | Energy flow in 2015.

rate of transmission and distribution, improved the conversion rate of processing, and significantly reduced the energy consumption compared with the other three scenarios. No policy changes were made in the BAU scenario. By 2050, coal-fired power accounted for 91.53% of thermal power generation, and gas-fired power accounted for 8.47%, with coal at 81.41% of total power generation energy consumption. The policy adjustment of the ISO scenario was basically consistent with BAU. In the ESO scenario, the purchase of natural gas and electricity increased from adjusting the energy structure. In the power generation module, the proportion of gas power generation was further improved, and gas power generation accounted for 28% of the total power generation by 2030 and 37% by 2050. In the ETD scenario, high energy consumption and high-pollution fuels were further reduced, and the ratio of gas-fired power generation further increased compared with the ESO

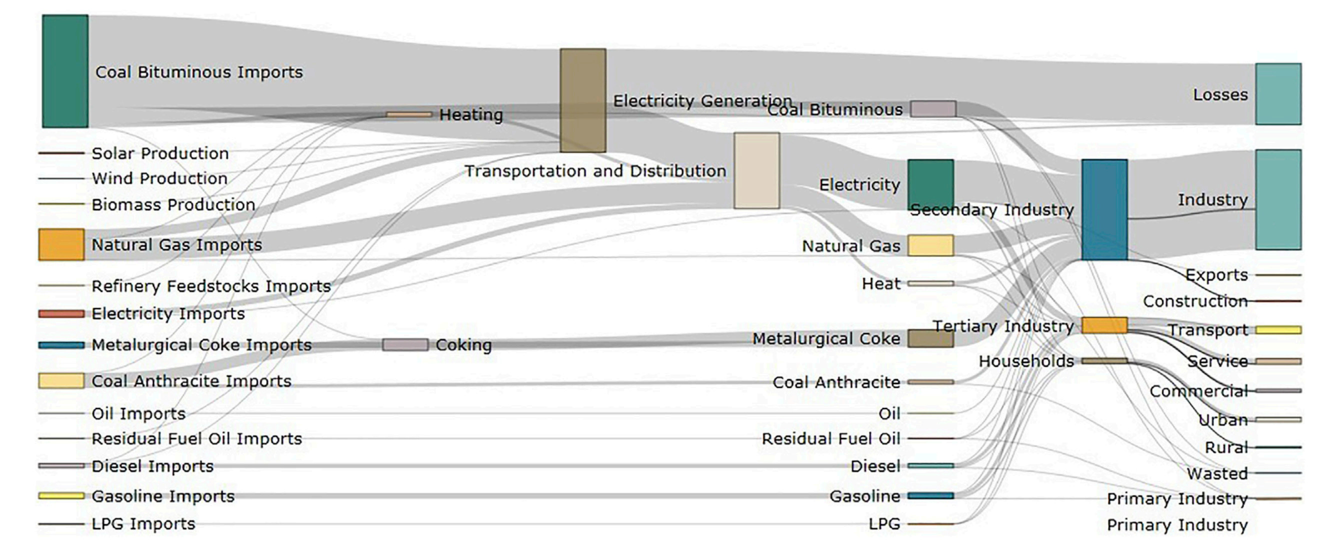

FIGURE 8 | Energy flows in 2030 under the BAU scenario.

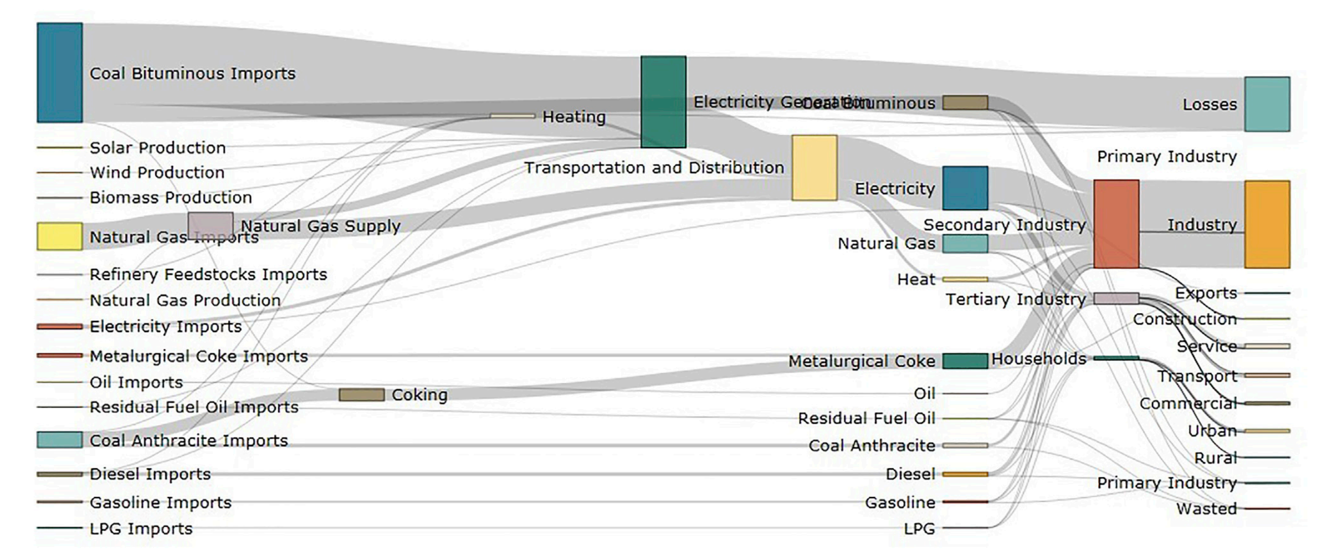

FIGURE 9 | Energy flows in 2050 under the BAU scenario.

scenario, with the proportion of gas-fired power generation reaching 35% by 2030 and 48% by 2050.

4.3 Energy Flows

According to the energy flow in 2015 (**Figure 7**), in the base year the consumption of coal accounted for 76.12% of the total energy consumption of the whole society, natural gas accounted for 10.57%, and electricity accounted for 5.34%. In the energy processing and conversion sector, coal-fired power generation was the main type. In terms of energy consumption by sector, industry, transport, and urban living accounted for 86.97, 5.38, and 2.69% of the total energy consumption.

The BAU scenario was planned in accordance with existing policies and development trends, and the future energy consumption of all sectors and the composition of all types of energy were basically similar to that of the base year (**Figures 8**, **9**). In the BAU scenario, coal still comprised the highest proportion of energy consumed in the future, and thermal power generation was still the main power generation component, and its future energy flow composition was similar to that of 2015.

After the adjustment of industrial structure, the total future energy consumption in the ISO scenario was significantly reduced. Although the proportion of coal was still the highest,

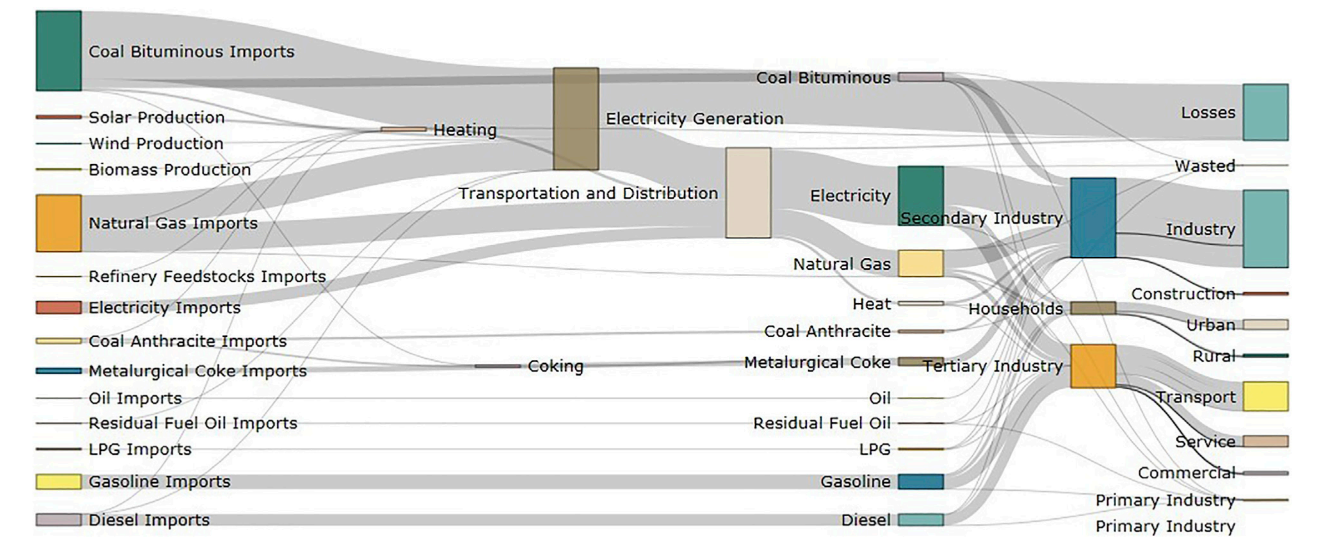

FIGURE 10 | Energy flow in 2030 under the ETD scenario.

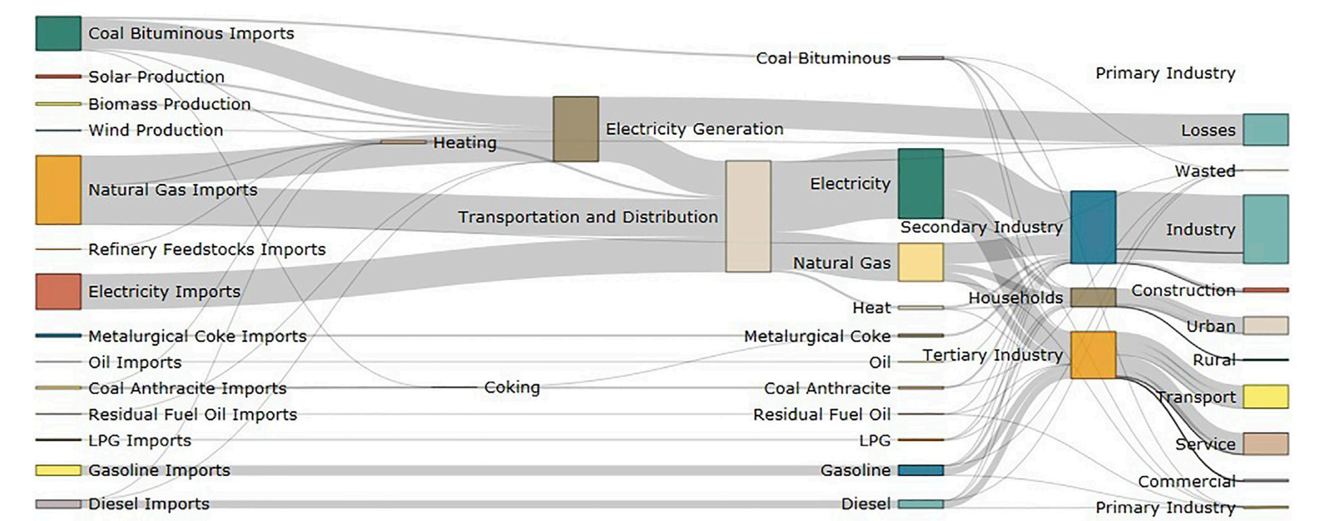

FIGURE 11 | Energy flow in 2050 under the ETD scenario.

it was reduced more significantly than that in the BAU scenario. The share of non-fossil energy consumption did not increase significantly. Of the various sectors, the energy consumption of the industrial sector decreased significantly. Based on the ISO scenario, the ESO scenario focused on the energy structure adjustment of the energy sectors. In this scenario, clean coal was implemented, the proportion of natural gas increased, and renewable energy was gradually developed. The import of natural gas increased, the proportion of renewable energy increased, the non-fossil proportion of the total energy consumption increased yearly, and the proportion of industrial energy consumption decreased. Based on the above scenarios, the ETD scenario continued increasing the use of natural gas to replace coal consumption, and the proportion of coal consumption further decreased. There was also a greater use of electricity and natural gas in energy consumption sectors, and the proportion of energy consumption in the industrial sector also showed a downward trend. Energy flow changes in the ETD scenario were the most complex, and energy flow diagrams for the ETD scenario are presented in **Figures 10**, **11**.

4.4 Carbon Emission

According to the direct and indirect carbon dioxide emissions generated by various sectors in Suzhou from 2020 to 2050 (**Figure 12**), it can be seen that the carbon emissions of various scenarios varied greatly. In the BAU scenario, carbon

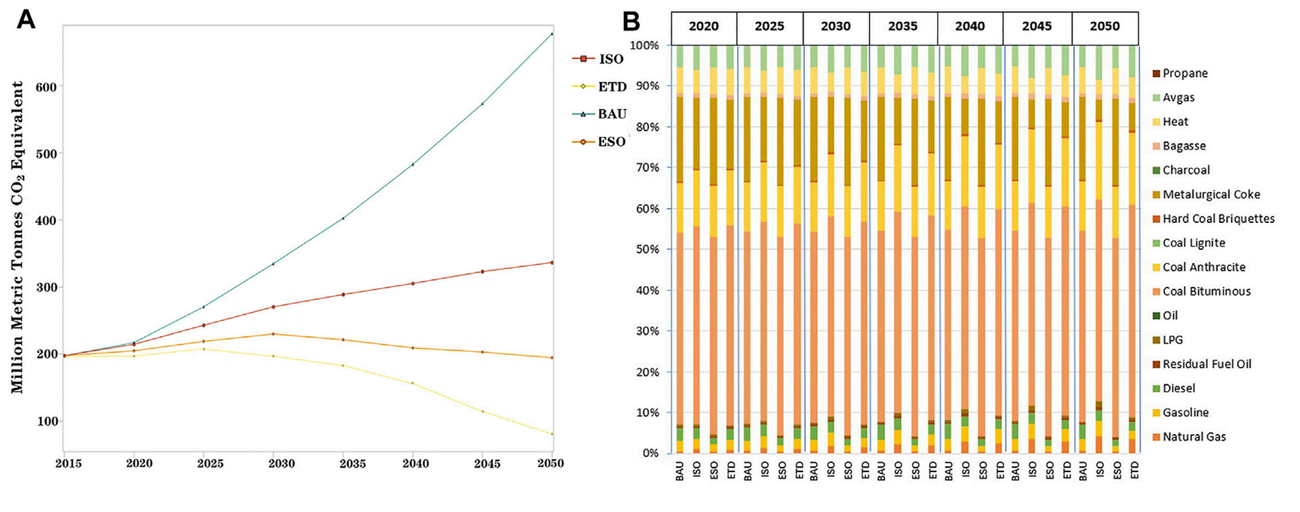

FIGURE 12 | (A) CO_2 emission of all scenarios in Suzhou and **(B)** share of carbon emissions by energy types and consumption sectors.

dioxide emissions were on the rise, with no inflection point, from 198.1 Mt in 2015 to 677.6 Mt in 2050. This indicated that environmental problems become serious when no measures are taken to reduce emissions. The carbon dioxide emission of the ISO scenario still showed an increasing trend, but the growth trend slowed down. Compared with the BAU scenario, carbon emission in 2050 decreased by 341 Mt, which failed to reach the final goal of carbon emission reduction in Suzhou. In the ESO scenario, the growth trend of carbon dioxide emissions showed an inflection point around 2030 and then declined. Carbon emissions in 2050 were similar to those in 2015 without a significant decrease, indicating that reasonable adjustment of the consumption structure can reduce carbon emissions. In the ETD scenario, carbon dioxide emissions showed a trend of first increasing and then decreasing, reaching the peak of carbon emissions during 2025–2030, and then showing a significant downward trend. Carbon emissions in 2050 were only 58.5 Mt, indicating that energy system optimization can effectively control carbon emissions caused by energy consumption. This was the best scenario for achieving a reduction in carbon dioxide emissions. In all scenarios, the sector that produced the most carbon emissions was the industry sector, followed by the transport sector. In terms of energy types, heavy consumption of hard coal was the main source of carbon emissions. This showed that while optimizing and upgrading the industrial structure, we should consider the technological upgrading and the use of clean energy in the process transformation industry and further expand the use of renewable energy, so as to jointly reduce carbon dioxide emissions and achieve the construction of carbon emission reduction targets in Suzhou.

5 DISCUSSION

This paper established the LEAP-Suzhou model under the constraint of carbon emissions. Four scenarios were set to study the important factors affecting urban energy system. The ISO scenario focused on the tertiary, secondary, and primary industrial structure optimization, led by the tertiary industry. The ESO scenario focused on the energy structure optimization that replaced coal with gas and renewable energy. In the ETD scenario, based on the optimization of the industrial and energy structures, the proportions of purchased clean electricity, purchased natural gas, and local renewable consumption continued to increase, and the energy utilization efficiency further improved. Specifically:

Most carbon emissions and energy consumption come from the industry sector. With the improvement of people's living standards and the development of tertiary industry, energy consumption in areas such as electricity production and supply, transportation, and households is expected to increase further. The average annual growth rates of total energy demand in the BAU, IOS and ESO scenarios were 3.6, 2.25, and 2.22%, respectively, and the total energy consumption in these three scenarios showed a sharp yearly upward trend, which did not allow Suzhou to take the path of sustainable energy development. In the ETD scenario, the total energy demand decreased from 75.40 million tons of standard coal in 2015 to 65.52 million tons in 2050, 194.44 million tons less than the BAU scenario. This scenario appeared to be at an inflection point around 2028, followed by a decline in energy consumption, which was a suitable path for Suzhou's energy transformation development. At the same time, in the ETD scenario, the proportion of high-energy-consuming industries gradually decreased, the proportion of renewable energy consumption continued to rise, the proportion of natural gas and outsourced electricity consumption increased substantially, and the industrial and energy structures gradually moved from medium-high level to high level. The carbon emission reduction effect of energy reform in Suzhou was remarkable. From the perspective of carbon emissions, both the BAU scenario and the ISO scenario showed an increasing trend of emissions, which was not conducive to the future development of Suzhou. The optimal scenario of energy consumption structure peaked around 2030 and then declined. This scenario achieved the effect of emission reduction, but the emission reduction degree in 2050 was not high. The ETD scenario reached the peak of emissions from 2025 to 2030, followed by an obvious downward trend. This scenario effectively realized the optimization of energy system emission reduction and was the most suitable for the long-term development of Suzhou.

There are several limitations to this study. First, 2015 was the base year. The data were not currently up-to-date, but they were the most complete and detailed data we could obtain. Most of the key parameters were based on existing planning or trend extrapolation, which cannot accurately predict future changes. So, the prediction result was uncertain. The actual energy consumption and carbon emission coefficients of ferrous metal smelting, iron and steel, coking, and other specific types of equipment were insufficient. The energy consumption and carbon emissions of each device could not be accounted for. The LEAP model was based on data but could not capture the spatial distribution of specific sectors. This study referred to previous studies but focused on the benchmark scenario of energy-saving and emission reduction benefit analysis under the comprehensive scenario of industrial structure optimization, energy structure optimization, and low-carbon technology. It did not measure absolute numbers but looked at relative trends across sectors. In future work, field investigations of specific sectors and equipment are needed.

6 CONCLUSION AND POLICY IMPLICATIONS

6.1 Conclusion

Taking Suzhou as an example, this paper established the LEAP-Suzhou model under the constraint of carbon emissions to research the important factors affecting future urban energy policies. Four scenarios were set. In addition to the BAU scenario, reference scenarios with 2015 as the base year were set. The ISO scenario was dominated by the optimization of the industrial structure, the ESO scenario was dominated by the optimization of the energy structure, and the ETD scenario was dominated by energy reform. The results indicated that most carbon emissions and energy consumption come from the industry sector, and the industrial structure policies, energy structure upgrading policies, energy efficiency improvement policies, and key technologies implemented by the LEAP-Suzhou model will significantly affect energy consumption and carbon emissions. Among them, the total energy demand of the ETD scenario decreased from 75.40 million tons of standard coal in 2015 to 65.52 million tons in 2050, 194.44 million tons less than the BAU scenario. This scenario effectively realizes the emission reduction optimization of the energy system and is most suitable for the long-term development of energy transformation development path of Suzhou. The research results successfully explore the path of energy and carbon emission optimization in Suzhou city, which can provide reference for the energy transformation of industrial cities and the realization of carbon peak and carbon neutrality, and provide strong support for the realization of regional sustainable development.

6.2 Policy Implications

Based on the LEAP-Suzhou model, this paper studied the trend in energy carbon emissions from energy production and consumption in Suzhou. The description of the energy flow path and key nodes is of guiding and theoretical significance to medium and long-term urban energy planning (Zhang and Lin, 2012; Al-mulali et al., 2013). Through a comparative analysis, the total energy consumption under the BAU, ISO and ESO scenarios showed a trend of sharp yearly increases, which was not conducive to Suzhou taking the road of sustainable energy development and to the construction of a green, low-carbon, environmental protection and energy-saving Suzhou. The ETD scenario reached its peak and appeared at an inflection point, which was suitable for Suzhou's energy transformation development path.

Therefore, in order to realize the low-carbon development of Suzhou, specific policies and measures are proposed for various sectors:

The supply and application of clean energy should be gradually improved, which will conform to the development direction of the future city energy system (Lin, 2018). Currently, biomass power generation continues to grow rapidly, with solar and wind energy entering the energy consumption system in 2011 and 2014, respectively. The proportion of renewable energy (photovoltaic, biomass, wind power) continues to rise, and the outsourcing of electricity continues to grow. In the ETD scenario, the proportion of renewable energy consumption continued to rise, and the proportion of natural gas and outsourced electricity consumption increased significantly. The industrial and energy structures gradually moved from medium-high to high level. The carbon emission reduction effect of energy reform in Suzhou has been remarkable, and the city has entered a new stage of high-quality development. The gradual improvement in the clean energy supply and application should be a main direction of Suzhou's energy system reform in the future (Bi et al., 2011).

At present, this is one of the best paths for Suzhou's energy transformation, which is mainly based on cross-regional optimal allocation and supplemented by local development and utilization (Zhang et al., 2015). Suzhou is extremely short of local conventional primary energy and renewable resource endowment. The energy system of Suzhou has gradually changed from the previous "local thermal power generation (coal and fuel oil) + local coking" to the cross-regional optimal allocation mode of "trans-regional purchased power generation + local thermal power generation (coal, natural gas, and fuel oil) + purchased coke + renewable energy generation." However, there remains a large gap between Suzhou's trans-regional energy allocation capacity and that of first-tier cities such as Beijing, Shanghai, Guangzhou, and Shenzhen. In the future, Suzhou energy transformation should focus on cross-regional optimal allocation and improve the ability of the city's high-quality resource allocation.

Product structure adjustment based on industrial structure optimization is one of the best paths for Suzhou's energy system transformation (Zu and Wang, 2019). Suzhou is currently in the critical period of industrial structure transformation (Jiang and Lin, 2012), with tertiary industry and secondary industry leading together. Computers, electrical machinery, steel, general equipment, chemical industry, and transportation equipment were the six new leading industries in Suzhou from 2015 to 2017. Suzhou should actively adjust the production and trade structure of energy-consuming industries and products, so as to promote industrial products to the upper reaches of the whole industrial chain, increase their added value, and reduce their energy consumption (Lang and Chen, 2019). At the same time, the industrial structure in Suzhou should be actively promoted; the industry of Suzhou should develop to the upstream and improve the level of technology and value-added rate.

The new normal economy, new forms of energy, and efficient energy management have moved the urban energy system to the stage of multi-objective and high-quality development. Suzhou's energy system has undergone three stages of ensuring supply, ensuring supply and controlling safety, and ensuring supply and improving efficiency, and has stepped onto the stage of multi-objective and high-quality development. Under the new normal economy, Suzhou, as a large energy consumption market with scarce resources, faces the pressure of double control of total energy consumption and consumption intensity. In the absence of new external energy channels, strict control of coal consumption, and unstable supply of natural gas, energy consumption efficiency, a clean energy supply, and optimal operation of the energy system are required to meet the higher requirements for efficient energy management (Kennedy et al., 2014). The urban energy Internet is a platform for the interconnection, comprehensive utilization, optimization, and sharing of all kinds of energy in the city, centering on electricity. Through the cross-border integration of talents, technologies, services and policies, new technologies and business models will be stimulated to foster new businesses, new forms of business, and a new economy in the field of urban energy (Zheng et al., 2010). First, the urban energy Internet promotes the development of power generation enterprises, equipment suppliers, electricity companies, and other upstream and downstream enterprises. Second, the urban energy Internet also greatly promotes the integration of the communication industry, Internet industry, law, finance, capital, and other fields in the city, and drives the innovation and development of relevant manufacturing and production-oriented services.

DATA AVAILABILITY STATEMENT

The original contributions presented in the study are included in the article/**Supplementary Material**, further inquiries can be directed to the corresponding author.

AUTHOR CONTRIBUTIONS

WS and YZ contributed to all aspects of this work; ZL and WS conducted data analysis, YZ and ZL wrote the main manuscript text; YY and CC gave some useful comments and suggestions to this work. All authors reviewed the manuscript.

FUNDING

This work was supported by State Key Laboratory of Resources and Environmental Information System, Guangdong Introducing Innovative and Entrepreneurial Teams (2019ZT08L213) and Guangdong Basic and Applied Basic Research Foundation (2020A1515011230).

ACKNOWLEDGMENTS

We like to thank the editors and reviewers for their helpful remarks.

SUPPLEMENTARY MATERIAL

The Supplementary Material for this article can be found online at: https://www.frontiersin.org/articles/10.3389/fenvs.2022.905471/full#supplementary-material

REFERENCES

Al-mulali, U., Fereidouni, H. G., Lee, J. Y. M., and Sab, C. N. B. C. (2013). Exploring the Relationship between Urbanization, Energy Consumption, and CO2 Emission in MENA Countries. *Renew. Sustain. Energy Rev.* 23, 107–112. doi:10.1016/j.rser.2013.02.041

Bi, J., Zhang, R., Wang, H., Liu, M., and Wu, Y. (2011). The Benchmarks of Carbon Emissions and Policy Implications for China's Cities: Case of Nanjing. *Energy Policy* 39, 4785–4794. doi:10.1016/j.enpol.2011.06.045

Chai, Q. M., Guo, H. Y., Liu, C. Y., Dong, L., Ju, L. X., Liu, C. S., et al. (2020). Global Climate Change and China's Action Scheme: Climate Governance of China in the 14th Five-Year Plan Period from 2021 to 2025(Conversation by Writing). *Yuejiang Acad. J.* 12, 36–58. doi:10.13878/j.cnki.yjxk.20210107.001

Chu, S., and Majumdar, A. (2012). Opportunities and Challenges for a Sustainable Energy Future. *Nature* 488, 294–303. doi:10.1038/nature11475

Deng, M. X., and Li, W. (2017). Scenario Analysis of the Supply-Side Structural Reform Influences on Industrial Carbon Emissions Based on LEAP Model in Yunnan Province. *China Environ. Sci.* 37, 786–794. doi:10.3969/j.issn.1000-6923.2017.02.053

Ehrlich, P. R., and Holdren, J. P. (1971). Impact of Population Growth. *Science* 171, 1212–1217. doi:10.1126/science.171.3977.1212

He, J. K. (2014). Situation and Countermeasures of Energy Development and Climate Change in China. *Econ. Rev. J.* 5, 16–20. doi:10.16528/j.cnki.22-1054/f.2014.05.001

Hong, S., Chung, Y., Kim, J., and Chun, D. (2016). Analysis on the Level of Contribution to the National Greenhouse Gas Reduction Target in Korean Transportation Sector Using LEAP Model. *Renew. Sustain. Energy Rev.* 60, 549–559. doi:10.1016/j.rser.2015.12.164

Hu, G., Ma, X., and Ji, J. (2019). Scenarios and Policies for Sustainable Urban Energy Development Based on LEAP Model - A Case Study of a Postindustrial City: Shenzhen China. *Appl. Energy* 238, 876–886. doi:10.1016/j.apenergy.2019.01.162

Jiang, Z., and Lin, B. (2012). China's Energy Demand and its Characteristics in the Industrialization and Urbanization Process. *Energy Policy* 49, 608–615. doi:10.1016/j.enpol.2013.04.059

Kennedy, C. A., Ibrahim, N., and Hoornweg, D. (2014). Low-carbon Infrastructure Strategies for Cities. *Nat. Clim. Change* 4, 343–346. doi:10.1038/nclimate2160

Lang, W., and Chen, Y. Z. (2019). Empirical Analysis of Energy Consumption Structure of China's High Energy Consumption Industry. *Econ. Rev. J.* 4, 95–102. doi:10.16528/j.cnki.22-1054/f.201904095

Le, Q. C., Andrew, R. M., Friedlingstein, P., Sitch, S., and Zhu, D. (2018). Global Carbon Budget 2017. *Earth Syst. Sci. Data.* 10, 405–448. doi:10.5194/essd-10-405-2018

Li, N., Yang, J. S., and Chen, J. R. (2021a). Opportunities and Challenges of Energy Industry under the Background of "Carbon Emission Peak" and "Carbon Neutrality. *Nat. Resour. Econ. China* 34, 63–69. doi:10.19676/j.cnki.1672-6995.000688

Li, Q., Hu, J., and Yu, B. (2021b). Spatiotemporal Patterns and Influencing Mechanism of Urban Residential Energy Consumption in China. *Energies* 14, 3864. doi:10.3390/en14133864

Liao, Y., and Wu, G. (2013). Carbon Emission Analysis of Energy Consumption of Industrial Enterprises above Designated Size in Suzhou. *China J. Commer.* 14, 176–178. doi:10.1007/s11069-019-03607-2

Lin, B. Q. (2018). The Period of Carrying Out Energy Revolution to Promote Low Carbon Clean Development in China. *China Ind. Econ.* 6, 15–23. doi:10.19581/j.cnki.ciejournal.2018.06.002

Liu, H., Lu, W. H., and Wei, J. (2019). Research on Innovation and Development Status and Promotion Countermeasures of Industrial Enterprises in Suzhou. *North. Econ. Trade* 4, 117–119. doi:10.1155/2021/8473021

Liu, J. B. (2021a). Carbon Neutralization: Building a Community of Human and Natural Life Together. *Fujian For.* 4, 1. doi:10.3969/j.issn.1003-4382.2021.04.002

Liu, Q., Wang, Q., and Wang, Y. (2016). Climate Financing in the Era of Paris Agreement: Global Progress, Governance Challenges and China's Countermeasures China Population. *Resour. Environ.* 26, 14–21. doi:10.3969/j.issn.1002-2104.2016.12.003

Liu, T., Wang, R., and Sun, B. J. (2015). Analysis on Peaking of Carbon Emission in Typical Coastal Lndustrial Cities of China. *China Popul. Resour. Environ.* 25, 25–28. doi:10.1371/journal.pone.0258147

Liu, Y. M., Timothy, O. R., and Li, J. Y. (2021b). Exploring the Relationship between Urbanization and Resource-Environment from the Decoupling Perspective: A Case Study of Suzhou. *J. Suzhou Univ. Sci. Technol. Sci. Ed.* 38, 71–78. doi:10.1007/s11356-021-15161-1

Liu, Z. F., Huang, H. H., Li, L., and Liu, Y. (2022). Green Manufacturing: the Inevitable Choice of Manufacturing Industry under the Goal of Carbon Peak and Carbon Neutralization. *Metal. Work. Metal. Cut.* 1, 15–19. doi:10.3969/j.issn.1674-1641.2022.01.014

Nieves, J. A., Aristizábal, A. J., Dyner, I., Báez, O., and Ospina, D. H. (2019). Energy Demand and Greenhouse Gas Emissions Analysis in Colombia: A LEAP Model Application. *Energy* 169, 380–397. doi:10.1016/j.energy.2018.12.051

Nuta, F. M., Nuta, A. C., Zamfir, C. G., Petrea, S. M., Munteanu, D., and Cristea, D. S. (2021). National Carbon Accounting—Analyzing the Impact of Urbanization and Energy-Related Factors upon CO^2 Emissions in Central–Eastern European Countries by Using Machine Learning Algorithms and Panel Data Analysis. *Energies* 14, 2775. doi:10.3390/en14102775

Pan, L. J., Xie, Y. B., and Li, W. (2013). An Analysis of Emission Reduction of Chief Air Pollutants and Greenhouse Gases in Beijing Based on the LEAP Model. *Procedia Environ. Sci.* 18, 347–352. doi:10.1016/j.proenv.2013.04.045

Ponce, P., and Khan, S. A. R. (2021). A Causal Link between Renewable Energy, Energy Efficiency, Property Rights, and CO2 Emissions in Developed Countries: A Road Map for Environmental Sustainability. *Environ. Sci. Pollut. Res.* 28, 37804–37817. doi:10.1007/s11356-021-12465-0

Shao, S., Yang, L., Yu, M., and Yu, M. (2011). Estimation, Characteristics, and Determinants of Energy-Related Industrial CO2 Emissions in Shanghai (China), 1994-2009. *Energy Policy* 39, 6476–6494. doi:10.1016/j.enpol.2011.07.049

Su, Y. J., Zheng, Z. B., Liu, B., and Bao, Y. (2013). Study on Influencing Factors and Countermeasures of Industrial Carbon Emission in Suzhou. *China J. Commer.* 17, 188–190. doi:10.3969/j.issn.1005-5800.2013.17.088

Sun, H., Hu, X. Y., and Nie, F. F. (2019). Spatio-temporal Evolution and Socio-Economic Drivers of Primary Air Pollutants from Energy Consumption in the Yangtze River Delta. *Chin. J. Environ. Manag.* 11, 71–78. doi:10.16868/j.cnki.1674-6252.2019.04.071

Wang, H. Z. (2016). Scenario Prediction of Tianjin Transportation Energy Consumption and Carbon Emission. *J. Arid Land Resour. Environ.* 30, 37–41. doi:10.13448/j.cnki.jalre.2016.212

Wang, S. H., He, M. X., Zhang, W., and Liu, X. N. (2021a). Research on Industrial Energy Intensity and Lts Influencing Factors in Beijing-Tianjin-Hebei Urban Agglomeration from the Perspective of Supply-Side Reform. *Geogr. Geo-Information Sci.* 37, 110–116. doi:10.1016/j.egyr.2022.02.283

Wang, Y., Tan, D. M., Zhang, J. T., Meng, N., Han, B. L., and Ouyang, Z. Y. (2020). The Impact of Urbanization on Carbon Emissions: Analysis of Panel Data from 158 Cities in China. *Acta Eco Sin.* 40, 7897–7907. doi:10.5846/stxb201911292591

Wang, Y., Zhao, H., Li, L., Liu, Z., and Liang, S. (2013). Carbon Dioxide Emission Drivers for a Typical Metropolis Using Input-Output Structural Decomposition Analysis. *Energy Policy* 58, 312–318. doi:10.1016/j.enpol.2013.03.022

Wang, Y. Z., Lin, W., Li, C. Y., Zhu, Y. L., Zhang, J., and Gao, F. (2021b). Comprehensive Evaluation of Energy Transition in Industrial Cities: A Case Study of Suzhou. *J. Glob. Energy Interconnect.* 4, 188–196. doi:10.3390/su8080746

Watts, N., Adger, W. N., Agnolucci, P., Blackstock, J., Byass, P., Cai, W., et al. (2015). Health and Climate Change: Policy Responses to Protect Public Health. *Lancet* 386 (10006), 1861–1914. doi:10.1016/S0140-6736(15)60854-6

Wu, X. P. (2019). Practice and Enlightenment of Development of Lnternational Low-Carbon City. *Res. Dev.* 5, 44–52. doi:10.13483/j.cnki.kfyj.2019.05.007

Xie, L. L., and Sun, H. X. (2021). The Evolution of Coordinated Development Mechanisms of Urban Agglomeration in Yangtze River Delta. *Shanghai Econ.* 5, 39–61. doi:10.3969/j.issn.1000-4211.2021.05.004

Xu, P., Shao, L., Geng, Z., Guo, M., Wei, Z., and Wu, Z. (2019). Consumption-Based Carbon Emissions of Tianjin Based on Multi-Scale Input-Output Analysis. *Sustainability* 11, 6270. doi:10.3390/su11226270

Yang, Y. M. (2021). The Source Apportionment of VoCs and Countermeasures and Suggestions for Emission Reduction in an Industrial City in Western China. Thesis. Lanzhou: Lanzhou University. doi:10.27204/d.cnki.glzhu.2021.000917

Zhang, C., and Lin, Y. (2012). Panel Estimation for Urbanization, Energy Consumption and CO2 Emissions: A Regional Analysis in China. *Energy Policy* 49, 488–498. doi:10.1016/j.enpol.2012.06.048

Zhang, H. (2018). Challenges Faced by Jiangsu in Developing "green Energy Substitution. *Real. Only* 12, 71–72. doi:10.3969/j.issn.1004-1605.2018.12.019

Zhang, L. H., Xiong, J., Ju, L. W., Wu, H. L., and Tan, Z. F. (2015). An Optimization Model for Inter-regional Energy Allocation under Consideration of Clean Energy. *J. Hunan Univ. Nat. Sci.* 42, 71–77. doi:10.16339/j.cnki.hdxbzkb.2015.04.011

Zhang, T. Z. (2021). Discussion on the Current Situation and Development Trend of Energy Utilization in China. *Territ. Nat. Resour. Study* 5, 76–78. doi:10.16202/j.cnki.tnrs.2021.05.019

Zheng, Y. F., Li, H. T., Wu, R. J., and Wang, L. X. (2010). The Impact of Technological Progress on China's CO^2 Impact of Emission Reduction. *Chin. Sci. Bull.* 55, 1555–1564. doi:10.1007/s11434-010-3241-1

Zhu, C. J. (2006). Analysis of Energy Consumption and Sustainable Development Strategy in Suzhou. *Energy China* 12, 34–37. doi:10.3969/j.issn.1003-2355.2006.12.009

Zhu, C. X., Xi, W. M., Sun, Q., Chen, J. J., Xie, D., Chen, Q., et al. (2020). Energy Transition Path for Urban Areas under New-type Urbanization: A Case Study on Suzhou City Wuzhong District. *Electr. Power* 53, 232–240. doi:10.11930/j.issn.1004-9649.201911057

Zu, X., and Wang, P. (2019). Study on the Mechanism of Lndustrial Structure Adjustment on the Optimization of Energy Consumption Structure. *Soft Sci.* 33, 11–16. doi:10.13956/j.ss.1001-8409.2019.05.03

Conflict of Interest: The authors declare that the research was conducted in the absence of any commercial or financial relationships that could be construed as a potential conflict of interest.

Publisher's Note: All claims expressed in this article are solely those of the authors and do not necessarily represent those of their affiliated organizations, or those of the publisher, the editors and the reviewers. Any product that may be evaluated in this article, or claim that may be made by its manufacturer, is not guaranteed or endorsed by the publisher.

frontiers | Frontiers in Environmental Science

ORIGINAL RESEARCH
published: 12 May 2022
doi: 10.3389/fenvs.2022.892414

Carrying Capacity of Water Resources for Renewable Energy Development in Arid Regions in Northwest China: A Case Study of Golmud, Qinghai

Wenjuan Hou[1], Xiaojie Li[2], Linsheng Yang[1,3], Wanquan Ta[4] and Xiaopeng Jia[4]*

[1]*Key Laboratory of Land Surface Pattern and Simulation, Institute of Geographic Sciences and Natural Resources Research, Chinese Academy of Sciences, Beijing, China,* [2]*College of Land Science and Technology, China Agricultural University, Beijing, China,* [3]*College of Resources and Environment, University of Chinese Academy of Sciences, Beijing, China,* [4]*Key Laboratory of Desert and Desertification, Northwest Institute of Eco-Environment and Resources, Chinese Academy of Sciences, Lanzhou, China*

Abstract: Northwest China has become a base for wind and solar energy development due to its rich wind and solar resources and large area of desert and unutilized land. However, whether the scarce water resources in the arid regions there can meet the requirements for renewable energy development is currently a pressing, critical problem. Therefore, the life cycle water footprint (WF) of the renewable energy industry—its wind energy, photovoltaic (PV), and concentrated solar power (CSP) electricity generation enterprises—in the basin area of Golmud, Qinghai, a typical arid region in Northwest China, has been investigated in this study. Water consumption by local renewable energy enterprises was estimated under current (2020) scenarios [i.e., different (local/vs. nonlocal) origins of equipment and raw materials used, and employees hired by these enterprises] and three future scenarios (i.e., different ratios between installed capacities of wind energy, PV, and CSP at a fixed total renewable energy electricity generation capacity assuming China's carbon emission will peak then). The results revealed that water consumption by local renewable energy enterprises in 2020 was 1.62×10^6–1.31×10^7 m^3, accounting for 0.07–0.6% of the current total water resources in the basin area of Golmud. Water consumption by the local salt chemistry industry, a pillar industry in Golmud whose water consumption is high, accounted for 2.69% of the total water resources being 4.24–34.37 times that of the local renewable energy industry. To reach the goal of carbon emissions peaking by 2030 requires an increase of 6.17×10^6 kW in the installed capacity for wind and solar power generation in Golmud, would translate into an increase of 1.57×10^7–6.46×10^7 m^3 in water consumption, this accounting for 7.15–19.35% of the remaining available water resources in the basin area of Golmud. Our results indicate that the expansion of the local renewable energy industry has exerted significant pressure on the already scarce water resources in Golmud. Therefore, future increases in the installed capacity for renewable energy electricity generation should be planned scientifically, by considering the availability of water resources as a constraint.

Keywords: arid region, solar and wind energy, water footprint of electricity generation, water resource requirement, scenario analysis

OPEN ACCESS

Edited by:
Monica Salvia, Institute of Methodologies for Environmental Analysis (IMAA), Italy

Reviewed by:
Hongbing Tan, Hohai University, China
Chunye Lin, Beijing Normal University, China

Correspondence:
Wenjuan Hou
houwenjuan@igsnrr.ac.cn

Specialty section:
This article was submitted to Environmental Economics and Management, a section of the journal Frontiers in Environmental Science

Received: *09 March 2022*
Accepted: *07 April 2022*
Published: *12 May 2022*

Citation:
Hou W, Li X, Yang L, Ta W and Jia X (2022) Carrying Capacity of Water Resources for Renewable Energy Development in Arid Regions in Northwest China: A Case Study of Golmud, Qinghai. Front. Environ. Sci. 10:892414. doi: 10.3389/fenvs.2022.892414

1 INTRODUCTION

The renewable energy industry has been developing rapidly against the backdrop of global warming (Celik and Ozgür, 2020). Since the Chinese President Xi Jinping declared China's goal to reach a peak in carbon emissions by 2030 and become carbon neutral by 2060 at the 75th session of the United Nations General Assembly in September 2020, China's electricity generation from wind, solar, hydraulic, and other renewable energy sources has been progressing rapidly. Northwest China boasts of a high solar radiation intensity and abundant wind resources (Zuo, 1981; Xue et al., 2001; Chen et al., 2011) and has a huge area of desert and unutilized land. Due to this sound base (comparative advantage) for wind and solar power generation (Cui et al., 2020), this region has been ranked at the top in China in terms of installed wind and solar power capacity (Wu et al., 2018). As evinced by the Report on China's Electric Power Development 2020, by the end of 2020, Inner Mongolia, Xinjiang, Ningxia in the Northwest China had a grid-connected installed wind power capacity greater than 10 MW; Qinghai, Xinjiang, Inner Mongolia, and Ningxia had an installed capacity of photovoltaic (PV) exceeding 10 MW; all of China's eight concentrated solar power (CSP) generation projects with a grid-connected installed capacity of above 5 MW were located in the northwest region (Qinghai, Gansu, and Inner Mongolia). Evidently, this vital region has taken a substantial lead in electricity generation output of wind energy, PV, and CSP.

China's enormous efforts to boost renewable energy electricity generation have been accompanied by water resource problems. Studies have shown that the ongoing global energy structure transition will significantly reduce the carbon footprint in the future, but will very likely increase the water footprint (WF) (Mekonnen et al., 2016). Electric power and thermal energy production are expected to further increase in the future, placing more pressure on the scarce freshwater resources in arid and semiarid regions. China is one of the world's major water-scarce countries, characterized by a per capita share of water resources that is 1/4 the global average (2200 m^3/person). The arid and semiarid regions in Northwest China, especially the Qaidam Basin in northwestern Qinghai, incur severe water scarcity, and the water resource crisis there is expected to be further aggravated by renewable energy development. To maintain a high conversion efficiency of the PV and CSP, PV cells and heliostats must be cleaned regularly (Meldrum et al., 2013; Bukhary et al., 2018). In arid desert areas, they must be cleaned more frequently due to the low vegetation coverage (Mani and Pillai, 2010). The vapor circulation systems and condensers for CSP generation also use large amounts of water (Fthenakis and Kim, 2010; Ali, 2017). By contrast, operational water consumption for wind power generation is almost zero. Only the water consumption during the operation of renewable energy enterprises has been described above. From the whole life-cycle perspective, the supply-chain WF is also a major source of water consumption, including the manufacturing of wind energy, PV, and CSP generation equipment and raw materials, as well as construction materials for facilities. For example, the large amount of electricity consumed for purifying silicon and other semiconductor materials is produced by fossil-fired power plants, whose water-cooling systems also consume water. Studies have shown that the whole-life-cycle water consumption for wind power generation in China was 0.64 L/kWh (Li et al., 2012), that for PV was 1.72 L/kWh, and that for CSP was respectively 2.74 and 7.36 times that for PV and wind power (Burkhardt et al., 2011). Furthermore, renewable energy development requires the immigration of technical workers, who, like consumers, will produce a demand for huge water resources.

Golmud, a city located at the central-south margin of China's Qaidam Desert, has an arid, low-precipitation climate but a long sunshine duration and high solar radiation intensity. Due to its rich wind and solar resources and large desert areas, Golmud's wind and solar power generation industry has undergone rapid development; however, this has been accompanied by significantly increasing water resource requirements. In addition, among Golmud's five major industries (including saline lake chemistry, oil and gas chemistry, and new coal chemistry), the saline lake chemistry alone consumes a vast amount of water (5.56×10^7 m^3/year). With the scale increase in renewable energy electricity generation in Northwest China, the mismatch between wind and solar resources and water resources is expected to worsen. Thus, rigorously quantifying the water resource requirements for renewable energy development in water-scarce Golmud has become a pressing, critical problem. Accordingly, here we estimated the current water resource requirements for renewable energy enterprises operations and by their employees. On this basis, we went on to predict their water consumption against the backdrop of climate change and renewable energy development. Our results provide a timely and theoretical basis for making the most of Golmud's natural advantages for renewable energy electricity generation and supporting China's sustainable energy structure transition.

2 MATERIALS AND METHODS

2.1 Brief Description of the Study Region

Golmud, a city under the jurisdiction of Haixi Mongol and Tibetan Autonomous Prefecture, is located in western Qinghai. The city consists of two geographically different areas: a basin area and a mountainous area (the Tanggula Mountains) (**Figure 1A**). Golmud has a typical arid plateaucontinental climate, with an average air temperature of −7.8°C in winter and 17.1°C in summer in the basin area, and a maximum annual sunshine duration of 3323.9h (in the Xiaozaohuo area). Spatially, precipitation in the basin area decreases from east to west, with an annual precipitation of 13.7–45.5 mm in 2019, representing an increase of 0.9% over previous years. Golmud has a large total geographical area encompassing 11.92 million ha, but the proportion of its utilizable land is low, with 3.90 million ha of cropland, 47,000 ha of urban and built-up land, and 7.97 million ha of other land use types. Qinghai, of which Golmud is a jurisdiction unit, is currently ranked first in China for the ratio of the output of renewable energy electricity generation to the total output of local electricity generation, and also ranks first in terms of the ratio of PV power generation (>20%) (**Figure 1B**). This study focused on the basin area of Golmud, which is located at the central-south margin of the Qaidam Basin, with an area of 7.14 million ha.

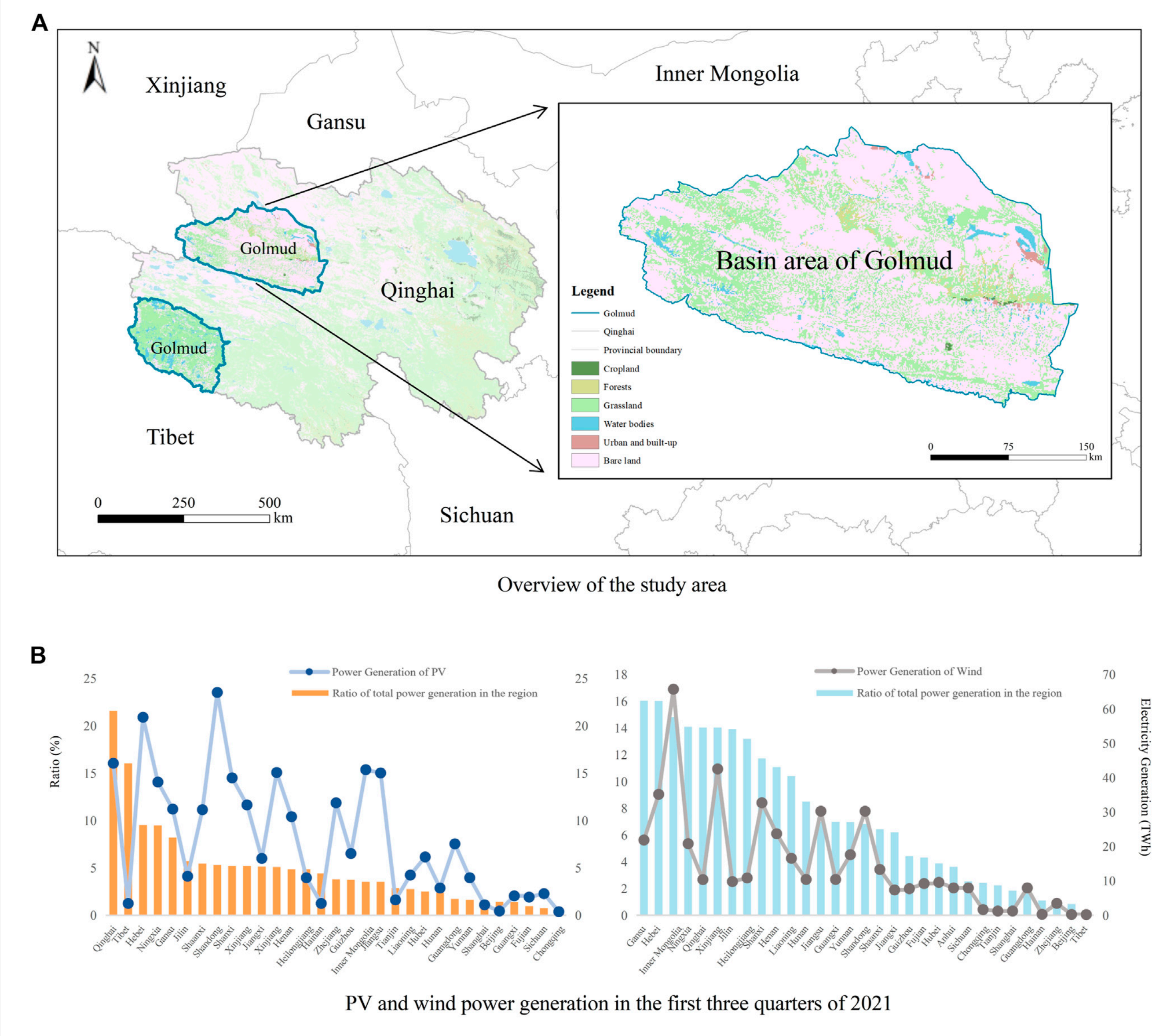

FIGURE 1 | Brief profile of geographical information **(A)** and electricity generation **(B)** in the study region.

Total water resources of the Golmud region are 7.24×10^9 m^3, among which, the total water resources in the basin area of Golmud is 2.26×10^9 m^3, and the surface water is 2.06×10^9 m^3. The total water consumption in the basin area of Golmud was 2.04×10^8 m^3 in 2015. Among them, agricultural water consumption was 1.78×10^8 m^3, accounting for 87.26% of the total water consumption, industrial consumption is 0.19×10^8 m^3 (9.31%), and domestic consumption was 0.03×10^8 m^3 (1.47%), and ecological consumption was 0.04×10^8 m^3 (1.96%) (Golmud Local Chronicles Compilation Committee, 2020).

2.2 Research Design

First, the water footprint (WF) of electricity generation and that of consumer were reviewed and estimated based on previous studies. Next, water consumption by the renewable energy enterprises in Golmud was assessed under four different current scenarios of the local/nonlocal origin of electricity generation equipment and raw materials used and of the employees. Then, the water consumption by these enterprises in 2030 was predicted under three different scenarios varying the scale and proportion of renewable energy installed capacities. The relations of temperature and precipitation to total water resources were quantified *via* multiple linear regression using meteorological and water resource data of 1997–2018. Based on the fitting results of multiple linear regression, the total water resources in basin area of Golmud in 2030 was predicted using the average of temperature and precipitation in the different models and scenarios in the Coupled Model Intercomparison Project Phase-6 (CMIP6). Finally, the water consumption by the renewable energy enterprises was analyzed vis-à-vis total available water resources, and the potential scale of renewable energy electricity generation

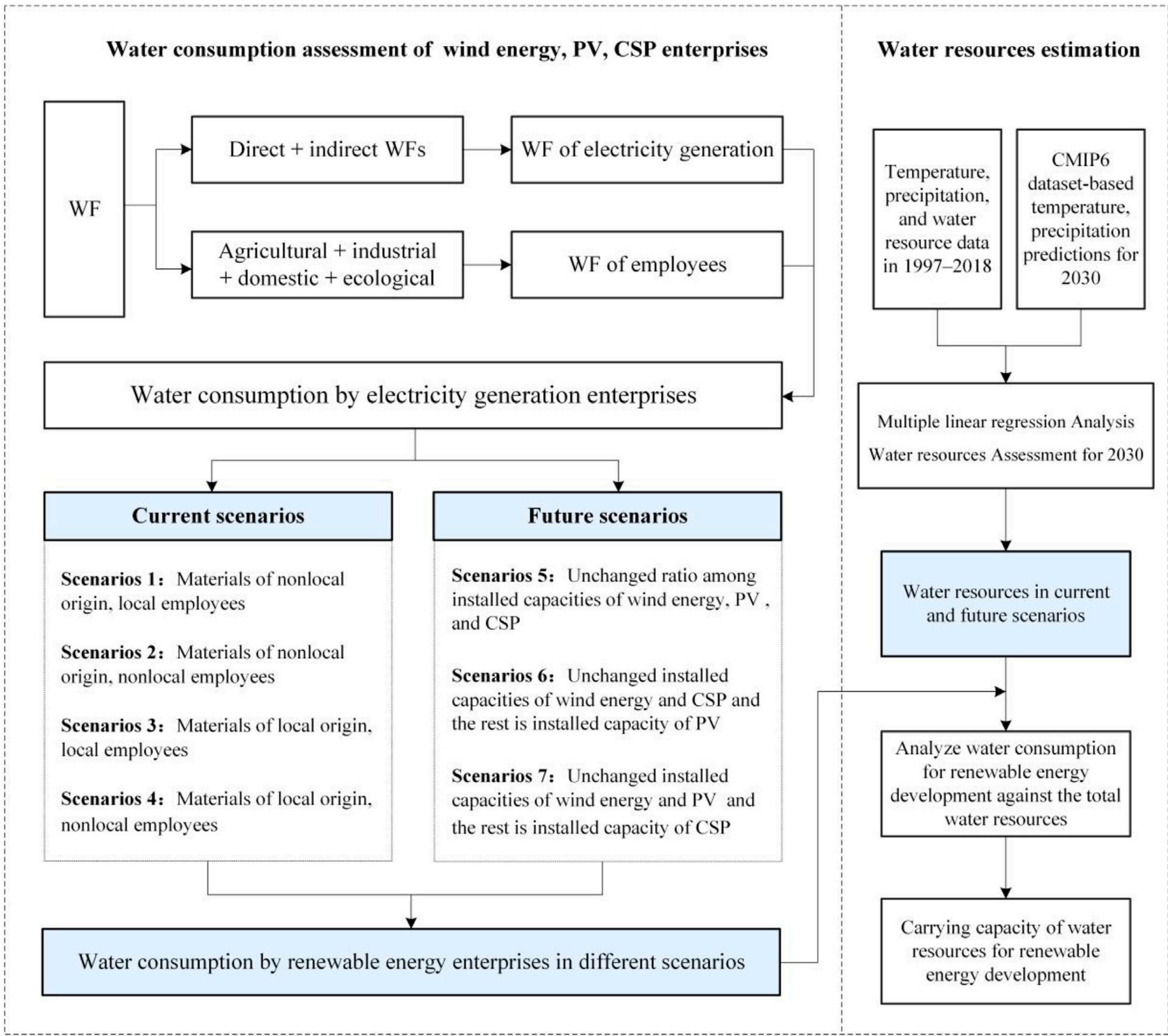

FIGURE 2 | Research framework of this study.

supportable by water resources in basin area of Golmud under current and future scenarios was estimated. The aim was to provide an empirically based reference for enhanced decision making on renewable energy development and water resource conservation in Golmud (**Figure 2**).

2.3 Method for Estimating the Water Consumption by Renewable Energy Enterprises

According to the water footprint evaluation theoretical system based on water footprint network (WFN) of Hoekstra et al. (2011) and Jia et al. (2012), the WF of an enterprise includes that of its operational WF and supply-chain WF. The operational WF refers to the WF directly arising from the product production and daily use by employees, while the supply-chain WF refers to the WF of raw materials and security services required for maintaining operations. Most researchers have assessed the WF of different types of renewable energy enterprises from the life cycle perspective (Burkhardt et al., 2011; Yang et al., 2015); that is, the WF covers that of operations, raw materials, and facility construction (Meldrum et al., 2014; Mekonnen et al., 2015). Compared with the WF theoretical system of Hoekstraand Hung (2003; 2011), there is this part of the difference between domestic and industrial water consumption by enterprise employees—that is, the WF resulting from daily security services. This was calculated separately in this study as the WF of enterprise employees. Based on its comprehensive consideration, water consumption by a renewable energy enterprise was divided into two parts: water consumption for power generation and that by employees.

2.3.1 Method for Estimating the Water Consumption for Electricity Generation

In this study, renewable energy enterprises were classified into three types according to the current main types of renewable energy used for power generation: PV, CSP, and wind power plants, and the WF of electricity generation was calculated by these enterprise types. The WFs of all three types of enterprises were summed as the total water requirement for electricity generation, as follows:

$$AWC_T = AWC_{E,PV} + AWC_{E,W} + AWC_{E,CSP} \tag{1}$$

where AWC_T is the total water consumption for electricity generation by renewable energy enterprises, $AWC_{E,PV}$ is the water consumption for PV generation, $AWC_{E,W}$ is the water consumption for wind power generation, and $AWC_{E,CSP}$ is the water consumption for CSP generation. *WF* was calculated on an annual basis. The water requirement for each type of electricity generation was calculated this way:

$$AWC = WF \times P(p) \tag{2}$$

where *WF* is the water footprint of a given type of renewable energy power generation (m^3/kWh), and $P(p)$ is the output of that type of renewable energy power generation (kWh). The *WF* data were obtained by reviewing previous studies of different types of renewable energy enterprises (See part 3.1). *P*(p) was calculated by multiplying the installed capacity and operating time of electricity generation.

2.3.2 Method for estimating the Water consumption by Employees

A water resource account is established for enterprise employees. The WF of an enterprise employee included the consumption of agricultural and manufactured products, domestic water, and ecological services:

$$WF_C = WF_{\mathrm{agr}} + WF_{ind} + WF_{liv} + WF_{eco} \tag{3}$$

where WF_C is the WF of an individual consumer, WF_{agr} is the agricultural WF of an individual consumer, WF_{ind} is the industrial WF of an individual consumer, WF_{liv} is the domestic WF of an individual consumer, and WF_{eco} is the ecological WF of an individual consumer.

The total employee WF of the renewable energy enterprises in basin area of Golmud was calculated by multiplying the number of employees in these enterprises and the per capita WF:

$$AWC_C = WF_C \times P(\mathrm{u}) \tag{4}$$

where AWC_C is the total water consumption by the employees, WC_C is the per consumer WF, and *P*(u) is the number of employees.

2.3.3 Scenario analysis

Considering that both the equipment and raw materials used and the employees hired by the renewable energy enterprises may be of local or nonlocal origin, four current scenarios were defined (**Table 1**). Three future scenarios of renewable energy development that considered the impact of climate change were also defined. Total water consumption for electricity generation by these enterprises in each scenario was calculated. In scenarios 1 and 2, all the equipment and raw materials used by the renewable energy enterprises were manufactured nonlocally, and all their employees were of local and nonlocal origin, respectively. In scenarios 3 and 4, all the equipment and raw materials were manufactured locally, and all the employees were of local and nonlocal origin, respectively. In scenarios 1 and 2, the renewable energy enterprises had an operational WF but lacked a supply-chain WF. In scenarios 3 and 4, the renewable energy enterprises had both operational and supply-chain WFs.

The future scenarios of renewable energy development and climate change were based on scenario 4, which entailed the largest water consumption. Three scenarios of renewable energy development (three different ratios between the installation capacities for wind energy, PV, and CSP generation) in Golmud in 2030—when China was assumed to peak in carbon emissions (with a total installed wind and solar power generation capacity of 1.2 GW)—were considered (**Table 1**). The annual output of wind and solar power generation in Golmud under these future scenarios was estimated by assuming the ratio of the total installed capacity in Golmud to the national total and the electricity generator operating time in 2020 would remain unchanged in 2030. Total water resources in the future scenarios were estimated using the average temperature and precipitation in 2030 as predicted by three models (BCC-CSM2-MR, MRI-ESM2, GFDL-ESM4) in the CMIP6 (https://esgf-node.llnl.gov/projects/cmip6/) and fitted multiple linear regression model. Considering the water resources in basin area of Golmud come from precipitation and melted ice and snow, so changes in both temperature and precipitation will drive changes in the total water resources. The multiple linear regression model was obtained from temperature, precipitation, and total water resources data from 1998 to 2016.

2.4 Data sources

The electricity generation WF of the three types of renewable energy enterprises (wind energy, PV, and CSP) was estimated by screening the results reported in the literature (see part 3.1), and the water footprint data applicable to this region are selected for study. The electricity generation output of Golmud's renewable energy enterprises *P*(p) was estimated by multiplying their current installed capacities, as published on the official website of the Golmud government (http://www.geermu.gov.cn/details?id=bb5cf28b7cab7b40017cc4c6d02b0142), and their PV and wind power generation operating time, as published on the official website of the National Energy Administration (http://www.nea.gov.cn/2020-02/28/c_138827910.htm, http://www.gov.cn/zhengce/zhengceku/2020-05/16/content_5512148.htm) or CSP generation operating time, as estimated by Li et al. (2012), assuming operation at full capacity of solar power plants under ideal solar radiation conditions. The installed capacity data of China's wind energy, PV, and CSP generation as of 2020 came from the Report on China's Electric Power

TABLE 1 | Definition of scenarios.

Factors considered Scenario description		Origin of materials	Origin of employees	Installed capacity of renewable energy		Climate change
Current scenarios	Scenario 1	Nonlocal origin	Local origin	2020 Certain installed capacity	Wind : PV : CSP = 18:82:1	2020
	Scenario 2	Nonlocal origin	Nonlocal origin			
	Scenario 3	Local origin	Local origin			
	Scenario 4	Local origin	Nonlocal origin			
Future scenarios	Scenario 5	Local origin	Nonlocal origin	2030 Certain installed capacity	Wind : PV : CSP ratio will remain unchanged	2030
	Scenario 6				The installed capacity for wind energy and CSP will remain unchanged, and that for PV will increase	
	Scenario 7				The installed capacity for wind energy and PV will remain unchanged, and that for CSP will increase	

TABLE 2 | Installed capacity and electricity generator operating time data of renewable energy enterprises in Golmud.

Renewable energy enterprises	Installed capacity (MW)	Generation operating time (h/year)
PV	4100	1511
Wind	900	1743
CSP	50	2000
Installed capacity of solar and wind in Golmud	5050	—
Installed capacity of solar and wind in China	540,000	—

Development 2020 (China Electric Planning and Engineering Institute, 2021). **Table 2** shows the data used for estimating the water consumption for electricity generation by the local renewable energy enterprises.

The data needed in the calculation of water consumption by the employees of local renewable energy enterprises includes: 1) The agricultural WF (per capita agricultural water consumption) was estimated by multiplying the amount of virtual water contained in a unit mass of agricultural and livestock products and their per capita consumption. The virtual water contained in a unit mass of agricultural and livestock products in Qinghai was derived from research data of the virtual water contained in a unit mass of agricultural and livestock products in Qinghai published on the official website of the Water Footprint Network (https://www.waterfootprint.org/en/); the virtual water contained in a unit mass of Chinese agricultural and livestock products estimated by Hoekstra et al. (2011); and the virtual water contained in the major agricultural and livestock products in Xinjiang, as estimated by Cheng et al. (2016). The per capita consumption data of agricultural and livestock products in Qinghai came from the Qinhai Statistical Yearbook 2020 (Qinghai Provincial Bureau of Statistics, 2020). Using the above data, the per capita agricultural WF in the study area was estimated by selecting 15 agricultural and livestock products generally consumed in China and in Golmud (**Table 3**). 2) The WF of industrial products is difficult to estimate using the method for agricultural products, due to the complexity of the manufacturing processes and technologies involved (Jia et al., 2012), so it is usually estimated based on their proportional relationship with agricultural products (Long et al., 2005). In this study, the virtual water contained in industrial products in Northwest China was estimated to be 7% of that contained in agricultural and livestock products, based on studies by the International Institute for Hydraulic and Environmental Engineering (2002), the researchers Old and Ksnce (2003) and Zhang and Shen (2017), with the different economic development levels of Chinese provinces considered accordingly. 3) The per capita domestic and ecological water consumption values in Qinghai were respectively estimated using data published in the China Statistical Yearbook 2020 (National Bureau of Statistics of the People's Republic Of China, 2020). 4) The number of employees in these enterprises P(u) was estimated based on a field survey in 2021 of renewable energy enterprises in Qinghai. The number of employees in an electricity generation enterprise is related to its capacity and type of electricity generation. Generally, the ratio of the number of employees to the installed capacity was about 3 persons/10 MW for wind energy and PV installed capacity and 18 persons/10 MW for CSP installed capacity (the CSP enterprises were in the start-up stage and used complex processes, thus requiring more employees for operations and maintenance). Applying the above employee/installed capacity ratios, the number of employees in a 4100 MW PV enterprise installed capacities in 2020 was estimated to be ca. 1230; likewise, that of a 900 MW wind power enterprise was estimated to be ca. 27, and that of a 50 MW CSP enterprise was estimated to be ca. 90. Using

TABLE 3 | Virtual water contents, per capita consumption of agricultural and livestock products and per capita agricultural WF.

Major agricultural and livestock products	Virtual water contents (m^3/kg)	Per capita consumption (kg/year)	Per capita agricultural WF (m^3/year/person)
Grain	1.13	108.1	122.153
Edible oil	2.36	9.7	22.892
Vegetable	0.1	54.7	5.47
Pork	2.21	8.7	19.227
Beef	12.6	9	113.4
Mutton	5.2	5.5	28.6
Poultry	3.65	3.4	12.41
Aquatic products	5	2	10
Egg	3.55	4.2	14.91
Milk	1	18.8	18.8
Fruits	1	28	28
Sugar	1.8	4.1	7.38
Tea	10.95	0.5	5.475
Tobacco	2.96	22.5	66.6
Alcohol	1.39	3.5	4.865
Total	—	—	480.18

these, the total annual water consumption by the employees of the local renewable energy enterprises was thus estimated. The number of employees in the 2030 future scenarios was also estimated using the above method.

The data of water resources in the study area came from the Qinghai Water Resource Communique 2020 (http://slj.haixi.gov.cn/info/1037/25916.htm). The climate data in 2030 was predicted using three models (BCC-CSM2-MR, MRI-ESM2, and GFDL-ESM4) in the CMIP6 data set (https://esgf-node.llnl.gov/projects/cmip6/). The predictions were calibrated, using the observational data from 2015 to 2020, to address differences between the simulation results yielded by the CMIP6 models for the basin area of Golmud and the observational data, thereby obtaining more accurate climate data for the future scenarios. The regression relationship of the total water resources as a function of precipitation and temperature was fitted using the observational data of the temperature, precipitation, and water resources calculated by observational data in Haixizhou, Qinghai in 1998–2016, as published in the Qinghai Water Resource Communique and on the official website of the China Meteorological Administration.

3 RESULTS AND ANALYSIS

3.1 WF of Electricity Generation and Employee for Renewable Energy Enterprises

Based on previous studies, the life-cycle WF of PV generation is different due to different PV panel materials (monocrystalline silicon, polycrystalline silicon, and thin-film cadmium telluride) they used. The WF of monocrystalline silicon, the PV cell material commonly used in the study area, was 1.72 L/kWh (Fthenakis and Kim, 2010). Of the whole-life-cycle WF (1.72 L/kWh), the water consumption for the manufacturing of PV equipment and power plant construction materials accounted for the majority (89%) (Wild-Scholten and Alsema, 2005). The whole life-cycle WF of terrestrial wind power generation was 0.64 L/kWh. Similar to PV power generation, the water consumption for the manufacturing of raw materials (including the iron, steel, and glass fiber for wind turbine generator manufacturing and power plant construction materials) accounted for the majority (99.4%) (Yang et al., 2015). Unlike wind power and PV, CSP has a high whole life-cycle WF of 4.71 L/kWh, with the operational WF (wet cooling and heliostat cleaning, etc.) accounting for the majority (89%) (Burkhardt et al., 2011). The water consumption for CSP generation was estimated based on wet cooling in this study, although dry cooling and hybrid cooling systems are also used for CSP generation (Fthenakis and Kim, 2010).

Using the formulas described in **Section 2** and data from the literature, the agricultural, industrial, domestic, and ecological WFs in Qinghai were estimated at 480.18, 33.61, 52.85, and 23.13 m^3/person/year, respectively. The agricultural WF was the highest, being 14.27, 9.09, and 20.76 times the industrial, domestic, and ecological WFs, respectively. The per capita water consumption in Qinghai was estimated at 589.77 m^3/year (**Figure 3**).

3.2 Water Consumption by Renewable Energy Enterprises Under Current Scenarios

Figure 4 shows the current water consumption by local renewable energy (wind and solar) enterprises estimated using the data and methods described above. In Scenario 1 (nonlocal origin of raw materials and local origin of employees), water consumption by the local renewable energy enterprises was minimally estimated at 1.62×10^6 m^3, most of which (72.9%) constituted water consumption by PV enterprises (1.18 ×

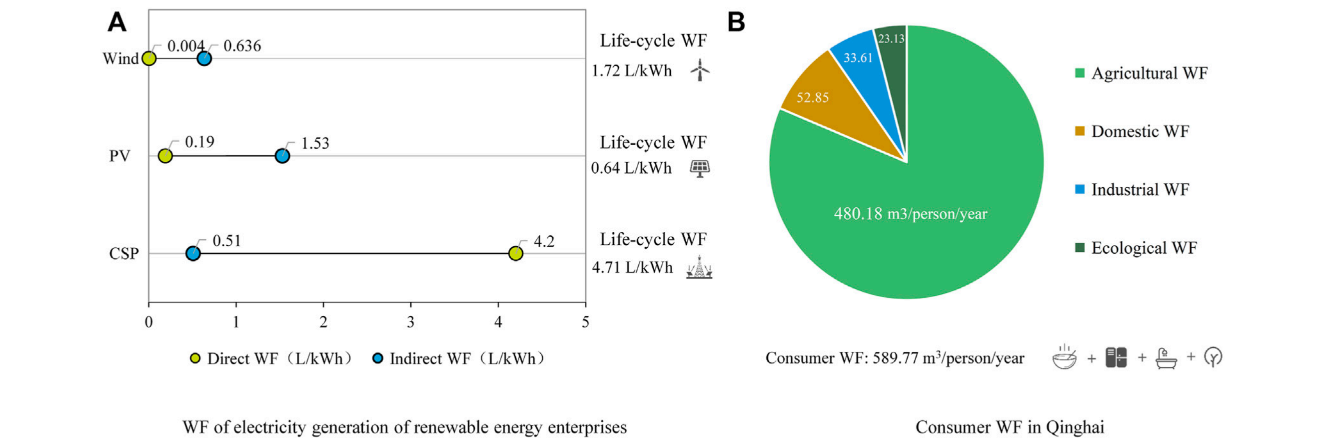

FIGURE 3 | WF of renewable energy enterprises: **(A)** electricity generation WF; **(B)** employee WF.

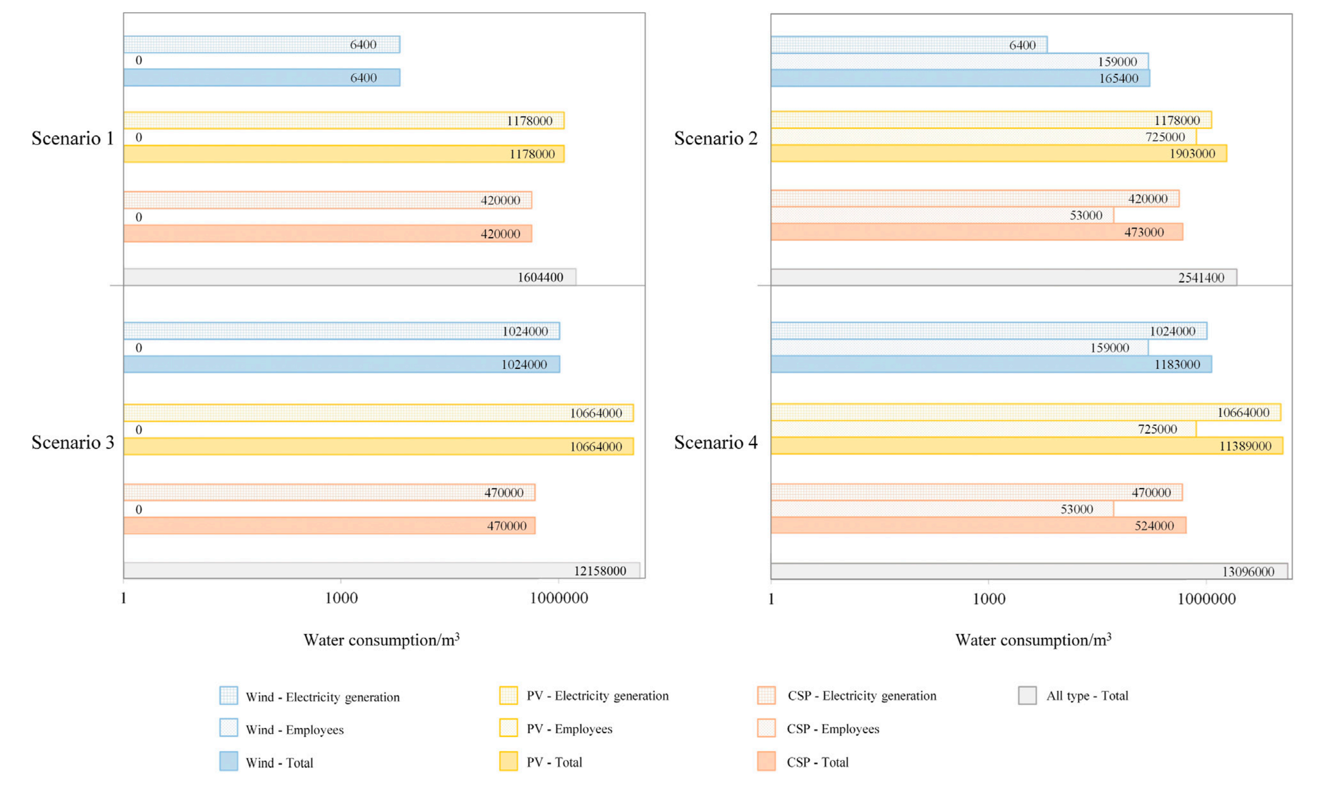

FIGURE 4 | Water consumption by renewable energy enterprises in Golmud under current scenarios.

10^6 m^3), followed by that of CSP enterprises (4.2×10^5 m^3). In Scenario 2, total water consumption increased to 2.54×10^6 m^3 due to the nonlocal origin of employees, with that by PV enterprises (1.90×10^6 m^3) again accounting for the majority of it. The WF of CSP was relatively large. In Scenario 1, the output generation of PV was 62 times that of CSP, but the water consumption for PV was only 2.8 times that of CSP. In Scenario 4 (local origin of raw materials and nonlocal origin of employees), total water consumption by local renewable energy enterprises was estimated at 1.31×10^7 m^3, the highest among the current scenarios, with that contributed by the PV enterprises increasing to 1.14×10^7 m^3. Annual water consumption by the renewable energy enterprises under the current scenarios was estimated in the range of 1.62×10^6–1.31×10^7 m^3. In 2020, water consumption by the three salt chemistry enterprises in Golmud was 5.56×10^7 m^3 (with a salt output of 5.56×10^7 t), being 4.24–34.37 times that of local renewable energy enterprises. In the 2020 scenarios, water consumption by the local renewable

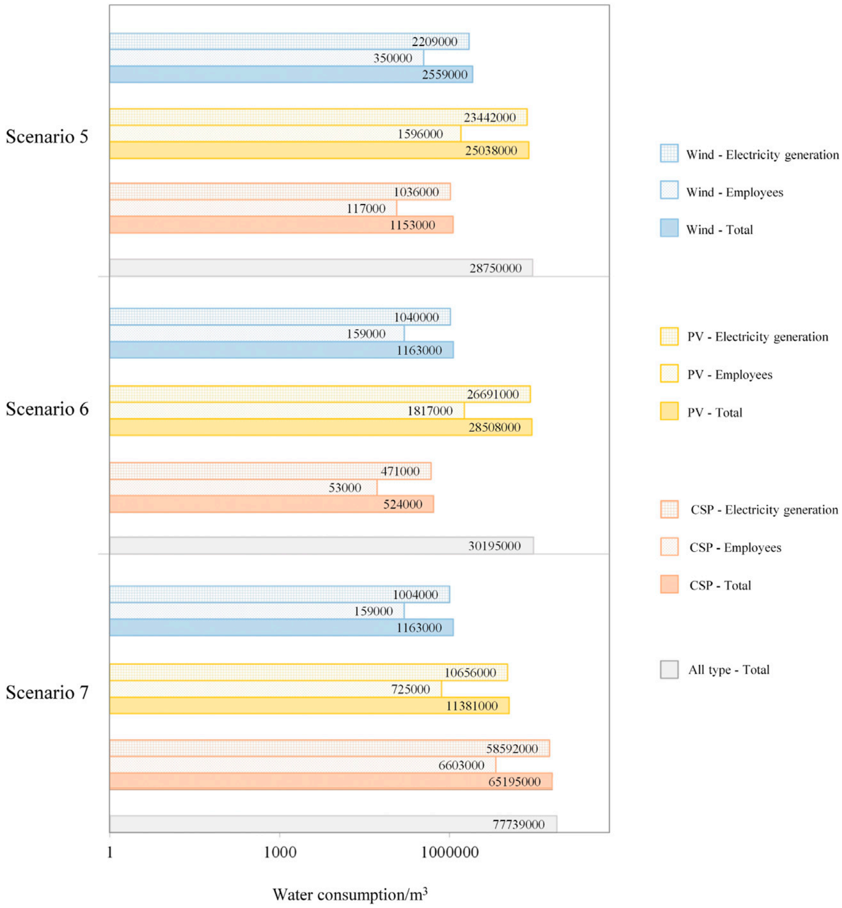

FIGURE 5 | Water consumption by renewable energy enterprises in Golmud under future scenarios.

energy enterprises accounted for 0.2–1.2% of the total water consumption and 1–6.8% of the industrial water consumption in Haixizhou, Qinghai (Water Resources Department of Qinghai Province, 2020).

The multiple-year average of annual total water resources in the basin area of Golmud was 2.06 × 10^9 m^3, and the ecological water consumption under natural conditions was removed, leaving 7.71 × 10^8 m^3 of utilizable water resources. In the four current scenarios, the water consumption by the local renewable energy enterprises accounted for 0.07%–0.6% of the total water resources and 0.21%–1.7% of the utilizable water resources. According to estimates by relevant government departments, the utilized water resources in the basin area of Golmud reached 3.69 × 10^8 m^3 in 2015, leaving only 4.02 × 10^8 m^3 of unused water resources, these mainly concentrated in the basins of the Nalinggele River and Tuolahai River basins. Assuming that all remaining water resources are utilizable and earmarked for renewable energy electricity generation (with the water consumption by consumers not included in the remaining amount), the available water resources can support an additional electricity generation capacity of 2.34×10^{11} kWh/year for PV, 6.28×10^{11} kWh/year for wind power, and 8.5×10^9 kWh/year for CSP. In Scenario 4 (with the highest water consumption among the current scenarios), water consumption by local renewable energy enterprises accounted for 30% of the remaining water resources. Thus, renewable energy development in Golmud could be shifted to those areas with more utilizable water resources, such as the Nalinggele River and Tuolaihai River basins.

3.3 Water Consumption by Renewable Energy Enterprises Under Future Scenarios

Among the future scenarios of climate change and installed capacity of renewable energy expansion, water consumption by local renewable energy enterprises was the highest (7.77 × 10^7 m^3) under Scenario 7, being 5.98 times that under Scenario 4 and 40% higher than the 2020 water consumption by Golmud's salt chemistry enterprises (**Figure 5**). The significant increase in the CSP installed capacity led to a significant increase in water consumption under Scenario 7 because whole life-cycle WF of CSP had reached up to 4.71 L/kWh, this 7.36 and 2.74 times that of wind power and PV, respectively. Furthermore, the number of employees required for per unit of CSP enterprises exceeded that of wind power or PV. The water consumption under Scenarios 5 and 6 were 2.88×10^7 and 3.02 × 10^7 m^3, thus respectively 54.9% and 57.0% greater than under

Scenario 4 (2020). This was a consequence of the doubling of wind power, PV, and CSP installed capacities in Scenario 5 and the significant increase in the installed PV capacity in Scenario 6 vis-à-vis the corresponding capacities in Scenario 4. The water consumption between Scenarios 5 and 6 differed by only 0.14×10^7 m^3. This was because the installed capacity of PV increased but the installed capacities of wind power and CSP decreased in Scenario 6 when compared with Scenario 5—that is, the increased water consumption for PV power generation was partially offset by the decreased water consumption for wind power and CSP generation and, more importantly, the installed capacities of CSP in these two future scenarios differed insignificantly.

Total water resources in the basin area of Golmud in the 2030 future scenarios (2.15×10^9 m^3, predicted using the temperature and precipitation data of CMIP6) increased by 4.4% (9.1×10^7 m^3) when compared with 2020. However, due to the significant increase in the installed capacity for renewable energy electricity generation, water consumption increased by 54.9–493.6% (2.88×10^7–7.77×10^7 m^3), accounting for 1.3%–3.6% of total water resources in 2030. The small increase in total water resources and significant increase in water consumption were expected to bring about a water crisis. In addition, the remaining water resources in 2015 reached a low level of 4.01×10^8 m^3—that is, renewable energy development under future scenarios was expected to consume 7.15%–19.35% of the remaining utilizable water resources, at a minimum.

4 DISCUSSION

Because the arid and semi-arid regions in Northwest China have high solar radiation intensity, they are deemed suitable for PV and CSP development projects. Yet the direct contradiction between high water consumption by renewable energy enterprises and long-term water resource scarcity in Northwest China inherently limits the potential increase in installed capacity of solar power there despite the rich solar energy resources it offers. In particular, CSP generation is expected to emerge as the main driver of solar power generation in China in the foreseeable future because of its advantages, such as integrated power generation and heat storage, 24-h continuous power supply, and capacity for peak regulation. In December 2018, China's first 100 MW-class molten-salt, tower-type CSP plant finished construction and commenced its grid-connected operation; this project is equipped with the world's largest, highest, and 24-h operating 100 MW-class molten salt tower. The State Grid has started planning a power system in Northwest China whereby fossil-fired power plants are completely replaced by CSP plants (http://www.cnste.org/html/huiyi/2021/0716/8118.html). However, the prerequisite wet cooling and the heliostat cleaning for maintaining CSP plants in desert areas together consume a tremendous amount of water resources. Undoubtedly, water resource is a factor constraining the renewable energy development in the arid and semi-arid regions of Northwest China. Thus, renewable energy development, especially the expansion of solar power generation, should be planned appropriately based on an accurate assessment of water resources available now and in the near future.

Furthermore, the quantity of water was primarily considered in the water consumption for renewable energy power generation in this study. Actually, the quality of water can also affect the efficiency of electricity generation from the various types of renewable energy sources (Meldrum et al., 2013). Nevertheless, given the present inadequate understanding of the mechanisms underlying the effects of water quality upon the efficiency of renewable energy power generation, water quality could be not considered in this study. Concerning our method to quantify water consumption, the WF of renewable energy power generation estimated here included blue water WF only, thus omitting gray water WF due to the difficulty to obtain sufficient local data on its parameters. Another challenge, more generally, is the relatively few studies on WF of PV, CSP, and wind power generation for China, especially the WF of CSP generation. Therefore, the WF estimates in our study was mainly based on the internationally unified standards of water consumption for renewable energy power generation. However, the operational and supply-chain WF of a given enterprise is influenced by its background environment—that is, enterprises in different geographical areas likely differ in the magnitude of their respective WF. Hence, the water consumption levels estimated in this study might be partially biased compared with the actual situation. Nonetheless, by considering multiple factors that are known to affect water consumption and estimating water consumption levels under four current and three future scenarios, the water consumption estimates reported here could be given as ranges of values, thereby mitigating the effect of a WF estimation deviation upon the results (and any inferences drawn from them).

5 CONCLUSION

For the current scenarios examined, the water resource requirements for wind power, PV, and CSP generation in Golmud ranged from 1.62×10^6 to 1.31×10^7 m^3, accounting for ca. 0.07%–0.6% of the current total water resources in Golmud. Scenario 1 (nonlocal origin of renewable energy electricity generation equipment and raw materials and local origin of employees) featured the lowest water consumption, whereas Scenario 4 (local origin of equipment and raw materials and nonlocal origin of employees) entailed the highest water consumption. The water consumption by Golmud's salt chemistry industry (5.56×10^7 m^3) is 4.24–34.37 times that of the local renewable energy industry—that is, the water resource requirement for the local renewable energy industry, despite being at the early stage of development, is also quite high. An increase of 6.17×10^6 kW in the installed capacity of wind and solar power under the 2030 scenarios requires an extra 1.57×10^7–6.46×10^7 m^3 in water resource appropriation for the local renewable energy industry, this representing 7.15%–19.35% of the remaining utilizable water resources in basin area of Golmud. Different ratios between the installed capacities of wind power, PV, and CSP lead to differing water resource requirements. Scenario 7 (unchanged installed capacity for wind power and PV generation and significantly increased installed capacity for CSP generation) has the maximum requirement of total water resources, at 7.77 ×

$10^7 m^3$, accounting for 3.6% of the total water resources in 2030. Scenarios 5 and 6 differ insignificantly in their water resource requirements. The small increase total water resources coupled with the huge expansion of the local renewable energy industry in 2030 are expected to place much greater pressure on Golmud's water resources.

DATA AVAILABILITY STATEMENT

The original contributions presented in the study are included in the article/Supplementary Material, further inquiries can be directed to the corresponding author.

AUTHOR CONTRIBUTIONS

WH: conceptualization, methodology, formal analysis, writing—original draft. XL: methodology, data curation, and visualization. LY is responsible for conceptualization, writing—reviewing and editing and project administration. WT and XJ are responsible for investigation, writing—review and editing as well.

FUNDING

This study was supported by the "Strategic Priority Research Program" of the Chinese Academy of Sciences (XDA23100403), and "Strategic Research Program" of the Chinese Academy of Sciences (GHJ-ZLZX-2021-18).

ACKNOWLEDGMENTS

The authors acknowledge the Chinese Academy of Sciences and Ministry of Science and Technology, with gratitude.

REFERENCES

Ali, B. (2017). The Cost of Conserved Water for Power Generation From Renewable Energy Technologies in Alberta, Canada. *Energy Convers. Manag.* 150, 201–213. doi:10.1016/j.enconman.2017.08.019

Bukhary, S., Ahmad, S., and Batista, J. (2018). Analyzing Land and Water Requirements for Solar Deployment in the Southwestern United States. *Renew. Sust. Energ. Rev.* 82 (3), 3288–3305. doi:10.1016/j.rser.2017.10.016

Burkhardt, J. J., III., Heath, G. A., and Turchi, C. S. (2011). Life Cycle Assessment of a Parabolic Trough Concentrating Solar Power Plant and the Impacts of Key Design Alternatives. *Environ. Sci. Technol.* 45, 2457–2464. doi:10.1021/es1033266

Celik, A. N., and Özgür, E. (2020). Review of Turkey's Photovoltaic Energy Status: Legal Structure, Existing Installed Power and Comparative Analysis. *Renew. Sust. Energ. Rev.* 134, 110344. doi:10.1016/j.rser.2020.110344

Chen, X., Song, Li., Huang, H., Liu, A., and Fan, S. (2011). Study on Characteristics of Wind Energy Resources in Two Typical Areas in China. *Acta Energiae Solaris Sinica* (3), 55–61.

Cheng, Z., Lu, B., Xiong, S., Wang, H., Hu, Y., and Zhang, Q. (2016). Analysis on Water Resources Carrying Capacity Based on Water Footprint Model in Xinjiang. *J. Water Res. Water Eng.* 27 (6), 54–59. doi:10.11705/j.issn.1672-643X.2016.06.10

China Electric Planning and Engineering Institute (2021). *Report on China's Electric Power Development 2020*. Beijing: People's Daily Press.

Cui, Y., Zhang, H., Zhong, W., Zhao, Y., Wang, Z., and Xu, B. (2020). Day-ahead Scheduling Considering Participation of Price-based Demand Response and CSP Plant in Wind Power Accommodation. *Power Syst. Technol.* 44 (1). doi:10.13335/j.1000-3673.pst.2019.0181

Fthenakis, V., and Kim, H. C. (2010). Life-cycle Uses of Water in U.S. Electricity Generation. *Renew. Sust. Energ. Rev.* 14, 2039–2048. doi:10.1016/j.rser.2010.03.008

Golmud Local Chronicles Compilation Committee (2020). *Golmud Yearbook*. Xi'an: Shaanxi Science and Technology Press.

Hoekstra, A. Y., Chapagain, A. K., Aldaya, M. M., and Mekonnen, M. M. (2011). *The Water Footprint Assessment Manual: Setting the Global Standard*. London: Earthscan.

Hoekstra, A. Y., and Hung, P. Q. (2003). "Virtual Water Trade: A Quantification of Virtual Water Flows Between Nations in Relation to Internation Corp Trade," in Proceedings of the International Expert Meeting on Virtual Water Trade 12, Delft, 25–47.

Jia, Y, Yan, Y, Wang, C, Liang, Y, Zhang, Y, Wu, G, et al. (2012). The Estimation and Application of the Water Footprint in Industrial Processes. *Acta Eco Sin* 32 (20), 6558–6565. doi:10.5846/stxb201201060030

Li, X., Feng, K., Siu, Y. L., and Hubacek, K. (2012). Energy-water Nexus of Wind Power in China: The Balancing Act between CO2 Emissions and Water Consumption. *Energy Policy* 45, 440–448. doi:10.1016/j.enpol.2012.02.054

Long, A., Zhang, Z., Xu, Z., and Su, Z. (2005). Analysis of Water Footprint and Consumption Pattern in Gansu Province. *Adv. Water Sci.* 16 (3), 418–425. doi:10.3321/j.issn:1001-6791.2005.03.019

Macknick, J., Meldrum, J., Nettles-Anderson, S., Heath, G., and Miara, A. (2014). Life Cycle Water Use for Photovoltaic Electricity Generation: A Review and Harmonization of Literature Estimates. *Environ. Res. Lett.* 8 (1), 1458–1460. doi:10.1109/pvsc.2014.6925190

Mani, M., and Pillai, R. (2010). Impact of Dust on Solar Photovoltaic (PV) Performance: Research Status, Challenges and Recommendations. *Renew. Sust. Energ. Rev.* 14 (9), 3124–3131. doi:10.1016/j.rser.2010.07.065

Mekonnen, M. M., Gerbens-Leenes, P. W., and Hoekstra, A. Y. (2016). Future Electricity: The Challenge of Reducing Both Carbon and Water Footprint. *Sci. Total Environ.* 569-570 (nov.1), 1282–1288. doi:10.1016/j.scitotenv.2016.06.204

Mekonnen, M. M., Gerbens-Leenes, P. W., and Hoekstra, A. Y. (2015). The Consumptive Water Footprint of Electricity and Heat: A Global Assessment. *Environ. Sci. Water Res. Technol.* 1 (3), 285–297. doi:10.1039/c5ew00026b

Meldrum, J., Nettles-Anderson, S., Heath, G., and Macknick, J. (2013). Life Cycle Water Use for Electricity Generation: A Review and Harmonization of Literature Estimates. *Environ. Res. Lett.* 8, 015031. doi:10.1088/1748-9326/8/1/015031

National Bureau of statistics of the people's Republic of China (2020). *China Statistical Yearbook*. Beijing: China Statistics Press.

Old, T., and Kance, S. (2003). "Virtual Water Trade to Japan and in the World. Virtual Water Trade," in Proceedings of the International Expert Meeting on Virtual Water Trade, 12-13 December 2002. Editor A. Y. Hoekstra Edited (Delft, Netherlands: Value Water Res. Rep. Ser).

Qinghai Provincial Bureau of statistics (2020). *Qinghai Investigation Team of National Bureau of Statistics QinghaiStatistical Yearbook*. Beijing: China Statistics Press.

Wild-Scholten, M. d., and Alsema, E. A. (2005). Environmental Life Cycle Inventory of Crystalline Silicon Photovoltaic Module Production. *MRS Proc.* 895, 304. doi:10.1557/proc-0895-g03-04

Wu, D., Wang, J., Li, H., Wang, Z., Zhang, N., and Kang, C. (2018). Research on Capacity and Delivery Sequence of Interconnected Northwestern-Southwestern Power Grid Towards Renewable Energy Accommodation. *Power Syst. Technol.* 42 (7). doi:10.13335/j.1000-3673.pst.2018.0697

Xue, H., Zhu, R., Yang, Z., and Yuan, C. (2001). Assessment of Wind Energy Reserves in China. *Acta Energiae Solaris Sinica* (02), 167–170. doi:10.3321/j.issn:0254-0096.2001.02.010

Yang, D., Liu, J., Yang, J., and Ding, N. (2015). Life-cycle Assessment of China's Multi-Crystalline Silicon Photovoltaic Modules Considering International Trade. *J. Clean. Prod.* 94, 35–45. doi:10.1016/j.jclepro.2015.02.003

Zhang, L., and Shen, J. (2017). Analysis on Temporal and Spatial Pattern Evolution and Driving Factors of Water Footprint Intensity in China. *Stat. Decis.* (17), 143–147. doi:10.13546/j.cnki.tjyjc.2017.17.033

Zuo, D. (1981). Solar-energy Resources in Beijing Region. *Scientia Geographica Sinica* 1 (1), 44–51. doi:10.13249/j.cnki.sgs.1981.01.005

Conflict of Interest: The authors declare that the research was conducted in the absence of any commercial or financial relationships that could be construed as a potential conflict of interest.

Publisher's Note: All claims expressed in this article are solely those of the authors and do not necessarily represent those of their affiliated organizations, or those of the publisher, the editors, and the reviewers. Any product that may be evaluated in this article, or claim that may be made by its manufacturer, is not guaranteed, or endorsed by the publisher.

Energy Use Greenization, Carbon Dioxide Emissions, and Economic Growth: An Empirical Analysis Based in China

Wang Xinmin[1], *Kashif Iqbal*[2]* *and Yichu Wang*[3]

[1]School of Business, Northwest Normal University, Lanzhou, China, [2]College of International Students, Wuxi University, Wuxi, China, [3]School of Oriental and African Studies, University of London, London, United Kingdom

Developing countries are constantly facing the problem of environmental degradation. Environmental degradation is caused by the consumption of non-renewable energy for economic growth, but the consequences of environmental degradation cannot be ignored. The main purpose of this study is to investigate the relationship between three variables (i.e., energy use greenization, CO_2 emission, and economic growth) in the case of China using simultaneous equation modeling techniques and data for the period 2000–2018. The results indicate that (1) there is a long-term equilibrium relationship between energy use greenization, carbon emissions, and economic growth in China. Energy use greenization not only reduces carbon dioxide emissions but also promotes sustainable economic growth in China. (2) Carbon emissions and economic growth have promoted energy use greenization, indicating that the pressures of environmental climate and economic transformation in China have forced energy use greenization to a certain extent. (3) The contribution rate of energy use greenization to economic growth shows an inverted U-shaped trend that rises first and then decreases subsequently, while carbon emissions have a relatively large contribution rate to green energy use and economic growth. These results have far-reaching policy directions for the environmental sustainability goals of the Chinese economy.

Keywords: energy use greenization, CO_2 emission, economic growth, energy economics, China

Edited by:
Jingli Fan,
China University of Mining and Technology, Beijing, China

Reviewed by:
Muhammad Mohsin,
Jiangsu University, China
Ugur Korkut Pata,
Osmaniye Korkut Ata University, Turkey

Correspondence:
Kashif Iqbal
kashii42@yahoo.com

Specialty section:
This article was submitted to Environmental Economics and Management, a section of the journal Frontiers in Environmental Science

Received: *07 February 2022*
Accepted: *13 May 2022*
Published: *30 June 2022*

Citation:
Xinmin W, Iqbal K and Wang Y (2022) Energy Use Greenization, Carbon Dioxide Emissions, and Economic Growth: An Empirical Analysis Based in China.
Front. Environ. Sci. 10:871001.
doi: 10.3389/fenvs.2022.871001

INTRODUCTION

Environmental issues, such as climate change and global warming, have become critical issues at the global level and have begun to pose a serious threat to sustainable development (Bekun et al., 2019; Yam et al., 2021). Owing to industrialization and urbanization, the world has experienced considerable economic growth over the past few decades (Li et al., 2021). Carbon dioxide emissions are likely to grow at the second-fastest pace on record this year as global economies recover from the COVID-19 recession and invest stimulus money into fossil fuels (Zheng et al., 2019a). Fossil fuels will remain an important source of the energy mix in many countries (Liang et al., 2022). The drastic economic development of the BRIC countries has led to a large number of environmental problems, especially the emission of carbon dioxide (Pata, 2021). Substantial economic growth is in one way or another related to fossil fuel consumption that produces large amounts of greenhouse gases (GHGs) in the environment, which warms the atmosphere (Pata and

Kumar, 2021; Yin et al., 2021). The increasing concentration of GHGs is primarily responsible for global warming and climate change. The production of GHGs is considered a major factor affecting carbon dioxide emissions (Wu et al., 2021). Climate change has certain adverse impacts on human health, and among many factors, carbon dioxide is the most important gas that deteriorates the environment and human health. Brazil, India, China, and South Africa are fast emerging economies (FECs) owing to their strong fundamental base and reliance on fossil fuel energy sources, leading to increased GHG emissions and adverse effects on human health (Liu et al., 2020). The European Union (EU) considers that renewable energy sources can mitigate the effects of climate change (Bekun et al., 2021c). Reducing CO_2 emissions has become the primary priority for all economies throughout the world. Countries ratified the United Nations Framework Convention on Climate Change in 1992 to slow the global climate crisis, which is also the premise and foundation of cooperation among countries worldwide. In 2015, the Paris Climate Change Summit established a sustainable development goal for 2030. With the rapid development of the Chinese economy, China's dependence on energy consumption is increasing every year. The overall energy consumption of China in 2018 was 4.644 billion tons of standard coal, 3.3% higher than the previous year, and the total carbon emissions were 2.5% higher than the preceding year (Zheng et al., 2020; Zhou et al., 2021). Although the proportion of coal consumption has decreased by 1.4% from the previous year, it still accounts for 59% of the total energy consumption (Liu and Cai., 2018). Based on the statistical report of the International Energy Agency (IEA), China is the world's largest emitter of CO_2 and carbon emissions still continue to increase rapidly. China is highly concerned about the climate change problem. China has increased its efforts to promote low-carbon development in recent years by efficiently reducing GHG emissions, effectively boosting the adaptive capacity of the climate and continuously improving systems and mechanisms of operation.

China has also contributed positively to the Paris Agreement's finalization, adopting stronger policies to achieve sustainable development by 2030 and carbon neutrality by 2060 (Chi et al., 2021). Zheng et al. (2019a) suggest that the energy intensity per person may greatly reduce CO_2 emissions from energy-related companies in China, and the gross domestic product (GDP) is a crucial factor influencing the increase in industrial CO_2 emissions. Renewable energy is considered an alternative to overcome global warming and an effective choice to continue fossil fuel growth (Zheng et al., 2019b). Renewable technologies help to reduce CO_2 emissions from conventional energy sources to achieve a sustainable energy consumption system (Asongu et al., 2018). Furthermore, energy-saving solutions can help close the gap between CO_2 emissions and economic growth, enabling long-term development. To achieve sustainable energy development, China needs to continuously promote energy use greenization, complete the economic transformation, control CO_2 emissions, and bear the responsibility of major countries to reduce CO_2 emissions from a strategic standpoint.

Thus, given this background, it is important to evaluate the nexuses between energy use greenization, CO_2 emissions, and economic growth in China. Some pioneering studies (Anwar, 2016; Ishaque, 2017; Shahzad et al., 2017) have empirically investigated the nexus between CO_2 emissions and macroeconomic variables on the economy as a whole. In China, only few studies exist on the relationship between energy use greenization, CO_2 emissions, and economic growth. Second, based on the generalized method of moments (GMM) and structural modeling, this study analyzes CO_2 emissions, energy use greenization, and economic growth by using simultaneous equations. The primary goal of using the simultaneous system approach is just to account for simultaneity issues to avoid potential problems in error estimations of econometric researchers (Baydoun and Aga, 2021). The results of this study will provide important information for the development of environment and economic growth policies.

The remainder of this study is structured in the following manner. First, we provide a literature review and the econometric models and data are then examined. Subsequently, empirical analysis and debate are presented. Finally, the findings are addressed, and the policy implications.

A BRIEF LITERATURE REVIEW

The literature has shown widespread concern about the links between energy use, economic growth, and CO_2 emissions. As mentioned previously, the present literature can be classified into three sections of research; the first section focuses on the relationship between energy use and economic growth. The relationship between energy and growth is of great interest to not only economists but also to policymakers, because of its significant policy implications. Some researchers suggest that both key macro-variables and economic growth are the most important pillars of energy use; thus, the application of these candidate series to energy development programs is advocated (He et al., 2021). Energy use directly and/or indirectly contributes to economic growth (Wu et al., 2021). Conversely, other studies showed that energy use is determined by economic growth and not vice versa (Lan et al., 2021); several studies also found that both true GDP and energy use are interdependent, and there is bidirectional causality between them (Bekun et al., 2021c). However, some studies found that there is no causal relationship between energy use and economic development (Bekun et al., 2021b; Fang et al., 2022). The development of clean energy has a positive impact on the economic growth of new EU members (Regulation of the European Parliament and of the Council, 2021). Moreover, renewable energy is a dynamic force for economic growth in the OECD and G-7 economies (Bekun et al., 2019). The development of renewable energy is an important part of green economic growth and it also depends on the implementation of environmental regulation policies, which have made important contributions to the development of renewable energy.

The second section focuses on renewable energy consumption and environmental issues. With the rapid development of green energy, more researchers have studied the fundamental contribution of green energy development to the mitigation of emissions at the national, regional, and world levels. Many recent studies have confirmed the beneficial effects of green energy on environmental quality (Bekun, 2022). For example, the use of green energy leads to a drop in CO_2 emissions (Bekun et al., 2021a; Irfan et al., 2022). The development of green energy has contributed significantly to environmental improvements in 85 developed and developing economies (Osobajo et al., 2020). In addition, several researchers have found a bidirectional causal relationship between green energy and environmental quality (Ahukaemere et al., 2020; Manta et al., 2020). However, the empirical results of some studies do not demonstrate a causal relationship between renewable energy consumption and environmental quality (Liu et al., 2021). Conversely, the exploitation of green energy has reduced CO_2 emissions in five selected African economies (Baydoun and Aga, 2021). In the face of economic growth trajectories, renewable energy is a panacea for sustainable development.

The third section of the literature examines the relationship between renewable energy and economic growth, and the validity of the Environmental Kuznets Curve (EKC) Hypothesis. According to the EKC hypothesis, the relationship between economic growth and environmental deterioration resembles an inverted U-shaped curve. Many scholars, such as Osobajo et al. (2020), have proven the inverted U-shaped relationship between economic growth and CO_2 emissions, but the "EKC hypothesis" was generally regarded as a phenomenon to be tested in the present research. In some existing studies, the inverted U-shaped curve confirms that the growth of low-income per capita intensifies environmental deterioration until it stabilizes at middle-income levels, at which point fresh growth leads to improved environmental conditions (Liu and Cai, 2018; Iqbal et al., 2022). Several studies have validated the EKC hypothesis in a single nation (Liu et al., 2019; Pata and Isik, 2021). However, the EKC hypothesis does not hold true for China (Pata and Aydin, 2020; Pata and Caglar, 2020). In five EU nations, there was an inverted U-shaped relationship between CO_2 emissions and economic development (Zheng et al., 2019a; Chen and Ma, 2021). Some studies found that economic growth boosts the usage of renewable energy (Chi et al., 2021). These findings suggest that the relationship between non-renewable energy, renewable energy, and economic growth appears to be U-shaped in the economy of India (Sarfraz et al., 2021). In the long run, CO_2 emissions have an N-shaped relationship with the real GDP per capita, rather than the traditional U-shaped curve given by the EKC hypothesis (Olivier and Peters, 2020). Through a comparative study, the economic growth in Australia accelerated CO_2 emissions. In the long run, Canadian trade appears to increase CO_2 emissions, while economic growth and urban population also boost CO_2 emissions (Shah et al., 2021).

Based on structural modeling and the GMM estimator, this study used simultaneous equations to analyze the relationship between energy use greenization, CO_2 emissions, and economic growth from an empirical research perspective, and the results were compared with those from existing research. The primary motivation for using the simultaneous system technology was to compensate for the simultaneity problems and prevent a potentially biased evaluation by econometric researchers (Hassan et al., 2019). The interconnection between economic growth, energy consumption, and CO_2 emissions has been examined extensively by researchers both at home and abroad, offering a solid framework for this research. China is rapidly developing as a country. China is the world's second-largest producer and consumer of energy and the second-largest emitter of CO_2. China faces enormous pressure from the international community to save energy and reduce emissions. The subject of this case study is the connection between China's energy use greenization, CO_2 emissions, economic growth, energy conservation, and emission reduction through energy policy and policy formulation.

Compared with that of previous studies, the marginal contribution of this study is as follows: first, based on the existing literature, the Cobb–Douglas production function model was used to introduce CO_2 emissions and construct a regression equation for carbon dioxide emissions. Second, an empirical study of the link between energy use greenization, CO_2 emissions, and economic growth was conducted through the simultaneous equation modeling approach. Third, this study uses the proportion of clean energy consumption such as natural gas, nuclear power, and hydropower in total energy consumption as a measure of energy use greenization.

MODEL BUILDING AND DATA

Model Building

To study the relationship between economic growth, CO_2 emissions, and energy use greenization, we used the Cobb–Douglas production function model, wherein the income is influenced by the level of technology, labor, and capital. Apart from these factors, energy as a potential factor in economic growth has also been cited (Rousseeuw and Yohai, 1984). Generally, the extended Cobb–Douglas production function is expressed as follows:

$$Y = AK^{\beta_1} L^{\beta_2} E^{\beta_3} e^{\varepsilon}, \quad (1)$$

where Y represents the income level; A represents the level of technology; K represents the capital; L represents the labor; E represents energy use; and β_1, β_2, and β_3, respectively, represent the output elastic coefficients of capital, labor, and energy use. There is a linear relation between CO_2 emissions (CE) and energy use, and at any time: E = b.CE at a specific level of technology. Furthermore, some energy economists discovered that renewable energy may reduce CO_2 emissions while also increasing economic growth; hence, renewable energy can be used as a component in the production function model (Tiwari, 2011; Mahjabeen, 2020; Venkatraja, 2020). Therefore, the extended Cobb–Douglas production function model is expressed as follows:

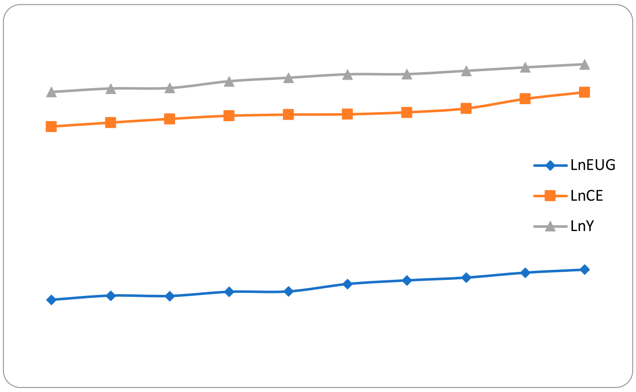

FIGURE 1 | Time series of lnEUG, lnCE, and lnY.

TABLE 1 | Descriptive statistics.

Variable	Mean	SD	Min	Max
CE_t	13.160	12.201	0.572	29.51
Y_t	3651	2026	5305.8	11,817.6
EUG_t	0.020	0.011	0.007	0.052
FD_t	0.412	0.132	0.189	0.603
F_t	1.756	2.632	-1.321	8.511
T_t	75.111	12.123	56.122	97.010
L_t	0.455	0.275	0.055	1.742
K_t	21.154	3.218	18.556	32.852
OP_t	47.701	30.102	15.521	100.514
U_t	0.445	0.273	0.054	1.746
EU_t	115.43	16.820	83.714	149.904

$$Y = AK^{\beta_1}L^{\beta_2}bCE^{\beta_3}RE^{\beta_4}e^{\varepsilon}. \quad (2)$$

We considered the logarithm of the Cobb–Douglas production function model **(2)** and obtained the following result:

$$\ln Y_t = \beta_0 + \beta_1 \ln CE_t + \beta_2 \ln EUG_t + \beta_3 \ln L_t + \beta_4 \ln K_t + \varepsilon_t, \quad (3)$$

where $\beta_0 = \ln A$; t is the subscript; T represents the time period; Y indicates the income level; CE indicates the CO_2 emissions per capita; EUG indicates energy use greenization; K represents the capital; L indicates labor; and ε is a random variable. The production function model was separated into multiple analysis models to inspect the relationship between energy use greenization, economic growth, and CO_2 emissions. These new models were established on the foundation of past theoretical and empirical research. Energy use greenization and CO_2 emissions can be used as the dependent or independent variables. To examine the causality of income, capital (K), labor (L), energy use (EU), squared GDP (Y^2), direct foreign investment (F), trade openness (T), oil prices (OP), financial development (FD), and urbanization (U) are defined as independent variables.

An empirical study of the link between energy use greenization, CO_2 emissions, and economic growth is conducted through the following three function models:

$$\ln Y_t = \beta_0 + \beta_1 \ln CE_t + \beta_2 \ln EUG_t + \beta_3 \ln K_t + \beta_4 \ln L_t + \varepsilon_t, \quad (4)$$

$$\ln CE_t = \beta_0 + \beta_1 \ln Y_t + \beta_2 \ln EUG_t + \beta_3 \ln Y_t^2 + \beta_4 \ln EU_t + \beta_5 \ln U_t + \beta_6 \ln F_t + \varepsilon_t, \quad (5)$$

$$\ln EUG_t = \beta_0 + \beta_1 \ln Y_t + \beta_2 \ln CE_t + \beta_3 \ln OP_t + \beta_4 \ln FD_t + \beta_5 \ln T_t + \varepsilon_t. \quad (6)$$

Model (4) shows that the GDP is affected by CO_2 emissions, renewable energy, labor, and capital (Danish et al., 2017). Model (5) indicates that the amount of CO_2 emissions is affected by the GDP per capita, renewable energy, energy use, squared GDP per capita, urbanization, and direct foreign investment (Lee and Brahmasrene, 2014). Model (6) indicates that energy use greenization is affected by the GDP, oil prices, CO_2 emissions, and external trade (Ishaque, 2017).

Models **(4–6)** are tested by using the GMM, which is a frequently used multidirectional model. The GMM can be used to solve the problem of endogeneity, and an effective and reliable evaluation is conducted when any heteroscedasticity occurs. In addition, two diagnostic examinations are required for estimating models **(4–6)**; namely, Hansen's test for excessive identification limits and Durbin–Wu–Hausman's (DWH) test for examining the issue of endogeneity (Engle and Granger, 1987). The first test provides proof of the validity of the instrumental variable. This tests the hypothesis that these instruments are suitable, and this hypothesis was consequently rejected. The second test was used to examine endogeneity issues in the three forecasted models. The alternative hypothesis affirms the endogeneity of the instruments. If the hypothesis is accepted, the technology of the instrumental variable is unsuitable.

Data and Descriptive Statistics

To evaluate models **(4–6)**, we collected the annual data of China from 2000 to 2018. These data are sourced from the Chinese Energy Statistic Yearbook and the Chinese Statistical Yearbook. To eliminate the possible heteroscedasticity problem, the horizontal time series data are processed by a natural logarithm to obtain lnEUG, lnCE, and lnY, as shown in **Figure 1**. **Figure 1** shows the changing trends of lnEUG, lnCE, and lnY. It shows that since 2000, the proportion of clean energy consumption in China generally transitioned from a slow increase (2000–2008) to a rapid increase (2009–2018); namely, from 5.5% in 2000 to 15.7% in 2018, indicating that China has achieved certain results in energy use greenization and energy consumption structure optimization. Simultaneously, although China's CO_2 emissions are increasing every year, the growth rate has slowed down significantly since 2012. This shows that the continuous optimization of the industrial structure and energy consumption structure has significantly reduced the growth rate of carbon emissions, even in 2016, which showed a negative growth of 0.3%. In addition, China's per capita GDP also showed a steady growth trend during the sample period, but the growth rate has declined in recent years.

TABLE 2 | Variable correlations.

Variable	CE_t	Y_t	EUG_t	FD_t	F_t	T_t	L_t	K_t	OP_t	U_t	EU_t
CE_t	1										
Y_t	0.701***	1									
EUG_t	-0.615**	0.150	1								
FD_t	0.691**	0.521**	0.705*	1							
F_t	0.284	0.163	0.322	0.540**	1						
T_t	0.558**	0.411	0.269	0.628*	0.728**	1					
L_t	0.420	0.499	0.498	0.702	0.309	0.436	1				
K_t	0.579	0.620**	0.371	0.624	0.477	0.415	0.535	1			
OP_t	0.561**	0.563***	0.620**	0.597**	0.581*	0633***	0.699*	0.584***	1		
U_t	0.401	0.519	0.310	0.400	0.381	0.469	0.601	0.506	0.604**	1	
EU_t	0.661***	0.401***	0.450*	0.489	0.503***	0.554***	0.400**	0.509*	0.593***	0.495*	1

Indicates significant paths: *$p < 0.05$, **$p < 0.01$, ***$p < 0.001$

TABLE 3 | Simultaneous equation generalized method of moment estimation for the models.

Dependent variables						
Independent variable	**Y (GDP per capita) model (4)**		**CO_2 (CO_2 emissions) model (5)**		**EUG (EU greenization) model (6)**	
	Coef	**P**	**Coef**	**P**	**Coef**	**P**
Y (GDP per capita)			0.701	(0.000)	0.221	(0.031)
Y^2 (squared GDP)			-0.092	(0.061)		
CE (CO_2 emissions)	-0.102	(0.019)			0.245	(0.000)
EUG (EU greenization)	0.063	(0.000)	-0.050	(0.000)		
K (capital)	0.412	(0.000)				
L (labor)	-0.192	(0.059)				
EU (energy use)			0.411	(0.000)		
U (urbanization)			0.152	(0.022)		
F (foreign direct investment)			0.111	(0.043)		
OP (oil prices)					0.109	(0.125)
FD (financial development)					0.210	(0.029)
T (trade openness)					0.112	(0.098)
Constant	7.211	(0.000)	4.521	(0.009)	11.001	(0.000)
Hansen's test (p)	13.216	(0.674)	20.514	(0.301)	18.011	(0.430)
DWH test (p)	5.001	(0.032)	10.401	(0.003)	6.331	(0.033)

Table 1 shows that during the sample period, the GDP per capita ranged from 5,305.8 to 11,817.6 Yuan; the per capita CO_2 emissions ranged from 0.57 to 29.5 tons; and energy use greenization accounted for 0.007–0.054% of the total ultimate energy consumption.

Table 2 shows that the GDP and CO_2 emissions per capita showed the largest correlation, whereas the urbanization variable showed the lowest. Moreover, there is a significant negative relationship between CO_2 emissions and energy use greenization. Energy use greenization is positively correlated with the GDP per capita, which implies that increasing energy use greenization in the total ultimate energy use may reduce CO_2 emissions per capita and increase the GDP per capita.

EMPIRICAL RESULTS AND DISCUSSION

Through Hansen's test and the DWH test, the evaluation coefficients of models **(4–6)** are presented in **Table 3**. The empirical findings of model **(4)** indicate that CO_2 emissions show a significant negative correlation with the GDP. If the per capita CO_2 emissions increase by 1%, the economic growth is expected to decrease by about 0.1%. This result was confirmed by the survey results of Pata (2018), who showed that Turkey's GDP per capita had not reached a level to reduce environmental pollution, and the consumption of renewable energy was not a solution to reduce CO_2 emissions. However, China's energy use greenization has a remarkable impact on economic growth, which confirms the growth hypothesis. These results are supported by the cases of developing countries (Zheng et al., 2019a; Iqbal et al., 2019). In addition, the capital and labor force coefficients show significantly positive and negative correlations with the economic growth, respectively.

The empirical results of model **(5)** show that the per capita GDP influences CO_2 emissions per capita. The research shows that there is a positive relationship between the per capita GDP and per capita CO_2 emissions. If the GDP per capita increases by 0.1%, the CO_2 emissions per capita are expected to increase by about 0.70%. This shows that the improvement of economic growth worsens the environmental quality. This result was confirmed by the findings of Höhne et al. (2011) for 15 European countries. We found a negative correlation between energy use greenization and CO_2 emissions. If energy use greenization increases by 1%, CO_2 emissions per capita are expected to decrease by about 0.05%. This result is the same as that in the references (Shahzad et al., 2017). However, our result contradicts the findings of one of the references (Shabani and Shahnazi, 2019). Energy use shows a significant positive correlation with CO_2 emissions per capita. If energy use increases by 1%, the CO_2 emissions per capita are expected to rise by about 0.41%. Similarly, urbanization and trade openness have positive correlations with CO_2 emissions per capita.

Finally, the empirical findings of model **(6)** display that the GDP per capita is significantly positive for energy use greenization at a level of 5%. Energy use greenization is expected to increase by about 0.22% if the economic growth increases by 1%. This finding shows that there is a positive and significant relationship between energy use greenization and economic growth, which implies that the increase in economic growth will lead to an increase in energy use greenization. Regarding the environmental variable, we found a positive correlation between CO_2 emissions per capita and the demand for renewable energy. If CO_2 emissions per capita increase by 1%, energy use greenization is expected to increase by about 0.24%. These results show that CO_2 emissions per capita increase environmental degradation and promote the production and consumption of carbon-free sustainable energy, while lower CO_2 emissions lead to lower renewable energy consumption. We also found a positive correlation between financial development and the demand for renewable energy. If financial development increased by 1%, the energy use greenization was expected to increase by about 0.21%. This result showed that financial development was an important catalyst to promote production and energy use greenization in China.

The aforementioned results indicated that (i) energy use greenization promotes per capita GDP growth; (ii) increased economic growth leads to higher CO_2 emissions, and continued increases in CO_2 emissions may reduce economic growth; and (iii) increased CO_2 emissions can boost the demand for renewable energy, thereby reducing CO_2 emissions.

DISCUSSION AND CONCLUSION

The main objective of this study was to investigate the relationship between CO_2 emissions, energy use greenization, and economic growth. Our findings show that energy use greenization may have narrowed the gap between China's economic growth and CO_2 emissions from 2000 to 2018. This study tested these interrelations using the simultaneous equation model approach. This approach enables us to simultaneously examine the relationship between energy use greenization, CO_2 emissions, and GDP. Our empirical results show that energy use greenization can promote economic growth. We also found that economic growth leads to increased CO_2 emissions, which promotes energy use greenization. Our findings also emphasize that energy use greenization can narrow the gap between China's economic growth and CO_2 emissions.

The key policy implications emerging from the aforementioned results are as follows. First, we found a significant relationship between the GDP and CO_2 emissions. The results indicate that economic growth leads to an increase in CO_2 emissions, and the continuous increase of CO_2 emissions reduces economic growth. Hence, to solve the contradiction between energy supply and security, economic growth, and environmental protection, the Chinese government has promulgated the Energy Law of the People's Republic of China. The Chinese government encourages the development of clean energy and defines hydropower, nuclear energy, natural gas, coal-bed methane, wind energy, biomass energy, solar energy, geothermal energy, and ocean energy as clean and low-carbon energy. Moreover, energy greenization should be an important component of the CO_2 emission mechanism. Increased CO_2 emissions can increase the demand for energy use greenization, thereby continuously reducing CO_2 emissions. Second, there is a significant relationship between energy use greenization and CO_2 emissions. An increase in CO_2 emissions can increase the demand for energy use greenization and continuously reduce CO_2 emissions. High fossil fuel consumption and the sharp increase in CO_2 emissions have brought severe challenges to the sustainable development of China's economy. Energy structure transformation and CO_2 emission reduction have become important issues for China. Therefore, China is geographically well-positioned and has a high potential for the production of renewable energy from solar and wind energy. The Chinese government has increased the proportion of renewable energy usage in total energy consumption through measures to adjust the energy structure. In terms of economic and social aspects, the Chinese government not only encourages energy use greenization, but also provides funds to improve renewable energy consumption and industrial energy use. China implements green finance policies and reduces investments in high-polluting and high-emission industries. These measures will enable China to profit entirely from the interests of energy use greenization. On the one hand, energy use greenization is changing the traditional energy consumption structure, transitioning from coal-fired cogeneration in the past to distributed energy structures, combined natural gas cooling, heating, and power, and complementary clean and renewable energy. Simultaneously, the peak adjustment capacity of clean energy reserves should also be improved to expand its utilization scope. Conversely, owing to China's high demand for coal in the short term, the development and application of coal cleaning technology need to be accelerated, and black energy (coal) needs to be transformed into green energy.

SUGGESTIONS AND POLICY IMPLEMENTATIONS

We need to acknowledge the positive role of energy use greenization in reducing CO_2 emissions to achieve sustainable economic growth. Simultaneously, as a developing country, China should pay special attention to maintaining economic growth and employment stability in the process of energy use greenization. Therefore, it is necessary to promote the transformation of the traditional energy production industry (such as coal and oil industries) to mechanization and intelligence, transition from simple resource mining to deep processing, and eliminate the backward production capacity. Some manufacturing industries (with large traditional energy consumption, such as power production and supply industries) need to be encouraged to purchase green raw materials and green production equipment, increase the proportion of clean energy and renewable energy input, and realize energy use greenization from the production side. For the green energy-related industries (such as the new energy vehicle industry), policy support, including subsidies and research and development tax incentives, is required in the initial stage of enterprise incubation and green technology research.

On the one hand, energy use greenization requires changing the traditional energy consumption structure, from the cogeneration of coal and power to distributed energy, cold, heat, and electricity systems, and complementary clean energy and renewable energy. Simultaneously, the peak regulation capacity of clean energy reserves should also be improved to expand its scope of utilization. Conversely, because China still has a high demand for coal in the short term, the development and application of clean coal technologies should be accelerated; these include carbon emission control technologies, carbon sequestration (including carbon capture), and clean coal combustion technologies, including circulating fluidized bed combustion to promote the transformation of coal to green energy. This study intends to accelerate the market-oriented reform of energy and the power system, and promote the role of the market mechanism on the sides of power generation and sales. In addition, with the continuous development of China's green economy, the related green energy industry has a large capital gap. Therefore, it is necessary to comprehensively use green financial methods, such as green credit, to meet the capital needs in the process of energy use greenization.

This study discusses the relationship between energy use greenization, CO_2 emissions, and economic growth, and provides a theoretical basis and policy recommendations for the sustainable promotion of energy use greenization in China. However, this study was only conducted at the national level and can be conducted at the regional or industry level in the future.

DATA AVAILABILITY STATEMENT

The original contributions presented in the study are included in the article/Supplementary Material; further inquiries can be directed to the corresponding author.

AUTHOR CONTRIBUTIONS

WX: writing an initial draft. KI coordinated the work and writing—analysis. YW: proofreading.

REFERENCES

Ahukaemere, C. M., Okolo, N., Aririguzo, B. N., and Uchenna, O. S. (2020). Tropical Soil Carbon Stocks in Relation to Fallow Age and Soil Depth. *Malays. J. Sustain. Agric.* 4, 05–09. doi:10.26480/mjsa.01.2020.05.09

Anwar, J. (2016). Analysis of Energy Security, Environmental Emission and Fuel Import Costs under Energy Import Reduction Targets: A Case of Pakistan. *Renew. Sustain. Energy Rev.* 65, 1065–1078. doi:10.1016/j.rser.2016.07.037

Asongu, S. A., Le Roux, S., and Biekpe, N. (2018). Enhancing ICT for Environmental Sustainability in Sub-Saharan Africa. *Technol. Forecast. Soc. Change* 127, 209–216. doi:10.1016/j.techfore.2017.09.022

Baydoun, H., and Aga, M. (2021). The Effect of Energy Consumption and Economic Growth on Environmental Sustainability in the Gcc Countries: Does Financial Development Matter? *Energies* 14, 5897. doi:10.3390/en14185897

Bekun, F. V., Alola, A. A., Gyamfi, B. A., and Ampomah, A. B. (2021a). The Environmental Aspects of Conventional and Clean Energy Policy in Sub-Saharan Africa: Is N-Shaped Hypothesis Valid? *Environ. Sci. Pollut. Res.* 28, 66695–66708. doi:10.1007/s11356-021-14758-w

Bekun, F. V., Alola, A. A., Gyamfi, B. A., and Yaw, S. S. (2021b). The Relevance of EKC Hypothesis in Energy Intensity Real-Output Trade-Off for Sustainable Environment in EU-27. *Environ. Sci. Pollut. Res.* 28, 51137–51148. doi:10.1007/s11356-021-14251-4

Bekun, F. V., Emir, F., and Sarkodie, S. A. (2019). Another Look at the Relationship between Energy Consumption, Carbon Dioxide Emissions, and Economic Growth in South Africa. *Sci. Total Environ.* 655, 759–765. doi:10.1016/j.scitotenv.2018.11.271

Bekun, F. V., Gyamfi, B. A., Onifade, S. T., and Agboola, M. O. (2021c). Beyond the Environmental Kuznets Curve in E7 Economies: Accounting for the Combined Impacts of Institutional Quality and Renewables. *J. Clean. Prod.* 314, 127924. doi:10.1016/j.jclepro.2021.127924

Bekun, F. V. (2022). Mitigating Emissions in India: Accounting for the Role of Real Income, Renewable Energy Consumption and Investment in Energy. *Ijeep* 12, 188–192. doi:10.32479/ijeep.12652

Chen, Y., and Ma, Y. (2021). Does Green Investment Improve Energy Firm Performance? *Energy Policy* 153, 112252. doi:10.1016/j.enpol.2021.112252

Chi, Y., Bai, G., Li, J., and Chen, B. (2021). Research on the Coordination of Energy in China's Economic Growth. *PLoS One* 16, e0251824–20. doi:10.1371/journal.pone.0251824

Danish et al. (2017). 'Role of renewable energy and non-renewable energy consumption on EKC: Evidence from Pakistan'. *Journal of Cleaner Production* 156, pp. 855–864. doi:10.1016/j.jclepro.2017.03.203

Engle, R. F., and Granger, C. W. J. (1987). Co-Integration and Error Correction: Representation, Estimation, and Testing. *Econometrica* 55, 251. doi:10.2307/1913236

Fang, Z., Razzaq, A., Mohsin, M., and Irfan, M. (2022). Spatial Spillovers and Threshold Effects of Internet Development and Entrepreneurship on Green Innovation Efficiency in China. *Technol. Soc.* 68, 101844. doi:10.1016/j.techsoc.2021.101844

Hassan, S. T., Xia, E., Huang, J., Khan, N. H., and Iqbal, K. (2019). Natural Resources , Globalization , and Economic Growth : Evidence from Pakistan. *Environ. Sci. Pollut. Res.* 26, 15527–15534. doi:10.1007/s11356-019-04890-z

He, G., Liu, X., and Cui, Z. (2021). Achieving Global Food Security by Focusing on Nitrogen Efficiency Potentials and Local Production. *Glob. Food Secur.* 29, 100536. doi:10.1016/j.gfs.2021.100536

Höhne, N., Blum, H., Fuglestvedt, J., Skeie, R. B., Kurosawa, A., Hu, G., et al. (2011). Contributions of Individual Countries' Emissions to Climate Change and Their Uncertainty. *Clim. Change* 106, 359–391. doi:10.1007/s10584-010-9930-6

Iqbal, K., Hassan, S. T., Peng, H., and Khurshaid (2019). Analyzing the Role of Information and Telecommunication Technology in Human Development: Panel Data Analysis. *Environ. Sci. Pollut. Res.* 26, 15153–15161. doi:10.1007/s11356-019-04918-4

Iqbal, K., Hassan, S. T., Wang, Y., Shah, M. H., Syed, M., and Khurshaid, K. (2022). To Achieve Carbon Neutrality Targets in Pakistan: New Insights of Information and Communication Technology and Economic Globalization. *Front. Environ. Sci.* 9, 1–10. doi:10.3389/fenvs.2021.805360

Irfan, M., Elavarasan, R. M., Ahmad, M., Mohsin, M., Dagar, V., and Hao, Y. (2022). Prioritizing and Overcoming Biomass Energy Barriers: Application of AHP and G-TOPSIS Approaches. *Technol. Forecast. Soc. Change* 177, 121524. doi:10.1016/j.techfore.2022.121524

Ishaque, H. (2017). Quantifying the Potential Impact of Pakistan's GHG Mitigation Policies for Coal-Fired Power Plants. *Energy Procedia* 142, 2809–2815. doi:10.1016/j.egypro.2017.12.426

Lan, Z., Zhao, Y., Zhang, J., Jiao, R., Khan, M. N., Sial, T. A., et al. (2021). Long-term Vegetation Restoration Increases Deep Soil Carbon Storage in the Northern Loess Plateau. *Sci. Rep.* 11, 1–11. doi:10.1038/s41598-021-93157-0

Lee, J. W., and Brahmasrene, T. (2014). ICT, CO_2 Emissions and Economic Growth: Evidence from a Panel of ASEAN. *Glob. Econ. Rev.* 43, 93–109. doi:10.1080/1226508X.2014.917803

Li, Z., Wang, J., and Che, S. (2021). Synergistic Effect of Carbon Trading Scheme on Carbon Dioxide and Atmospheric Pollutants. *Sustainability* 13, 5403. doi:10.3390/su13105403

Liang, X., Lu, T., and Yishake, G. (2022). How to Promote Residents' Use of Green Space: An Empirically Grounded Agent-Based Modeling Approach. *Urban For. Urban Green.* 67, 127435. doi:10.1016/j.ufug.2021.127435

Liu, J.-L., Ma, C.-Q., Ren, Y.-S., and Zhao, X.-W. (2020). Do Real Output and Renewable Energy Consumption BRICS Countries. *Energies*, 1

Liu, J., Yang, Q., Zhang, Y., Sun, W., and Xu, Y. (2019). Analysis of CO_2 Emissions in China's Manufacturing Industry Based on Extended Logarithmic Mean Division Index Decomposition. *Sustainability* 11, 226. doi:10.3390/su11010226

Liu, Y., Jiao, R., Zhao, L., and Liu, K. (2021). Impact of Greenization on the Marginal Utility of Intensity of Carbon Emissions and Factors Affecting it in China. *Energy Eng. J. Assoc. Energy Eng.* 118, 363–378. doi:10.32604/EE.2021.013472

Liu, Z., and Cai, B. (2018). High-resolution Carbon Emissions Data for Chinese Cities. *Belfer Cent. Sci. Int. Aff.* Cambridge, Mass Harvard Univ. 1–29.

Manta, A. G., Florea, N. M., Bădîrcea, R. M., Popescu, J., Cîrciumaru, D., and Doran, M. D. (2020). The Nexus between Carbon Emissions, Energy Use, Economic Growth and Financial Development: Evidence from Central and Eastern European Countries. *Sustainability* 12, 7747. doi:10.3390/SU12187747

Olivier, J. G. J., and Peters, J. A. H. W. (2020). Trends in Global CO_2 and Total Greenhouse Gas Emissions. *PBL Neth. Environ. Assess. Agency* 2020, 70.

Osobajo, O. A., Otitoju, A., Otitoju, M. A., and Oke, A. (2020). The Impact of Energy Consumption and Economic Growth on Carbon Dioxide Emissions. *Sustainability* 12, 7965. doi:10.3390/SU12197965

Pata, U. K. (2021). Linking Renewable Energy, Globalization, Agriculture, CO_2 Emissions and Ecological Frootprint in BRIC Countries: a Sustainability Perspective. *Renew. Energy* 173, 197–208. doi:10.1016/j.renene.2021.03.125

Pata, U. K., and Aydin, M. (2020). Testing the EKC Hypothesis for the Top Six Hydropower Energy-Consuming Countries: Evidence from Fourier Bootstrap ARDL Procedure. *J. Clean. Prod.* 264, 121699. doi:10.1016/j.jclepro.2020.121699

Pata, U. K., and Caglar, A. E. (2021). Investigating the EKC Hypothesis with Renewable Energy Consumption, Human Capital, Globalization and Trade Openness for China: Evidence from Augmented ARDL Approach with a Structural Break. *energy* 216, 119220. doi:10.1016/j.energy.2020.119220

Pata, U. K., and Isik, C. (2021). Determinants of the Load Capacity Factor in China: A Novel Dynamic ARDL Approach for Ecological Footprint Accounting. *Resour. Policy* 74, 102313. doi:10.1016/j.resourpol.2021.102313

Pata, U. K., and Kumar, A. (2021). The Influence of Hydropower and Coal Consumption on Greenhouse Gas Emissions: A Comparison between China and India. *Water* 13 (10), 1387. doi:10.3390/w13101387

Pata, U. K. (2018). Renewable Energy Consumption, Urbanization, Financial Development, Income and CO_2 Emissions in Turkey: Testing EKC Hypothesis with Structural Breaks. *J. Clean. Prod.* 187, 770–779. doi:10.1016/j.jclepro.2018.03.236

Regulation of the European Parliament and of the Council (2021). Regulation of the European Parliament and of the Council Amending. *Eur. Comm.* 0197.

Rousseeuw, P., and Yohai, V., 1984, *Robust Regression by Means of S-Estimators*. 256–272. doi:10.1007/978-1-4615-7821-5_15

Sarfraz, M., Ivascu, L., Belu, R., and Artene, A. (2021). Accentuating the Interconnection between Business Sustainability and Organizational Performance in the Context of the Circular Economy: The Moderating Role of Organizational Competitiveness. *Bus. Strat. Env.* 30, 2108–2118. doi:10.1002/bse.2735

Shabani, Z. D., and Shahnazi, R. (2019). Energy Consumption, Carbon Dioxide Emissions, Information and Communications Technology, and Gross Domestic Product in Iranian Economic Sectors: A Panel Causality Analysis. *Energy* 169, 1064–1078. doi:10.1016/j.energy.2018.11.062

Shah, S. G. M., Sarfraz, M., and Ivascu, L. (2021). Assessing the Interrelationship Corporate Environmental Responsibility, Innovative Strategies, Cognitive and Hierarchical CEO: A Stakeholder Theory Perspective. *Corp. Soc. Responsib. Environ. Manag.* 28, 457–473. doi:10.1002/csr.2061

Shahzad, S. J. H., Kumar, R. R., Zakaria, M., and Hurr, M. (2017). Carbon Emission, Energy Consumption, Trade Openness and Financial Development in Pakistan: A Revisit. *Renew. Sustain. Energy Rev.* 70, 185–192. doi:10.1016/j.rser.2016.11.042

Wu, X., Liu, Z., Yin, L., Zheng, W., Song, L., Tian, J., et al. (2021). A Haze Prediction Model in Chengdu Based on Lstm. *Atmosphere* 12, 1479. doi:10.3390/atmos12111479

Yam, G., Tripathi, O. P., and Das, D. N. (2021). Modelling of Total Soil Carbon Using Readily Available Soil Variables in Temperate Forest of Eastern Himalaya, Northeast India. *Geol. Ecol. Landscapes* 5, 209–216. doi:10.1080/24749508.2019.1706295

Yin, L., Wang, L., Huang, W., Liu, S., Yang, B., and Zheng, W. (2021). Spatiotemporal Analysis of Haze in Beijing Based on the Multi-Convolution Model. *Atmosphere* 12, 1408. doi:10.3390/atmos12111408

Yuelan, P., Akbar, M. W., Hafeez, M., Ahmad, M., Zia, Z., and Ullah, S. (2019). The Nexus of Fiscal Policy Instruments and Environmental Degradation in China. *Environ. Sci. Pollut. Res.* 26, 28919–28932. doi:10.1007/s11356-019-06071-4

Zheng, J., Mi, Z., Coffman, D. M., Milcheva, S., Shan, Y., Guan, D., et al. (2019a). Regional Development and Carbon Emissions in China. *Energy Econ.* 81, 25–36. doi:10.1016/j.eneco.2019.03.003

Zheng, J., Mi, Z., Coffman, D. M., Shan, Y., Guan, D., and Wang, S. (2019b). The Slowdown in China's Carbon Emissions Growth in the New Phase of Economic Development. *One Earth* 1, 240–253. doi:10.1016/j.oneear.2019.10.007

Zheng, X., Lu, Y., Yuan, J., Baninla, Y., Zhang, S., Stenseth, N. C., et al. (2020). Drivers of Change in China's Energy-Related CO_2 Emissions. *Proc. Natl. Acad. Sci. U.S.A.* 117, 29–36. doi:10.1073/pnas.1908513117

Zhou, Y., Zhang, J., and Hu, S. (2021). Regression Analysis and Driving Force Model Building of CO_2 Emissions in China. *Sci. Rep.* 11, 1–14. doi:10.1038/s41598-021-86183-5

Tiwari, A. (2011). Tourism, Exports and FDI as a Means of Growth: Evidence from four Asian Countries. *Rom. Econ. J.* 14 (40), 131–151.

Mahjabeen, N. (2020). Renewable Energy, Institutional Stability, Environment and Economic Growth Nexus of D-8 Countries. *Mendeley Data* 29 (1), 1–10. doi:10.17632/y6tdzbn9cf.1

Venkatraja, B. (2020). Does Renewable Energy Affect Economic Growth? Evidence From Panel Data Estimation of BRIC Countries. *Int. J. Sustain. Dev. World Ecol.* 27 (2), 107–113. doi:10.1080/13504509.2019.1679274

Conflict of Interest: The authors declare that the research was conducted in the absence of any commercial or financial relationships that could be construed as a potential conflict of interest.

Publisher's Note: All claims expressed in this article are solely those of the authors and do not necessarily represent those of their affiliated organizations, or those of the publisher, the editors, and the reviewers. Any product that may be evaluated in this article, or claim that may be made by its manufacturer, is not guaranteed or endorsed by the publisher.

ORIGINAL RESEARCH
published: 08 July 2022
doi: 10.3389/fenrg.2022.889877

Check for updates

Construction and Application of a Carbon Emission Model for China's Coal Production Enterprises and Result Analysis

Yang Li[1], *Xiangyang Jin*[1,2]*, *Guoliang Wang*[2], *Yuqi Ren*[1], *Huiqi Tan*[1] *and Na Li*[1]

[1]*School of Energy and Mining Engineering, China University of Mining and Technology-Beijing, Beijing, China,* [2]*China Coal Technology and Engineering Group International Engineering Co Ltd, Beijing, China*

Edited by:
Jingying Fu,
Chinese Academy of Sciences (CAS), China

Reviewed by:
Yuntao Liang,
CCTEG Shenyang Research Institute, China
Shaobin Wang,
Chinese Academy of Sciences (CAS), China
Fangtian Wang,
China University of Mining and Technology, China

****Correspondence:***
Xiangyang Jin
45805801@qq.com

Specialty section:
This article was submitted to Sustainable Energy Systems and Policies,
a section of the journal Frontiers in Energy Research

Received: *04 March 2022*
Accepted: *09 June 2022*
Published: *08 July 2022*

Citation:
Li Y, Jin X, Wang G, Ren Y, Tan H and Li N (2022) Construction and Application of a Carbon Emission Model for China's Coal Production Enterprises and Result Analysis. Front. Energy Res. 10:889877. doi: 10.3389/fenrg.2022.889877

To achieve the national goal of "peak carbon emissions and carbon neutrality," a specific action plan is needed. Therefore, it is particularly important to scientifically calculate the total carbon emissions of enterprises in various industries. According to the related enterprises' characteristics, this study adopts different-source methods to construct the carbon emission calculation model. Carbon dioxide emissions are calculated based on the gas grade, and the results are as follows: *1*) Carbon emissions of enterprises are significantly different with various gas grades; *2*) gas dissipation accounts for more than 80% of carbon emissions of relevant enterprises, so the gas content in the coal seam increases the effect of carbon emissions; and *3*) with the increase in mining depth, carbon emissions are increasing. This innovation of study is, first, comprehensively analyzing the carbon emission sources of relevant enterprises from six aspects, including fuel combustion, torch burning, CH_4 and CO_2 dissipation, net purchased electricity and heat implication, coal gangue storage and utilization, and coal transportation. Moreover, the source–sink relationship method is proposed when the CH_4 and CO_2 dissipation is calculated, which avoids human errors such as inaccurate measurement of the actual statistical method and the difficulty of obtaining calculation parameters, thus more accurately calculating the total carbon emissions. The source–sink relationship method can be applied in open coal pits to solve the carbon emission calculation. Implementing green and low-carbon development and achieving the goal of peak carbon emissions and carbon neutrality is significant.

Keywords: coal production enterprises, total carbon emissions, calculating model, calculating method, classified accounting

INTRODUCTION

Greenhouse gas emissions (CO_2, CH_4, N_2O, HFCs, PFCs, SF_6, *etc.*) caused by human activities such as agriculture and the exploitation of fossil energy such as coal, oil, and natural gas lead to a rise in the concentration of greenhouse gases, the enhancement of the greenhouse effect, global warming, and the frequent occurrence of extreme weather. To protect our environment, 200 contracting parties signed the Paris Agreement, which clearly stated that "by the end of this century, the global average temperature rise shall be maintained within 2°C relative to the preindustrial level, and efforts shall be made to control the global average temperature rise within 1.5°C to reduce the risks and impacts of climate change" (Cai F et al., 2022).

In 2019, global carbon emissions were 40.1 billion tons of carbon dioxide, 86% of which came from fossil fuels (Wang X. et al., 2021). Among them, coal, as an important fossil energy source, accounted for 27% of the world's primary energy in 2019 (BP, 2020). Carbon makes up more than 60% of coal. As an energy source and industrial raw material, coal creates a large amount of CO_2 emissions at the production end (coal production enterprises) and consumption end (coal power companies, heating companies, coal-to-chemical companies, building materials companies, *etc.*). Due to China's energy features of the "rich coal, poor oil, and less natural gas," the proportion of coal in total energy consumption was much higher than the world average, between 60% and 70% for many years (Li et al., 2021). In recent years, with the rapid development of new energy sources and the technical improvement of fossil energy, the proportion of coal in total energy consumption dropped to below 60% for the first time in 2018 and to 56.8% in 2020 (Ministry of Natural Resources, PRC, 2021). According to the *Guiding Opinions on the High-Quality Development of the Coal Industry during the Fourteenth Five-Year Plan*, by 2025, domestic coal production will be controlled at approximately 4.1 billion tons, and national coal consumption will be controlled at approximately 4.2 billion tons, with average annual consumption growth of approximately 1%.

To achieve the goal of carbon neutrality, China must completely change the energy structure dominated by coal and increase the proportion of noncarbon energy sources. Coal production enterprises are facing serious pressure of industrial optimization and adjustment and stress on the supply chain and the public. On 22 April 2021, at the Earth Day Leaders' Climate Summit, Xi Jinping proposed that China will strictly control coal power projects and the growth of coal consumption during the "14th Five-Year Plan" period and gradually decrease coal consumption during the "15th Five-Year Plan" period. Coal control will be a major means for China to reduce carbon emissions in the future (Xinhuanet, 2021). To formulate carbon reduction policies for the coal industry, the responsible department of the coal industry should accurately verify the carbon emission data of coal production enterprises and study the characteristics and trends of carbon emissions. Therefore, a simple carbon emission model for coal production enterprises should be constructed; it should have a wide application range and be easily accessible.

At present, the research on the construction of carbon emission models for coal production enterprises in domestic and foreign academic circles primarily focuses on the research of model construction methods, the determination of carbon emission sources, and the prediction of methane emissions. The main research results of the model construction method and carbon emission source determination are as follows. IPCC (2006) presented calculation methods for total carbon emissions in the production process of power generation, coke, and lignite briquette (Intergovernmental Panel on Climate Change, 2006). Liu and Wang (2013) established measurement models of corporate carbon emissions, taking the coal power industry chain as the mainline and applying the whole life cycle analysis method, which was divided into mining, washing, thermal power generation, and gas power generation (Liu and Wang, 2013). The National Development and Reform Commission (2014) promulgated the *Guidelines for Accounting Methods and Reporting of Greenhouse Gas Emissions from China*'s Coal Production Enterprises (Trial) (AMCC) to build an accounting model from four aspects, including fuel combustion, torch burning, CH_4 and CO_2 escape, and net purchased electricity and heat implications (National Development and Reform Commission of the People's Republic of China, 2014). Wang, Wen, and Zhu (2015) studied CMM emission characteristics and designed a coefficient-intensity factor methodology integrated with IPCC methodology to increase its applicability to regional circumstances (Wang et al., 2015). Wang B. J. et al. (2019) presented the status and hot spots reported in studies on the carbon emissions of the coal mining industry in China (Wang B. et al., 2019). Wang et al. (2022) built a source-driven CO_2 emissions accounting model for the coal development sectors using the emissions factor method (Wang B. et al., 2019). Zhou et al. (2020) used the life cycle (LCA) method to study and establish a carbon emission calculation model of the whole process of coal production enterprises from the aspects of mining, ventilation, drainage, power consumption, transportation, and closure activities (Zhou et al., 2020). The main research results of methane emission prediction are as follows. Based on numerical analysis, Brodny and Tutak (2016) proposed the mechanism of CMM release from a mined rock mass and a rockfall goaf, which was released to the surface and into the atmosphere through a ventilation system (Brodny and Tutak, 2016). Tutak and Brodny (2019) studied the methodology of predicting methane emissions based on artificial neural networks and selected statistical methods (Magdalena et al., 2019). According to AMCC, Ren et al. (2022) established the carbon emission calculation model in the process of coal development, calculated the carbon emissions in the process of coal development, analyzed the carbon emission characteristics of different links, and put forward the technical methods of carbon emission reduction in the process of coal development from the three links of production energy consumption, gas emissions, and post-mining activities (Ren et al., 2022).

Most of the above carbon emission models are constructed by the different-source method, and many studies have been carried out on carbon emission sources. However, the following problems have been identified: *1*) for carbon emission calculation of the key influencing factor methane, the statistical measurement method is adopted, which requires many parameters that are difficult to obtain, and some parameters use empirical data; *2*) empirical data are used for CH_4 emission factors of open-pit mining and post-mining activities, resulting in inaccurate calculation results; *3*) the unsystematic emission of greenhouse gases from ground fissures and closed pits is not considered, resulting in a smaller value being calculated for carbon emission; and *4*) due to the different gas content in coal seams, the carbon emission per unit of coal output varies greatly. The existing research results have not been classified and evaluated according to the gas

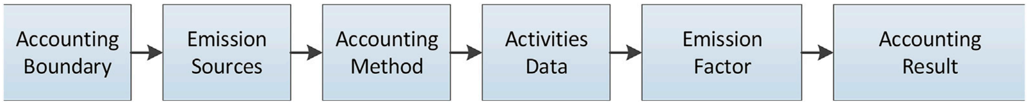

FIGURE 1 | Steps of carbon emission calculation.

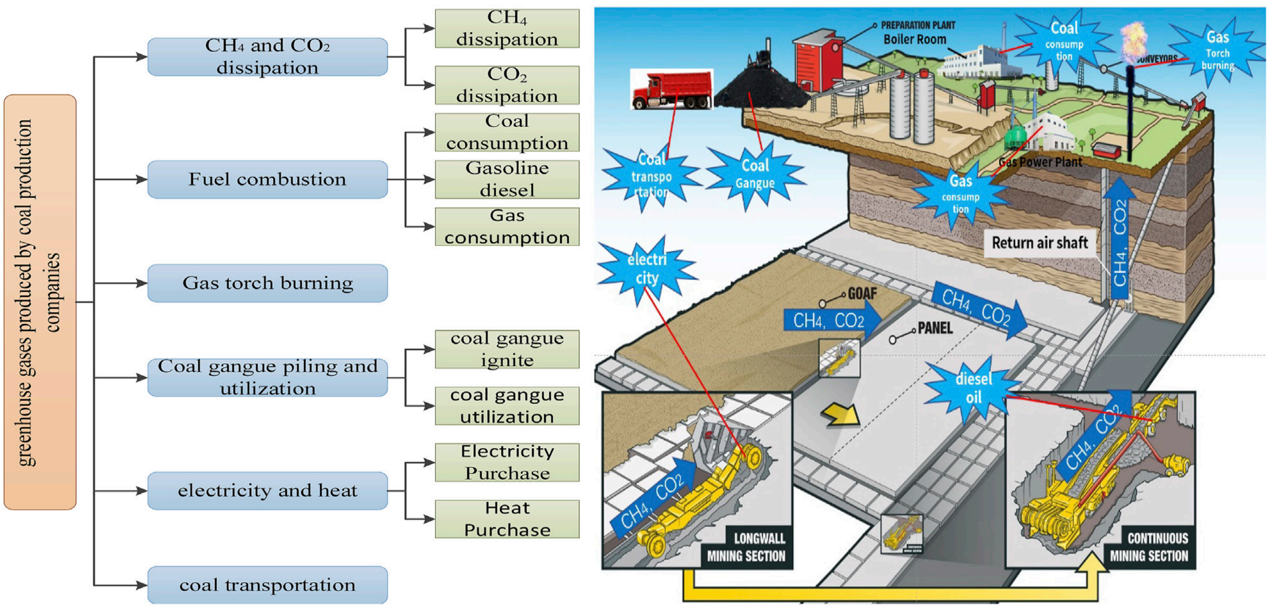

FIGURE 2 | Greenhouse gas emission sources of coal production enterprises.

grade. Therefore, it is impossible to scientifically guide the responsible departments of the coal industry to formulate plans and carbon reduction policies. Because of the problems above, this study optimizes the carbon emission model of coal production enterprises and proposes the source–sink relationship method for the calculation of methane and CO_2 emissions. At the same time, based on the coal mine gas grade, the carbon emissions are calculated using the established model, and the emission data are analyzed and predicted. The main significance of this research is as follows: *1*) to provide a simpler and more accurate calculation method of carbon emissions so that the government and coal production enterprises can have an accurate and objective understanding of the carbon emissions of coal mines; *2*) to determine the key factors affecting the carbon emissions of coal production enterprises and calculate the carbon emissions per ton and the trend of coal mines with different gas grades so that the coal mines can understand the composition of their own carbon emissions to take more targeted measures to reduce carbon emissions from the source; *3*) to understand the carbon emission status of the coal industry and provide a scientific basis for the formulation of a carbon neutralization planning strategy; and *4*) to formulate targeted policies according to the carbon emission characteristics of coal production enterprises.

CONSTRUCTION METHOD OF CARBON EMISSION MODEL FOR COAL PRODUCTION ENTERPRISES

According to the carbon emission calculation process, referring to *the* IPCC (2006) *Guidelines for National Greenhouse Gas Inventories* and AMCC, a carbon emission model for coal production enterprises is constructed. The steps of the carbon emission calculation are shown in **Figure 1**.

Determine the Accounting Boundary

A coal production enterprise is engaged in coal mining and washing activities within China. Therefore, the accounting boundary should be the process from coal removal to transportation, crushing, washing, and processing into commercial coal. However, since product coal and coal gangue must be transported over long distances in the subsequent utilization link, the CH_4 dissipation process is relatively slow and continues until the coal is finally used. Therefore, to ensure

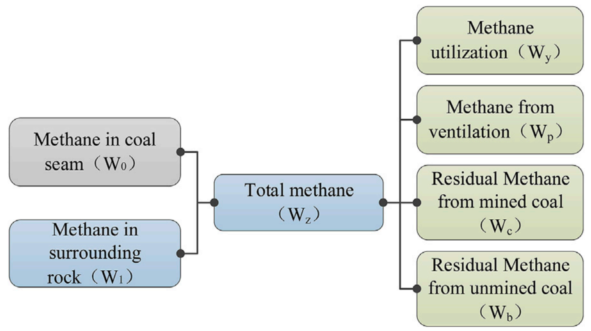

FIGURE 3 | Source–sink relationship of CH_4 in coal production enterprises.

the calculation accuracy of carbon emissions, the accounting boundary should be extended to the end-users of coal, involving the transportation of coal and coal gangue, excluding the end users' consumption of coal. In other words, all the links before the end-users are included.

The facilities within the accounting boundary comprise the primary and auxiliary production systems, administrative welfare facilities, and transportation links to end-users. The primary production systems include coal mining, coal tunnel excavation, coal washing, and processing. Auxiliary production systems include lifting, ventilation, transportation, drainage, compressed air, gas extraction systems, power supply and distribution, heating, refrigeration, mechanical repair, coal gangue storage, and environmental protection facilities. Administrative welfare facilities include offices, accommodations, bathrooms, and canteens. Transportation links include automobiles, railways, and water transportation.

Identify Emission Sources

The types of greenhouse gases made by coal production companies are divided into direct and indirect emissions. Direct emissions are methane (CH_4) and CO_2 dissipation emissions, fuel combustion CO_2 emissions, torch burning CO_2 emissions, coal gangue storage and utilization, and coal transportation to users. Indirect emissions are CO_2 emissions implied by the net purchase of electricity and heat (Climate change response Department of national development and Reform Commission, 2011). The specific analysis is as follows:

(1) Carbon emissions from CH_4 and CO_2 dissipation: the dissipation emissions of CH_4 and CO_2 from coal production and post-mining activities. The coal production link includes the escape of coal mining, excavation, and transportation activities from shaft, pumping station, and ground fissures, and the post-mining activities refer to the CO_2 emission from the free and adsorbed CH_4 and CO_2 in the coal, which is slowly released into the atmosphere during the coal transportation, storage, and processing. After the mine is closed, the residual CH_4 and CO_2 pass through the fracture zone and the unclosed shafts and finally dissipate into the atmosphere.

(2) Fuel combustion carbon emissions: the CO_2 emissions generated by the full combustion of coal, gas, gasoline, diesel, and other fossil fuels with oxygen through boilers, self-provided power plants, standby generators, gas power generation equipment, and transportation vehicles.

(3) Carbon emissions from torch burning: the CO_2 emissions generated by the torch burning of gas from coal mines for safety and environmental protection purposes.

(4) Carbon emissions from coal gangue storage and utilization: the coal gangue produced by the tunneling system and washing is temporarily stored in the gangue site. Gangue will produce CH_4 and CO_2, and some will ignite spontaneously, leading to carbon emissions. Coal gangue is transported to low-calorific value power plants or gangue brick factories for comprehensive utilization, and carbon emissions will be released during the transportation process. The CH_4 and CO_2 dissipation of coal gangue are counted in (1).

(5) Carbon emissions implied by net purchases of electricity and heat: the CO_2 emissions from fuel combustion during the production process corresponding to the annual net purchase of electricity or heat (steam, hot water) by coal production enterprises. Emissions actually occur in those electricity or heat production enterprises but are triggered by the consumption activities of the coal production companies and calculated in their total emissions.

(6) Carbon emissions from coal transportation: coal production is located in Inner Mongolia, Shanxi, and Shaanxi. The total raw coal production of these three provinces in 2020 was 2.752 billion tons, accounting for 71% of the national raw coal production (Statistics Bureau of the People's Republic of China, 2020). The coal from the three provinces was transported to the coast along the Yangtze River, North China, and Northeast China. The annual net transfer volume reached 1.5 to 1.6 billion tons, with an average transportation distance of 1,204 km (Coalrennet, 2020). The long-distance transportation of coal not only led to severe carbon emissions from vehicle fuel but also caused the residual CH_4 and CO_2 of the coal to dissipate into the atmosphere. The carbon emissions of this part are counted in (1).

TABLE 1 | Desorption time of 90% gas from lump coal with different particle sizes.

Coal sample size	1 μm (seconds)	10 μm	100 μm	1 mm	1 cm	1 m
Discharge time	4.6	10 min	100 h	1 month	15 years	150,000 years

Method for determination of residual gas content of coal (LI D.,1992).

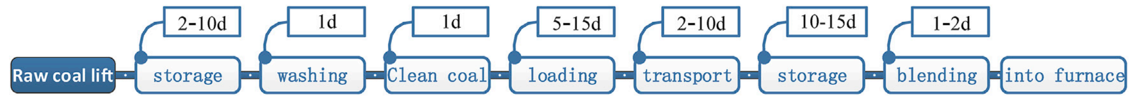

FIGURE 4 | Whole life cycle process of raw coal.

The sources of greenhouse gas emissions from coal production enterprises are shown in **Figure 2**.

CONSTRUCTION OF THE CARBON EMISSION MODEL OF COAL PRODUCTION ENTERPRISES

Referring to *AMCC*, by using a different-source method to construct an accounting model, the total greenhouse gas (GHG) emissions of coal mine production enterprises are equal to the sum of the carbon emissions from CH_4 and CO_2 dissipation, fossil fuel combustion, torch burning, coal gangue storage and utilization, and the net purchased electricity and heat. Please see the following formula:

$$E_{GHG} = E_{CH_4 dissipation} \times GWP_{CH_4} + E_{CO_2 dissipation} + E_{CO_2 burn} + E_{CO_2 torch} + E_{CO_2 gangue} + E_{CO_2 electricity} + E_{CO_2 heat}. \quad (1)$$

E_{GHG} is total enterprise greenhouse gas emissions, ton·CO_2 equivalent.

$E_{CH4dissipation}$ is dissipation emissions of CH_4, tons·CH_4.

GWP_{CH4} is the global warming potential (GWP) value of CH_4 compared to CO_2, taken as 28 (IPCC, 2014).

$E_{CO2\ dissipation}$ is CO_2 dissipation emissions, tons·CO_2.

$E_{CO2\ burn}$ is CO_2 emissions from fossil fuel combustion, tons·CO_2.

$E_{CO2\ torch}$ is CO_2 emissions from gas torch burning, tons·CO_2.

$E_{CO2\ gangue}$ is CO_2 emissions from coal gangue storage and utilization, ton·CO_2.

$E_{CO2\ electricity}$ is CO_2 emissions implied by the company's net purchase of electricity, ton·CO_2.

$E_{CO2heat}$ is CO_2 emissions implied by the net purchase of heat by the company, ton·CO_2.

Dissipation Emissions of CH_4 and CO_2

The dissipation emissions of CH_4 and CO_2 are the key and difficult point for coal production enterprises to calculate carbon emissions. Affected by mining disturbance, the original CH_4 and CO_2 in the coal seam and surrounding rocks begin to desorb, and the pressure and content of CH_4 and CO_2 begin to decrease over time. The desorbed CH_4 and CO_2 enter the gas drainage system or flow into the coal mine ventilation system. The remaining CH_4 and CO_2 in the extracted coal enter the surface production system along with the raw coal and are slowly released into the atmosphere during the process of crushing, washing, storage, and transportation, which constitute the dissipation emissions of CH_4 and CO_2 from post-mining activities. The residual CH_4 and CO_2 in the gob and protective coal pillars that have not been completely desorbed in adjacent coal seams will continue to be slowly released. Even after the mine is closed, CH_4 and CO_2 will still enter the atmosphere through mining gallery cracks, geological structures, and poorly closed shafts.

The source–sink relationship of mine CH_4 (CO_2) is shown in **Figure 3**.

According to the above analysis, the dissipation emissions of CH_4 and CO_2 can be calculated by two methods: the measured statistics method and the source–sink relationship method.

Dissipation Emissions of CH_4

(1) Measured statistics method:

$$E_{CH_4 dissipation} = E_{CH_4 direct} + E_{CH_4 mined} + E_{CH_4 unsystematic}. \quad (2)$$

$E_{CH4\ dissipation}$ is annual CH_4 emissions, t/a.

$E_{CH4direct}$ is the amount of CH_4 emitted directly into the atmosphere by the ventilation system or gas extraction system, t/a.

$E_{CH4mined}$ is the amount of CH_4 emitted after the raw coal is mined until it is transported to the coal users, t/a.

$E_{CH4unsystematic}$ is the unsystematic discharged CH_4 that has not entered the mine ventilation system and passes through cracks, faults, and uncomplete closed shafts, t/a.

① Calculation of $E_{CH4direct}$:

$$E_{CH_4 direct} = \left(\sum Q_{CH_4 ventilate} + \left(\sum Q_{CH_4 drainage} - Q_{CH_4 torch} - Q_{CH_4 usage}\right)\right) \times \rho_{CH_4}, \quad (3)$$

$$Q_{CH4ventilate} \sum T \left(\frac{1}{N}\sum_{N=1}^{n}(Q_{return-air} \times C_{return-air})n \times 60 \times 10^{-4}\right)T. \quad (4)$$

$Q_{CH4ventilate}$ is the amount of CH_4 in the airflow in the air-return roadway in 1 year, 10,000 Nm^3/year.

$Q_{CH4drainage}$, $Q_{CH4torch}$, $Q_{CH4usage}$ are, in the gas drainage system, the amount of drainage, torch burning, and gas used, which can be directly read through the gas drainage system, 10,000 Nm^3/year.

ρ_{CH4} is the density of CH_4 under standard conditions of 7.17 tons of CH_4/10,000 Nm^3.

T is the operating hours of the mine in the current year, h.

n is the nth monitoring of the air-return roadway within 1 h.

N is the number of monitoring of the air-return roadway within 1 h.

$Q_{air-return}$ is the nth monitored wind flow in the air-return roadway, Nm^3/min.

$C_{air-return}$ is the volume concentration of CH_4 monitored for the nth time in the air-return roadway, dimensionless, with a value range of 0–1.

② Calculation of $E_{CH4mined}$:

$$E_{CH_4 mined} = \left(AD_{coal} \times Q_{CH_4 residual}\right) \times 10^{-4} \times \rho_{CH_4}. \quad (5)$$

TABLE 2 | Data of carbon emission of Lingzhida coal mine in 2020.

Average air volume of No.1 air-return shaft (m^3/min)	**Gas concentration of No.1 air-return shaft (%)**	**CO_2 concentration of No. 1 air-return shaft (%)**	**Original gas content of mining coal seam (m^3/t)**
11,570	0.06	0.06	1.69
Original CO_2 content of mining coal seam (m^3/t)	**Diesel consumption (t)**	**Electricity purchase per year (MWh)**	**Raw coal output (MTPA)**
1.89	49	33,748	1.76

Provided by Lingzhida coal mine.

TABLE 3 | Calculation results of CO_2 emission of Lingzhida coal mine.

Serial number	**Emission source**	**Activity data**	**GWP/emission factor**		**CO_2 emission equivalent (t)**	**Proportion (%)**
		Burning amount/ dissipation amount (t)	**Carbon content (ton carbon/ ton or 10,000 Nm^3)**	**Carbon oxidation rate (%)**		
1	CH_4 dissipation	4,635 (measured statistical method) 5,971 (source–sink relationship method)	GWP = 28		167,199 (source–sink relationship method)	81.05
2	CO_2 dissipation	18,348	The density is 19.7 ton/ 10,000 Nm^3		18,348	8.89
3	Diesel	49 t	0.8615704	98	154	0.11
4	Purchased electricity	33,748 MWh	0.6101 t/MWh		20,590	9.98
5	Total				206,291	
6	Carbon emission per ton of coal				0.12	

Authors' calculation.

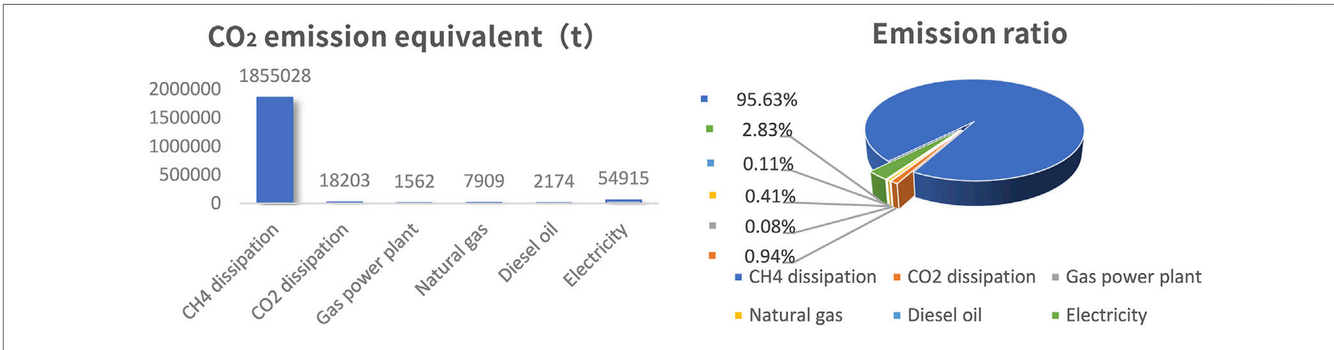

FIGURE 5 | Carbon emission by source and emission proportion of Wangpo coal mine.

AD_{coal} is the annual output of raw coal, t/a.

$Q_{CH4residual}$ is the residual gas content for the mined raw coal, m^3/t.

The gas desorption in coal is complex, comprising penetration and diffusion, and is affected by temperature, air pressure, particle size, coal quality, and exposure time. After research, the theoretical calculation of the time required for lump coal to desorb 90% of the gas is shown in **Table 1** (Li, 1992).

According to the *Design Code of Boiler House* and the *Technical Conditions of Coal for Chain Grate Boiler*, the maximum size of power coal is 50 mm. **Table 1** shows that, for raw coal with a particle size of 10 mm, it takes 15 years to desorb 90% of the gas. Therefore, it is difficult to accurately determine the CH_4 emissions from coal production enterprises' post-mining activities. For the transportation and storage of coal products from coal production enterprises to end users, the dissipation emissions of CH_4 and CO_2 cannot be calculated due to the uncertain time of gas desorption. Hence, the life cycle method is adopted to extend the calculation boundary of coal production enterprises to the links of coal transportation and coal gangue utilization. As more than 50% of China's coal is used for

TABLE 4 | Data of carbon emission of Wangpo coal mine in 2020.

Average air volume of No.1 air shaft (m^3/min)	Gas concentration of No.1 air shaft (%)	CO_2 concentration of No. 1 air shaft (%)	Average air volume of No. 2 air shaft (m^3/min)	Gas concentration of No. 2 air shaft (%)	CO_2 concentration of air shaft 2 (%)
11,443	0.31	0.032	14,290	0.35	0.035
Original gas content of mining coal seam (m^3/t)	**Original gas content of overlying coal seam (m^3/t)**	**Residual gas (m^3/t)**	**Annual gas drainage (Nm^3)**	**Annual gas utilization (Nm^3)**	**Annual gas discharge of drainage system (Nm^3)**
11.0	11.0	3.29	28741800	7134900	21606900
Diesel consumption (t)	**Natural gas consumption (m3)**	**Electricity purchase (MWh)**	**Raw coal output (MTPA)**		
702	3658536	90010	3.0		

Provided by Wangpo coal mine.

TABLE 5 | Calculation results of CO_2 emission of Wangpo coal mine.

Serial number	Emission source	Activity data	GWP/emission factor		CO_2 emission equivalent(t)	Proportion (%)
		Burning amount/ dissipation amount (t)	Carbon content (ton carbon/ ton or 10,000 Nm^3)	Carbon oxidation rate (%)		
1	CH_4 dissipation	61,851 (measured statistical method) 66,251 (source–sink relationship method)	GWP = 28		1,855,028 (source–sink relationship method)	95.63
2	CO_2 dissipation	18,203	CO_2 concentration is 10% of CH_4, the density is 19.7 ton/10,000 Nm^3		18,203	0.94
3	Gas power plant	713.49 ten thousand Nm^3	0.637694	99	1562	0.08
4	Natural gas	365.85 ten thousand Nm^3	5.956443	99	7909	0.41
5	Diesel oil	702 t	0.8615704	98	2174	0.11
6	Purchased electricity	90010 MWh	0.6101 t/MWh		54,915	2.83
7	Total				1939791	
8	Carbon emission per ton of coal				0.65	

Authors' calculation.

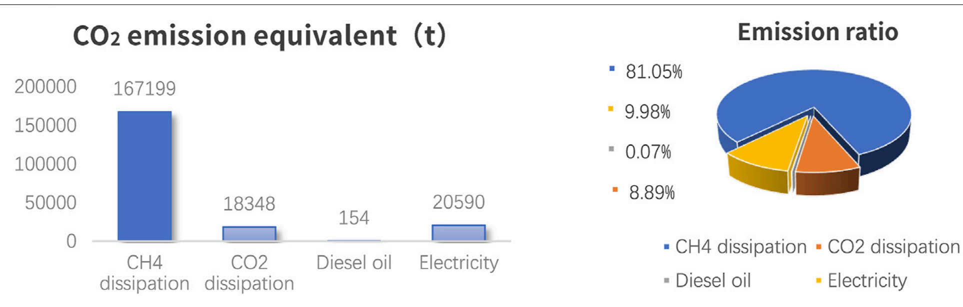

FIGURE 6 | Carbon emission by source and emission proportion of Lingzhida coal mine.

thermal power generation, to improve boiler efficiency and fuel utilization, coal is ground into pulverized coal before being blown into the furnace through the air carrying less than 75% of the pulverized coal, with a particle size less than 90 μm.

The process is shown in **Figure 4**.

Figure 4 shows that the raw coal undergoes multiple processes, such as crushing, screening, washing, long-distance transportation, storage, coal blending, and coal grinding, over a period of 30–60 days. During this time, the residual CH_4 and CO_2 of the coal are nearly zero:

TABLE 6 | Data of carbon emission of Zhongheng coal mine in 2020.

Average air volume of No.1 air-return shaft (m^3/min)	Gas concentration of No.1 air-return shaft (%)	CO_2 concentration of No. 1 air-return shaft (%)	Average air volume of No. 2 air-return shaft (m^3/min)	Gas concentration of No. 2 air-return shaft (%)
6,500	0.18	0.06	4,200	0.14
CO_2 concentration of air-return shaft 2 (%)	**Original gas content of mining coal seam (m^3/t)**	**Original gas content of overlying coal seam (m^3/t)**	**Residual gas (m^3/t)**	**Annual gas drainage (Nm^3)**
0.06	13.88	8–14.5	4.6	14,150,000
Annual gas utilization (Nm^3)	**Annual gas discharge of drainage system (Nm^3)**	**Electricity purchase (MWh)**	**Raw coal output (MTPA)**	
11,010,000	3,140,000	13,000	0.92	

Provided by Zhongheng coal mine.

TABLE 7 | Calculation results of CO_2 emission of Zhongheng coal mine.

Serial number	Emission source	Activity data	GWP/emission factor		CO_2 emission equivalent(t)	Proportion (%)
		Burning amount/dissipation amount (t)	Carbon content (ton carbon/ton or 10,000 Nm^3)	Carbon oxidation rate (%)		
1	CH_4 dissipation	14,945 (measured statistical method) 17,742 (source–sink relationship method)	GWP = 28		496,778 (source–sink relationship method)	96.32
2	CO_2 dissipation	8,475	The density is 19.7 Ton/10,000 Nm^3		8,475	1.64
3	Gas power plant	1101 ten thousand Nm^3	0.637694	99	2,549	0.08
4	Purchased electricity	13,000 MWh	0.6101 t/MWh		7,931	1.54
5	Total				515,733	
6	Carbon emission per ton of coal				0.56	

Authors' calculation.

③ Calculation of $E_{CH4unsystematic}$:

$$E_{CH_4unsystematic} = \left(AD_{unmined} \times Q_{CH_4residual}\right) \times 10^{-4} \times \rho_{CH_4}. \quad (6)$$

$AD_{unmined}$ is the amount of coal resources affected by mining in the current year, t/a.

$Q_{CH4residual}$ is the residual gas content of unmined coal, m^3/t.

The actual measured statistical method is simple and easy to implement and can be used in coal mines with continuous monitoring conditions. However, there are the following problems:

a. Due to the different intensities of coal mining, the gas concentration varies greatly.
b. On the cross-section of the air-return roadway, the gas concentration is different at different locations.
c. The CH_4 content of mined raw coal and unmined coal has a wide variation range, which cannot be continuously measured.
d. Not applicable to open-pit coal mines.

(2) Source–sink relationship method:

As shown in **Figure 3**, the source of CH_4 is the desorption of CH_4 in coal seams and surrounding rocks affected by mining and driving, and finally, CH_4 is released into the atmosphere and gas extraction and utilization system. Therefore, the total amount of CH_4 that finally dissipates into the atmosphere is composed of three parts: the amount of gas exhausted through ventilation, the dissipation of residual CH_4 of the mined coal, and the fractured but not mined coal:

$$W_{CH_40} + W_{CH_41} = W_{CH_4y} + \left(W_{CH_4p} + W_{CH_4c} + W_{CH_4b}\right), \quad (7)$$

$$W_{CH_40} + W_{CH_41} = W_{CH_4y} + E_{CH_4dissipation}. \quad (8)$$

Combining formulas **(7)** and **(8)**, we can conclude the following formula:

$$E_{CH_4dissipation} = W_{CH_40} + W_{CH_41} - W_{CH_4y}. \quad (9)$$

W_{CH40} is annual CH_4 emissions from coal seams affected by mining disturbance, t/a.

W_{CH41} is annual CH_4 emissions from surrounding rocks affected by mining disturbance, t/a.

W_{CH4y} is the annual utilization of CH_4, t/a.

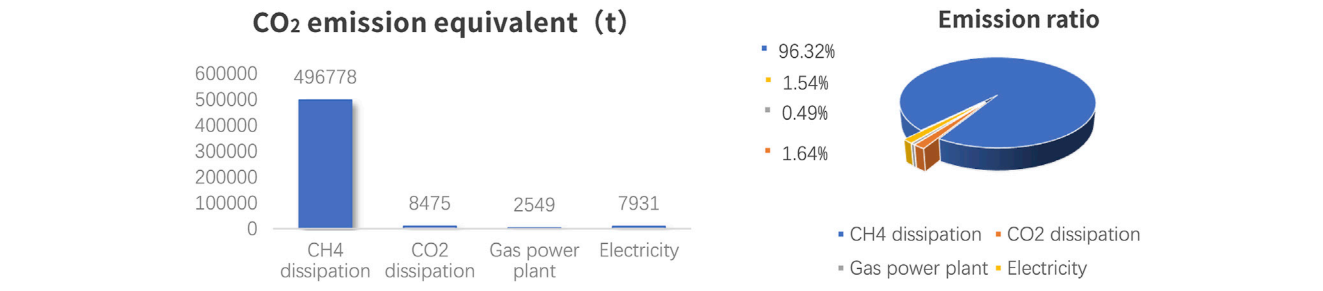

FIGURE 7 | Carbon emission by source and emission proportion of Zhongheng coal mine.

Among them, the calculation of W_{CH40} is shown as follows:

$$W_{CH_40} = \sum\left(AD_{affected}\times Q_{CH_4original}\right)\times 10^{-4}\times\rho_{CH_4}. \quad (10)$$

$AD_{affected}$ is the amount of coal resource affected by mining and driving that year, t/a.

$Q_{CH4original}$ is the original gas content of the coal seam that shall be calculated by the coal seam slice.

By the original gas content value of the surrounding rock or the estimation method, WCH_{41} is calculated as follows:

$$W_{CH_41} = k\times W_{CH_40}. \quad (11)$$

k means the gas emission coefficient of the surrounding rock is 0.2–0.5. When the roof is managed by the total collapse method and the surrounding rock has more carbon content, k will take a larger value. When the backfilling method is used, k will take a small value. When the surrounding rock is tight, k will take a smaller value.

The source–sink relationship method employs the law of conservation of mass to indirectly calculate the annual CH_4 emissions. It uses a few parameters, making the calculation simple. However, it does not consider the amount of CH_4 permanently remaining in the underground mine that did not dissipate into the atmosphere, leading to a large calculated value. Nevertheless, in the long run, the calculation result of the source–sink relationship method is more reasonable, it can calculate the impact on the atmosphere of CH_4 emitted by coal production enterprises throughout the life cycle, and it is also suitable for open-pit coal mines and should be put into use first.

Dissipation Emissions of CO_2

The calculation of CO_2 dissipation emissions is the same as that of CH_4 dissipation emissions. The calculation formula is as follows:

$$E_{CO_2\,dissipation} = E_{CO_2\,direct} + E_{CO_2\,mined} + E_{CO_2\,unsystematic}$$

$$\begin{cases} E_{CO_2\,direct} = \left(\sum Q_{CO_2\,ventilate} + \left(\sum Q_{CO_2\,drainage} - Q_{CO_2\,usage}\right)\right)\times\rho_{CO_2} \\ Q_{CO_2 ventilate} = \sum T\left(\frac{1}{N}\sum_{N=1}^{n}(Q_{return-air}\times C_{return-air})n\times 60\times 10^{-4}\right)T \\ E_{CO_2\,mined} = \left(AD_{coal}\times Q_{CO_2\,residual}\right)\times 10^{-4}\times\rho_{CO_2} \\ E_{CO_2\,unsystematic} = \left(AD_{unmined}\times Q_{CO_2\,residual}\right)\times 10^{-4}\times\rho_{CO_2} \end{cases}. \quad (12)$$

$$or:\ E_{CO_2\,disipation} = W_{CO_20} + W_{CO_21} - W_{CO_2y}$$

The parameters' meaning in the calculation of CO_2 fugitive emissions above is similar to the calculation formula of CH_4 in **3.1.1**.

ρ_{CO2} is CO_2 density under standard conditions, 19.7 tons of CO_2/10,000 Nm^3.

Emissions of CO_2 From Fuel Combustion

Fossil fuels need to be used to ensure the production and continuity of coal mines. For example, boilers are used in heating and hot water systems, hot blast stoves are used for shaft air intake heating, diesel vehicles are used in underground auxiliary transportation, and gasoline is used in ground vehicles. Fuel combustion CO_2 emissions are the different fossil fuel combustion volumes of facilities of coal mining enterprises, multiplied by the corresponding fuel carbon content and carbon oxidation rate and then accumulated layer by layer as follows:

$$E_{CO_2burn} = \sum_j\sum_i\left(AD_{i,j}\times CC_{i,j}\times OF_{i,j}\times 44/12\right). \quad (13)$$

$E_{CO2burn}$ means CO_2 emissions from fossil fuel combustion, tons/year.

i are types of fossil fuels.

j is the serial number of the combustion facility.

$AD_{i,j}$ is the consumption of fossil fuel type i burned in the combustion facility j in tons for solid or liquid fuels, and 10,000 Nm^3 (volume under standard conditions) for gas fuels. The volume under non-standard conditions needs to be converted into standard conditions for calculation.

$CC_{i,j}$ is the carbon content of the fossil fuel i burned in the combustion facility j measured in units of ton carbon per ton of fuel for solid and liquid fuels and measured per ton of carbon per 10,000 Nm^3 for gaseous fuels.

$OF_{i,j}$ means the carbon oxidation rate of fossil fuel i in the combustion facility j is dimensionless, and the value range is 0–1, which can be measured by enterprises. The default value is not measured. The carbon oxidation rate of liquid fuels is 0.98 and that of gas fuels (including CBM or CMM, which is used as fuel by enterprises through recycling) is taken as 0.99. When solid fuel is not measured, it is taken as 1 (Ministry of ecology and environment, 2021).

44/12 is the molecular weight conversion coefficient of CO_2 and carbon (C).

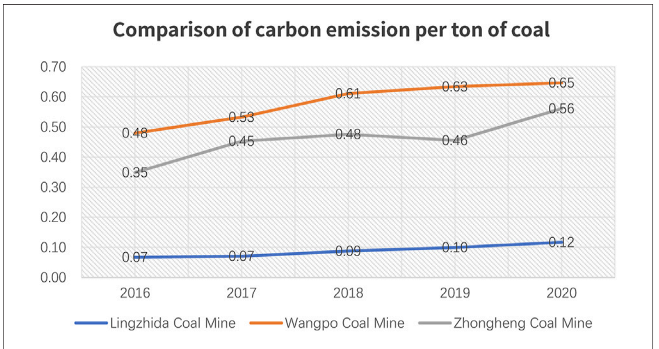

FIGURE 8 | Comparison of carbon emission per ton of coal.

In

$$CC_i = NCV_i \times EF_i, \quad (14)$$

NCV_i is net calorific value of fossil fuel type i, GJ/ton.

EF_i is the carbon content per calorific value of the fossil fuel type *i*, ton carbon/GJ, and the EFi of common fuels can be obtained from the relevant table (Climate change response Department of national development and Reform Commission, 2011).

CO_2 Emissions From Torch Burning

Before the gas is discharged into the atmosphere, it is burned with a torch. The combustion product is CO_2. The calculation formula is shown in **Eq. 15**. However, due to environmental protection requirements, it has rarely been used:

$$E_{CO_2 torch} = Q_{gastorch} \times CC_{nonCO_2} \times OF_{torch} \times 44/12. \quad (15)$$

$E_{CO2torch}$ means CO_2 emissions from coal bed methane (CBM) (coal mine methane (CMM)) torch burning, tons·CO_2;

$Q_{gastorch}$ means torch burning volume (mixed volume) of coalbed methane (coal mine methane), 10,000 Nm^3; CC_{nonCO2} means the total carbon content of other carbon-containing compounds except for CO_2 in CBM or CMM, a ton of carbon/10,000 Nm^3, can be calculated after actual measurement of each gas component; OF_{torch} means the carbon oxidation rate of the torch burning is dimensionless, and the value range is 0–1. When there is no actual measured value, it is taken as 0.99.

CO_2 Emissions From Coal Gangue Storage and Utilization

Coal gangue storage and utilization will bring carbon emissions from the following links: ① coal gangue storage spontaneous combustion, resulting in CO_2 emissions, and ② CH_4 and CO_2 dissipation from coal gangue storage and transportation, which has been included in Formula **(5)**. Carbon emissions generated by coal gangue transport vehicles have been considered in road transport companies, and calculation will not be repeated for coal production companies. The calculation formula is shown as follows:

$$E_{CO_2 gangue} = AD_{gangue} \times CC_{gangue} \times OF_{gangue} \times 44/12. \quad (16)$$

$E_{CO2gangue}$ means CO_2 emissions from coal gangue storage and utilization, ton·CO_2.

AD_{gangue} is annual production of coal gangue, t/a.

CC_{gangue} is the carbon content of coal gangue, ton of carbon per ton of fuel.

OF_{gangue} is the carbon oxidation rate of coal gangue, 1 if no actual measurement is available.

Implied CO_2 Emissions From Net Purchased Electricity and Heat

For production and life needs, coal production enterprises, especially in recent years, have gradually achieved mechanization, automation, and intelligence, requiring a large amount of electricity. Additionally, industrial and civil building heating, shaft air-intake heating, and bathing, among others, sometimes need to purchase heat, and it is necessary to calculate the implied CO_2 emissions from both electricity purchased and heat. The necessary calculations are shown as follows:

$$E_{CO_2 electricity} = AD_{electricity} \times EF_{electricity}, \quad (17)$$

$$E_{CO_2 heat} = AD_{heat} \times EF_{heat}. \quad (18)$$

$E_{CO2electricity}$ is CO_2 emissions implied by the net purchased electricity of the company, ton·CO_2.

$E_{CO2heat}$ is CO_2 emissions implied by the net heat purchased by the company, ton·CO_2.

$AD_{electricity}$ is the power consumption of the company's net purchases, megawatt-hours (MWh). AD_{heat} is the heat consumption of the company's net purchase, GJ, in respect of hot water or steam measured by mass. It can be converted into the heat unit GJ.

$EF_{electricity}$ is the CO_2 emission factor for electricity supply, ton CO_2/MWh. The emission factor corresponding to the power purchased from the grid and the power supplied by the self-provided power plant adopts the 2015 national grid average emission factor of 0.6101tCO_2/MWh.

EF_{heat} is the CO_2 emission factor for the heating power supply, ton CO_2/GJ, provided by the heating company. The default value is 0.11tCO_2/GJ.

CASE STUDY, RESULT ANALYSIS, AND TOTAL CARBON EMISSION ESTIMATION

According to the model, the factors affecting carbon emissions of coal production enterprises are CH_4 dissipation, CO_2 dissipation, fuel combustion, and purchased power. Due to the different gas contents in coal seams, CH_4 dissipation varies greatly among coal mines. Therefore, to accurately identify the key factors affecting coal mine carbon emissions and estimate the carbon emissions per ton of coal, representative coal mines should be selected for research according to the gas grade. According to the *AMCC*, approximately 90% of China's coal production comes from underground coal mines. According to the gas content of and emissions from coal seams, underground coal mines are divided into three categories: low gas mines, high gas mines, and coal and gas outburst mines. This study selects one case from each of the three types of coal mines for research and verifies the model in the Lingzhida coal mine.

Case Study and Model Verification of a Low Gas Mine

Overview of the Lingzhida Coal Mine

The Lingzhida coal mine, located in Changzhi City, Shanxi Province, belongs to the Changzhi mining area of the Qinshui coalfield. The area of the field is 17.6874 km^2, and the minable coal seams in the field are the No. 3 coal seam and No. 15 coal seam. The production capacity of the Lingzhida coal mine is 1.50 MTPA. At present, the No. 15 coal seam is mined from shallow to deep. The thickness of the coal seam is 3.5 m. It uses fully mechanized mining and full height mining at the same time. The gas content of coal seam 15 is 1.3–4.9 m^3/t, which is a low gas mine. The main carbon emission sources of the Lingzhida coal mine are the return air shaft, raw coal storage yard, coal washing plant, railway loading station, gangue storage plant, underground and ground-level diesel locomotives, and electrical equipment.

Carbon Emission Calculation

The main carbon emission sources of the Lingzhida coal mine are CH_4 and CO_2 dissipation, fossil fuel combustion (diesel), and purchased electricity.

The relevant data of 2020 are shown in **Table 2**.

The data in **Table 2** are substituted into the calculation model constructed above, in which CH_4 dissipation is calculated according to the measured statistical method and the source–sink relationship method, and the larger value is used. The calculated results are shown in **Table 3**.

The carbon emission ratio of the Lingzhida coal mine is shown in **Figure 5**.

Model validation

In order to verify the carbon emission calculation model constructed in this study, the calculation method in *AMCC* is used to calculate the CO_2 emissions of the Lingzhida coal mine.

The calculation formula is as follows:

$E_{GHG} = E_{CH4dissipation} \times GWP_{CH4} + E_{CO2dissipation} + E_{CO2burn} + E_{CO2torch} + E_{CO2electricity} + E_{CO2heat}$,

$E_{CH4dissipation} = E_{CH4ug} + E_{CH4mined}$,

$E_{CH4ug} = ((\sum Q_{CH4ventilate} + (\sum Q_{CH4drainage} - Q_{CH4torch} - Q_{CH4usage})) \times \rho_{CH4} = 2616t$,

$E_{CH4\ mined} = 1760000 \times 0.6/1000 = 1056t$。 1760000 is the annual output, and 0.6 is selected according to the default value in *AMCC*, 0.6 kg CH_4/ton of raw coal,

$E_{CH4\ dissipation} = 3672t, E_{CO2\ dissipation} = 7188t, E_{CO2\ burn} = 154t, E_{CO2\ torch} = 0, E_{CO2\ electricity} = 20590t, E_{CO2\ heat} = 0$,

$E_{GHG} = 3672 \times 28 + 7188 + 154 + 0 + 20590 + 0 = 130748$ t.

The above calculation results are 36.6% lower than the calculation model constructed in this study (**Table 3**) because the model in *AMCC* ignores the unsystematic emission of CH_4 and the default value of post-mining activities is too small and additionally ignores the unsystematic emission of CO_2 and the dissipation of post-mining activities.

Because the values of unsystematic emissions and post-mining activities are difficult to obtain, the source–sink relationship method effectively calculates the dissipation of CH_4 and CO_2.

Case Study of a High Gas Mine

Overview of the Wangpo Coal Mine

The Wangpo coal mine, an underground typical high gas mining area, located in northwestern Jincheng city, Shanxi Province, belongs to the Jincheng mining area of the Qinshui coalfield, covering an area of 25.3652 km^2. The mineable coal seams in the field are No. 3, No. 9, and No. 15. Among them, the average spacing between No. 3 and No. 9 is 48.27 m, and the average spacing between No. 9 and No. 15 is 38.85 m. The upper part of No. 3 is located in No. 1 and No. 2, which is approximately 0.3 m thick and non-mineable. The spacing is 15 m between No. 2 and No. 3 and 30 m between No. 1 and No. 3. The production capacity of the Wangpo coal mine is 3.0 MTPA. At present, coal seam 3 is mined from shallow to deep. The thickness of the coal seam is 5.76 m. It is mined by fully mechanized top coal caving. The gas content of No. 3 is 5.02–18.77 m^3/t, which signifies a high gas mine. The main carbon emission sources of the Wangpo coal mine are the No. 1 return air shaft, No. 2 return air shaft, raw coal storage yard, coal washing plant, railway loading station, gangue storage plant, gas boiler room, gas power station, gas extraction station, underground and ground-level diesel locomotives, and electrical equipment.

Carbon Emission Calculation

The main carbon emission sources of the Wangpo coal mine are CH_4 and CO_2 dissipation, fossil fuel combustion (diesel, gas, and natural gas), and purchased electricity.

The relevant data for 2020 are shown in **Table 4**.

The carbon emission model created in this study is used to calculate the carbon emissions of the Wangpo coal mine. The calculation results are shown in **Table 5**.

The carbon emission ratio of the Wangpo coal mine is shown in **Figure 6**.

Case Study of a Coal and Gas Outburst Mine

Overview of the Zhongheng Coal Mine

The Zhongheng coal mine, located in Hongguo Town, Panxian County, Guizhou Province, belongs to the Panxian coalfield. The Panxian coal field is the main coking coal base in China. Most of the coal mines are coal and gas outburst mines. The area of the minefield is 2.9078 km^2, and the minable coal seams in the field are coal seams 1, 3, 4, 8, 12, 15-1, 15-3, 20-1, 22, 23, 24, and 25. The production capacity of the Zhongheng coal mine is 0.90 MTPA. At present, the No. 15-1 coal seam is mined from shallow to deep. The thickness of the coal seam is 2.07 m. It uses fully mechanized mining and full height mining at the same time. The gas content of coal seam 15-1 is 13.88 m^3/t, and the Zhongheng coal mine is a coal and gas outburst mine. The main carbon emission sources of the Zhongheng coal mine are the return air shaft, raw coal storage yard, coal washing plant, gangue storage plant, gas power station, gas extraction station, and electrical equipment.

Carbon Emission Calculation

The main carbon emission sources of the Wangpo coal mine are CH_4 and CO_2 dissipation, fossil fuel combustion (gas), and purchased electricity.

The relevant data for 2020 are shown in **Table 6**.

The carbon emission model created in this study is used to calculate the carbon emissions of the Zhongheng coal mine. The calculation results are shown in **Table 7**.

The carbon emission ratio of the Zhongheng coal mine is shown in **Figure 7**.

Analysis and Comparison of Carbon Emission Data

The comparison of carbon emissions per ton of coal in the Lingzhida coal mine, Wangpo coal mine, and Zhongheng coal mine from 2016 to 2020 is shown in **Figure 8**.

The following conclusions can be drawn from **Figures 5–8**:

① Gas dissipation accounts for more than 80% of the carbon emissions of coal production enterprises, including more than 95% of high gas mines and coal and gas outburst mines. Therefore, coal seam gas content is the key factor affecting the carbon emissions of coal production enterprises.

② For coal mines with different gas grades, the carbon emissions per unit of coal output vary greatly. The carbon emissions per ton of low gas coal mines are significantly lower than those of high gas coal mines and coal and gas outburst coal mines, and the carbon emissions per ton of high gas coal mines and coal and gas outburst coal mines are equivalent.

③ With the increase in mining depth, the carbon emissions of coal production enterprises increase year by year.

Estimation of Total Carbon Emissions in the Coal Industry

In 2020, China's raw coal output will be 3.902 billion tons (Statistics Bureau of the People's Republic of China, 2020). The annual output of high gas and coal and gas outburst mines in China accounts for 32.7% of the total output (Sun, 2014), which is 1.276 billion tons, whereas the annual output of low gas mines is 2.626 billion tons. According to the results of carbon emissions per ton of coal shown in **Figure 8**, it is estimated that, in 2020, the carbon emission equivalent of high gas and coal and gas outburst mines was approximately 770 million tons, the carbon emission equivalent of low gas coal mines was approximately 320 million tons, and the carbon emission equivalent of coal production enterprises was 1.09 billion tons.

DISCUSSION

Compared with the calculation model in *AMCC*, the carbon emission model of coal production enterprises established in this study optimizes the calculation method of CH_4 dissipation and CO_2 dissipation, which makes the calculation simpler and the result more objective. It is suitable for solving the problem of calculating the empirical value of open-pit coal mines. The conclusion is verified by the application of the model in the Lingzhida coal mine.

The calculation of carbon emissions of three types of coal mines indicated that gas content is the key influencing factor, and the carbon emissions per ton of coal vary greatly among coal production enterprises with different gas grades. By calculating the carbon emissions per ton of coal, the total carbon emissions of the coal industry are estimated to be 1.09 billion tons. The former conclusion is consistent with the conclusion that the carbon emissions of gas emissions account for the highest proportion in *Characteristics Of Carbon Emissions During Coal Development And Technical Approvals For Carbon Neutral Development* (Ren et al., 2022), but the total carbon emissions are higher than the 593 million tons estimated in the paper, mainly due to different calculation models. These conclusions are helpful for coal mines to take targeted measures to reduce carbon emissions and for the government to formulate industry planning and policies.

Limited by time and data acquisition, this study selects three types of coal mines to calculate the carbon emissions per ton of coal and then estimates the carbon emissions of coal mines in China. There are few samples, and the estimated value is inaccurate. In future research, the number of samples will be increased.

CONCLUSION AND POLICY RECOMMENDATIONS

Conclusion

(1) CH_4 dissipation is calculated by the measured statistics method and the source–sink relationship method. The latter calculation result can better reflect the carbon emission activities of coal production enterprises and is suitable for open-pit coal mines.
(2) Coal seam gas content is the key factor affecting the carbon emissions of coal production enterprises, especially in high gas coal mines and coal and gas outburst coal mines, where the proportion of gas dissipation carbon emissions accounts for more than 95%. Therefore, improving the utilization rate of drainage and studying the utilization of low-concentration gas is an important aspect of green coal mining.
(3) Coal mines with different gas grades have huge differences in carbon emissions per unit of coal output. Therefore, carbon reduction policies are formulated according to classification.
(4) The model established in this study estimated that the total carbon emissions of the coal industry will be 1.09 billion tons in 2020, and with the increase in mining depth, the coal seam gas content will increase. If the gas utilization rate is not improved, the carbon emissions will increase. Therefore, policymakers should focus attention on the carbon emissions of the coal industry.

Policy recommendations

The following suggestions are put forward for the responsible department of the coal industry's response to the national carbon neutralization policy.

(1) To calculate the total carbon emissions and composition of coal production enterprises accurately.

Coal projects that require large investments have a strong effect on economics and are difficult for local governments and enterprises to control the investment impulse. From January to May 2021, the total profit of the national coal mining and beneficiary industry was 161.44 billion (Yuan, 2021), a year-on-year increase of 109.4% (Statistics Bureau of the People's Republic of China. From January to May 2021). The later the carbon reaches the peak, the greater the peak carbon emission is and the more difficult it is to realize carbon neutrality in the future. Thus, in the context of carbon neutrality, local governments should enhance risk awareness and replan high-carbon projects guided by the goal of carbon neutrality. To this end, the responsible department of the coal industry should accurately calculate the total carbon emissions and composition of China's coal production enterprises and organize the preparation of the carbon peak and carbon neutrality roadmap of coal production enterprises as soon as possible.

(2) To incorporate coal mine methane emission control into the carbon emission reduction development plan.

As methane dissipation is a key influencing factor of carbon emissions, it is suggested to incorporate coal mine methane emission control into the development plan of carbon emission reduction as soon as possible, formulate methane control objectives and paths, and comprehensively improve the control level of methane emissions. This is a key measure for the coal industry to achieve the goal of peak carbon and carbon neutrality.

(3) To establish more stringent gas drainage and utilization regulation so that all gas should be drained and used only when it can be used.

The existing gas extraction and utilization regulations have low requirements on the gas extraction and utilization rate and lack effective supervision and punishment, resulting in the gas treatment of coal production enterprises mainly addressing air exhaust, so a large amount of gas is directly discharged into the atmosphere. For air exhaust, only the gas concentration of the air-return roadway is controlled; as long as the air volume is large enough, more gas can be discharged. According to research, air exhaust gas accounts for 80% of the total gas emissions of coal mines (Xie et al., 2010). For this reason, stricter gas drainage and utilization regulations must be established, and a coal mine should control not only the concentration of air exhaust gas but also the amount of air exhaust gas per ton of raw coal produced. For gas drainage and utilization, it is also necessary to increase the drainage ratio and utilization ratio so that it can be extracted and used most effectively.

(4) To conduct research on bringing CH_4 into the carbon emission trading market.

The carbon emission trading market is an important measure to reduce carbon emissions by using the market mechanism of "punishing enterprises with more carbon emissions and rewarding enterprises with (fewer) carbon emissions." Bringing methane into the carbon emission trading market is conducive to forcing enterprises to carry out technological transformation and upgrading, improve the utilization rate of gas drainage, and reduce direct gas discharge. It helps encourage coal production enterprises to achieve low-cost carbon emission reduction targets.

(5) To strengthen the prevention and control of spontaneous combustion of coal and gangue, coal gangue must be comprehensively utilized to achieve energy conservation and emission reduction.

The spontaneous combustion of coal and gangue hills produces a large amount of carbon emissions, pollutes the environment, and occupies land resources. If coal gangue is comprehensively utilized, it will not only save energy but also reduce carbon emissions and save land resources. The annual output of coal gangue in China is approximately 700 million tons, and the comprehensive utilization rate of coal gangue resources is 72.2% (Yang and Xu, 2021). At present, the main methods of comprehensive utilization of coal gangue resources include coal gangue power generation, underground filling materials, building materials, road construction, and backfilling of subsidence areas.

(6) To change the concept of "a big horse pulling a small carriage" in coal mine equipment selection and carry out energy-saving transformation of coal mine equipment.

In recent years, coal production enterprises have had better profits to pursue equipment reliability, and they generally choose mining equipment that does not match the capacity of the underground coal mine. The one-sided pursuit of equipment reliability and the selected equipment power requirements consume much electricity, resulting in many indirect carbon emissions through purchasing power. By changing the idea of "a big horse pulling a small carriage" in equipment selection and energy-saving transformation of coal mine equipment, the indirect carbon emissions of purchased electricity can be reduced by over 30%.

(7) To establish the exit schedule of coal production enterprises.

The basic data sheet shall be established by coal mines, and the government will entrust scientific research institutions to measure the gas content of all coal seams in the country to conduct carbon verification. According to the road map of peak carbon and carbon neutrality in the coal industry and the scenario prediction of the end of coal consumption, combined with the service life and carbon emissions of coal mines, the exit schedule of coal production enterprises will be formulated. Detailed plans for the exit schedule, energy supply security, employment resettlement, transformation of related industries, social security and so on should be made.

(8) To strengthen the regulation of coal and power imports and reduce the production of high gas coal mines and long-distance coal transportation.

China's coal production and selling regions are seriously uneven. Only five provinces and regions, namely, Inner Mongolia, Shanxi, Shaanxi, Guizhou, and Xinjiang, have more coal production than consumption. Guizhou and Xinjiang are mainly transporting coal to neighboring provinces. Large amounts of coal from the three provinces of Inner Mongolia, Shanxi, and Shaanxi are transported to the coastal, riverside, northern, and northeastern regions of the country. For the southeast coastal area, the annual coal consumption is approximately 900 million tons, of which the imported coal is 250 million tons. In China, the southeast coastal areas use Indonesian coal, which reduces the carbon emissions of long-distance coal transportation. At the same time, coal in Indonesia has a low gas content, which can greatly reduce the carbon emissions caused by gas dissipation. For Northeast China and North China, researchers can study the import of coal or electricity from Russia and Mongolia. To ensure energy security, China can obtain resources through purchase, equity participation, collaborative development of coal resources, and other collaboration methods. Chinese coal enterprises should be encouraged to go global; incorporate overseas resource development into national strategies; and gain support in finance, banking, insurance, taxation, and technical assistance, among others. In addition, to maintain the stable import of coal, long-term contracts should be signed.

DATA AVAILABILITY STATEMENT

The original contributions presented in the study are included in the article/Supplementary Material. Further inquiries can be directed to the corresponding author.

AUTHOR CONTRIBUTIONS

Conceptualization: YL. Data curation: XJ. Formal analysis: GW and YR. Investigation; HT. Methodology: YL and XJ. Software: NL. Validation: XJ. Writing—original draft: XJ, GW, and YR. Writing—review and editing: HT and NL.

FUNDING

The study was supported by the National Natural Science Foundation Sciences (no. 52074293) and Natural Science Foundation of Hebei Province (no. E2020402041).

REFERENCES

BP (2020). *Statistical Review of World Energy 2020*, 69th edn. London: Royal Dutch Shell.

Brodny, J., and Tutak, M. (2016).*Analysis of Methane Emission into the Atmosphere as a Result of Mining Activity*. 16th ed. Sofia, Bulgaria: International Multidisciplinary Scientific GeoConference SGEM 3, 83–90. Book 4.

Cai, F., Yang, L., Yuan, Y., and Taghizadeh-Hesary, F. (2022). The Application of an Improved Fuzzy Comprehensive Evaluation in Coal Quality Rating: The Case Study of China. *Front. Energy Res.* 9, 752472. doi:10.3389/fenrg.2021.752472

Climate change response Department of national development and Reform Commission, (2011). *Guidelines for the Preparation of Provincial Greenhouse Gas Inventories (For Trial Implementation)*. China: National Development and Reform Commission.

Coalrennet (2020). *Since October, the Average Transportation Distance of National Coal Transportation Orders Has Been 1204*. China: Meitanren. km[EB/OL]. http://www.coalren.org/bencandy.php?fid=214&id=34427.

Intergovernmental Panel on Climate Change (2006). *IPCC Guidelines for National Greenhouse Gas Inventoriess EnergyStationary Combustion*, 2. Japan: IGES. Availabe at: https://www.ipcc-nggip.iges.or.jp/public/2006gl/pdf/2_Volume2/V2_2_Ch2_Stationary_Combustion.pdf (Accessed June 27, 2021).

Li, D. (1992). Method for Determination of Residual Gas Content of Coal. *J. Saf. Coal. Min.* (09), 5–8.

Li, P., Yu, H., Zhang, J., Du, M., and Xiong, J. (2021). Coal Supply Sustainability in China: A New Comprehensive Evaluation Methodology. *Front. Energy Res.* 9, 701719. doi:10.3389/fenrg.2021.701719

Liu, J., and Wang, C. (2013). Carbon Emission Calculation and Evaluation of Coal Enterprise. *J. Coal. Min. Technol.* 18 (6), 99–102. doi:10.13532/j.cnki.cn11-3677/td.2013.06.030

Ministry of ecology and environment (2021). *Guidelines for Accounting Methods and Reporting of Greenhouse Gas Emissions by Enterprises Power Generation Facilities*. China: Ministry of Ecology and Environment.

Ministry of Natural Resources PRC (2021). *China Mineral Resources 2020*. China: Ministry of Land and Resources.

National Development and Reform Commission of the people's Republic of China (2014). *Guidelines for Accounting Methods and Reporting of Greenhouse Gas Emissions of China's Coal Production Enterprises (For Trial Implementation)*. China: National Development and Reform Commission.

IPCC (2014). *Climate Change 2014: Synthesis Report. Contribution of Working Groups I, II and III to the Fifth Assessment Report of the Intergovernmental Panel on Climate Change Core Writing Team*. Editors Pachauri R. K. and Meyer L. A. (Geneva, Switzerland: IPCC), 151.

Ren, Shihua, Xie, Yachen, Jiao, Xiaomiao, Xie, Heping, et al. (2022). Characteristics of Carbon Emissions during Coal Development and Technical Approaches for Carbon Neutral Development. *J. Adv. Eng. Sci.* 54 (1), 60–68. doi:10.15961/j.jsuese.202100924

Statistics Bureau of the people's Republic of China (2020). *China Statistical Yearbook*. China: National Bureau of Statistics.

Statistics Bureau of the people's Republic of China (2021). *From January to May 2021, the Profits of Industrial Enterprises above Designated Size Increased by 83.4% Year-On-Year, with an Average Increase of 21.7% in Two Years*. China: National Bureau of Statistics. [EB/OL] http://www.stats.gov.cn/tjsj/zxfb/202106/t20210627_1818792.html.

Sun, Q. (2014). Research on Status Quo and Prevention Countermeasures of Coal Mine Gas Disaster in China. *J. Saf. Coal. Min.* 40 (03), 116–119. doi:10.19880/j.cnki.ccm.2014.03.027

Tutak, M., and Brodny, J. (2019). Forecasting Methane Emissions from Hard Coal Mines Including the Methane Drainage Process. *Energies* 12 (20), 3840. doi:10.3390/en12203840

Wang, B., Cui, C.-Q., Zhao, Y.-X., Chen, M., and Yuan, X.-C. (2019b). Climate Change Mitigation in the Coal Mining Industry: Low-Carbon Pathways and Mine Safety Indicators. *Nat. Hazards* 95 (1-2), 25–38. doi:10.1007/s11069-018-3438-1

Wang, B. J., Zhao, J. L., and Wei, Y. X. (2019a). Carbon Emission Quota Allocating on Coal and Electric Power Enterprises under Carbon Trading Pilot in China: Mathematical Formulation and Solution Technique. *J. Clean. Prod.* 239, 118104. doi:10.1016/j.jclepro.2019.118104

Wang, N., Wen, Z., and Zhu, T. (2015). An Estimation of Regional Emission Intensity of Coal Mine Methane Based on Coefficient-Intensity Factor Methodology Using China as a Case Study. *Greenh. Gas. Sci. Technol.* 5, 437–448. doi:10.1002/ghg.1485

Wang, X., Li, L., and Zhao, F. (2021). Decomposition Analysis of CO2 Emissions in Northeast China: Insights From Investment Factors. *Front. Energy Res.* 9, 777290. doi:10.3389/fenrg.2021.777290

Wang, X., Liang, S., Wang, H., Huang, S., and Liao, B. (2022). Do Fossil-Fuel Price Distortions Impact the Low-Carbon Transition in China's Energy Intensive Industries? *Front. Energy Res.* 9, 805224. doi:10.3389/fenrg.2021.805224

Xie, K., Yuan, M., Ma, K., Li, B., and Chen, W. (2010). Research on the Utilization of Ventilation Air Methane in Colliery in China. *Coal. Mine. Mod.* 95 (2), 1–2. doi:10.3969/j.issn.1009-0797.2010.02.001

Xinhuanet (2021). *Xi Jinping's Speech at the "leaders Climate Summit.* China: Xinhuanet. [EB/OL]. http://www.xinhuanet.com/politics/leaders/2021-04/22/c_1127363132.htm.

Yang, F., and Xu, H. (2021). Analysis on the Development Path of Ecological Environment Protection and Resources Comprehensive Utilization in Coal Industry during the 14th Five-Year Plan Period. *J. China Coal.* 47 (5), 73–82. doi:10.19880/j.cnki.ccm.2021.05.012

Yuan, L. (2021). Study on the Development Strategy of Coal Mine Safety in China. *J. China Coal.* 47 (6), 1–6. doi:10.19880/j.cnki.ccm.2021.06.001

Zhou, A., Hu, J., and Wang, K. (2020). Carbon Emission Assessment and Control Measures for Coal Mining in China. *Environ. Earth. Sci.* 79, 461. doi:10.1007/s12665-020-09189-8

Conflict of Interest: Author XJ is employed by China Coal Technology and Engineering Group International Engineering Co., Ltd. and studied at China University of Mining and Technology-Beijing. Author GW is employed by China Coal Technology and Engineering Group International Engineering Co., Ltd.

The remaining authors declare that the research was conducted in the absence of any commercial or financial relationships that could be construed as a potential conflict of interest.

Publisher's Note: All claims expressed in this article are solely those of the authors and do not necessarily represent those of their affiliated organizations or those of the publisher, the editors, and the reviewers. Any product that may be evaluated in this article, or claim that may be made by its manufacturer, is not guaranteed or endorsed by the publisher.

frontiers | Frontiers in Environmental Science

TYPE Brief Research Report
PUBLISHED 26 July 2022
DOI 10.3389/fenvs.2022.934236

OPEN ACCESS

EDITED BY
Monica Salvia,
Institute of Methodologies for Environmental Analysis (IMAA), Italy

REVIEWED BY
Nicola Epicoco,
University of L'Aquila, Italy
Haozhi Pan,
Shanghai Jiao Tong University, China

*CORRESPONDENCE
Byron Ioannou,
b.ioannou@frederick.ac.cy

SPECIALTY SECTION
This article was submitted to Environmental Economics and Management, a section of the journal Frontiers in Environmental Science

RECEIVED 02 May 2022
ACCEPTED 08 July 2022
PUBLISHED 26 July 2022

CITATION
Mouzas AJ, Ioannou B and Fokaides P (2022), The establishment of an intermodal walkability index for use in car oriented urban environments: The case of Nicosia.
Front. Environ. Sci. 10:934236.
doi: 10.3389/fenvs.2022.934236

The establishment of an intermodal walkability index for use in car oriented urban environments: The case of Nicosia

Antony John Mouzas[1], Byron Ioannou[2]* and Paris Fokaides[3]

[1]School of Pure and Applied Sciences, Open University of Cyprus, Latsia, Cyprus, [2]School of Engineering, Frederick University, Nicosia, Cyprus, [3]Faculty of Civil Engineering and Architecture, Kaunas University of Technology, Kaunas, Lithuania

Sustainable mobility has been considered key in the pursuit of sustainable development in urban environments. During the last decades, a lot of innovative initiatives have been proposed and examined, most of them were site-specific and highly relevant to the local context. This case study review focuses on Nicosia, a car oriented, medium sized city, and attempts to define an intermodal walkability index for the city center. In a city like Nicosia where more than 90% of the daily trips are done completely by car, encouraging intermodal mobility with walking as part of the trip is an important first step to sustainable mobility. The aim of the paper is to present a model based upon the most impactful sustainability indicators when referring to pedestrian mobility, and therefore will create an intermodal walkability index for grading the walkability of an urban environment, in our case a particular, car-oriented one. The index was developed by using the latest version of pyQGIS, due to the fact that the algorithms that are being used in the calculation of this index are already part of the geospatial analysis toolbox contained within QGIS. The paper uses as a case study the municipality of Nicosia in Cyprus where it was proven that pedestrian transportation can be graded in terms of walkability from the private car drop point. The study has also discovered that the use of primary electricity generation and fossil fuels for transport can be reduced if problematic areas that have a low or negative sustainability score are managed in ways that will increase the score.

KEYWORDS

sustainable mobility, walkability index, QGIS, urban design, car-oriented

Introduction and literature review

Intermodal walkability is the combination of pedestrian movement with any other mean of transport in order to complete a full journey (Chidambara, 2019). This case study review focuses on Nicosia and attempts to define an intermodal walkability index for the city center. The center of the conurbation is approachable in more than 90% of the movements by private cars seeking a parking place near their destination. Intramodality means the use of different transportation means in one journey, in our case is car with walking. Our case study is innovative because it proposes a walkability index for a medium-sized car-oriented city like Nicosia. Our lab results derive through the proper selection of indicators and their assessment through QGIS, an Open Source Geographic Information System (GIS) that allows browsing and map creation in the way conventional GIS software does.

The aim of the literature review is to highlight different walkability index methodologies in order to provide a common ground for the current case study application. Walkability is one of the universal challenges, very crucial to making cities resilient, as briefly mentioned in the UN Sustainable Development Goal 11 (SDG11) in the 2030 Agenda. A number of cities try to develop plans based on walkability to overcome issues such as traffic congestion, air pollution, low level of physical activities among people, and high level of carbon emissions (Epicoco and Falagario, 2022). Friendly walking neighborhoods provide a high-level pedestrian environment (Ruiz-Padillo et al., 2018) shaped by different agents. Compact city and the city of 15 min is a very popular model for achieving walkability and sustainable mobility for the future cities. Already since Lin and Yang 2006 quote the high sustainability potential of compact city in a preliminary assessment which is again confirmed by Bibri et al. (2020) with detailed interviews and secondary data. Additionally, Yao et al. (2022) emphasizes on the efficiency and the economic growth stability achieved through these models.

Designing a walkable network that approaches every part of each conurbation creates a multi-modal, functional city with mobility choices making urban space inclusive. However, in a lot of cases design has proven inadequate if not accompanied by monitoring, and evaluation but also information tools channelizing the citizen's mobility behaviors. Walkability indexes are a tool for providing a meaningful assessment of the fabric in total that could be utilized by authorities, urban and transportation planners but also citizens in order to improve the walkable capacity of specific parts of a city or the city as a sum.

Walkability index methodologies are based on grading either peoples' perceptions, or measurable spatial attributes. It is also usual to plan the process in steps like 1) problem description; 2) evaluation walkability; 3) understanding of the available assessment methods; 4) proposing a new framework adjusted to the specific local attributes (Abastante, et al., 2021). There are different approaches to data collection including in-field inspections of pedestrian paths and crossings or retrieving spatial data like density, land use mix, and street connectivity in order to grade the network facility. Other approaches are more related to health and passive exercise than physical space attributes, there are studies that use at the beginning a conventional prospective study design and a novel space-syntax measurement but the aim is to identify relationships between neighborhood walkability with specific routes in the city (Giles-Cortie et al., 2014; Koohsari et al., 2018; Garau et al., 2020; Caseli et al., 2021; Frank et al., 2021). Densities and the relevant lifestyle routines are also determinants of mobility behaviors and especially where there is an urban/rural transition (Molina-García et al., 2020).

Various comments on the applicability of a walkability index suggest that it is more easily applied when it is comprehensive, simple, and flexible (Fan et al., 2018). Under this aspect, there are more simplified approaches where the indicators are standardized and transformed to a value between 0 and 1 before the assessment process. (Motieyan et al., 2022). Ruiz-Padillo et al. (2018) use a similar approach to quantifying urban environment characteristics. In these cases, as well as in Manzolli et al. (2021) there is a significant focus on multicriteria evaluation approaches. In all these cases the need of including more variables has damaged simplicity and comprehensiveness. There are even more detailed approaches as Chidambara (2019), which suggest a detailed approach of more than 30 indicators relevant to geometries, traffic, accessibility, crossings, safety, liveliness, etc. Such approaches could enable measuring the comparability between different areas or the impact of specific projects but are certainly hard to apply in large-scale and preliminary assessments.

In order to overcome this gap, some approaches provide sophisticated tools like grid cells, connected to a relevant database (Hino et al., 2022), connecting land uses to focal points or the geometries of walking space (Caseli et al., 2021), or grouping parameters according to the nature of the information (Abastante, et al., 2021). There are also other approaches that base their evaluations on extended questionnaires and individual judgments by different social groups, for example, tourists (Stockton et al., 2016; Bassiri et al., 2021). The issue of last mile performance evaluation has found in two papers (Chen et al., 2021; Garces et al., 2021) lie in the logic of the current case study review since in both the cases there is an attempt to provide planning interventions with measurable assessment in order to improve transit connectivity and eliminate mobility inequality across neighborhoods.

In our opinion, the approaches that retain simplicity and comprehensiveness suggest a blend of four environmental attributes example residential dwelling density, intersection density/street connectivity, land use mix, and retail floor area

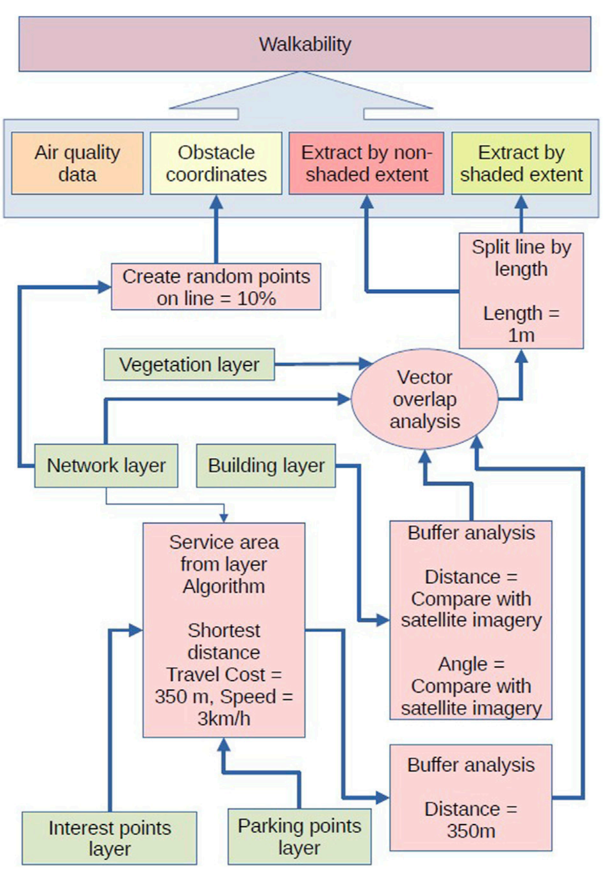

FIGURE 1
Case study flow chart.

ratio, or focus exclusively on densities (Mayne et al., 2013; Giles-Cortie et al., 2014; Fan et al., 2018; Rundle et al., 2019; Frank et al., 2021; Motieyan et al., 2022). Indexes should have a common background in order to be comparable and valid, but at the same time, there is a flexibility in integrating particular local features. Proximity, distance from service points and areas as well as comfort and easiness of pedestrian movement are some universal and more used parameters through the literature review.

Method: Building a walkability index for Nicosia

Our approach examines the total area of the Municipality of Nicosia, which is composed of a number of distinct neighborhoods. For this case, we follow the simplified approaches from the literature, suitable for large-scale preliminary studies. Nicosia, the capital city, is the largest of the five conurbations of the southern part of the island controlled by the Republic of Cyprus. The total population is estimated more than 250,000 inhabitants (approximately 28% of the total population under the control of the Republic, according to CyStat) extremely dispersed covering a total area of around 200 km^2. Nicosia is since 1974 a divided city with its northern part of approximately 90,000 inhabitants being out of the direct control of the Republic. Urban sprawl and low densities are the main reason that consolidates a car-oriented community where more than 90% of the daily movements is carried by private vehicles (Republic of Cyprus, 2020). The Municipality of Nicosia, which serves as the city center, has currently the 1/5 of the city's population and due to the division lies at the north edge of the city past controlled by the formal state. As the city center has a more complete network of activities and functions as the main destination for the whole conurbation.

The basic hypothesis of the current walkability index that differentiates this approach from similar literature cases is that we assume that the origin of the pedestrian movement is the drop-off parking place. In the particular conditions of Nicosia, a car-oriented city, part of traffic and congestion are usually caused by each driver's attempt to park as close to his destination as he or she can, minimizing his or her walking distance. Under these circumstances, increasing intermodal walkability is of high importance.

In order to create an intermodal walkability index for Nicosia, we created a sequence of steps, similar to most of the cases examined in the literature review (see Figure 1, Flow Chart). At first, a GIS database containing points of interest has been built. Secondly, physical attributes were extracted from the satellite images and added to the GIS database, including buildings, vegetation, and road network. Then specific case study areas have been selected in order to provide a functional network layer in order to maximize the scope of each movement. In the next step, spatial data for neighboring land uses were retrieved from open sources and added to the database. At the same time parking, lots and parking points are also added. The index derives from an algorithm calculating positive and negative grading and, in this way, measuring the intensity of the overlapping 3 min areas and also benefited by their physical attributes (Figure 2). Finally, the index indicates the attractiveness of specific locations as more accessible than others in terms of intermodal walkability. The GIS database has been built on a vector basis as a network data structure (link-node graph) in order to enable the analysis of the existing pedestrian network system. All the selected pedestrian paths available in the public space, sidewalks, and pedestrian crossings have been mapped in the database, associating each link with a series of qualitative and quantitative attributes. In order to derive the correct aspects of shading and for what area, there was the digitization of the existing buildings in the satellite imagery that was within these two tolerance zones. The buildings that have been digitized can be considered sustainable in terms of their close proximity to the points of interest and the parking points.

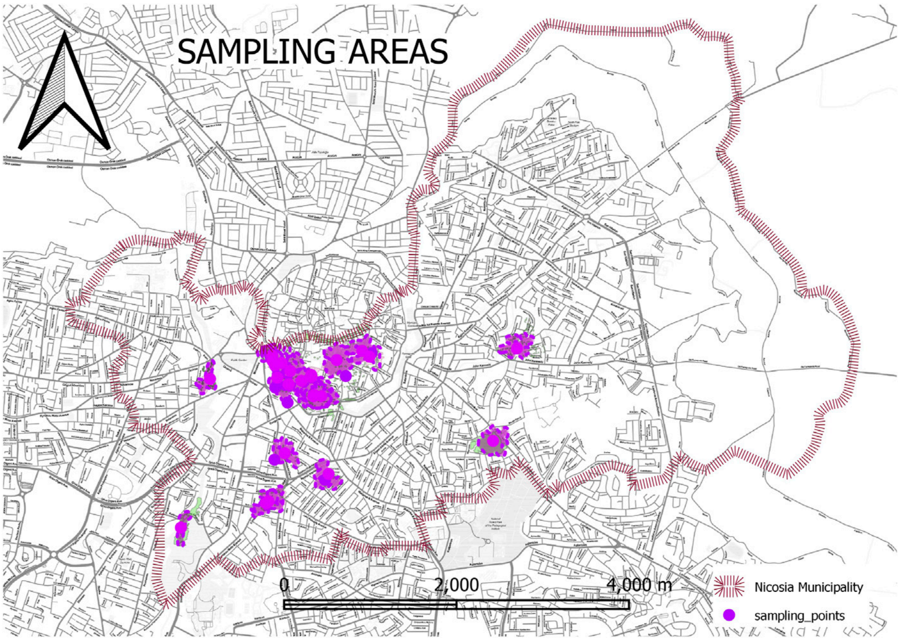

FIGURE 2
Sampling area.

Results

Figure 2 indicates the boundary of the sample area at the Municipality of Nicosia. Archived satellite imagery was analyzed and the highest quality satellite imagery of the Nicosia municipality was gathered and it was used for geospatial analysis. In terms of physical attributes from satellite images three variables were considered:

- shading (binary)—shaded areas +1, unshaded −1 (extracted from satellite imagery and also from existing buildings shade direction)
- mobility (binary)—areas within tolerance distance get +1, outside the zone is −1
- vegetation cover (binary)—segments with vegetation cover receive +1, no vegetation −1.

The processing of these data has resulted, firstly, in a series of thematic maps that identify the main critical issues related to the degree of the walkability of each link and crossing, secondly, in the calculation of a walkability index, detecting whether the pedestrian network is able to meet the needs of all users, even the most vulnerable ones, such as those with limited mobility.

The boundary of the specific study area was selected in order to have a functional network layer and the boundary to which the scope of the sustainability index will function. Along with these two layers, there must also be points of interest that pedestrians are willing to visit and would constitute a rational and declared target for the pedestrian destination. Data about leisure, amenity, office, shop, tourism, and sports destinations were collected from open sources and added to the GIS database. In addition to this, stopping points for parking points will act as an origin for the pedestrians to begin a theoretical journey. Gathering these aspects will allow for the walkability index to extract the sampling areas that will be most beneficial for public investment and public funds through maintenance, and also which have the highest levels of connectivity regarding modal transportation.

In the beginning, we gathered networks in the entire municipality. On the initial analysis of this network, there were aspects that were inaccurate for our purposes and had to be simplified, such example a cemetery sampling area, which has two parking lots adjacent to it and the footpaths within the cemetery have been identified by the algorithm as shaded paths due to a large amount of vegetation. Also, through this refinement network lines that were found to be incomplete were adjusted in order to reflect reality. There are points in the network that radiate out from the boundaries of the municipality and therefore these were considered also as origin points for motor vehicles for our purposes.

These data points were coupled with various interest points located in the municipality, as well as the various parking lots that visitors use for disembarking into the city. These three points created the foundation for our analysis, by using the serviceable

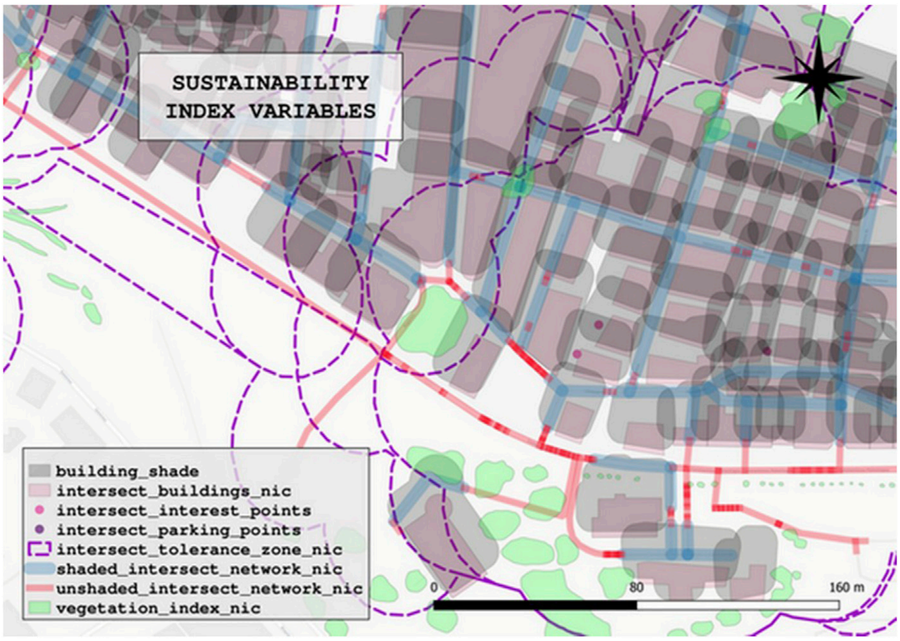

FIGURE 3
Intermodal walkability index variables.

area of both the parking lots and the interest points. The total serviceable areas around each interest and parking point, create a tolerance zone to which pedestrians are able to reach within 5 min at an average speed of 3 km/h (Bohannon and Andrews, 2011). This led to the perception that traffic that travels into the municipality uses these parking spaces to disembark from their vehicles in order to walk to various interest points that exist within the municipality. This also creates an overlapping area that we can consider more sustainable.

This is a view of the before mentioned overlapping areas in the algorithm, delineated by the red circular shape file, and as we can see there is an interesting point directly adjacent to two parking points and the areas that are in purple are the network areas that are within the serviceable distance of the parking lot and the lighter blue areas are the serviceable distance within a cemetery, in this case, our interest point.

These before-mentioned details have led to the conclusion that there is a sampling area of increased capacity to enable sustainable mobility in the municipality of Nicosia. This capacity is evident by the confluence of the networks that join interest points with facilities for private and public motor vehicle parking. The areas in the purple are the intersect of these two areas showing the exact size of the network with the adjacent buildings and vegetation cover can be seen in green. After the sampling area has been gathered using the methodology mentioned above, aspects of shading of the buildings were given an average value in order to reflect a 2 1/2 floor building, which is from our site observation the average height. Buildings that were quite tall were adjusted to reflect the taller building aspects and the shading that was cast upon the ground. Due to the fact that air quality is generally constant, and temperature although fluctuating is constant at any given time, and also given that the climate of Cyprus is generally hot rather than cold, areas of the network that were in full sunlight were given a negative score and areas of the network that were in the complete shade were given a positive score (Figures 2, 3).

The aspect of an obstacle coverage of the network was conceived and therefore set to random intervals in the network, resulting in a total of 10% of the network being obstructed. This 10% of obstruction includes cars that are parked on the pavement, for payment quality, inadequate paving, and lack of paving. The lines in red are very cautionary -2 on the score. This means that they are exposed and offered little to no walkability and therefore do not offer a sustainable method of pedestrian mobility, while the areas in blue and green have a higher score and in fact, a positive score means that it is a pleasant and short distance experience for pedestrians as well as being near the points of interest that the pedestrians desire to walk to. And therefore Figure 4 summarizes the intermodal walkability index of the Nicosia municipality.

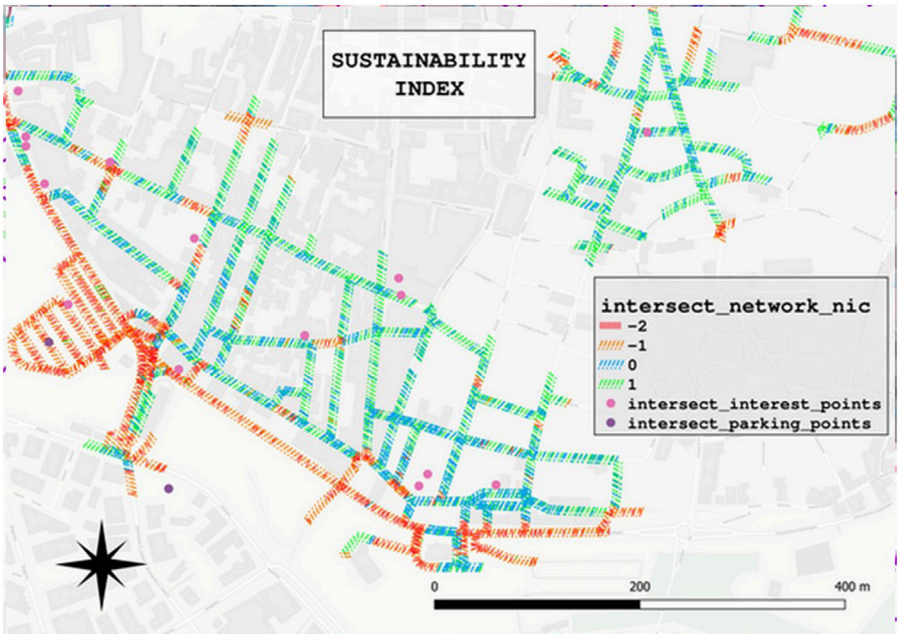

FIGURE 4
Intermodal walkability index final output.

Discussion

The use of this methodology for the quantification and establishment of a walkability index allows for an accurate evaluation of sustainable mobility within private vehicle-oriented cities, with lower public transportation access and usage. Our contribution adds to the last mile approach for intermodal mobility (Chen et al., 2021; Garces et al., 2021). This methodology will benefit from live weather and air quality data for more accurate, time-series data on walkability scores. Applications in other climate types, such as those with heavy rain or snow, would perceptibly have the same negative score as high-temperature climates. Although areas have been tagged as needing simplification or exclusion, we can see that areas that have a positive shade index, adequate vegetation cover, and the relative parking and interest points are in close proximity have positive walkability scores and are therefore more attractive for pedestrians using these forms of modal mobility.

Evaluating walkability from the private car drop point could provide a long-term benefit to the locational strategies of private investors as well as public planning processes, especially for cities with low densities and structural barriers to promoting conventional sustainable mobility strategies. In this context, the use of primary electricity generation and fossil fuels for transport can be reduced if problematic areas that have a low or negative walkability score are supported towards the increase of their score.

The main insight from the case study is that local problems need tailored approaches to be solved. Literature has revealed a huge number of parameters that shape walkability but this effort avoided just copying best practices in order to design a custom-made tool for Nicosia where servicing, as well as shaded and comfortable walking is significantly important. An important benefit of this approach is that it could be applied and function without any large-scale interventions in transportation and mobility planning. The tool can improve the walkability of the existing network and of course become more efficient if sustainable mobility measures are implemented. A minor barrier has to with the accuracy of the available data on the 3d model of the city which can be certainly improved in the following years. Another barrier has to do with monitoring and updating the database, especially concerning the fields relevant to green.

Future design and planning could benefit from our tool that could be more sophisticated, and updated frequently with temperature and air quality data, which would affect the score of the network walkability. Also, this index could integrate microscale data from crowdsourcing, for example, the detection of various different obstacles that can be found whilst navigating these areas as a pedestrian, which is also very well known to the pedestrians themselves. And finally, it could also include perceptions of the comfort, the aesthetics, and the social attributes of the users. In any case and as it was evident from the literature review, the density of destinations and the geometry of the network are the decisive elements, already integrated into the index. Under these options, sustainable mobility plans and urban renewal projects could base on a more accurate and detailed base of the city's performance and thus increase the efficiency of their interventions.

Data availability statement

The raw data supporting the conclusions of this article will be made available by the authors, without undue reservation.

Author contributions

AJM has contributed this paper by designing the walkability index through his MSc thesis at the Open University of Cyprus, supervised by PF and BI. PF and BI guided the main author of the paper in terms of literature review, methodology design and the structure of the research.

Funding

The current publication was funded by Frederick University Research Fund.

Conflict of interest

The authors declare that the research was conducted in the absence of any commercial or financial relationships that could be construed as a potential conflict of interest.

Publisher's note

References

Abastante, F., Gaballo, M., and La Riccia, L. (2021). "Investigate walkability: An assessment model to support urban development processes," in *Smart and sustainable planning for cities and regions. SSPCR 2019. Green energy and technology*. Editors A. Bisello, D. Vettorato, H. Haarstad, and J. Borsboom-van Beurden (Cham: Springer). doi:10.1007/978-3-030-57332-4_13

Bassiri, A., Allan, A., Pieters, J., and Davison, G. (2021). "Developing a GIS-based tourist walkability index based on the AURIN walkability toolkit—case study: Sydney CBD," in *Urban informatics and future cities. The urban book series*. Editors S. C. M. Geertman, C. Pettit, R. Goodspeed, and A. Staffans (Cham: Springer). doi:10.1007/978-3-030-76059-5_13

Bibri, S., Krogstie, J., and Kärrholmd, M. (2020). *Compact city planning and development: Emerging practices and strategies for achieving the goals of sustainability*. Developments in the Built Environment Science Direct. doi:10.1016/j.dibe.2020.100021

Bohannon, R., and Andrews, W. (2011). Normal walking speed: A descriptive meta-analysis. *Physiotherapy* 97 (3), 182–189. doi:10.1016/j.physio.2010.12.004

Caselli, B., Rossetti, S., Ignaccolo, M., Zazzi, M., and Torrisi, V. (2021). "Towards the definition of a comprehensive walkability index for historical centres," in *Computational science and its applications - ICCSA 2021. Lecture notes in computer science*. Editors O. Gervasi, et al. (Cham: Springer), 12958. doi:10.1007/978-3-030-87016-4_36

Chen, S., Yan, X., Pan, H., and Deald, B. (2021). Using big data for last mile performance evaluation: An accessibility-based approach. *Travel Behav. Soc.* 25, 153–163. doi:10.1016/j.tbs.2021.06.003

Chidambara (2019). "Walking the first/last mile to/from transit: Placemaking a key determinant," in *Public space in the new urban Agenda: Research into implementation urban planning*. Editors M. Mehaffy, T. Haas, and P. Elmlund, 4, 183–195. doi:10.17645/up.v4i2.2017

Cyprus Statistical Service (2022). Population. Available at: https://www.cystat.gov.cy/en/SubthemeStatistics?s=46 (Accessed March 31, 2022).

Epicoco, N., and Falagario, M. (2022). Decision support tools for developing sustainable transportation systems in the eu: A review of research needs, barriers, and trends. *Res. Transp. Bus. Manag.* 43, 100819. doi:10.1016/j.rtbm.2022.100819

Fan, P., Wan, G., Xu, L., Park, H., Xie, Y., Liu, Y., et al. (2018). Walkability in urban landscapes: A comparative study of four large cities in China. *Landsc. Ecol.* 33, 323–340. doi:10.1007/s10980-017-0602-z

Frank, L., Appleyard, B., Ulmer, J., Chapman, J., and Fox, E. (2021). Comparing walkability methods: Creation of street-smart walk score and efficacy of a code-based 3D walkability index. *J. Transp. Health* 21, 101005101005. doi:10.1016/j.jth.2020.101005

Garau, C., Annunziata, A., and Yamu, C. (2020). A walkability assessment tool coupling multi-criteria analysis and space syntax: The case study of iglesias, Italy. *Eur. Plan. Stud.*, 1–23. doi:10.1080/09654313.2020.1761947

Garces, E., Tomei, J., Franco, C., and Dynerc, I. (2021). Lessons from last mile electrification in Colombia: Examining the policy framework and outcomes for sustainability. *Energy Res. Soc. Sci.* 79, 102156. doi:10.1016/j.erss.2021.102156

Giles-Corti, B., Macaulay, G., Middleton, N., Boruff, B., Bull, F., Butterworth, J., et al. (2014). Developing a research and practice tool to measure walkability: A demonstration project. *Health promot. J. austr.* 25 (3), 160–166. doi:10.1071/HE14050

Hino, K., Baba, H., Kim, H., and Shimizu, H. (2022). Validation of a Japanese walkability index using large-scale step count data of Yokohama citizens. *Cities* 123, 103614. doi:10.1016/j.cities.2022.103614

Koohsari, M. J., Oka, K., Shibata, A., Liao, Y., Hanibuchi, T., Owen, N., et al. (2018). Associations of neighbourhood walkability indices with weight gain. *Int. J. Behav. Nutr. Phys. Act.* 15, 33. doi:10.1186/s12966-018-0668-2

Lin, J., and Yang, A. (2006). Does the compact-city paradigm foster sustainability? *Environ. Plann. B. Plann. Des.* 33 (3), 365–380. doi:10.1068/b31174

Manzolli, J., Oliveira, A., and Neto, M. (2021). Evaluating walkability through a multi-criteria decision analysis approach: A lisbon case study. *Sustainability* 13, 1450. doi:10.3390/su13031450

Mayne, D. J., Morgan, G. G., Willmore, A., Rose, N., Jalaludin, B., Bambrick, H., et al. (2013). An objective index of walkability for research and planning in the sydney metropolitan region of new south wales, Australia: An ecological study. *Int. J. Health Geogr.* 12, 61. doi:10.1186/1476-072X-12-61

Molina-García, J., Campos, S., García-Massó, X., Herrador-Colmenero, M., Galvez-Fernandez, P., Molina-Soberanes, D., et al. (2020). Different neighborhood walkability indexes for active commuting to school are necessary for urban and rural children and adolescents. *Int. J. Behav. Nutr. Phys. Act.* 17, 124. doi:10.1186/s12966-020-01028-0

Motieyan, H., Kaviari, F., and Mostofi, N. (2022). Quantifying walking capability: A novel aggregated index based on spatial perspective and analyses. *Pap. Reg. Sci.* 101, 483–503. doi:10.1111/pirs.12652

Republic of Cyprus (2020). *Cyprus' integrated National Energy and Climate Plan*. Nicosia: Republic of Cyprus.

Ruiz-Padillo, A., Pasqual, F., Larranaga Uriarte, A., and Cybis, H. (2018). Application of multi-criteria decision analysis methods for assessing walkability: A case study in porto alegre, Brazil. *Transp. Res. Part D Transp. Environ.* 6, 855–871. doi:10.1016/j.trd.2018.07.016

Rundle, A. G., Chen, Y., Quinn, J. W., Rahai, N., Bartley, K., Mooney, S. J., et al. (2019). Development of a neighborhood walkability index for studying neighborhood physical activity contexts in communities across the U.S. Over the past three decades. *J. Urban Health* 96 (4), 583–590. doi:10.1007/s11524-019-00370-4

Stockton, J. C., Duke-Williams, O., Stamatakis, E., Mindell, J. S., Brunner, E. J., and Shelton, N. J. (2016). Development of a novel walkability index for london, United Kingdom: Cross-sectional application to the whitehall II study. *BMC Public Health* 16, 416. doi:10.1186/s12889-016-3012-2

Yao, Y., Pan, H., Cui, X., and Wang, Z. (2022). Do compact cities have higher efficiencies of agglomeration economies? A dynamic panel model with compactness indicators. *Land Use Policy* 115, 106005. doi:10.1016/j.landusepol.2022.106005

TYPE Original Research
PUBLISHED 06 September 2022
DOI 10.3389/fenvs.2022.978076

Low-carbon city pilot policy, fiscal pressure, and carbon productivity: Evidence from china

Yun Yang[1]* and Chunli Peng[2]*

[1]School of Economics, Tianjin University of Commerce, Tianjin, China, [2]School of Management, National Defense University, Beijing, China

OPEN ACCESS

EDITED BY
Ayman Elshkaki,
Key Laboratory of Resource Utilization and Environmental Restoration, Institute of Geographic Sciences and Natural Resources Research (CAS), China

REVIEWED BY
Luigi Aldieri,
University of Salerno, Italy
Elchin Suleymanov,
Baku Enginering University, Azerbaijan

*CORRESPONDENCE
Chunli Peng,
pcl-1990@163.com
Yun Yang,
yangyunpaper@126.com

SPECIALTY SECTION
This article was submitted to Environmental Economics and Management,
a section of the journal
Frontiers in Environmental Science

RECEIVED 25 June 2022
ACCEPTED 30 July 2022
PUBLISHED 06 September 2022

CITATION
Yang Y and Peng C (2022), Low-carbon city pilot policy, fiscal pressure, and carbon productivity: Evidence from china.
Front. Environ. Sci. 10:978076.
doi: 10.3389/fenvs.2022.978076

The implementation of the low-carbon city pilot policy is an important measure to reduce carbon emissions and promote low-carbon economic development in China. However, the resulting fiscal pressure may be counterproductive. The aim of this paper is to investigate the impacts of the low-carbon city pilot policy and fiscal pressure on carbon productivity. Based on the data of 282 cities in China over the period 2005 to 2017, this paper uses the staggered difference-in-differences (DID) model to identify the causal relationship among the low-carbon city pilot policy, fiscal pressure, and carbon productivity. The results show that this pilot policy can significantly improve carbon productivity and that the improvement effect presents a dynamic and persistent feature. However, the fiscal pressure resulting from this pilot policy can reduce carbon productivity, and the degree of reduction depends on the status of fiscal pressure. Increased fiscal pressure has a negative impact on carbon productivity, which is heterogeneous with different levels of economic development. Moreover, the mediation effect analysis finds that this pilot policy affects carbon productivity by adjusting the energy production and consumption structure, enhancing green technology innovation capabilities, and increasing the number of low-carbon-type enterprises entering the market. This paper provides new ideas for improving carbon productivity without increasing fiscal pressure. It also recommends that fiscal pressure cannot be ignored in the implementation of the low-carbon city pilot policy.

KEYWORDS

low-carbon city pilot, fiscal pressure, carbon productivity, staggered DID, mediation effect

1 Introduction

In recent years, extreme weather conditions related to global warming have frequently occurred, highlighting the challenges to high-quality economic development. Therefore, effective strategies to improve carbon productivity and reduce carbon emissions have elicited increasing attention. The goal of the low-carbon policy is to promote carbon productivity and enhance the development of a low-carbon economy. However, Tao and Li (2021) found that China's low-carbon city pilot policy had a negatively impact on economic growth and fiscal revenue, thus aggravating the fiscal pressure on local governments. To alleviate fiscal pressure, local governments may relax environmental regulations to induce more pollution-intensive enterprises, thereby increasing the degree of industrial pollution (Wang and Zhang, 2017; Bai et al., 2019; Huang and Zhou, 2020). This raises the question of whether the fiscal pressure brought about by the low-carbon city pilot policy reduces carbon productivity. Under the condition of controlling for the impact of fiscal pressure brought about by this pilot policy, can the low-carbon city pilot policy still improve carbon productivity?Clarifying the above problems will not only unveil the internal relationship between the low-carbon city pilot policy and carbon productivity but also provide policy implications for further improving the latter.

The low-carbon city pilot policy is an important way to significantly reduce carbon emissions (Huo et al., 2022; Liu et al., 2022; Ren et al., 2022), and it has positive spillover effects (Liu, 2022). Most of the literatures have focused on the ways in which the low-carbon policy affects carbon emissions. First, the low-carbon city pilot policy can promote urban green total factor productivity (Cheng et al., 2019; Qiu et al., 2021). Second, the low-carbon city pilot policy can promote the green technology innovations of enterprises, and its green innovation effect is reflected in patent applications for energy conservation and alternative energy production (Chen et al., 2022; Pan et al., 2022). An increase in the use of clean energy has been shown to reduce coal-fired power generation and carbon emissions (Fell and Kaffine, 2018; Huo et al., 2022; Zhou et al., 2022). Third, carbon tax increases the cost of carbon consumption and significantly reduces carbon emissions (Nordhaus, 2006; Andersson, 2019). Moreover, carbon tax and research and development (R&D) subsidies can encourage companies to innovate clean technologies, thereby reducing pollutant emissions and promoting output growth (Acemoglu et al., 2016; Aghion et al., 2016). Fourth, the carbon emission trading system is also conducive to low-carbon technology innovation and carbon emission reduction (Calel and Dechezleprêtre, 2016; Li et al., 2022).

However, in the implementation of the low-carbon city pilot policy, local governments may directly shutdown high-energy-consuming enterprises, which can lead to reductions in the tax base and tax revenue. In turn, this can increase the fiscal pressure on local governments. On the one hand, to alleviate fiscal pressure, local governments can increase the number of industrial enterprises and relax environmental regulations to promote the proliferation of more pollution-intensive enterprises, thus increasing the degree of industrial pollution (Wang and Zhang, 2017; Huang and Zhou, 2020). On the other hand, local governments can increase fiscal revenues through non-tax methods, which will increase the actual non-tax burden of enterprises (Peng et al., 2020; Zhao and Fan, 2020). In both cases, regardless of which way is chosen to alleviate fiscal pressure, it may have a negative impact on enhancing carbon productivity.

In general, the above literature contribute to the impacts and mechanisms of the low-carbon city pilot policy on carbon emissions, as well as the rise in fiscal pressure, leading to the relaxation of low-carbon environmental regulations by local governments. However, there are still some shortcomings. First, the relationship among the low-carbon city pilot policy, fiscal pressure, and carbon productivity has not been established. In fact, the low-carbon city pilot policy may lead to increased fiscal pressure that will prompt the local government loosening its environmental regulations, which may increase carbon emissions and reduce carbon productivity. Second, the existing literature does not consider the impact of fiscal pressure brought about by the low-carbon city pilot policy. This not only not only has the problem of biased estimation results caused by the omission of variables, but also fails to fully understand the role of the low-carbon city pilot policy. Only perceiving the positive aspects of the pilot policy will not be conducive to providing effective strategies for solving fiscal pressure problems. It will have a perverse effect on reducing carbon emissions and improving carbon productivity.

The aims of this paper are twofold. First, it investigates whether the low-carbon city pilot policy and fiscal pressure brought about by the low-carbon city pilot policy affect carbon productivity. This will not only establish a full understanding of the impact of the low-carbon city pilot policy but also resloves the problem of estimation bias caused by the omission of variables to avoid only seeing the positive impacts of the pilot policy. Second, this study deconstructs the mediation mechanism of the low-carbon city pilot policy on carbon productivity and discusses the heterogeneity of the impact of the pilot policy between different regions and economic development levels, which will enhance the understanding of the impacts of the low-carbon city pilot policy.

Based on the background of the low-carbon city pilot policy and the proposed hypothesis, this paper obtains data from 282 cities in China over the period 2005–2017 and then uses the staggered difference-in-differences (DID) model to identify the relationships among the low-carbon city pilot policy, fiscal pressure, and carbon productivity. The results are as follows:1) the low-carbon city pilot policy can significantly improve carbon productivity, and the impact is persistent; 2) the fiscal pressure resulting from the low-carbon city pilot policy will reduce carbon productivity, and the degree of decline depends on the status of fiscal pressure; (3) increased fiscal pressure will reduce carbon productivity, and the degree of reduction is heterogeneous with different levels of economic development; and 4) the mediation effect analysis shows that the low-carbon city pilot policy affects carbon productivity by adjusting the structure of energy production and consumption, enhancing the ability for green technology innovation and increasing the number of low-carbon-type enterprises entering the market. In this sense, this paper delivers new ideas and supplements the existing literature on the impacts of such a pilot policy.

Compared to the existing literature, the marginal contributions of this paper are as follows. *First*, most existing studies focus on whether the low-carbon city pilot policy can reduce carbon emission and the negative relationship between this pilot policy and economic growth. This paper incorporates fiscal pressure into the analysis of the impacts of such a pilot policy on carbon productivity, which not only provides an explanation for the negative relationship between the pilot policy and economic growth (Tao and Li, 2021) but also solves the estimation bias problem caused by the omission of variables. In addition, without controlling for the impact of fiscal pressure brought about by this pilot policy, the size of the impact of the low-carbon city pilot policy is similar to that reported by Huo et al. (2022) and Liu (2022). However, after controlling for the impact of the fiscal pressure brought about by the pilot policy, the impact of the low-carbon city pilot policy is greater, which is significantly different from that of Huo et al. (2022) and Liu (2022). Meanwhile, the impact of the fiscal pressure brought about by this pilot policy is the opposite; the ultimate impact of the low-carbon city pilot policy also depends on the status of fiscal pressure. *Second*, studies on the effects of the low-carbon city pilot policy usually use technological innovation and energy structure as mediation variables to analyze the mediation effect (Huo et al., 2022; Liu et al., 2022). Apart from these, this paper adds the registration number of low-carbon-type enterprises and fiscal pressure brought about by this pilot policy as additional mediation variables, thus expanding the literature on the impact path of the low-carbon city pilot policy on carbon productivity. *Third*, in terms of policy implications, this paper evidences that the fiscal pressure brought about by the implementation of the low-carbon city pilot policy will reduce carbon productivity. However, if the implementation of this policy can raise the low-carbon access standards for new enterprises, optimize the low-carbon technology level of existing enterprises, and adjust the energy structure, this policy will not increase the fiscal pressure. On the contrary, it will help improve carbon productivity and resolve fiscal pressure.

The remainder of this paper is organized as follows. Section 2 presents the background of the low-carbon city pilot policy and proposes the theoretical hypotheses. Section 3 describes the empirical model and data. Section 4 delivers the results of the estimation and robustness tests. Section 5 discusses the impacts of heterogeneity and the mediation effects. Finally, Section 6 provides the conclusions and policy implications.

2 Background of the low-carbon city pilot policy and theoretical hypothesis

2.1 Background of the low-carbon city pilot policy

China is the largest manufacturing country globally; hence, it is considered "the world's factory." However, the rapid development of the manufacturing industry has been inevitably accompanied by massive energy consumption, and many industries that use traditional fossil fuel energy have emitted large amounts of carbon dioxide (CO_2). To reduce carbon emissions, the Chinese government has actively adopted measures and committed to the realization of global carbon emission reduction. At the 15th Session of the Conference of the Parties to the United Nations Framework Convention on Climate Change held in Copenhagen, Denmark in 2009, the Chinese government pledged that by 2020, the country's carbon dioxide emissions per unit of gross domestic product (GDP) would be reduced by 40–45% compared to 2005 figures, Such an effort represents a huge contribution to emission reduction efforts. In particular, Chairman Xi Jinping proposed that China would strive to achieve a carbon peak by 2030 and carbon neutrality by 2060 during the general debate held at the 75th United Nations General Assembly in September 2020, thus representing China's action plan for achieving its carbon emission reduction targets.

After the Chinese State Council proposed the goal of controlling greenhouse gas (GHG) emissions in November 2009, the National Development and Reform Commission (NDRC) announced its plan to reduce carbon emissions by issuing the "Notice on the Implementation of thePilot Policy for Low-Carbon Provinces, Regions, and Low-carbon Cities" (Development and Reform Climate [2010] No. 1587) in July 2010. This policy requires low-carbon pilot cities to formulate their own action goals, key tasks, and response measures to control GHG emissions, advocate low-carbon production and consumption, and formulate supporting policies conducive to achieving low-carbon and green development. This policy also aimed to establish an industrial system characterized by low carbon emissions to reduce the intensity of carbon emissions and promote carbon productivity. The first batch of selected low-carbon cities consisted of eight cities, including Tianjin and Chongqing, which were further expanded in 2012. In april 2012, the Climate Department of the NDRC issued the "Notice on Organizing the Recommendation and Declaring the Second Batch of low-carbon Pilot Provinces and Cities" (Development and Reform Climate [2012] No. 3760). This batch comprised 28 cities, including Beijing and Shanghai. After that, the NDRC issued the "Notice on Carrying Out the Third Batch of National Low-carbon City Pilot Policy Work" (Development and Reform Climate [2017] No. 66) in January

2017, this time including 45 cities (e.g., Wuhai City) in the third batch of selected areas.

Thus far, a total of 81 cities have been selected as low-carbon city pilot policy areas. In terms of geographical distribution, these areas include cities in the Eastern, Central, and Western regions, such as cities in the south and north of the Qinling Mountains and the Huai River. From the perspective of location, the selected areas include provincial capital cities, municipalities directly under the Central Government, and general prefecture-level cities. With respect to economic development level, the list comprises cities in both economically developed and underdeveloped areas in the Central and Western regions. Generally, the selected areas for the low-carbon city pilot thoroughly represent a broad spectrum of Chinese cities with varying characteristics.

2.2 Theoretical hypothesis

The low-carbon city pilot policy affects carbon productivity in several ways. *First*, traditional fossil energy sources, such as raw coal and coke, have high CO_2 emissions. Low-carbon cities reduce the proportion of traditional fossil energy use, increase the use of clean energy (e.g., hydropower, wind power, and solar energy), and reduce carbon emission by adjusting their respective energy structures (Liu et al., 2022). *Second*, the low-carbon city pilot policy requires the acceleration of low-carbon technology demonstration, promotion, and application. In terms of policy, carbon tax and R&D subsidies can encourage companies to invest in cleaner production and technological innovations, reduce carbon emissions, increase carbon productivity, and promote low-carbon economy growth (Acemoglu et al., 2016; Aghion et al., 2016). In other words, such a policy can promote the progress of low-carbon technology and increase the number of green patent applications, thus improving carbon productivity. *Third*, different from Acemoglu et al.(2016), Huo et al.(2022) and Liu et al. (2022) argued that to reduce carbon emissions by adjusting the energy structure and promoting low-carbon technology innovation, if the local government improves the low-carbon technology access standards of enterprises and expands the number of low-carbon-type enterprises entering the market, it can reduce the overall carbon emission intensity and improve carbon productivity. Accordingly, the first hypothesis is proposed:

Hypothesis 1. The low-carbon city pilot policy can improve carbon productivity, and the mediation effect of this pilot policy operates by adjusting the energy structure, increasing the number of low-carbon-type enterprises entering the market, and enhancing green technology innovation.

To alleviate fiscal pressure, local governments may adopt two measures. *First*, they could increase the number of high-energy-consuming industrial enterprises and relax environmental regulations, thus increasing the number of pollution-intensive enterprises (Wang and Zhang, 2017; Huang and Zhou, 2020). Although this will increase fiscal revenue and alleviate fiscal pressure, it will also increase carbon emissions and lead to a decline in carbon productivity. *Second*, they could alleviate fiscal pressure by increasing the actual non-tax burden of enterprises (Peng et al., 2020; Zhao and Fan, 2020). Such an increase leads to a concomitant increase in policy uncertainty and operating costs for enterprises. Excessive non-tax burdens lead to insufficient funds for low-carbon technological innovation. At the same time, enterprises may cease operations due to excessive non-tax burdens, which is seriously detrimental to carbon emission reduction and carbon productivity improvement. In addition, strengthening tax collection and management and increasing the non-tax burden will have a distorting effect on investment in capital factors and reduce the efficiency of capital allocation (Huang and Deng, 2020), which are also not conducive to improving carbon productivity. Unlike Huang and Zhou (2020), Zhao and Fan (2021), and other studies, we link fiscal pressure to carbon productivity, recognizing the role of fiscal pressure. Accordingly, the second hypothesis is proposed:

Hypothesis 2. An increase in fiscal pressure leads to the decline of carbon productivity.

During the implementation of the low-carbon city pilot policy, some enterprises with high energy and resource consumption may be shut down, thereby reducing government revenues and increasing fiscal pressure. To alleviate the fiscal pressure, local governments either increase the intensity of tax collection and management(Huang and Zhou, 2020) or increase non-tax collection efforts(Peng et al., 2020; Zhao and Fan, 2020), or both, which will increase the actual burden on enterprises. As a result, enterprises do not have enough funds for the research and development and use of low-carbon clean technologies, which will not help reduce carbon emissions and improve carbon productivity. When the tax and non-tax burdens of enterprises have reached high levels, and there is no way to further increase the intensity of tax and non-tax collection, local governments have to relax environmental regulations again and increase the entry of high-energy-consuming enterprises, resulting in increased carbon emissions and lower carbon productivity.

By contrast, during the implementation of the low-carbon city pilot policy, if the local government provides policy support for the low-carbon clean technology transformation of stock enterprises (note: high-polluting enterprises must be closed), such action can stabilize the tax base and improve carbon productivity. In addition, the low-carbon technology access standards for new enterprises should be improved to enable them to meet the requirements of low-carbon development, thereby expanding the tax base and reducing the intensity of carbon emissions. The above measures will not increase fiscal pressure but will alleviate fiscal pressure and improve carbon productivity. Accordingly, the third hypothesis is proposed:

Hypothesis 3. The fiscal pressure brought about by the low-carbon city pilot policy will hinder the improvement of carbon productivity. However, if the local government increases the policy support for the optimization of low-carbon technologies of existing enterprises and raises the low-carbon access standards for new enterprises, such a pilot policy will not lead to increased fiscal pressure. Moreover, carbon productivity will be reduced.

3 Methodology

3.1 Empirical model

This paper examines the impacts of the low-carbon city pilot policy in 2010 and 2012. Referring to the methods of Angrist and Pischke (2008), Callaway and Sant'Anna (2021), and Baker et al. (2022), the staggered DID model is used for estimation. The benchmark model is set as follows:

$$CP_{it} = \beta_0 + \beta_1 Treat_i * Post_{it} + \beta_2 Treat_i * Post_{it} * FP_{it} + \sum_{k=1}^{n} \phi_j X_{jit} + \mu_i + \theta_t + \varepsilon_{it}, \quad (1)$$

where i stands for city, t stands for year, CP_{it} denotes carbon productivity, $Treat_i$ stands for whether city i is a low-carbon pilot city, $Post_{it}$ is a time dummy variable of the low-carbon city pilot policy, $Treat_i * Post_{it} * FP_{it}$ is the interaction term of the dummy variable of the low-carbon city pilot policy and its fiscal pressure, μ_i is the city-specific fixed effect, θ_t is the year-specific fixed effect, ε_{it} is the random disturbance term, and X_{jit} is a set of control variables, including investment growth rate (IGR_{it}), population growth rate (PGR_{it}), trade competitiveness (TC_{it}), human capital level (HC_{it}), and fiscal pressure (FP_{it}). Moreover, to investigate whether there is a time-lag effect in the impact of the low-carbon city pilot policy on carbon productivity, the model is set as follows:

$$CP_{it} = \beta_0 + \beta_1 Treat_i * Post_{it-1} + \beta_2 Treat_i * Post_{it-1} * FP_{it} + \sum_{k=1}^{n} \phi_j X_{jit} + \mu_i + \theta_t + \varepsilon_{it} \quad (2)$$

where $Post_{it-1}$ is one period lag of the low-carbon city pilot policy. The other variables are the same as those in Eq. 1.

To test whether the staggered DID model satisfies the assumption of parallel trends and to examine the dynamic effects of the low-carbon city pilot policy over time, this paper draws on the methods of Jacobson et al. (1993), Freyaldenhoven et al. (2019), and Sun and Abraham (2021) and adopts the event analysis method for estimation. The model is set as follows:

$$CP_{it} = \beta_0 + \sum_{k=2005}^{t} \beta_k Treat_i * D_{it}^k + \beta_2 Treat_i * Post_{it} * FP_{it} + \sum_{k=1}^{n} \phi_j X_{jit} + \mu_i + \theta_t + \varepsilon_{it}, \quad (3)$$

where i stands for city, t stands for year, $Treat_i$ is a dummy variable representing whether city i is a low-carbon city, and D_{it}^k is the time dummy variable, D_{it}^k is assigned a value of one in k year and 0 for other years. The coefficient of β^k is the interaction term ($Treat_i * D_{it}^k$) that measures the difference between the treatment group and the control group during the period of the low-carbon city pilot policy. The other variables are the same as those in Eq. 1.

3.2 Variables

3.2.1 Dependent variable

This paper refers to the method of Shao et al. (2014) and Hu and Liu (2016) to measure carbon productivity as follows:

$$CP_{it} = \frac{GDP_{it}}{(CO_2)_{it}}, \quad (4)$$

where i stands for city, t stands for year, CP_{it} denotes carbon productivity, GDP_{it} is the city's gross domestic product(unit: yuan, ¥), and $(CO_2)_{it}$ is the city's total CO_2 emissions (unit: kilograms).

3.2.2 Independent variables

According to the basic steps of the staggered DID model, two dummy variables related to the low-carbon city pilot policy are constructed. The first one consists of the group dummy variable of the low-carbon city pilot policy ($Treat_i$), namely, the control group and the treatment group, in which the low-carbon city is defined as the treatment group and is assigned a value of 1, while the non-low-carbon city is defined as the control group and is assigned a value of 0. The second consists of the time dummy variable of the low-carbon city pilot policy($Post_{it}$). If the city i is selected as a low-carbon pilot area in year t, the time dummy variable of the low-carbon city pilot policy($Post_{it}$) is assigned a value of one in year t and subsequent years, while the others are assigned a value of 0.

The low-carbon city pilot policy($Treat_i \times Post_{it}$), which is a dummy variable, is measured by the interaction term of the group dummy variable of the low-carbon city pilot policy($Treat_i$) and the time dummy variable of the low-carbon city pilot policy($Post_{it}$).

Fiscal pressure (FP_{it}) is obtained as follows: calculate the difference between the general budget expenditure and tax revenue, and then divide it by the general budget expenditure.

The fiscal pressure brought about by the low-carbon city pilot policy($Treat_i \times Post_{it} \times FP_{it}$) is measured by the interaction

TABLE 1 Variable definitions and descriptive statistics.

Variables	Definitions	Observations	Mean	Standard deviation	Minimum	Maximum
CP	Carbon Productivity	3,666	5.871	2.967	1.990	12.592
Treat*Post	Low-carbon City Pilot Policy	3,666	0.060	0.238	0.000	1.000
Treat*Post*FP	FP brought about by the Treat*Post	3,666	0.029	0.127	0.000	0.892
FP	Fiscal Pressure	3,666	0.641	0.194	0.228	0.892
IGR	Investment Growth Rate	3,666	0.683	0.248	0.304	1.176
PGR	Population Growth Rate	3,666	0.057	0.043	−0.016	0.149
TC	Trade Competitiveness	3,666	0.314	0.441	−0.657	0.944
HC	Human Capital Level	3,666	1.197	0.375	0.735	2.278

term of the low-carbon city pilot policy($Treat_i \times Post_{it}$) and fiscal pressure (FP_{it}).

3.2.3 Control variables

With reference to the research of Liu (2022), Huo et al. (2022), and Ren et al. (2022). The selected control variables are as follows: investment growth rate (IGR_{it}), population growth rate (PGR_{it}), trade competitiveness (TC_{it}), and human capital level (HC_{it}). Investment growth rate (IGR_{it}) is measured by the annual growth rate of fixed asset investments, while population growth rate (PGR_{it}) is measured by the annual natural growth rate of the population. Trade competitiveness (TC_{it}) is obtained as follows: calculate the difference between the trade imports and exports, get the sum of the total imports and exports, and then calculate the ratio of that difference to the total. In addition, human capital level (HC_{it}) is measured as follows: get the sum of the number of students in colleges and universities*16 + the number of ordinary middle schools*9 + the number of ordinary primary schools*6, and then divide by the total population.

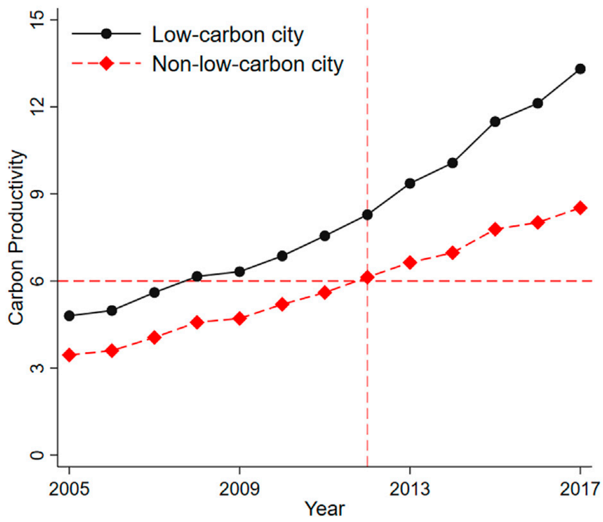

FIGURE 1
Carbon productivities of low-carbon and non-low-carbon cities.

3.3 Data

Fixed asset investment, population growth rate, GDP, general budget expenditure, human capital, and trade import and export data were sourced from the China Statistics for Regional Economy Database and China City Statistics Database of the EPS DATA platform. CO_2 emission data came from the China Carbon Accounting Database (CEADS), while the tax revenue data were sourced from the China Statistics for Regional Economy Database of the EPS DATA platform and China Economic Database of the CEIC data platform. For these different sources of data, we matched by city and year to obtain the required data.

After obtaining the data, we further processed them according to the following principles: 1) For any city with missing GDP data for 5 years or more, we deleted the sample data of the city. 2) Next, we deleted city samples whose numbers of corresponding years in the city code were less than 14 (i.e., the data whose statistical year was less than 14 years). 3) We used the three-period moving average method to make up for missing data. 4) After filling in the missing data, if the sample number of all indicators in any city was less than 13, the sample data of that city was deleted. 5) Except for the dummy variables of the low-carbon city pilot policy, other variables were winsorized at the level of 5%. 6) Given that Jiyuan City is a county-level city and the Daxing'an Mountains region has missing data, the samples from these two regions were deleted, leaving a total of 34 low-carbon pilot cities. In this way, we obtained the sample data for 282 cities in China over the period 2005–2017. The variables and their descriptive statistical characteristics are shown in Table 1.

Subsequently, we divided the whole sample of carbon productivity into two sample groups: the low-carbon city group and the non-low-carbon city group. Then, we

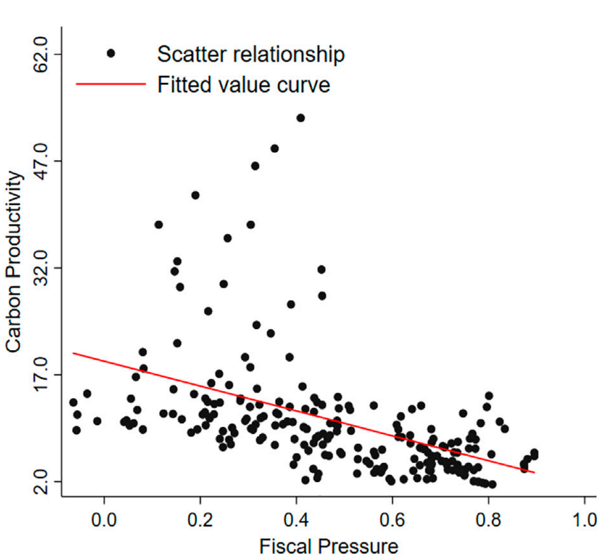

FIGURE 2
Scattered relationship between fiscal pressure and carbon productivity.

calculated the average value of the carbon productivity in each group every year. Finally, we plotted them. The trend chart of carbon productivity is displayed in Figure 1. In addition, we plotted a scatter diagram to present the relationship between fiscal pressure and carbon productivity, as shown in Figure 2.

Figure 1 indicates that before 2012, carbon productivity met the parallel assumption in both low-carbon and non-low-carbon cities. However, since 2012, the changes in the carbon productivity of the low-carbon cities have become significantly higher than those of non-low-carbon cities. These results initially reflect that the low-carbon city pilot policy strongly promotes carbon productivity. The results in Figure 2 demonstrate that a negative relationship between fiscal pressure and carbon productivity, that is, the greater the fiscal pressure, the lower the carbon productivity.

4 Empirical result analysis and robustness test

4.1 Parallel trend and heterogeneous treatment effect test

When using the staggered DID model to estimate the impacts of the low-carbon city pilot policy and fiscal pressure on carbon productivity, one necessary condition is that the control and treatment groups must meet the parallel trend assumption. If there is a difference in the time trend of carbon productivity between low-carbon and non-low-carbon cities before the launch of the low-carbon city pilot policy, it can be inferred that the difference is not caused by this pilot policy. In addition, although the staggered DID model estimates the average treatment effect of the low-carbon city pilot policy, the impacts of this policy in different years are not shown. Therefore, to test whether the staggered DID model is a suitable method, we used the event analysis method to test the parallel trends and dynamic effects of the low-carbon city pilot policy. This specific method involves the following procedure: first, generate the interaction term of a low-carbon city pilot policy group dummy variable and the year dummy variable, then estimate the coefficient of the interaction term to obtain the dynamic effect of the low-carbon city pilot policy. The results are shown in Figure 3.

Figure 3 plots the estimated results of the coefficients of the interaction term between the low-carbon city pilot policy group dummy variable and the year dummy variable under a 95% confidence interval (CI). Evidently, the coefficients of the interaction term are all around 0 in the years before the start of the low-carbon city pilot policy, suggesting that before the pilot policy was started, there was no significant difference between the treatment and control groups. Hence, the conditions for the assumption of parallel trends are established. After the launch of the pilot policy, the coefficient is positive and increases significantly, showing a stable trend. At this point, the estimated coefficients of the control and treatment groups are significantly different, which indicates that the implementation of the low-carbon city pilot policy significantly improves the carbon productivity of low-carbon cities.

The two-way fixed effects (FE) regression of the staggered DID model is a popular method to evaluate treatment effects. However, if the error term is not mean zero conditional on group and period, this can lead to the problem of heterogenous treatment effects (Gardner, 2021). de Chaisemartin and D'Haultfoeuille (2020) demonstrated that in several DID models, the two-way FE estimator is a weighted sum of the treatment effect in each group and period. If the average treatment effects (ATEs) are heterogeneous across groups or periods, it will result in the question of negative weights. The two-way FE estimators of the staggered DID model do not identify the typical effect of the treatment. To test whether heterogeneous treatment effects exist, de Chaisemartin and D'Haultfoeuille (2020) recommended computing the weights attached to the two-way FE regression of the staggered DID model and calculating the ratio of the coefficient of variable and the standard deviation of the weights. If many weights are negative and if the ratio is small, we should use the new method to estimate the staggered DID model. Thus, referring to the method of de Chaisemartin and D'Haultfoeuille (2020), we computed the weight of the treated group and periods. The results are shown in Table 2.

In Table 2, the results indicate that under the condition of the estimation of the two-way FE of the staggered DID model, there are 220 positive weights and 0 negative weights. Moreover, the standard deviation of the treatment effect across the low-carbon cities and years is 0.879, which is

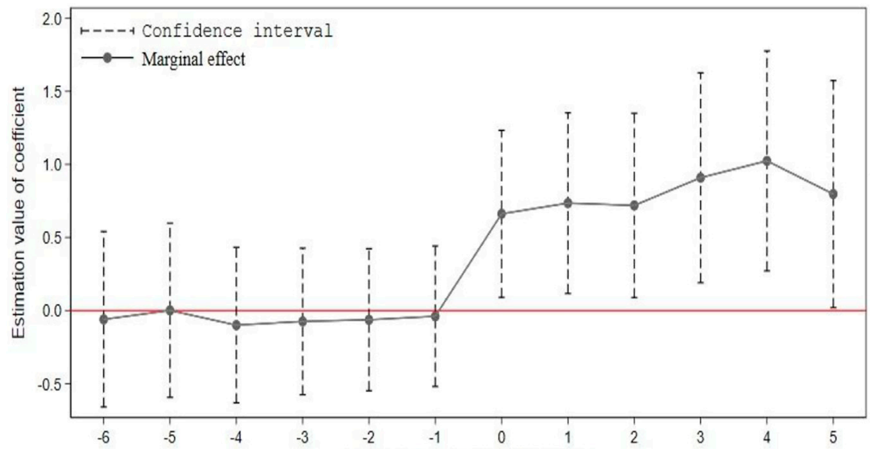

FIGURE 3
Dynamic effect of low-carbon city pilot policy.

TABLE 2 Estimation of weights.

	Positive Weights	Negative Weights
Number of weights	220	0
Sum of weights	1	-
Standard deviation of the treatment effect	0.879	-

greater than 0. Thus, we can use the two-way FE regression of the staggered DID model to estimate the treatment effect of the low-carbon city pilot policy.

4.2 Baseline DID model estimation

As a major policy measure to promote carbon productivity, the low-carbon city pilot policy advocates low-carbon production and consumption, which can undoubtedly reduce CO_2 emissions and improve the quality of economic development. Therefore, the implementation of this pilot policy provides a quasi-natural experiment for this study. We used a staggered DID model to estimate the impacts of the policy and fiscal pressure on carbon productivity. The results are provided in Table 3.

In Table 3, Columns (1)–3) show the results of the staggered DID estimation under the conditions of controlling for only the year FE, only the city FE, and both types of FE, respectively. Columns (4)–6) present the effects of one period lag of the low-carbon city pilot policy. The results indicate that the coefficients pass the significance test after controlling for both the city and year FE, regardless of whether it is the current period or one lag period.

Specifically, Column 3) shows that when the city and year FE are controlled simultaneously, the coefficient of $Treat{*}Post$ is significant for 1.318 at the 1% level, which indicates that the low-carbon city pilot policy can significantly promote carbon productivity. The coefficient of $Treat{*}Post{*}FP$ is significant for–2.722, which means that the fiscal pressure brought about by the low-carbon city pilot policy will reduce carbon productivity, and the degree of reduction depends on the status of fiscal pressure. The coefficient of fiscal pressure (FP) is significant for –0.931, which suggests that an increase in fiscal pressure will decrease carbon productivity. Peng et al. (2020) and Zhao and Fan (2021) explained that the government might relax environmental regulations to relieve fiscal pressure, which can result in an increase in high-energy-consuming enterprises that reduces carbon productivity. As seen in Column (6), after controlling for the city FE and the year FE, the coefficients of $Treat{*}Post_{-1}$, $Treat{*}Post{*}FP$ and fiscal pressure (FP) are 0.609, –1.309, and –1.157, respectively, all of which are significant at the 1% level. These results demonstrate that the effects of the low-carbon city pilot policy are persistent. Hence, Hypotheses one to three are verified. In other words, we cannot ignore the negative effects of fiscal pressure on carbon productivity when implementing the low-carbon city pilot policy.

TABLE 3 Benchmark estimation results.

Variables	Carbon Productivity (*CP*)					
	(1)	(2)	(3)	(4)	(5)	(6)
Treat ∗ *Post*	4.451***	3.155***	1.318***			
	(0.331)	(0.377)	(0.242)			
$Treat * Post_{-1}$				2.244***	1.740***	0.609***
				(0.217)	(0.317)	(0.138)
Treat ∗ *Post* ∗ *FP*	−5.352***	−5.793***	−2.722***	−0.956**	−2.969***	−1.309***
	(0.635)	(0.789)	(0.463)	(0.409)	(0.583)	(0.259)
FP	2.376***	−3.869***	−0.931***	2.138***	−4.106***	−1.157***
	(0.470)	(0.231)	(0.340)	(0.492)	(0.249)	(0.350)
IGR	5.016***	−1.320***	0.386**	4.800***	−1.351***	0.417**
	(0.151)	(0.226)	(0.156)	(0.160)	(0.233)	(0.163)
PGR	3.304***	2.746***	3.443***	3.143***	2.796***	3.847***
	(0.873)	(0.967)	(0.613)	(0.867)	(0.998)	(0.610)
HC	−1.512***	0.846***	1.308***	−1.704***	0.920***	1.267***
	(0.219)	(0.133)	(0.164)	(0.228)	(0.140)	(0.175)
TC	0.105	0.273***	0.291***	0.071	0.304***	0.260***
	(0.085)	(0.093)	(0.066)	(0.089)	(0.099)	(0.069)
Constant	2.401***	7.977***	4.350***	3.042***	8.282***	4.699***
	(0.464)	(0.275)	(0.330)	(0.478)	(0.288)	(0.342)
Year fixed effect	NO	YES	YES	NO	YES	YES
City fixed effect	YES	NO	YES	YES	NO	YES
Observations	3,666	3,666	3,666	3,384	3,384	3,384
Number of cities	282	282	282	282	282	282
R_squared	0.782	0.412	0.904	0.792	0.383	0.908
Fvalue	343.823	160.546	22.838	256.637	133.955	20.006

Note: ***, **, and * indicate significance at the 1, 5, and 10% levels, respectively. Robust standard errors are reported in parentheses.

4.3 Robustness test

To verify whether the relationship among the low-carbon city pilot policy, fiscal pressure, and carbon productivity is robust, we test the robustness of the conclusions by taking a series of measures, including index substitution, the Tobit-DID model of data merging processing, and counterfactual testing methods.

4.3.1 Robustness analysis after carbon productivity Is substituted by $lnCO_2$

A similar indicator to carbon productivity is carbon emissions. We use the logarithm of the total carbon emissions ($lnCO_2$) as an alternative indicator of carbon productivity and then estimate the model. In doing so, it is also helpful to compare the connections and differences between this paper and the study by Huo et al. (2022) and Liu et al. (2022) and explore whether the fiscal pressure brought about by the low-carbon city pilot policy is a factor that cannot be ignored. The estimated results are provided in Table 4.

Columns (3)–4) in Table 4 indicate that, without controlling for the effects of the interaction term of the low-carbon city pilot policy and fiscal pressure(*Treat*∗*Post*∗*FP*), the coefficient of *Treat*∗*Post* is significant for -0.040. This estimated coefficient size is similar to the results obtained by Huo et al. (2022) and Liu et al. (2022). When controlling for the influence of the interaction term of the low-carbon city pilot policy and fiscal pressure(*Treat*∗*Post*∗*FP*), the coefficient of *Treat*∗*Post* is -0.165, while the coefficient of *Treat*∗*Post*∗*FP* is 0.252. Both are significant at the 1% level. These results reveal that the low-carbon city pilot policy can reduce carbon emissions and improve carbon productivity; however, the fiscal pressure brought about by this pilot policy will increase carbon emissions and reduce carbon productivity.

At the same time, compared to those that do not control for the influence of the interaction term of the low-carbon city pilot policy and fiscal pressure(*Treat*∗*Post*∗*FP*), under the condition of controlling the influence of *Treat*∗*Post*∗*FP*, the results indicate that not only is the coefficient of *Treat*∗*Post* larger, but the coefficient of *Treat*∗*Post*∗*FP* is also significantly positive,

TABLE 4 Estimations after using lnCO_2.

Variables	Carbon Emission ($\ln CO_2$)			
	Without $Treat*Post*FP$ (Huo et al., 2022)	With $Treat*Post*FP$ (The way of this paper)	Without $Treat*Post*FP$ (Huo et al., 2022)	With $Treat*Post*FP$ (The way of this paper)
	(1)	(2)	(3)	(4)
$Treat*Post$	−0.039***	−0.175***	−0.040***	−0.165***
	(0.009)	(0.024)	(0.009)	(0.023)
$Treat*Post*FP$		0.276***		0.252***
		(0.040)		(0.039)
FP			-0.050*	-0.064**
			(0.027)	(0.027)
Constant	23.704***	23.704***	23.622***	23.627***
	(0.001)	(0.001)	(0.030)	(0.030)
Control variables	NO	NO	YES	YES
Year fixed effect	YES	YES	YES	YES
City fixed effect	YES	YES	YES	YES
Observations	3,666	3,666	3,666	3,666
Number of cities	282	282	282	282
R_squared	0.989	0.989	0.989	0.990
Fvalue	19.444	27.244	15.018	16.971

Note: ***, **, and * indicate significance at the 1, 5, and 10% levels, respectively. Robust standard errors are reported in parentheses.

which implies that the ultimate impact of the low-carbon city pilot policy also depends on the status of fiscal pressure, that is, the marginal impact is $\beta_1 + \beta_2 * FP$.This is significantly different from the study of Huo et al. (2022) and Liu et al. (2022), where they obtained the impact as β_1.Therefore, ignoring the impact of the fiscal pressure brought about by the low-carbon city pilot policy will lead to not only a biased evaluation of the effect of the pilot policy but also a failure to recognize the negative side of this pilot policy, which will be detrimental to reducing carbon emissions and improving carbon productivity.

4.3.2 Robustness analysis after substituted by secondary industry and industrial carbon productivity

The low-carbon city pilot policy advocates low-carbon production and consumption. Secondary industry, especially the industrial sector, is the main source of CO_2 emissions. This means that if the secondary industry and the industrial sector carbon productivity in a low-carbon city are significantly improved, then the pilot policy will be able to promote carbon productivity; otherwise, the pilot policy is invalid. We used the ratio of secondary industry output value (unit: yuan) and industrial output value (unit: yuan) to CO_2 emissions(unit: kilogram) to measure the secondary industry and industrial sector carbon productivity. Subsequently, the GDP carbon productivity in the staggered DID model in Eq. 2 was substituted by the secondary industry carbon productivity and industrial sector carbon productivity. After controlling for the city FE and the year FE, we estimated the impacts of the low-carbon city pilot policy and fiscal pressure on carbon productivity. To examine the continuous effects of the low-carbon city pilot policy, we estimated the impact of the one period lag of interaction term($Treat*Post_{-1}$). The results are shown in Table 5.

Table 5 presents the estimated results after replacements with secondary industry carbon productivity. In Columns 1) and (2), the coefficient of $Treat*Post$ is 1.093 and the coefficient of $Treat*Post*FP$ is −1.847, both pass the significance test. In Column (2), the coefficient of $Treat*Post_{-1}$ is significant for 0.659, while the coefficient of $Treat*Post*FP$ is significant for −0.900. These results suggest that the low-carbon city pilot policy strongly promotes carbon productivity in secondary industry, and this promotion has a persistent character. The fiscal pressure brought about by the policy hinders the improvement of carbon productivity in the same industry.

In Column (3), after substituting carbon productivity with industrial sector, the coefficient of $Treat*Post$ is significant for 0.761, while the coefficient of $Treat*Post*FP$ is significant for −1.511. In Column(4), the coefficients of $Treat*Post_{-1}$ and $Treat*Post*FS$ are significant for 0.422 and −0.789 at the 1%

TABLE 5 Estimations after using the secondary industry and industrial carbon productivity.

Variables	Secondary Industry Carbon Productivity		Industrial Carbon Productivity	
	(1)	(2)	(3)	(4)
$Treat*Post$	1.093***		0.761***	
	(0.222)		(0.203)	
$Treat*Post_{-1}$		0.659***		0.422***
		(0.126)		(0.113)
$Treat*Post*FP$	−1.847***	−0.900***	−1.511***	−0.789***
	(0.387)	(0.201)	(0.352)	(0.178)
FP	−0.262	−0.305	−0.341	−0.268
	(0.270)	(0.288)	(0.249)	(0.263)
Constant	2.252***	2.407***	2.689***	2.762***
	(0.246)	(0.260)	(0.228)	(0.239)
Control variables	YES	YES	YES	YES
Year fixed effect	YES	YES	YES	YES
City fixed effect	YES	YES	YES	YES
Observations	3,666	3,384	3,666	3,384
Number of cities	282	282	282	282
R_squared	0.863	0.870	0.856	0.864
Fvalue	13.056	12.715	7.579	6.871

Note: ***, **, and * indicate significance at the 1, 5, and 10% levels, respectively. Robust standard errors are reported in parentheses.

level, respectively. These results indicate that the low-carbon city pilot policy promotes carbon productivity in the industrial sector, but the fiscal pressure brought about by the low-carbon city pilot policy reduces carbon productivity in industrial sector. Therefore, the conclusion that the low-carbon city pilot policy can promote carbon productivity is robust. At the same time, the conclusion that the fiscal pressure brought about by the policy can decrease carbon productivity is also robust, and the extent of such decline depends on the magnitude of the fiscal pressure.

4.3.3 Censored data and tobit-DID estimation

To deal with the possible adverse effects of variable singular values, we used the winsorize method to deal with all variables at the 5% level, which resulted in the problem of censored data. Although we observed the data for all samples, data with variable values below the 5% level were censored to the 5% level, and those with values above the 95% level were censored to the 95% level. However, the potential issue with censored data is that the estimates of the staggered DID model with two-way FE are inconsistent. To solve this problem, the method of censored regression (i.e., Tobit model estimation) was adopted. Therefore, we used the panel Tobit-DID model to estimate the impacts of the low-carbon city pilot policy and fiscal pressure on carbon productivity. The estimation results are provided in Table 6.

In Table 6, Columns 1) and 2) indicate that, without controlling for the influence of other variables, the coefficients of both current period $Treat*Post$ and one period lag of $Treat*Post_{-1}$ are significantly greater than 0, suggesting that the impact of the low-carbon city pilot policy on carbon productivity is robust. At the same time, the coefficients of $Treat*Post*FP$ and FP are negative, which confirms that the negative effect of fiscal pressure brought about by the policy on carbon productivity is also robust. Under the condition of controlling for the influence of other variables, Columns 3) and 4) show that the impacts of the policy and fiscal pressure on carbon productivity remain unchanged. Therefore, the effects of the low-carbon city pilot policy are robust.

4.3.4 Counterfactual testing

We tested the relationship among the low-carbon city pilot policy, fiscal pressure, and carbon productivity through indicator substitution and Tobit-DID methods, all of results reveal that the conclusions are robust. However, a further placebo test is needed to determine whether counterfactual experiments in different cities and in different periods can yield consistent conclusions. The basic idea involved the selection of a total of 34 cities as low-carbon cities in 2010 and 2012, with 248 unselected cities. Initially, there were 36 low-carbon pilot cities, but Jiyuan City is a county-level city and the Daxinganling area has missing data. Thus, the samples from these two pilot areas were deleted. Next, we randomly selected 34 cities from 282 cities as "pseudo-low-carbon cities." Assuming that these 34 cities were selected as low-carbon cities, namely, the treatment group, and the other cities

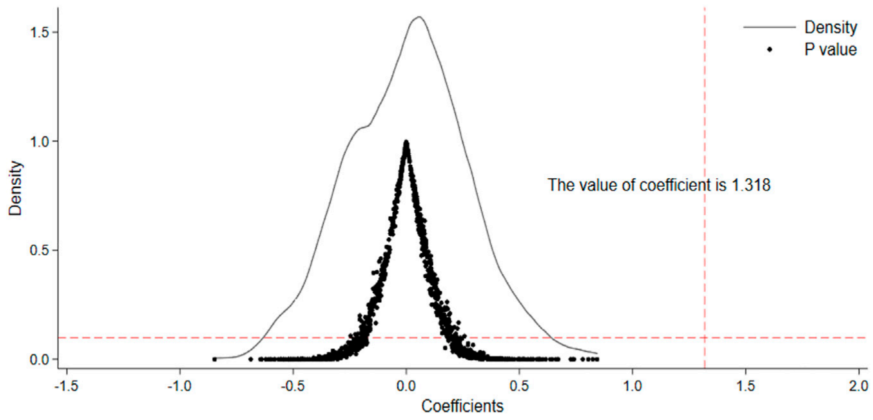

FIGURE 4
The placebo effects of thelow-carbon city pilot policy. Note: The figures show the distribution of estimated coefficients and corresponding *p*-values of the pseudo-low-carbon city pilot dummy variables sampled 1,000 times. The vertical dashed line represents the estimated value of the true coefficient, while the horizontal dashed line represents a value of 0.1.

TABLE 6 Tobit-DID estimation results.

Variables	Carbon Productivity (*CP*)			
	(1)	(2)	(3)	(4)
*Treat*Post*	1.457***		0.943***	
	(0.424)		(0.222)	
$Treat*Post_{-1}$		1.527***		1.078***
		(0.421)		(0.250)
*Treat*Post*FP*	−2.141	−2.722	−2.513	−2.846*
	(2.218)	(2.486)	(1.550)	(1.670)
FP	3.485	3.529	2.332	2.389
	(2.358)	(2.433)	(1.536)	(1.643)
Constant	−0.087	0.098	−0.056	0.015
	(0.426)	(0.417)	(0.213)	(0.220)
Control variables	NO	NO	YES	YES
Year fixed effect	YES	YES	YES	YES
City fixed effect	YES	YES	YES	YES
Observations	3,666	3,384	3,666	3,384
Number of cities	282	282	282	282
R_squared	0.013	0.014	0.131	0.126
LLvalue	−7197.071	−6475.852	−6331.831	−5744.990

Note: ***, **, and * indicate significance at the 1, 5, and 10% levels, respectively. Robust standard errors are reported in parentheses.

comprised the control group, then more than 500 random samples were taken to complete the placebo test.

However, the pilot policy times of the two batches of selected low-carbon cities vary, and this factor cannot be ignored in counterfactual experiments. Therefore, in the quasi-natural experiment using the staggered DID model to evaluate the effects of the low-carbon city pilot policy, it is necessary to use the placebo test method to conduct the counterfactual experiments. The specific methods are as follows. First, we used the "sample"command to randomly select a year as a pseudo-low-carbon city pilot policy year, after which we randomly selected 34 cities as pseudo-low-carbon cities and kept the city code and year from which the sample was drawn. Then, the sample was matched with the original data, and the cities that were successfully matched were classified as the pseudo-low-carbon cities (i.e., the samples of the treatment group); the cities that were not matched became the samples of the control group. Then, the dummy variable of the pseudo-low-carbon city pilot policy was generated by comparing the sequential relationship between each period and the pseudo-low-carbon city pilot policy year. Based on this estimation, the estimated coefficient, standard error, and *p*-value of the pseudo-low-carbon city pilot policy dummy variable were obtained. We repeated this process 1,000 times to obtain the results of the placebo effect test of the low-carbon city pilot policy. The detailed results are shown in Figure 4.

The results in Figure 4 reveal that the estimated coefficients of the pseudo-low-carbon city pilot policy are basically around 0, and the corresponding *p*-values are all greater than 0.1. Hence, the estimated value of the low-carbon city pilot policy in the real staggered DID model is not obtained by chance or coincidence, so the influence of random factors or other similar policies can almost be ignored. This finding further illustrates that the estimated coefficient of the low-carbon city pilot policy is robust, which evidences that the pilot policy effectively promotes carbon productivity.

5 Discussion of the heterogeneity and mediation effects

In this section, we carry out two aspects of research. First, we conduct a heterogeneous analysis of the effects of the low-carbon

TABLE 7 Estimations under different regional conditions.

Variables	Carbon Productivity (*CP*)			
	Eastern, Central and Western Regions		North and South Regions	
	Central and Western Regions	Eastern Regions	North Regions	South Regions
	(1)	(2)	(3)	(4)
*Treat**Post*	1.450***	1.182***	1.580***	0.497*
	(0.341)	(0.356)	(0.510)	(0.257)
*Treat**Post**FP*	−3.038***	−2.743***	−3.206***	−1.462***
	(0.558)	(0.884)	(0.773)	(0.531)
FP	−3.684***	2.633***	−1.731***	0.064
	(0.466)	(0.447)	(0.431)	(0.403)
Constant	5.940***	3.524***	3.236***	6.816***
	(0.449)	(0.444)	(0.428)	(0.399)
Control variables	YES	YES	YES	YES
Year fixed effect	YES	YES	YES	YES
City fixed effect	YES	YES	YES	YES
Observations	2,366	1,300	1911	1755
Number of cities	182	100	147	135
R_squared	0.891	0.922	0.885	0.932
Fvalue	27.992	13.290	23.771	3.705

Note: ***, **, and * indicate significance at the 1, 5, and 10% levels, respectively. Robust standard errors are reported in parentheses.

city pilot policy and fiscal pressure on carbon productivity and test whether this effect is the same under different conditions of geographic location and economic development levels. Second, we perform a test of the effect of the mediation mechanism, explore the mechanism by which the pilot policy and fiscal pressure affect carbon productivity, and provide multiple mediation mechanisms for the impact of the low-carbon city pilot policy on carbon productivity.

5.1 Analysis of heterogeneity

There may be differences in the effects of the low-carbon city pilot policy under different geographic locations and economic development levels. Thus, we conducted heterogeneity analyses based on these aspects and discussed the reasons for any potential differences.

5.1.1 Heterogeneity test in different geographical locations

To distinguish the impact of geographic location on the effect of the low-carbon city pilot policy, we divided the sample based on two geographic locations. First, we divided the entire sample into cities from the Eastern region and those from the Central and Western regions. The Eastern region included 11 Eastern provinces and cities, such as Beijing and Tianjin. The corresponding city samples were the samples of the Eastern region. The corresponding city samples of other provinces, municipalities, and districts comprised the samples of the Central and Western regions. Second, we divided the entire sample into groups consisting of samples from the southern and northern cities. China was divided into Northern and Southern regions along the Qinling–Huai River line. Most of the cities in Jiangsu, most of the cities in Anhui, and a small part of the cities in Shaanxi, Chongqing, Sichuan, and 17 other provinces, cities, and districts comprised the group of southern cities. Other provinces, municipalities, and districts made up the northern region. The cities corresponding to other provinces, municipalities, and districts were comprised northern cities. After dividing the sample groups, we adopted the staggered DID model for estimation. The results are provided in Table 7.

Table 7 presents the estimation results of the staggered DID model under different regional conditions. In Columns 1) and (2), it is apparent that the coefficients of *Treat**Post* are significantly greater than 0, whilethe coefficients of *Treat**Post**FP* are significantly less than 0 in the Eastern, Central, and Western regions. In Columns 3) and (4), the coefficients of *Treat**Post* are significantly greater than 0, and the coefficients of *Treat**Post**FP* are significantly less than 0 in

TABLE 8 Estimations under different economic development levels.

Variables	Carbon Productivity (*CP*)			
	Size of GDP		Per Capita GDP	
	small	large	low	high
	(1)	(2)	(3)	(4)
*Treat*Post*	−0.946	1.258***	0.792	1.338***
	(0.839)	(0.258)	(0.524)	(0.295)
*Treat*Post*FP*	0.789	−3.028***	−1.342*	−3.583***
	(1.400)	(0.517)	(0.723)	(0.688)
FP	−3.103***	0.950**	−2.673***	−0.020
	(0.475)	(0.462)	(0.474)	(0.470)
Constant	4.564***	6.034***	6.222***	4.625***
	(0.541)	(0.401)	(0.468)	(0.462)
Control variables	YES	YES	YES	YES
Year fixed effect	YES	YES	YES	YES
City fixed effect	YES	YES	YES	YES
Observations	1833	1833	1833	1833
Number of cities	141	141	141	141
R_squared	0.890	0.916	0.902	0.901
Fvalue	20.192	6.813	10.382	12.516

Note: ***, **, and * indicate significance at the 1, 5, and 10% levels, respectively. Robust standard errors are reported in parentheses.

both the Southern and Northern regions. These results indicate that whether in the Eastern, Central and Western regions or the Southern and Northern regions, the low-carbon city pilot policy significantly promotes carbon productivity, but the fiscal pressure resulting from this pilot policy have an adverse impact on carbon productivity.

At the same time, the results show that the coefficients of *FP* in the Eastern and Southern regions are both positive, while the coefficients of *FP* in the Northern, Central, and Western regions are negative. Compared with the Northern, Central, and Western regions, an increase in fiscal pressure can promote carbon productivity in the Southern and Eastern regions. The likely reason is that the region turned fiscal pressure into a driving force to create conditions and environments that are conducive to economic development, which would increases carbon productivity and provides a possible explanation for the North–South and East–West regional differences in economic development.

5.1.2 Heterogeneity of the difference in the level of economic development

One fact that cannot be ignored is that the level of economic development itself may also have an influence on carbon productivity, which may affect the effective of the low-carbon city pilot policy. To characterize such an impact, we adopted the following methods. First, we examined whether there are differences in the effects of the low-carbon city pilot policy under different conditions of GDP size. To this end, we calculated the average GDP of each city in the sample period, sorted the averaged GDP according to size and divided the sorted data into two groups: the cities with small GDPs and those with large GDPs. Then, we used the staggered DID model to perform the estimation. Second, we also investigated whether there are differences in the effects of the low-carbon city pilot policy under different per capita GDP levels. For this, we calculated the average per capita GDP of each city in the sample period, sorted the average per capita GDP, and divided the sorted per capita GDP into city groups with low and high per capita GDP. Finally, we performed the estimation after grouping. The results are displayed in Table 8.

Table 8 presents the estimated results of the low-carbon city pilot policy effects under different sizes of GDP and levels of per capita GDP. Columns 1) and 2) show that in the city group with small GDPs, the coefficients of *Treat*Post* and *Treat*Post*FP* are not significant, while the coefficients of *FP* are significantly negative. In the city group with large GDPs, the coefficients of *Treat*Post* and *FP* are significantly greater than 0, and the coefficient of *Treat*Post*FP* is significantly less than 0. A possible reason is that most of the low-carbon pilot projects are located in provincial capital cities, and most cities with small GDPs are located in non-provincial capital cities, where such a pilot policy has not yet been implemented. Therefore, the impacts of the low-carbon city pilot policy on their carbon productivity are not obvious. However, relative to cities with large GDPs, increased fiscal pressure can reduce the carbon productivity levels in cities with small GDPs.

The results in Columns 3) and 4) in Table 8 indicate that under the condition of cities with low levels of per capita GDP, the coefficient of *Treat*Post* is positive but not significant; the coefficient of *Treat*Post*FP* is significantly negative at the 10% level, and the coefficient of *FP* is significantly less than 0. Under the condition of cities with high levels of per capita GDP, the coefficients of *Treat*Post* and *Treat*Post*FP* both pass the significance test, and the coefficients of *FP* are positive. Therefore, compared to cities with high levels of per capita GDP, in cities with low levels of per capita GDP do not display an obvious effect of the low-carbon city pilot policy. A possible reason is that most of the cities selected for the low-carbon pilot areas are located in provincial capitals and economically developed cities with high per capita GDP levels. Meanwhile, most cities with low per capita GDP levels are not within the scope of such a policy pilot region, as reflected in the small impact of the low-carbon city pilot policy on them. However, compared to cities with high levels of per capita GDP, cities with low levels of per capita GDP suffer from increased fiscal pressure, which will be detrimental to carbon productivity.

5.2 Test of the mediation effect.

The impacts of the low-carbon city pilot policy and fiscal pressure on carbon productivity are mainly achieved through technological innovation and progress, closing or restricting the production of high-energy-consuming enterprises, restricting new high-energy-consuming enterprises, and increasing the use of clean energy. At the same time, closing down enterprises will increase fiscal pressure. To resolve this problem, some local governments will partially relax restrictions on the development of high-energy-consuming industries. In view of this, we introduced four mediation variables: "energy structure,""the number of green patent applications,""the number of registrations of low-carbon-type enterprises," and "fiscal pressure brought about by the low-carbon city pilot policy." We constructed the mediation effect model of the low-carbon city pilot policy and fiscal pressure on carbon productivity and tested the mediation effect of the policy.

Among them, the number of green patent applications ($\ln(NP)$) is measured by using the natural logarithm of the number of green patent applications. The relevant data came from the State Intellectual Property Office. The registration number of low-carbon-type enterprises ($NLCE$) is measured by the ratio of registration of non-high energy-consuming companies to the total population. The original data sourced from Liu (2019) were shared on GitHub. The fiscal pressure brought about by the low-carbon city pilot policy ($Treat \times Post \times FP$) is measured by the interaction term between the dummy variables of the low-carbon city pilot policy and fiscal pressure. The original fiscal expenditure and tax data used to measure fiscal pressure were derived from the CEIC Database and the China Statistics for Regional Economy Database of the EPS DATA platform. The energy structure includes two measurement indicators: the ratio of electricity consumption to total energy consumption (PSE_{it}) and non-thermal power generation (NTP_{it}). The specific measurement methods are as follows:

$$PSE_{it} = PSE_{jit} = \frac{\left(NL_{jit} \Big/ \sum_{s=1}^{S} NL_{jst}\right) * PC_{jt}}{\left((CO_2)_{jit} \Big/ \sum_{s=1}^{S} (CO_2)_{jst}\right) * TEC_{jt}}, \quad (5)$$

$$NTP_{it} = NTP_{jit} = \frac{NL_{jit}}{\sum_{s=1}^{S} NL_{jst}} * \left(TEG_{jt} - TPG_{jt}\right), \quad (6)$$

where j stands for province, i stands for city, t stands for year, S stands for the total number of cities, CO_2 denotes carbon dioxide emissions, TEC_{jt} is total energy consumption, PC_{jt} is total power consumption, TEG_{jt} is total power generation, TPG_{jt} is thermal power generation, and NL_{jit} is night light brightness. When calculating the ratio of electricity consumption to total energy consumption, we converted the electricity consumption into standard coal usingthe method of 0.1229 kg/kWh and then calculated its ratio. The raw data of night light brightness was collected by the Operational Linescan System (OLS) carried by the US Defense Meteorological Satellite Program (DMSP) and the Visible Infrared Imaging Radiometer Suite (VIIRS) of the Suomi National Polar Orbiting Partnership Satellite(Suomi-NPP) (Li and Gong, 2019). The light data in this paper were sourced from the Mark Community Database, and such data were processed by saturation correction and continuous correction. We still used the staggered DID model to estimate the mediation effect model.

We refer to the methods of Baron and Kenny (1986), Imai et al. (2010), and Hicks and Tingley (2011) to construct a model of the mediation effect of the low-carbon city pilot policy on carbon productivity:

$$CP_{it} = \beta_0 + \beta_1 Treat_i * Post_{it} + \sum_{k=1}^{n} \phi_j X_{jit} + \mu_i + \varepsilon_{it}, \quad (7)$$

$$M_{it} = \beta_0 + \beta_1 Treat_i * Post_{it} + \sum_{k=1}^{n} \phi_j X_{jit} + \mu_i + \varepsilon_{it}, \quad (8)$$

$$CP_{it} = \beta_0 + \beta_1 Treat_i * Post_{it} + \beta_2 M_{it} + \sum_{k=1}^{n} \phi_j X_{jit} + \mu_i + \varepsilon_{it}, \quad (9)$$

where i stands for city, t stands for year, CP_{it} denotes carbon productivity, $Treat_i * Post_{it}$ is a dummy variable of the low-carbon city pilot policy, and M_{it} is a mediation variable, including energy structure (PSE_{it} and NTP_{it}), the number of green patent applications($\ln(NP_{it})$), the number of registrations of low-carbon-type enterprises ($NLCE_{it}$), and the fiscal pressure brought about by the low-carbon city pilot policy ($Treat_i \times Post_{it} \times FP_{it}$). μ_i is the city FE, θ_t is the year FE, ε_{it} is a random disturbance item, and X_{jit} is a set of control variables, including investment growth rate (IGR_{it}), population growth rate (PGR_{it}), trade competitiveness (TC_{it}), human capital levels (HC_{it}), and fiscal pressure (FP_{it}). The measurement method is the same as that in Eq. 1. The data source is specified in Section 3.3 of this paper.

5.2.1 Mediation effect based on energy structure

In the process of implementing the low-carbon city pilot policy, there is a need to involve the change of energy structure. This is because raw coal, coking coal, and other traditional fossil energy sources not only contain high sulfur elements but also cause high CO_2 carbon emissions. However, the use of electrical energy, especially hydropower, wind, and solar power, can effectively reduce carbon dioxide emissions. As for the change of energy structure, it is assumed that for energy consumption, the proportion of electric energy in total energy consumption will increase. For energy production, there will be a big push to develop clean energy sources, such as hydro, wind, and solar, which means that non-thermal power generation will increase. This development

TABLE 9 Estimation results based on energy structure.

Variables	Channels for the Proportion of Electricity Consumption			Channels for Non-Thermal Power Generation		
	(1)	(2)	(3)	(4)	(5)	(6)
	CP	*PSE*	*CP*	*CP*	*NTP*	*CP*
Treat∗Post	1.819***	0.037***	1.512***	1.819***	41.269***	1.173***
	(0.144)	(0.004)	(0.142)	(0.144)	(4.806)	(0.143)
PSE or NTP			8.226***			0.016***
			(0.849)			(0.001)
Constant	2.489***	0.133***	1.395***	2.489***	−48.101***	3.242***
	(0.466)	(0.013)	(0.461)	(0.466)	(11.828)	(0.453)
Control variables	YES	YES	YES	YES	YES	YES
City fixed effect	YES	YES	YES	YES	YES	YES
Mediation effect			0.034***			0.660***
Observations	3,666	3,666	3,666	3,666	3,666	3,666
Number of cities	282	282	282	282	282	282
R_squared	0.777	0.872	0.796	0.777	0.779	0.803
F value	359.097	74.912	338.400	359.097	83.690	370.776

Note: ***, **, and * indicate significance at the 1, 5, and 10% levels, respectively. Robust standard errors are reported in parentheses.

will effectively boost carbon productivity. Based on the mediation variables of electricity consumption ratio and non-thermal power generation, the stepwise regression coefficient method was used to estimate the mediation effect model based on the energy structure, after which we calculated the size of the mediation effect. The results are shown in Table 9.

In Table 9, when examining the mediation channels for the proportion of electricity consumption, Column 1) indicates that the coefficient of *Treat∗Post* is significant for 1.819. The coefficient of *Treat∗Post* is significant for 0.037, as shown in Column (2), which implies that the low-carbon city pilot policy can promote the proportion of electricity consumption. In Column (3), the coefficient of *Treat∗Post* is significant for 1.512, the coefficient of *PSE* is also significant for 8.226, and the mediation effect is 0.037, which indicates that the low-carbon city pilot policy promotes carbon productivity by affecting the energy consumption structure. Furthermore, after considering the mediation channels for non-thermal power generation, Column 5) shows that the coefficient of *Treat∗Post* is 41.269, which suggests that the low-carbon city pilot policy has a significant impact on clean energy production. Meanwhile, in Column (6), the coefficient of *Treat∗Post* is significant for 1.173, and the coefficient of *NTP* is significant for 0.016. Hence, the estimated mediation effect value is 0.660, which indicates the establishment of the mediation mechanism by which the low-carbon city pilot policy affects carbon productivity through the change in the energy production structure and consumption structure.

5.2.2 Mediation effect based on the number of green patent applications

The low-carbon city pilot policy advocates low-carbon production and consumption. In the production field, this effort will inevitably lead to greener and cleaner production technological progress, which is reflected in the expansion of green patent applications. At the same time, the expansion of the number of green patents will produce corresponding rewards, such as improved clean production capacity, lower carbon emissions, and higher carbon productivity. Therefore, based on the number of green patent applications, we used the stepwise regression coefficient method to estimate the mediation effect model and then calculated the size of the mediation effect. The results are provided in Table 10.

In Table 10, without controlling for the influence of other variables, Column 1) shows that the coefficient of *Treat∗Post* is significantly positive. Column 2) specifies that the coefficient of *Treat∗Post* is significantly greater than 0, which means that the low-carbon city pilot policy promotes the application of green patents. Column 3) reveals that the coefficients of *Treat∗Post* and $\ln(NP)$ are significantly greater than 0, which indicates that the establishment of the mediation mechanism of the impact of the low-carbon city pilot policy on carbon productivity. Furthermore, after controlling for the influence of other variables, Column 5) shows that the coefficient of *Treat∗Post* is 0.789, which indicates that the low-carbon city pilot policy significantly boosts the number of green patent applications. In Column (6), the coefficient of *Treat∗Post* is significant for 0.913,

TABLE 10 Estimation results based on the number of green patent applications.

Variables	(1)	(2)	(3)	(4)	(5)	(6)
	CP	$\ln(NP)$	CP	CP	$\ln(NP)$	CP
$Treat{*}Post$	2.784***	1.324***	0.994***	1.819***	0.789***	0.913***
	(0.129)	(0.059)	(0.128)	(0.144)	(0.059)	(0.131)
$\ln(NP)$			1.352***			1.149***
			(0.022)			(0.028)
Constant	5.704***	3.464***	1.021***	2.489***	2.597***	-0.494
	(0.030)	(0.017)	(0.078)	(0.466)	(0.269)	(0.372)
Control variables	NO	NO	NO	YES	YES	YES
Cityfixed effect	YES	YES	YES	YES	YES	YES
Mediation effect			1.790***			0.907***
Observations	3,666	3,666	3,666	3,384	3,384	3,384
Number of cities	282	282	282	282	282	282
R_squared	0.644	0.648	0.850	0.777	0.807	0.859
Fvalue	465.774	499.404	2040.464	359.097	515.374	643.504

Note: ***, **, and * indicate significance at the 1, 5, and 10% levels, respectively. Robust standard errors are reported in parentheses.

and the coefficient of $\ln(NP)$ is 1.149. The mediation effect value obtained from 0.789 × 1.149 is 0.907, which means that the mediation mechanism for the impact of the low-carbon city pilot policy on carbon productivity through green and low-carbon technological progress is established.

5.2.3 Mediation effect based on the number of registrations of low-carbon-type enterprises

One of the most direct ways for the government to implement the low-carbon city pilot policy is to restrict the development of high-energy-consuming industries. Specifically, local governments can reduce their approval for high-carbon-type enterprises and expand access for low-carbon-type enterprises. Thus, the number of registrations of high-carbon-type enterprises will be declined, and those of low-carbon-type enterprises will be increased. If the low-carbon city pilot policy increases the number of registrations of low-carbon-type enterprises, then the pilot policy supports the development of low-carbon enterprises, in turn, improves carbon productivity. In view of this, we estimated the mediation mechanism effect model based on the number of registrations of low-carbon-type enterprises under the conditions of not controlling and controlling for the influences of other variables. The results are shown in Table 11.

In Table 11, without controlling the influence of other variables, Column 2) shows that the coefficient of $Treat{*}Post$ is significantly greater than 0. This result suggests that the low-carbon city pilot policy has increased the number of registrations of low-carbon-type enterprises. In Column (3), the coefficient of $Treat{*}Post$ is positive, and the coefficient of $NLCE$ is also significantly positive. Furthermore, under the condition of controlling for the influence of other variables, Column 5) shows that the coefficient of $Treat{*}Post$ is significant for 0.074. In Column (6), the coefficient of $NLCE$ is significant for 0.078 at the 1% level; thus, the mediation effect value can be calculated as 0.001. This result supports the validity of the hypothesis that the low-carbon city pilot policy can improve carbon productivity by affecting the number of low-carbon-type enterprises entering the market.

5.2.4 Mediation effect based on fiscal pressure brought about by the low-carbon city pilot policy

In the actual implementation of the low-carbon city pilot policy, some high-energy-consuming enterprises will inevitably be shut down, which will eliminate some tax sources. In the case of rigid growth of government expenditure, the fiscal expenditure gap will increase, as will fiscal pressure on the local government. Especially in the case of economic downturns and fiscal difficulties, local governments are likely to respond to fiscal pressure by loosening restrictions on the development of high-energy-consuming enterprises, which will adversely affect carbon productivity. In this regard, it is necessary to minimize the adverse effects. This paper used the interaction term between the dummy variable of the low-carbon city pilot policy and the fiscal pressure to describe the fiscal pressure brought about by such a pilot policy, after which we estimated the mediation effects based on this mediation variable. The results are provided in Table 12.

In Table 12, under the condition of controlling for the influence of other variables, Column 2) reports that the

TABLE 11 Estimation results based on the number of registrations of low-carbon-type enterprises.

Variables	(1)	(2)	(3)	(4)	(5)	(6)
	CP	*NLCF*	*CP*	*CP*	*NLCF*	*CP*
Treat*Post	2.784***	0.572***	2.654***	1.819***	0.074	1.813***
	(0.129)	(0.192)	(0.133)	(0.144)	(0.192)	(0.143)
NLCE			0.227***			0.078***
			(0.016)			(0.014)
Constant	5.704***	2.531***	5.129***	2.489***	−1.189*	2.582***
	(0.030)	(0.030)	(0.048)	(0.466)	(0.712)	(0.466)
Control variables	NO	NO	NO	YES	YES	YES
City fixed effect	YES	YES	YES	YES	YES	YES
Mediation effect			0.130***			0.001
Observations	3,666	3,666	3,666	3,384	3,384	3,384
Number of cities	282	282	282	282	282	282
R_squared	0.644	0.753	0.663	0.777	0.776	0.779
Fvalue	465.774	8.936	331.318	359.097	59.348	307.866

Note: ***, **, and * indicate significance at the 1, 5, and 10% levels, respectively. Robust standard errors are reported in parentheses.

TABLE 12 Estimation results based on the fiscal pressure brought about by the low-carbon city pilot policy.

Variables	(1)	(2)	(3)	(4)	(5)	(6)
	CP	*T***reat***Post*FP*	*CP*	*CP*	*T***reat***Post*FP*	*CP*
Treat*Post	2.784***	0.494***	4.101***	1.819***	0.492***	4.451***
	(0.129)	(0.011)	(0.323)	(0.144)	(0.011)	(0.331)
Treat*Post*FP			−2.664***			−5.352***
			(0.593)			(0.635)
Constant	5.704***	-0.000	5.703***	2.489***	-0.016	2.401***
	(0.030)	(0.001)	(0.030)	(0.466)	(0.012)	(0.464)
Control variables	NO	NO	NO	YES	YES	YES
City fixed effect	YES	YES	YES	YES	YES	YES
Mediation effect			−1.316***			−2.633***
Observations	3,666	3,666	3,666	3,384	3,384	3,384
Number of cities	282	282	282	282	282	282
R_squared	0.644	0.911	0.645	0.777	0.913	0.782
Fvalues	465.774	2,126.140	251.095	359.097	395.914	343.823

Note: ***, **, and * indicate significance at the 1, 5, and 10% levels, respectively. Robust standard errors are reported in parentheses.

coefficient of *Treat*Post* is significantly greater than 0. In Column (3), the coefficient of *Treat*Post* is greater than 0, and the coefficient of *Treat*Post*FP* is less than 0. These results indicate that the mediation effect exists. Furthermore, under the condition of controlling for the influence of other variables, In Column 6) shows that the coefficient of *Treat*Post* is significant for 0.492, which implies that the direct effects of the low-carbon city pilot policy are significant. At the same time, in Column(5) the coefficient of *Treat*Post* is significant for 0.492. In Column (6), the coefficient of *Treat*Post*FP* is significant for–5.352 at the 1% level, and the value of the mediation effect is–2.633. These results illustrate that the hypothesis that the low-carbon city pilot policy influences carbon productivity through the mediation mechanism of fiscal pressure is valid. Thus, Hypothesis three is confirmed.

10.3389/fenvs.2022.978076

6 Conclusion and policy implications

The low-carbon city pilot policy is an important measure for China to promote carbon productivity, as it provides a certain degree of experience and demonstrations for China to achieve a carbon peak in 2030. At the same time, the low-carbon city pilot policy will affect the development of high-energy-consuming enterprises and the tax base to some extent, which may lead to an increase in fiscal pressure. Several results were obtained in this paper. First, the low-carbon city pilot policy can significantly improve carbon productivity, and the improvement effect presents a dynamic and persistent feature. Second, the fiscal pressure resulting from the low-carbon city pilot policy will reduce carbon productivity, and the degree of reduction depends on the status of fiscal pressure. Third, an increase in fiscal pressure will significantly decrease carbon productivity, which is heterogeneous with different levels of economic development. Finally, the examination of the mediation effect found that the low-carbon city pilot policy improves carbon productivity by affecting the energy structure, green and low-carbon technological progress, and the entry of low-carbon-type enterprises. However, the fiscal pressure brought about by the low-carbon city pilot policy has a negative impact on the improvement of carbon productivity, whose influence we cannot ignore. Therefore, the issue of how to improve carbon productivity without affecting fiscal pressure is a scientific problem. In relation to this, optimizing the low-carbon clean technology of existing enterprises and raising the low-carbon technology access standards of new enterprises may be a feasible strategy.

The conclusions drawn from the above research can offer inspiration to developing countries for improving carbon productivity in several ways. First, these countries can expand the scope of their low-carbon city pilot policy and provide policy support for improving carbon productivity. In the process of expanding the scope of such policies, the central government must strictly select the criteria, clarify the conditions and requirements for selection, and plan the strategic tasks for the development of low-carbon cities. Second, the low-carbon technology level of existing enterprises must be optimized, and the low-carbon technology access standards of new enterprises must be raised. A fact that cannot be ignored is that in the process of promoting a low-carbon economy, some local governments still need to bridge the gap between their policy approaches and local economic development conditions and resource endowments. Solving one problem can lead to the emergence of another problem. Therefore, in the process of improving carbon productivity, attention should be allocated to resolving fiscal pressure and preventing fiscal risks. Third and finally, there is a need to adjust the energy structure and improve energy efficiency. The use of traditional energy sources, such as thermal power, raw coal, crude oil, and gasoline, will lead to the emission ofmassive amounts of CO_2. However, emerging energy sources, such as hydropower, wind power, and solar energy, do not generate carbon emissions. This means that if the structure of energy production and consumption can be improved to produce and use cleaner energy, which can directly reduce carbon emissions and promote carbon productivity. At the same time, even if the energy structure remains unchanged, improving energy efficiency can also promote carbon productivity.

Although our research has given rise to valuable conclusions, it still has certain limitations. First, in view of the limitations involving carbon emission data, the latest annual data were not obtained for analysis. Second, an analysis based on micro-level (enterprise) data has not been performed. In the future, we will expand and analyze these two aspects to provide strong evidence for the relationship among the low-carbon city pilot policy, fiscal pressure, and carbon productivity.

Data availability statement

The original contributions presented in the study are included in the article/supplementary material further inquiries can be directed to the corresponding author.

Author contributions

YY contributed to methodology, funding acquisition, writing—original draft preparation; CP contributed to conceptualization, writing—review, editing. All authors contributed to the article and approved the submitted version.

Funding

This paper was sponsored by the Launching Project of New Staff in Social Science of Tianjin University of Commerce (2022) (Grant No. 22KYQD14).

Acknowledgments

The authors would like to thank the editor for their attentive and friendly service, and also thank the reviewers for their constructive comments and suggestions in this paper.

Conflict of interest

The authors declare that the research was conducted in the absence of any commercial or financial relationships that could be construed as a potential conflict of interest.

Publisher's note

All claims expressed in this article are solely those of the authors and do not necessarily represent those of their affiliated organizations, or those of the publisher, the editors and the reviewers. Any product that may be evaluated in this article, or claim that may be made by its manufacturer, is not guaranteed or endorsed by the publisher.

References

Acemoglu, D., Akcigit, U., Hanley, D., and Kerr, W. (2016). Transition to clean technology. *J. Political Econ.* 124 (1), 52–104. doi:10.1086/684511

Aghion, P., Dechezleprêtre, A., Hemous, D., Martin, R., and Van Reenen, J. (2016). Carbon taxes, path dependency, and directed technical change: Evidence from the auto industry. *J. Political Econ.* 124 (1), 1–51. doi:10.1086/684581

Andersson, J. J. (2019). Carbon taxes and CO_2 emissions: Sweden as a case study. *Am. Econ. J. Econ. Policy* 11 (4), 1–30. doi:10.1257/pol.20170144

Angrist, J. D., and Pischke, J. S. (2008). *Mostly harmless econometrics*. New Jersey: Princeton University Press.

Bai, J., Lu, J., and Li, S. (2019). Fiscal pressure, tax competition and environmental pollution. *Environ. Resour. Econ. (Dordr).* 73 (2), 431–447. doi:10.1007/s10640-018-0269-1

Baker, A. C., Larcker, D. F., and Wang, C. C. Y. (2022). How much should we trust staggered difference-in-differences estimates? *J. Financial Econ.* 144 (2), 370–395. doi:10.1016/j.jfineco.2022.01.004

Baron, R. M., and Kenny, D. A. (1986). The moderator–mediator variable distinction in social psychological research: Conceptual, strategic, and statistical considerations. *J. Personality Soc. Psychol.* 51 (6), 1173–1182. doi:10.1037/0022-3514.51.6.1173

Calel, R., and Dechezleprêtre, A. (2016). Environmental policy and directed technological change: Evidence from the European carbon market. *Rev. Econ. Statistics* 98 (1), 173–191. doi:10.1162/REST_a_00470

Callaway, B., and Sant'Anna, P. H. C. (2021). Difference-in-differences with multiple time periods. *J. Econ.* 225 (2), 200–230. doi:10.1016/j.jeconom.2020.12.001

Chen, C., Lin, Y., Lv, N., Zhang, W., and Sun, Y. (2022). Can government low-carbon regulation stimulate urban green innovation? Quasi-experimental evidence from China's low-carbon city pilot policy. *Appl. Econ.* 2022, 1–21. doi:10.1080/00036846.2022.2072466

Cheng, J., Yi, J., Dai, S., and Xiong, Y. (2019). Can low-carbon city construction facilitate green growth? Evidence from China's pilot low-carbon city initiative. *J. Clean. Prod.* 231, 1158–1170. doi:10.1016/j.jclepro.2019.05.327

de Chaisemartin, C., and D'Haultfoeuille, X. (2020). Two-way fixed effects estimators with heterogeneous treatment effects. *Am. Econ. Rev.* 110 (9), 2964–2996. doi:10.1257/aer.20181169

Fell, H., and Kaffine, D. T. (2018). The fall of coal: Joint impacts of fuel prices and renewables on generation and emissions. *Am. Econ. J. Econ. Policy* 10 (2), 90–116. doi:10.1257/pol.20150321

Freyaldenhoven, S., Hansen, C., and Shapiro, J. M. (2019). Pre-event trends in the panel event-study design. *Am. Econ. Rev.* 109 (9), 3307–3338. doi:10.1257/aer.20180609

Gardner, J. (2021). *Two-stage differences in differences*. USA: University of Mississippi. Working paper.

Hicks, R., and Tingley, D. (2011). Causal mediation analysis. *Stata J.* 11 (4), 605–619. doi:10.1177/1536867X1201100407

Hu, X., and Liu, C. (2016). Carbon productivity: A case study in the Australian constr-uction industry. *J. Clean. Prod.* 112, 2354–2362. doi:10.1016/j.jclepro.2015.10.042

Huang, S., and Deng, Y. (2020). Fiscal pressure, distortion of enterprise factor input and economic performance. *Fiscal Res.* 3, 85–100. doi:10.19477/j.cnki.11-1077/f.2020.03.007

Huang, Y., and Zhou, Y. (2020). How does vertical fiscal imbalance affect environmental pollution in China? New perspective to explore fiscal reform's pollution effect. *Environ. Sci. Pollut. Res.* 27 (25), 31969–31982. doi:10.1007/s11356-020-09072-w

Huo, W., Qi, J., Yang, T., Liu, J., Liu, M., and Zhou, Z. (2022). Effects of China's pilot low-carbon city policy on carbon emission reduction: A quasi-natural experiment based on satellite data. *Technol. Forecast. Soc. Change* 175, 121422. doi:10.1016/j.techfore.2021.121422

Imai, K., Keele, L., and Tingley, D. (2010). A general approach to causal mediation analysis. *Psychol. Methods* 15 (4), 309–334. doi:10.1037/a0020761

Jacobson, L. S., LaLonde, R. J., and Sullivan, D. G. (1993). Earnings losses of displaced workers. *Am. Econ. Rev.* 83 (4), 685–709.

Li, C., Qi, Y., Liu, S., and Wang, X. (2022). Do carbon ETS pilots improve cities' green total factor productivity? Evidence from a quasi-natural experiment in China. *Energy Econ.* 108, 105931. doi:10.1016/j.eneco.2022.105931

Li, X., and Gong, L. (2019). Correction and fitting of night light images of DMSP/OLS and VIIRS/D-NB. *Bull. Surv. Mapp.* 7, 138–146. doi:10.13474/j.cnki.11-2246.2019.0236

Liu, F. (2022). The impact of China's low-carbon city pilot policy on carbon emissions: Based on the multi-period DID model. *Environ. Sci. Pollut. Res. Int.* doi:10.1007/s11356-022-20188-z

Liu, W. (2019). *Enterprise-Registration-Data-of-ChineseMainland[EB/OL]*. Available at: https://github.com/imhuste-r/Enter-prise-Registration-Data-of-Chinese-Mainland, 2019-06-01.

Liu, X., Li, Y., Chen, X., and Liu, J. (2022). Evaluation of low carbon city pilot policy effect on carbon abatement in China: An empirical evidence based on time-varying DID model. *Cities* 123, 103582. doi:10.1016/j.cities.2022.103582

Nordhaus, W. D. (2006). After kyoto: Alternative mechanisms to control global warming. *Am. Econ. Rev.* 96 (2), 31–34. doi:10.1257/000282806777211964

Pan, A., Zhang, W., Shi, X., and Dai, L. (2022). Climate policy and low-carbon innovation: Evidence from low-carbon city pilots in China. *Energy Econ.* 112, 106129. doi:10.1016/j.eneco.2022.106129

Peng, F., Xu, W., Lu, P., and Wu, H. (2020). Unexpected shocks of non-tax burdens: A study based on the "VAT reform. *Econ. Res.* 55 (11), 67–83.

Qiu, S., Wang, Z., and Liu, S. (2021). The policy outcomes of low-carbon city construction on urban green development: Evidence from a quasi-natural experiment conducted in China. *Sustain. Cities Soc.* 66, 102699. doi:10.1016/j.scs.2020.102699

Ren, H., Gu, G., and Zhou, H. (2022). Assessing the low-carbon city pilot policy on carbon emission from consumption and production in China: How underlying mechanism and spatial spillover effect? *Environ. Sci. Pollut. Res. Int.* doi:10.1007/s11356-022-21005-3

Shao, C., Guan, Y., Wan, Z., Guo, C., Chu, C., and Ju, M. (2014). Performance and decomposition analyses of carbon emissions from industrial energy consumption in Tianjin, China. *J. Clean. Prod.* 64, 590–601. doi:10.1016/j.jclepro.2013.08.017

Sun, L., and Abraham, S. (2021). Estimating dynamic treatment effects in event studies with heterogeneou-s treatment effects. *J. Econ.* 225 (2), 175–199. doi:10.16/j.jeconom.2020.09.006

Tao, D., and Li, C. (2021). Environmental regulation, local fiscal pressure and actual corporate tax burden. *Econ. Sci.* 3, 83–95. doi:10.12088/PKU.jjkx.2021.03.07

Wang, R., and Zhang, Q. (2017). Local governments' fiscal pressure and the dependence on polluting industries in China. *China & World Econ.* 25 (4), 109–130. doi:10.1111/cwe.12209

Zhao, R., and Fan, Z. (2020). Pension reform, collection and management incentives and corporate contri-bution rates. *China Ind. Econ.* 9, 61–79. doi:10.19477/j.cnki.11-1077/f.2021.06.003

Zhou, Q., Cui, X., Ni, H., and Gong, L. (2022). The impact of environmental regulation policy on firms' energy-saving behavior: A quasi-natural experiment based on China's low-carbon pilot city policy. *Resour. Policy* 76, 102538. doi:10.1016/j.resourpol.2021.102538

frontiers | Frontiers in Environmental Science

TYPE Original Research
PUBLISHED 23 September 2022
DOI 10.3389/fenvs.2022.983319

OPEN ACCESS

EDITED BY
Jingying Fu,
Institute of Geographic Sciences and Natural Resources Research (CAS), China

REVIEWED BY
Wenjie Xu,
Zhejiang University, China
Lei Zhou,
Chongqing University, China
Zhi-Guo Yu,
Nanjing University of Information Science and Technology, China

*CORRESPONDENCE
Ruiwen Yan,
yanruiwen819@hotmail.com

SPECIALTY SECTION
This article was submitted to Environmental Economics and Management,
a section of the journal Frontiers in Environmental Science

RECEIVED 30 June 2022
ACCEPTED 26 August 2022
PUBLISHED 23 September 2022

CITATION
Xi F, Yan R, Shi J, Zhang J and Wang R (2022), Pumped storage power station using abandoned mine in the Yellow River basin: A feasibility analysis under the perspective of carbon neutrality.
Front. Environ. Sci. 10:983319.
doi: 10.3389/fenvs.2022.983319

Pumped storage power station using abandoned mine in the Yellow River basin: A feasibility analysis under the perspective of carbon neutrality

Furui Xi[1,2], Ruiwen Yan[3]*, Jusong Shi[1,2], Jinde Zhang[1,2] and Runping Wang[4]

[1]Key Laboratory of Mine Ecological Effects and Systematic Restoration, Ministry of Natural Resources, Beijing, China, [2]China Institute of Geo-Environment Monitoring, Beijing, China, [3]College of Geoscience and Surveying Engineering, China University of Mining and Technology (Beijing), Beijing, China, [4]School of Geography and Information Engineering, China University of Geosciences, Wuhan, China

Greenhouse gas emissions, mainly CO_2, lead to global climate change, and the resulting ecological environment problems bring severe challenges to human survival and development. As the world's largest developing country and carbon emitter, China is facing the dual pressure of socio-economic development and carbon emission reduction. In order to cope with global climate change and achieve the goal of carbon neutrality and carbon peak as soon as possible, China needs to accelerate the optimization of energy structure, gradually increase the proportion of renewable energy utilization, and accelerate the solution of the bottleneck problem of renewable energy storage. As an energy basin, the Yellow River basin is a key demonstration area to promote energy system reform in China. There are a large number of abandoned mines in the Yellow River basin, which provide a new idea to build pumped storage power stations using abandoned mines (PSPSuM) for renewable energy storage. From the perspective of multidisciplinary integration, this study deeply discusses the relevant evaluation principles and technical key points of constructing PSPSuM in the region, and preliminarily carries out the feasibility assessment. The results show that 91 PSPSuM can be built in the Yellow River basin, with a total installed capacity of 15,830 MW, comprehensively considering the aspects of spatial size, spatial structure and space stability.

KEYWORDS
pumped storage power station, abandoned mine, yellow river basin, feasibility analysis, carbon neutrality

1 Introduction

Since the Industrial Revolution, the utilization of fossil energy such as coal, oil and natural gas has given rise to the dramatic increase in labor productivity and in the development of human society. However, the fossil energy also has brought about carbon emission, which is on continuous growth and has become the main cause of global climate warming. For more than 200 years, CO_2 concentrations has been on the rise, from around 280 ppm before the industrial revolution to 419 ppm in 2021 (NOAA, 2021). The cumulative amount of carbon dioxide (CO_2) from fossil fuel burning has reached 2.2 trillion tons. The global average surface temperature has increased by about 1.1°C, making 2011–2020 the warmest decade on record. In 2018, the United Nations Intergovernmental Panel on Climate Change (IPCC) released the Special Report on Global Warming 1.5°C (IPCC, 2018), which pointed out that global temperature has been observed to get higher, and the impact on human beings, when the temperature rise reached 2°C, is much more serious than the early prediction. The working Group I report of the Sixth Assessment Report of the Intergovernmental Panel on Climate Change (IPCC) released in 2021 shows that human activities have caused unprecedented changes in the climate system (IPCC, 2021). The past 50 years since 1970 have been the warmest in the last two thousand years, and global warming, as predicted, will continue to stick around until the middle of the century.

Global warming, caused by CO_2 emission of greenhouse gases, is considered as a non-traditional security issue worldwidely. Greenhouse effect has triggered serious ecological environment problems, affecting almost every corner on Earth. Those problems, including temperature rising, sea level increase, and frequent extreme weather, have brought severe challenges to human survival and development, particularly on global food supply, water, ecosystem, energy, infrastructure and human life (CSG, 2021; Huang et al., 2021). As the world's second largest economy, China's annual CO_2 emissions have listed the top of the world. In terms of total energy consumption, in 2020, China consumed 4.98 billion tons of standard coal, ranking first in the world, accounting for 30.9% of the global total consumption, and more than the United States (13.9%), India (7.2%) and Russia (4.5%) combined (Su et al., 2021). Energy-related carbon dioxide emissions are about 9.9 billion tons, accounting for 1/3 of the global sum (BP, 2021), and carbon emissions per unit GDP are 6.7 tons of carbon dioxide/$10,000, both are far higher than the world average. From the perspective of energy consumption structure, fossil fuels such as coal, oil and natural gas are the main sources, accounting for more than 84% in 2020 (BP, 2021). In particular, coal consumption accounts for more than half, much higher than the average proportion in the global energy consumption structure.

China's rapid economic growth is accompanied by an increasing demand of energy, and carbon emissions are still rising and have not yet peaked. Facing with strong international pressure to reduce carbon emissions, as the world's largest developing country and carbon emitter, Chinese government pledged at the Copenhagen Climate Change Conference to reduce carbon emissions per unit of GDP by 40%–45% by 2020, compared with 2005. In 2016, Chinese government formally signed Paris Agreement, solemnly committing to carbon peak by 2030. In September 2020, at the 75th Session of the United Nations General Assembly, China made an earnest commitment to the world that it would strive to achieve the goal of peaking carbon dioxide emissions by 2030 and achieve carbon neutrality by 2060 (Liu et al., 2019; Xi, 2020; Zhang and Xi, 2020; Huang and Xie., 2021). To deliver these promises, Chinese government is balancing socio-economic development and carbon emissions, which is not only a major decision in China, but also a heated discussed topic concerning the whole society.

Energy is one of the important material basis of economic and social development, as well as the main source of carbon emissions. To ensure a smooth realization of carbon neutral in China as promised, China's green low carbon development on energy structure is gearing up for the new challenge. The situation is not favorable, the energy consumption is going up, resource constraints are tightened, and the environmental pressure is aggravated. Under these circumstances, reducing the consumption of traditional fossil fuels while increasing the development and utilization of clean and renewable energy is an imposition. According to preliminary calculation, in 2020, the proportion of renewable energy in China's total energy consumption will increase to 15.9%, a significant increase of 8.5% compared with 2005. The total installed capacity of renewable energy power generation will reach 980 million kW, accounting for 44.7% of the total installed capacity. The utilization of renewable energy is an important measure for China, to solve current resource and environmental problems, mitigate and adapt to climate change, and realize the sustainable development of the resource-environment coupling system. China gives priority to renewable energy development, and vigorously develops and utilizes renewable energy. In 2020, green and low-carbon energy from wind power, photovoltaic, hydropower, biomass power and nuclear power reached 280 million kW, 250 million kW, 370 million kW, 29.52 million kW, and 49.89 million kW respectively, reaching 2.6 trillion kWh of electricity generated from non-fossil energy sources, accounting for more than one third of China's electricity consumption (CPEM, 2021). The installed capacity of photovoltaic and wind power increased by more than 3,000 times and 200 times, compared to the year of 2005.

China is rich in renewable energy, but the actual utilization efficiency is relatively low. The main reason is the renewable energy, particularly wind and solar energy, is restricted by the natural geographical conditions, making it intermittent, volatile and unstable. In the actual process of exploitation and utilization, a large amount of wind and solar power are abandoned. In order to use renewable energy efficiently, stably and safely, as well as to achieve the strategic goal by 2030, more than 1.2 billion kW wind and solar power should be generated (CPEM, 2021), corresponding energy storage facilities are needed. Energy storage is the core technology to achieve the large-scale development of renewable energy, the construction of a new power system and achieve the carbon neutrality goal. As electrical energy carrier, energy storage can effectively slow a large-scale new energy power grid volatility and intermittent, promote the balance of power system in the operation of the power and load, improve the safety, economy and flexibility of power grid operation. As carbon neutral has become a global consensus, the proportion of new energy in the whole energy system will increase rapidly, and energy storage technology is also ushering in explosive growth.

Pumped storage technology is currently the most mature, economical and the one that employs large-scale development conditions among all the green low carbon flexible adjustment technology in power system. Pumped storage power station (PSPS) is a clean and efficient renewable energy storage facilities, which can build new renewable energy power system combined with wind, solar power, nuclear power and thermal power. However, the terrain divide, the large amount of land space occupation and other constraints seriously restrict the build-ability of PSPS. After mining, a large amount of usable space is left on the surface and underground, and a PSPS with gravitational potential energy difference can be built by using multiple open pit with height difference, combination of open pit and underground space or pure underground space. In this case, using a large amount of above-ground and underground space of abandoned mines will eliminate the constraints of the site selection of PSPS and greatly increase their build-ability in plains and areas with limited surface space.

In the areas rich in new energy, using the ground and underground space of abandoned mines to build PSPS can, on the one hand, greatly save the surface construction land, avoid the waste of a large amount of underground space, and realize the deep ecological restoration of abandoned mines (Xi et al., 2020). On the other hand, it can effectively alleviate China's renewable energy storage crisis, promote the transformation and upgrading of energy structure, and greatly reduce carbon emission intensity. It is of great strategic significance for China to achieve the goal of carbon peak and carbon neutrality as soon as possible, and is a new form of PSPS development and construction worthy of in-depth study and promotion.

China's Yellow River basin is called energy basin with abundant resources including coal (Xi, 2019), oil, natural gas and non-ferrous metal. Its coal reserves are large and complete in types, and its coal production accounts for about 70% of the total national output, making it China's significant energy, chemical, raw materials and basic industry base (Jin, 2019; Gao et al., 2002). Therefore, the Yellow River basin is a key area for China to promote transformation and upgrading energy system, build an efficient modern energy system with clean and low carbon emissions, and to achieve the strategic goal of carbon neutrality and carbon peak. The Yellow River basin has a huge number of abandoned mines, which leaves a large amount of ground and underground space that can be reused (Zhang and Xi, 2020). At the same time, the Yellow River basin is rich in wind and solar energy, and the abandoned mines have a high spatial correlation with renewable energy areas. How to make full use of these abandoned Spaces to build PSPS and realize efficient and flexible storage of renewable energy is a scientific and technical problem that needs to be solved urgently.

2 Study area

2.1 Overview of the Yellow River basin

The Yellow River is the second longest river in China. It originates in the Yuogu Zonglie basin at the northern foot of Bayan Kala Mountain in Qinghai Province. The main body of the Yellow River, with a total length of 5,464 km, flows through nine provinces and regions in Qinghai, Sichuan, Gansu, Ningxia, Inner Mongolia, Shaanxi, Shanxi, Henan, and Shandong, and finally empty into the Bohai Sea. The Yellow River is seen as the mother river of China, and the Yellow River basin is an important birthplace of Chinese civilization, as well as an important ecological barrier and economic zone in China. Located between 95°59'—118°58′ E and 31°56'—42°03′ N (Figure 1), the Yellow River basin covers 27% of China's total land area. In 2018, provinces along the Yellow River had a total population of 420 million, accounting for 30.3% of China's population. Their regional GNP exceeded 23.9 trillion yuan, accounting for 26.5% of China's GDP in 2018 (Xi et al., 2022).

2.2 Energy structure

The Yellow River basin is rich in coal, oil, natural gas, non-ferrous metals and other mineral resources. The reserves of coal and natural gas account for 75% and 61% of the national basic reserves respectively. Among the 14 coal bases in China, nine coal bases including shendong, Northern Shaanxi, Eastern Ningxia, Western Shandong, Huanglong, Henan, Northern Shanxi, Jinzhong and Eastern Shanxi are located in the Yellow River basin (NEA, 2021).

Figures 2–8 show the energy Structure of provinces in the Yellow River basin from 2015 to 2021 (Peng and Bi., 2020). On the whole, except Sichuan province and Qinghai province in the upper Reaches of the Yellow River, where hydropower is the main power system, the other seven provinces rich in energy and

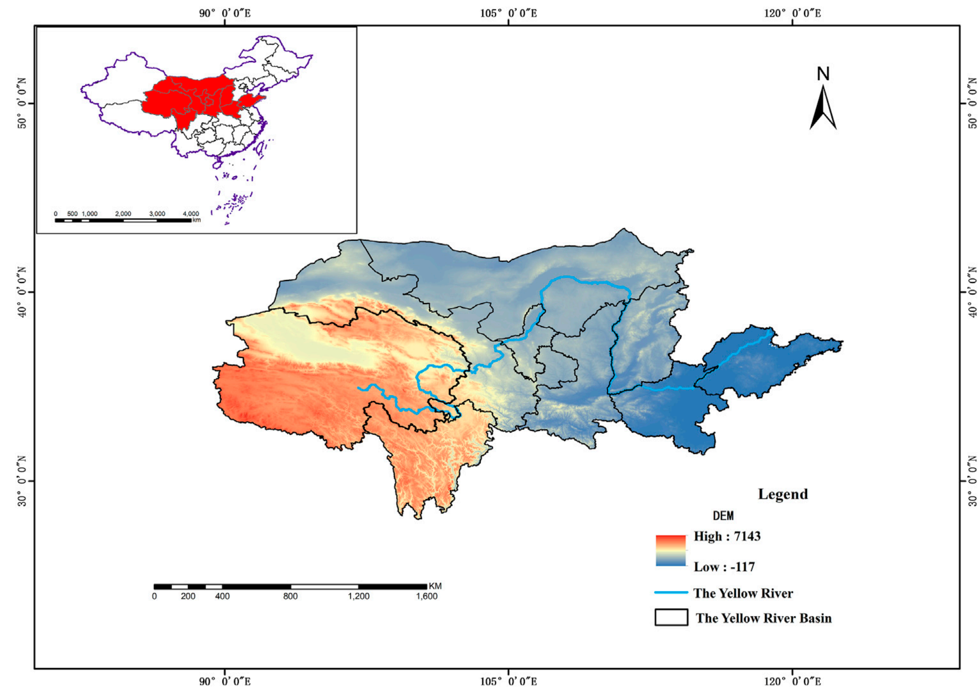

FIGURE 1
Location of the Yellow River basin.

mineral resources are mainly based on thermal power generation, and the proportion of renewable energy generation is relatively low. With the rapid socio-economic development in the Yellow River basin, the demand for energy in all provinces is increasing year by year. Thermal power generation and renewable energy generation in most provinces show a slow growth trend. Only the thermal power generation in Shandong province and Henan province shows an inverted U-shaped trend. In the solar energy enrichment area, the overall development and utilization degree of renewable energy is not high, and the proportion of renewable energy generation is relatively low.

For many years, the Yellow River basin, as China's main energy industry gathering area, formed a low-end industrial structure dominated by mining, energy and chemical industry (Zhang and Xi, 2020). The large-scale development and utilization of mineral resources indeed strongly support the rapid development of industrialization and urbanization in the Yellow River basin, but they also bring great pressure to the regional ecological environment. The Yellow River basin has gradually become one of the regions with the most concentrated carbon emissions in China. Under the guidance of carbon neutrality goal, the industrial structure adjustment in the Yellow River basin will be around the transformation of low carbon on its supply chain and the upgrading its low-end industry structure. It means vigorously promoting regional renewable energy development and utilization, and increasing the renewable energy's proportion in primary energy consumption structure. The middle and upper reaches of the Yellow River basin, with abundant wind and solar energy resources, provides basic guarantee conditions for the implementation of these measures (Zhang H et al., 2022). However, it should also be noted that the phenomenon of abandoning wind and solar energy is common in the area, and the development and construction of new energy storage system urgently need to be strengthened. The construction of PSPS by utilizing the space of a large number of abandoned mines in the Yellow River basin provides an action path worthy of in-depth study and discussion.

2.3 Distribution of abandoned mines

According to the research from China Geological Survey, there are 8,429 mines in the Yellow River basin according to the types of mineral resources. The number of non-metallic mines in the Yellow River basin is 6,803, accounting for 80.71%. The second is Metal mines, 989 in total, accounting for 11.73%; energy mines are the least, with a total of 630, accounting for 7.47%. According to the mine scale, small mines in the area have the most, with a total of 8,178, accounting for 97.02%. Secondly, there are 170 medium-sized mines, accounting for 2.02%; There

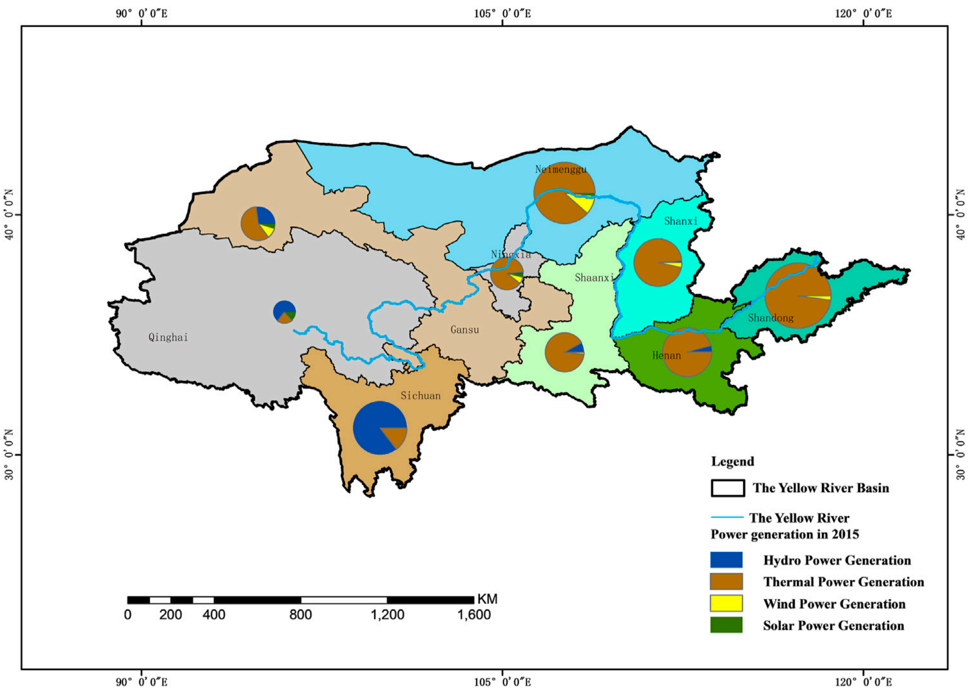

FIGURE 2
Energy structure of the Yellow River basin in 2015.

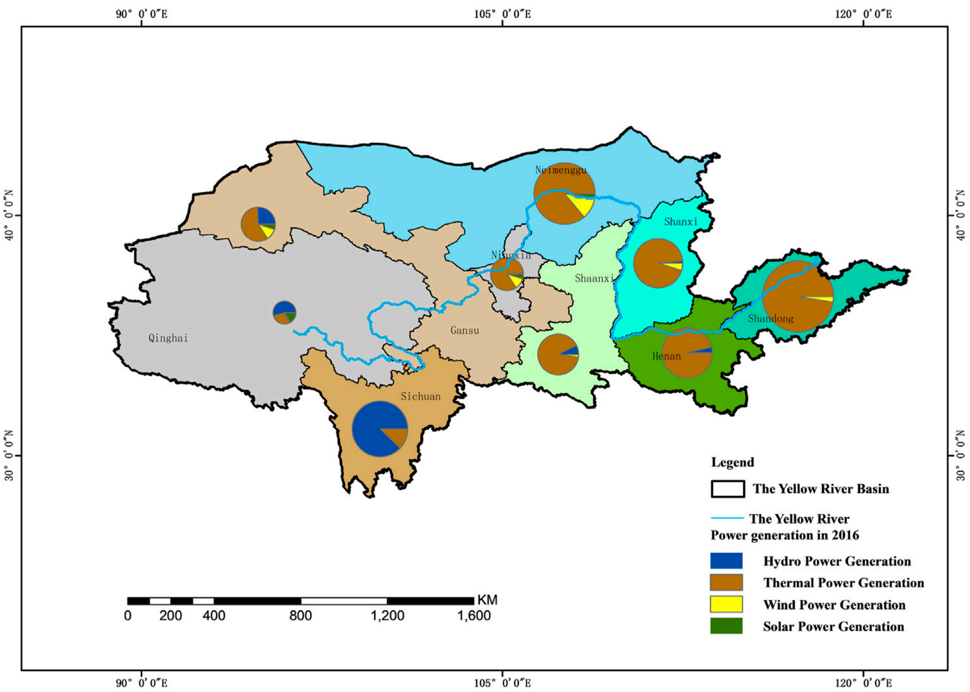

FIGURE 3
Energy structure of the Yellow River basin in 2016.

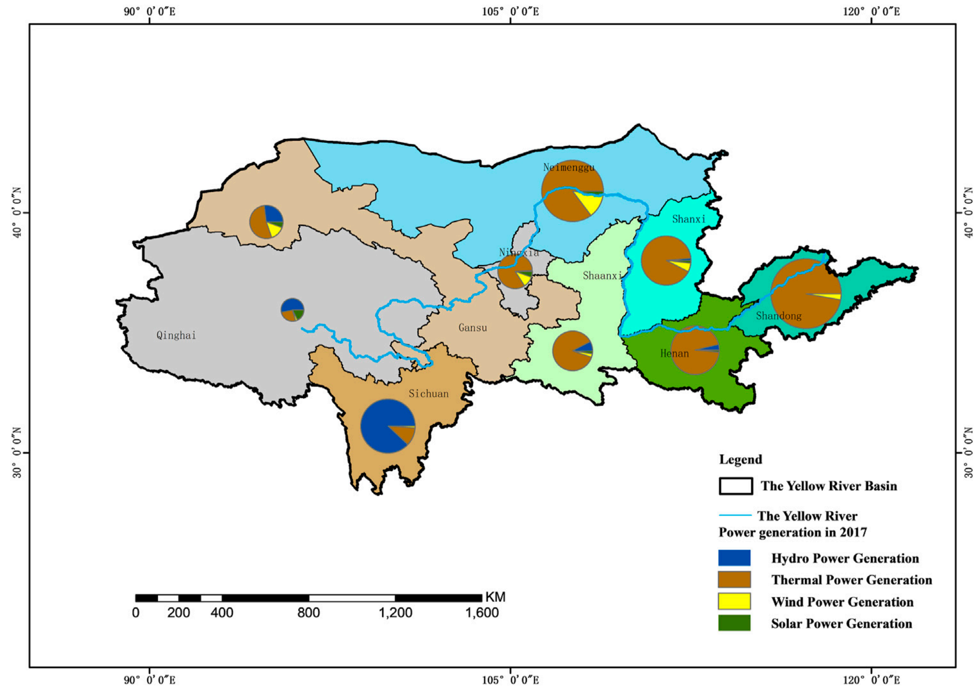

FIGURE 4
Energy structure of the Yellow River basin in 2017.

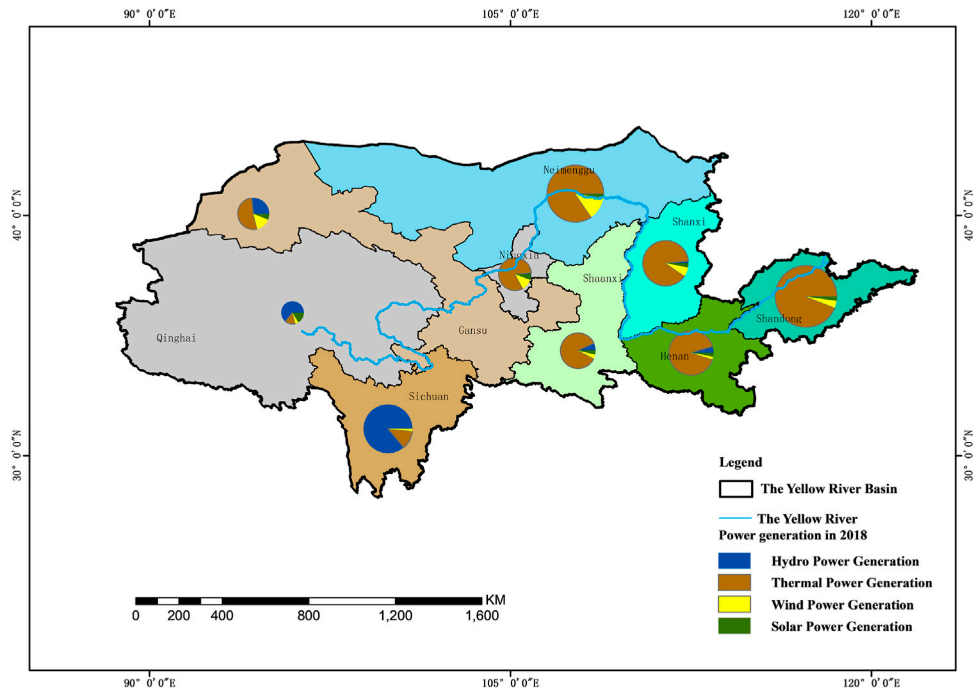

FIGURE 5
Energy structure of the Yellow River basin in 2018.

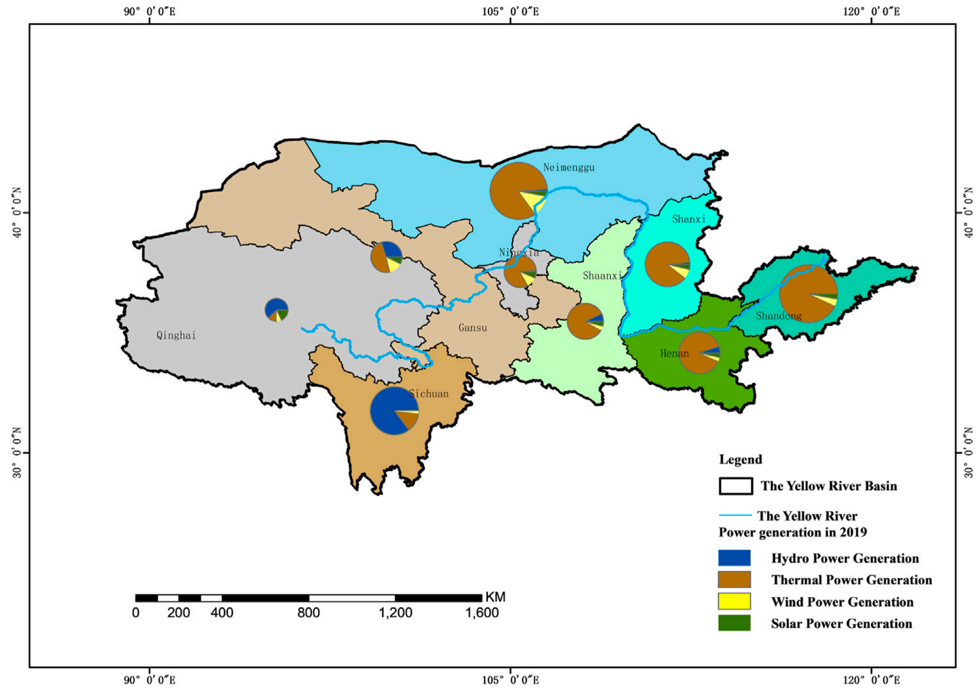

FIGURE 6
Energy structure of the Yellow River basin in 2019.

are 81 large mines in total, accounting for 0.96%. The spatial distribution of abandoned mines in each province is shown in Figure 9.

According to the preliminary estimate of China Geological Survey, taking into account the proportional relationship between the mining scale and the usable underground space, based on an average underground space resource of 600,000 m^3 per mine, and effective utilization coefficient of underground space more than 60%, it is estimated that abandoned mines in the Yellow River basin can provide about 300,000 m^3 underground space, providing a broad space conditions for the construction of PSPS.

3 Introduction of PSPS

3.1 Development history of PSPS

PSPS uses the gravitational potential energy of water as an energy medium to complete energy conversion and storage. When there is energy storage demand, electric energy is used to pump the water from the lower reservoir to the upper reservoir, and the electric energy is converted into the gravitational potential energy of water and stored. When there is a request for energy utilization, the water is released from the upper reservoir to lower reservoir, and the generator is driven by turbine to generate electricity, in this way the gravitational potential energy of water is converted into electricity.

The application history of PSPS can be traced back to more than 100 years ago. In 1901, the world's first PSPS prototype patent was submitted in the United States, and was approved by the United States Patent Office in 1917. The patent content is to convert the wind energy generated by the windmill on the ground into potential energy of water, through the underground water pump, turbines, generators and other devices which can be used to store wind energy in times of energy crisis (U.S. Patent, 1917).

Although pumped storage technology was invented earlier, it was not until the 1970s, along with the large-scale development and utilization of nuclear energy in Europe, that PSPS were really widely promoted and applied, mainly used to balance the fluctuation of daily power supply caused by unstable nuclear energy (Boust, 2012). Compared with other energy storage facilities, the PSPS has a higher energy conversion efficiency (up to about 80%). At the same time, the storage capacity can be flexibly adjusted by the area of the storage area and water head. Due to the large capacity, long life and efficient characteristics, PSPS has become the ideal storage facilities for energy storage. Huge applications demand has greatly promoted the development of the pumped storage industry. Since the 1970s, many scientific research institutions of Europe embarked on pumped storage related scientific research, published many representative works during this period (ANL, 1976; EPRI,

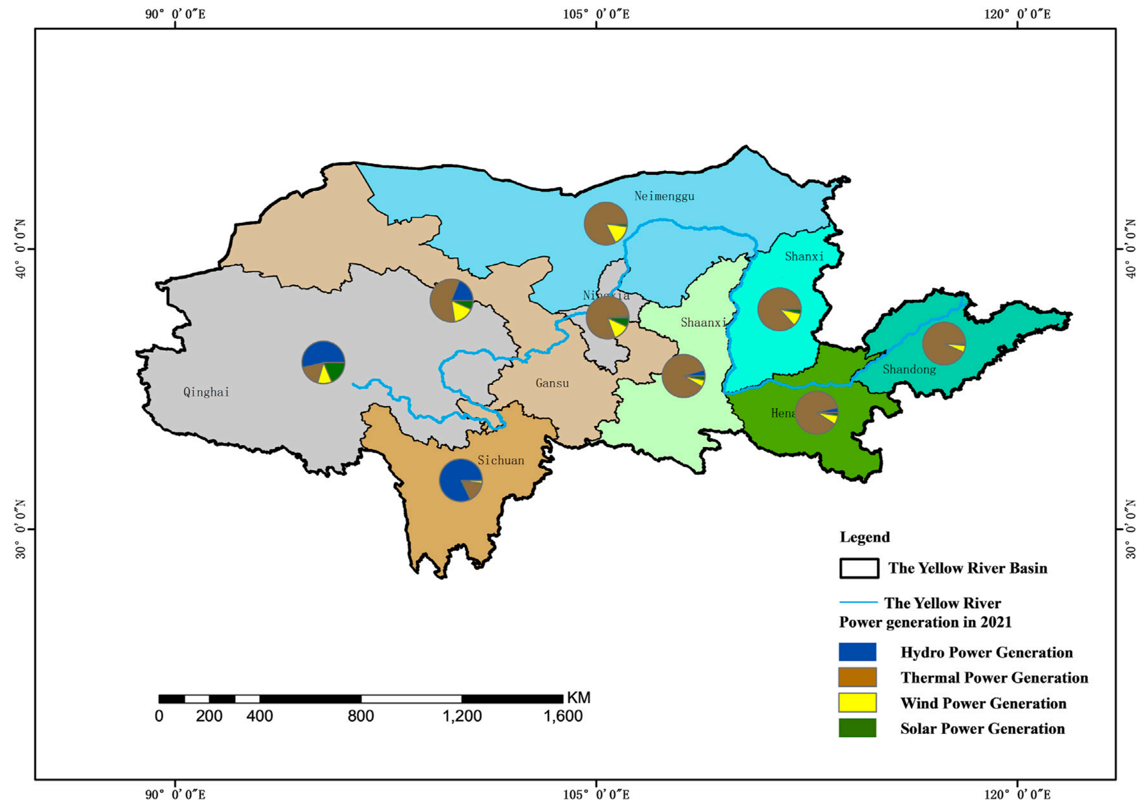

FIGURE 7
Energy structure of the Yellow River basin in 2021.

1976; NASA, 1976; Walia and McCreath, 1976; HEC, 1977; Chas, 1978; Tam et al., 1979; Chang and Thompson, 1980; Chang and Thompson, 1980; Xie et al., 2015; Yuan, 2017; Luo et al., 2018).

With the continuous application of pumped storage technology development, the requirements of terrain and the interference effect on the ground landscape gradually unfolded. PSPS requires a larger water head to complete the conversion of water potential energy, which can only be adopted in the region with great relief (hilly mountain area, for example). Plain regions, such as the gentle terrain, limits the application of pumped storage technology. At the same time, surface water storage facilities will have a certain degree of aesthetic impact on the ecological landscape. With the enhancement of people's awareness of ecological protection, the environmental impact of the above-ground PSPS also limits its large-scale application. Based on this, the researchers in European countries and America gradually shifted their study from above-ground to underground, and embarked on the feasibility study of underground PSPS, including underground construction requirements of PSPS, the location criteria and evaluation of construction cost, etc., The more representative research results are from the Argonne national laboratory (ANL, 1976). The report systemic evaluated the potential of building underground PSPS in the United States. It discusses the principle for the site selection of PSPS, and points out the strength of surrounding rock for the construction of water reservoir plays an important role. Also, it further argues that intrusive rocks and metamorphic rocks with low permeability are more suitable for the construction of underground PSPS than sedimentary rocks. At the same time, the report also evaluates the construction cost, pointing out that the construction of above-ground reservoir and auxiliary cavern has little impact on the total construction cost of underground PSPS, and the construction cost mainly comes from the construction of underground water reservoir.

3.2 Overview of the development of PSPS in China

According to the PSPS construction plan of the National Energy Administration of China (HPDGI, 2022), by 2020, China's total planned installed capacity of PSPS (including existing sites) will be about 13,000 kW, as shown in Figure 10. Among them, East China Power Grid has the largest total installed capacity, about 41 million kW, followed by North China Power Grid and Central China Power Grid, and Southwest Power Grid has the smallest total installed capacity,

FIGURE 8
Change trend of energy structure in the Yellow River basin from 2015 to 2021.

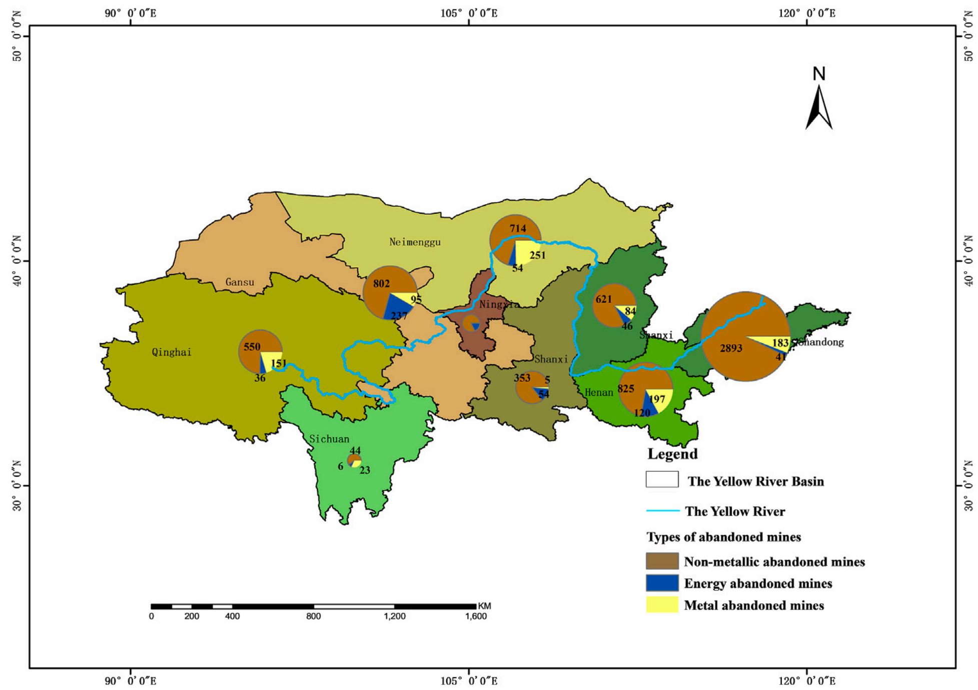

FIGURE 9
Spatial distribution of abandoned mines in the Yellow River basin.

10.3389/fenvs.2022.983319

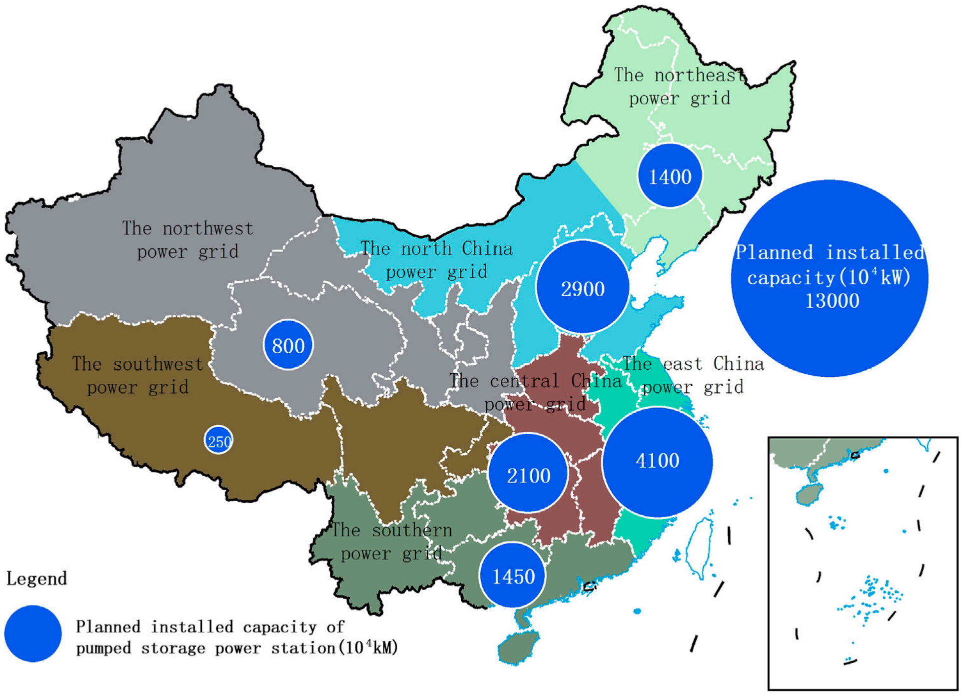

FIGURE 10
Spatial distribution of planned installed capacity of PSPS.

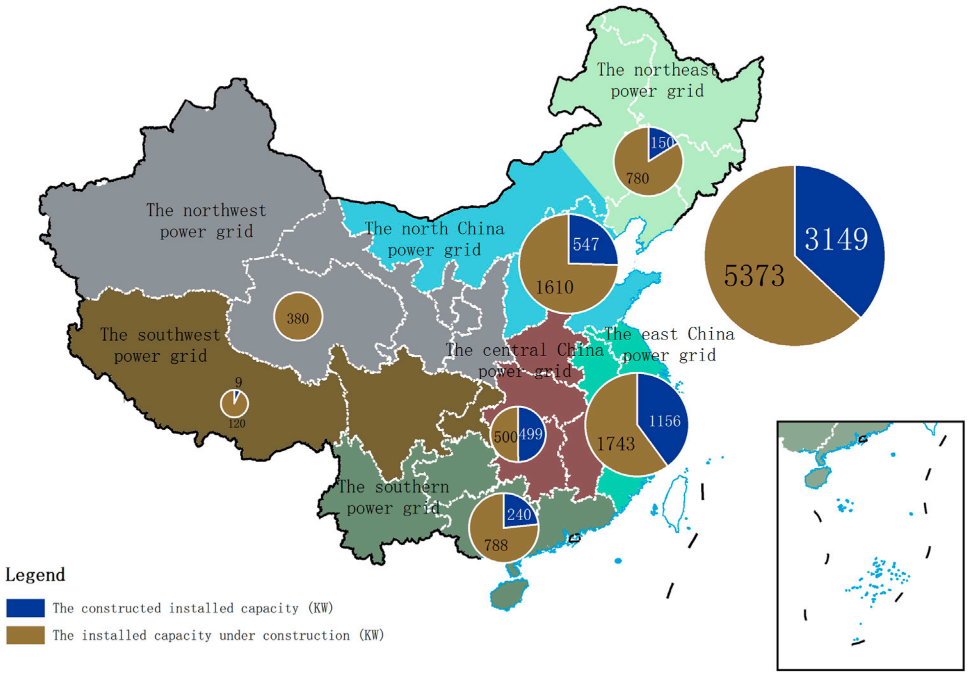

FIGURE 11
Existing installed capacity of PSPS in China.

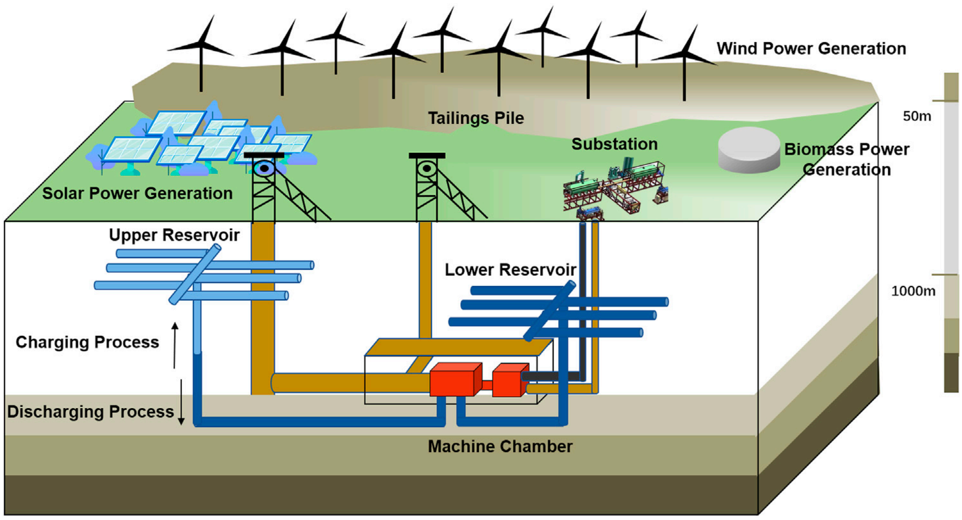

FIGURE 12
Concept of PSPSuM.

about 2.5 million kW. Compared with other countries in the world, China's overall development speed of PSPS is relatively fast, and the PSPS under construction ranks first in the world. The total installed capacity of PSPS in China is 31.49 million kW. The installed capacity of North China, East China, Central China, Northeast China, South China and Southwest power grid regions is 5.47 million kW, 11.56 million kW, 4.99 million kW, 1.5 million kW, 7.88 million kW and 90 million kW, respectively. The installed capacity of PSPS in East China Power Grid is the largest, followed by that in South China power grid and North China Power grid, as shown in Figure 11.

PSPS has the capacity to track system load fast, to carry out smooth and rapid adjustment of active power and reactive power, and to bear the important role of reactive dynamic support. The coordinated operation of PSPS and new energy generation can significantly improve the comprehensive utilization rate of renewable energy. However, from the perspective of renewable energy endowment and utilization efficiency, it is still necessary to accelerate the development of PSPS in a scientific and orderly way in the Yellow River basin.

4 Feasibility analysis of pumped storage power station using abandoned mine (PSPSuM) in the Yellow River basin

4.1 Concept of PSPSuM

PSPS require a relatively large water head to complete the conversion of hydraulic potential energy, but the relatively flat terrain in a large number of plain areas limits the large-scale application. Therefore, the construction of underground PSPS has become an inevitable choice to solve the bottleneck problem of renewable energy storage. Abandoned mines have large underground space and water head, And the underground space with relatively stable mechanical properties of surrounding rock can provide safe and reliable space guarantee for upper and lower reservoirs and machine caverns.

At the same time, the shaft makes the traffic convenient and the large amount of mine water after purification treatment can be enough water resource for upper and lower reservoir. Making full use of the underground space with stable structures in the abandoned mines to build underground PSPS, on the one hand, can effectively save the construction cost of underground water reservoir; On the other hand, it can avoid the influence of the construction of above-ground water storage engineering facilities on the surface landscape and reduce the ecological disturbance effect (Xi et al., 2020). The concept of PSPSuM is shown in Figure 12.

Back in the 1980s, TU delft in Netherlands had conducted a feasibility study on the use of abandoned coal mine to construct PSPS. Although the final results show that at the time, due to the limited technical and economic conditions, the use of abandoned coal mine to underground PSPS is not viable (Busch and Kaiser, 2013), the research pointed out the subsequent research direction, and extended the research boundary. In 1993, the United States built mount Hope Semi-underground PSPS in New Jersey by using open pit iron mine. In 2009, funded by the German Federal Ministry of Environmental Protection and Nuclear Energy Safety (BMU), the German Energy Research Center of Lower Saxony (EFZN) carried out the construction of underground PSPSuM (Schmidt et al., 2011; Busch and Kaiser, 2013; BMWI 2014). It determined that six mining areas in Germany, including Erzgebirge, Harz and Siegerland, were suitable or partially suitable for the construction of underground PSPSuM. According to preliminary estimates, up to 10 GW of installed capacity could be built in these mining areas under ideal conditions. In 2018, RAG group, together with other local scientific research institutes, carried out the feasibility study of abandoned coal mine PSPS in Prosper-Haniel mining area, which has built the world's first abandoned coal mine PSPS model with a installed capacity of 200 MW (UDE, 2014).

4.2 Technical essential

In general, a series of studies from suitability analysis to engineering design have been carried out on PSPSuM in the world, and the possibility and technical key points of constructing PSPSuM for renewable energy storage have been discussed. The studies show that using abandoned mines to build PSPS can be an effective means of renewable energy storage under the strategic condition of new energy transformation, and it is also operable in construction and implementation in terms of technical conditions risk assessment, environmental planning and economic benefits, and project approval. However, the planning and construction of an PSPSuM is a complex multi-disciplinary challenge, which requires an overall consideration of various disciplines including rock mechanics, mining, mining surveying, machinery manufacturing, power system, economics, ecology and law, and the coordination of scientific research forces of various professional disciplines to carry out comprehensive evaluation.

4.2.1 Rock mechanics

The stability of the surrounding rock of abandoned mine is the precondition to the construction of PSPSuM, including water reservoirs, machine cavern and mechanical stability of transportation roadway. The basic indicators for evaluating the stability of surrounding rock include formation lithology, rock mechanics, Initial stress state of underground space, Rock stress-strain, hydraulic characteristics, Water-rock coupling effect, Mining depth, exploitation method and so on.

In general, compared with sedimentary rock, intrusive rock and metamorphic rock with low permeability, are more suitable for building underground PSPS. When the design of the PSPS begins, the first step should be the analysis and research on the stability of surrounding rock. The mechanical properties of surrounding rock under the coupling effects of water and rock should be analyzed to reveal the boundary conditions of surrounding rock instability. Then, based on the analysis results, a scheme for planning of underground water reservoir, and for the stability of surrounding rock in areas with weak supporting structure should be mapped out.

4.2.2 Mine planning

According to the mining conditions and the structure of underground space, the capacity of underground space, mining depth and its topological relationship with ore deposit type should be analyzed. The limitation indexes such as shaft access and mine closure time should be estimated, and the suitability of underground PSPSuM is preliminarily evaluated.

1) Type of deposit: According to the strike of the deposit, it can be roughly divided into inclined and horizontal ones, and according to the distribution of the deposit, it can be roughly categorized into lenticular or massive. Generally speaking, for the construction of underground PSPSuM, the type of horizontal massive deposit is the ideal condition to achieve large capacity storage.
2) Mining depth: mining depth determines the hydraulic head of the PSPS, which indirectly determines the energy storage capacity. Generally speaking, hydraulic head can also be realized through the combination of multiple shafts and tunnel systems.
3) Underground space capacity and its topological relationship: besides mining depth, underground space capacity is another important index that determines the storage capacity of PSPSuM. The topological relationship of underground space determines the planning and configuration of underground space, including storage space machine chamber and other auxiliary chambers.
4) Supporting conditions: the supporting conditions of abandoned mine are important factors to improve the stability of surrounding rock. Under normal circumstances, the support measures of underground auxiliary chamber are relatively complete and the stability of surrounding rock is good, while the support measures of goaf are relatively weak and the stability of surrounding rock is poor. Compared with the abandoned mine with longer closure time, the abandoned mine with shorter closure time has better supporting condition.
5) Transportability of shaft: Large machinery and equipment of PSPSuM need to be transported to underground mechanical chamber through shaft. For power station with large energy storage capacity, the diameter of shaft is an important factor restricting the transportability of machine.
6) Mine closure time: mine closure time can not only be used as an indicator to judge the integrity of support measures, but also determine the reuse degree. Generally speaking, the mine that is about to be closed has not implemented the closure procedure, so the transportation channel can be opened without additional cost. Moreover, there is also real-time information about mine water changing state in those

mines, which is convenient for the construction planning of PSPS.

Through the analysis of the related parameters of abandoned mine, 3d visualization models of abandoned mine space can be mapped out using geographic information system and mining aided design software. Then combined with the mechanical characteristics of surrounding rock, the well-rounded design concerning the upper and lower water reservoirs, Penstock, machine cavern, auxiliary traffic and underground transmission line can be arranged.

4.2.3 Machine arrangement

It mainly includes the selection of hydraulic machinery components according to the evaluation indexes such as the hydraulic head of the PSPS, the storage capacity of the abandoned mine shaft, and the space volume of the mechanical chamber. At the same time, the rational configuration of the machines (pump, turbine, generator), debugging of mechanical performance and carrying out mechanical operation scenario simulation should also be considered.

4.2.4 Energy system design

Based on the design principle of energy management system, the framework conditions of renewable energy grid connection should be analysed. Combined with the constraints of power balance, the operation constraints of PSPS and renewable energy consumption, The power conversion efficiency under different scenarios should be calculated by professional power system simulation software to simulate public power grid. At the same time, economic benefit evaluation under different coupling scenarios should also be carried out, and the bottleneck data of public power grid will be analysed in cooperation with researchers from other disciplines, with the goal to minimize the total operation cost of the combined power generation system and improve the power generation efficiency.

4.2.5 Compliance

The researches on relevant laws and regulations of existing abandoned mines and PSPS, should be carried out. Based on relevant engineering fields involved in the construction, operation and maintenance of underground PSPSuM, the potential legal constraints should be analyzed according to the current laws and regulations in various fields, and the legal compliance of PSPSuM should be determined.

4.2.6 Environmental implication

The construction and operation process of underground PSPS will inevitably affect the local ecological environment. Therefore, at the beginning of planning, detailed environmental impact assessment should be carried out according to the actual situation of abandoned mines and planned engineering activities, focusing on the analysis of engineering activities' impact on water resources, biodiversity and landscape. The potential influence of water environment and water ecology, and the activation effect of water-rock interaction on harmful substances in mine should be evaluated. Renewable energy development (especially photovoltaic power plants) and PSPS construction also have potential impacts on habitats and animal migration paths, which should be subject to thematic assessment at the time of planning. In addition, the potential impact of the layout of surface transmission lines and the construction of substation facilities on the landscape should also be taken into account, especially when the power station is built around the city area.

4.2.7 Economical efficiency

Relevant studies in Germany have found that under the premise of ensuring the operation safety, compared with traditional energy storage forms, economical efficiency is the key factor restricting the feasibility of PSPSuM (Schmidt et al., 2011). The main factors influencing the construction cost should be detected before the construction process of PSPSuM. The simulation studies, which focus on the cost-benefit under the conditions of different energy storage capacity of PSPSuM, provides cost optimalization potential. Together with researchers from related science domains, a solution to reduce the construction cost of PSPSuM can be proposed, after a sophisticated analysis on underground water reservoir, mechanical configuration, power system planning, energy market and other factors.

4.3 Potential estimation

The Yellow River basin has a vast land area and excellent resource and environmental endowment. Solar energy and wind energy resources are abundant and widely distributed in the Yellow River basin. At the same time, the huge above-ground and underground space left by numerous and widely distributed abandoned mines in the Yellow River basin has laid a good foundation for the storage of renewable energy. Especially in Qinghai, Gansu, Inner Mongolia in the Northwest of the Yellow River basin, there is a high spatial correlation between the renewable energy enrichment areas, mainly wind and solar energy, and the mining areas. The preliminary analysis and research on the potential of PSPSuM should be carried out under with full reference to the international pilot study examples, which aims to unify the interdisciplinary theories concerning rock mechanics, mining,

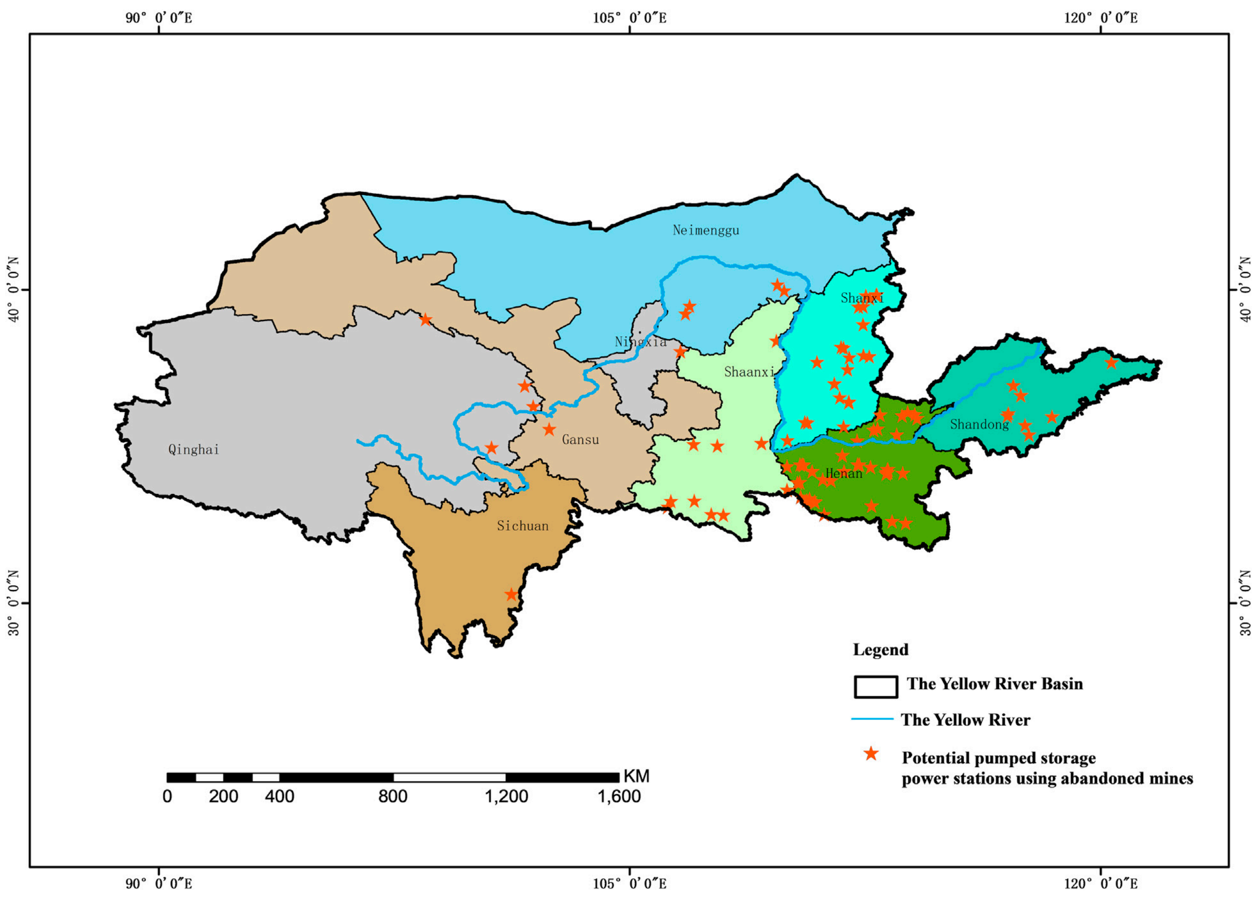

FIGURE 13
Spatial distribution of potential PSPSuM in the Yellow River basin.

mining surveying, machinery manufacturing, power system, economics, ecology and law.

Based on the national mine geological environment survey database from China Geological Survey (Li and Zhang, 2018), the preliminary potential analysis of PSPSuM in the Yellow River basin is mainly based on four indicators: the availability of underground space, the spatial structure, the geo-environmental conditions and the installed capacity. Firstly, the available underground space and its spatial structure of abandoned mine were estimated, according to the basic information such as the actual production capacity, the amount of ore produced, the area of mined-out area, the maximum mining depth, the maximum mining thickness and the mining method. Secondly, according to the requirements of the PSPSuM for the stability of surrounding rock, the abandoned mine whose geological environment conditions meet the safety requirements of engineering construction and operation is selected. Finally, 100 MW is taken as the minimum installed capacity. Taking into account selection indicators such as space size, space structure and stability, 91 abandoned mines suitable for the construction of PSPSuM were selected in the Yellow River basin, with a total estimated installed capacity of 15,830 MW. Their spatial distribution is shown in Figure 13.

TABLE 1 Main characteristics of the PSPSuM.

Parameters	Value
Mean water level of upper reservoir Z_u (m)	100
Volume of upper reservoir V (m^3)	658,000
Mean water level of lower reservoir Z_l (m)	560
Volume of lower reservoir V_l (m^3)	726,000
Operating time full load t (s)	180,000
Length of the water tunnel l (m)	2,150
Penstock diameter d (m)	2
Flow velocity v (m/s)	2.5
Resistance coefficient μ	0.018
Pump efficiency η_p (%)	85%
Turbine efficiency η_t (%)	90%
Efficiency coefficient η_e (%)	80%

4.4 Case study

The charging and power generating process is simulated in an abandoned mine selected from the Yellow River basin for the construction of a PSPSuM. The specific parameters of the PSPSuM are shown in Table1.

4.4.1 Charging process

In the charging process, the electric power generated by renewable energy is used to pump water from the lower reservoir to the upper reservoir. In this way, the electric power is converted into the gravity potential energy of water. The pumping flow Q is calculated by the following Formula:

$$Q = \frac{V}{t} \tag{1}$$

In this process, the frictional resistance along the flowing path and the sharp change of local boundary will lead to head loss, which is calculated by the following formulas:

$$H_l = H_f + H_b \tag{2}$$

$$H_f = \mu \frac{lv^2}{2dg} \tag{3}$$

$$H_b = \frac{v^2}{2g} \tag{4}$$

The actual average pumping head is determined by the average water level of upper and lower reservoirs and the head loss, as follows:

$$H_c = Z_l - Z_u + H_l \tag{5}$$

The maximum power consumption of the pumping process, that is, the power generated by renewable energy consumed by charging, is calculated by the following formula:

$$W_c = \frac{H_c V g\rho}{\eta_p} \tag{6}$$

4.4.2 Discharging process

In the process of power generation, water flows from the upper reservoir through the penstock, drives the generator and finally flows to the lower reservoir to convert the gravitational potential energy of water into electrical power. The average head of power generation is calculated as follows:

$$H_d = Z_l - Z_u - H_l \tag{7}$$

The maximum generated electric power is calculated by the following formula:

$$W_d = H_d V g\rho\eta_t \tag{8}$$

Thus, it can be concluded that the installed capacity of PSPSuM is:

TABLE 2 Power Conversion of the charging and discharging process.

Parameters	Value
Pumping flow Q (m^3/s)	36.56
Head loss H_l (m)	6.49
Pumping head H_c (m)	466.49
Power head H_d (m)	453.51
Power storage by Charging W_c (kW h)	7.44×10^5
Power generation by discharging W_d (kW h)	7.3×10^5
Installed capacity P (MW)	130
Annual power generation W_g (kW h year^{-1})	2.37×10^8

$$P = H_d Q g\eta_e \tag{9}$$

The power conversion of the charging and discharging process are shown in Table 2.

5 Discussion

According to the preliminary evaluation results of PSPSuM in the Yellow River basin, With 100 MW as the minimum installed capacity, at least 91 PSPSuM can be built by utilizing existing abandoned mines under the consideration of underground space, spatial structure and surrounding rock stability. The total installed capacity reaches 15830 MW. Based on an average full load time of 5 h, a single charging can store 7.92 × 10^7 kWh of renewable energy. 1 kWh is equivalent to 0.123 kg standard coal heat conversion, so a single discharging can be converted into 0.97 × 10^4 tons of standard coal. According to the average annual charging and discharging cycle times of 400, 0.39 million tons of standard coal could be saved annually, reducing carbon dioxide emissions of about one million tons. The effect is very prominent.

Wind and solar power resources in China is mainly concentrated along the provinces of Qinghai, Inner Mongolia and Gansu of the Yellow River basin. In those regions, the landscape are mainly plains with wind-blown sands, gobi, deserts and other unused lands. In the future, these areas can make full use of excellent renewable energy endowment to speed up the construction of large wind and solar power base (Zhang Y et al., 2022). At the same time, they are one of the most enrichment areas of China's coal resources. Therefore, In the future, a variety of energy forms and complementary energy technologies can be integrated and utilized in the region. The abandoned mines with large above-ground and underground space in these regions should be used to construct PSPSuM, adjusting to local conditions. The factors, such as regional electricity supply, the waste of wind power, energy storage capacity and the mutability of electricity, should be fully considered to utilize renewable energy in the Yellow River basin, relying on the established inter-provincial transmission channels and thermal power point-to-point network transmission channels.

The natural environment and socio-economic development levels are highly different between China and developed countries in Europe and the United States. Those differences predetermined the diverse features of the abandoned mines and the methods in reusing them. Compared to those countries mentioned above, abandoned mines in China are unique in their complex mine geological environment, problems left over by governance in the past, and insufficient restoration and serious ecological environmental impacts. Therefore, the reusing process of abandoned mines in China should first focus on solving the ecological environment problems, carrying out ecological restoration.

Based on the geological conditions and underground space distribution characteristics of different abandoned mines in different regions, research of underground space exploration should be carried out to analyze the influence of geological conditions on the suitability of underground PSPSuM. From the technical and economic perspectives, the multi-disciplinary research on the planning should also be carried out to form a set of practical engineering design and implementation scheme.

The construction of pumped storage power station in abandoned mines is a systematic project of interdisciplinary integration. Although some key scientific and technological problems have been properly solved according to international studies and engineering designs. However, there are still some key scientific issues, such as the influence of hydrogeology, hydrochemistry characteristics and groundwater circulation process on the site selection of PSPSuM, and the influence of the stability and tightness of surrounding rock mass on the construction and operation of PSPSuM, which need to be further studied by subsequent scholars (Bian et al., 2021).

In this study, the evaluation of the potential of PSPSuM in the Yellow River basin shows only a preliminary estimation result. Only the space size, space structure and space stability of abandoned mines are considered, and only the installed capacity larger than 100 MW are taken as the evaluation objects, so the evaluation results have certain limitations. The comprehensive and accurate potential assessment needs to take into account of other constraints such as regional renewable energy distribution, regional energy demand, ecological assessment and transmission infrastructure, combined with a thorough look into the existing energy base, energy storage site layout and regional energy configuration characteristics.

6 Conclusion

China's strategic goals of "carbon neutrality" and "carbon peak" have pointed out an important direction for the development of the energy industry. As the main energy industry gathering area in China, the Yellow River basin is bound to take on an irreplaceable historical mission in the process of energy industry restructuring in the coming decades. Under the guidance of carbon neutrality, the Yellow River basin should vigorously promote the development and utilization of renewable energy in the region, and increase the proportion of renewable energy in the primary energy consumption structure. Abundant wind and solar energy resources in the Yellow River basin provide basic guarantee conditions.

The renewable energy in the Yellow River basin can not be fully developed and effectively utilized due to the random fluctuation characteristics of wind and photovoltaic power generation system, the relatively low load level of power grid and the insufficient peak regulation capacity. PSPS, as the most large-scale and technologically mature way of energy storage, can effectively improve the acceptance capacity of power grid for wind and solar power generation. The large amount of ground and underground space left by abandoned mines in the Yellow River basin provides favorable space guarantee for the construction of PSPSuM and storage of renewable energy.

Using abandoned mines to build PSPS can be an effective means to develop renewable energy storage under the new energy transformation strategy. However, the planning and construction in abandoned mine is a complex multi-disciplinary challenge, which requires an overall consideration of a variety of disciplines including rock mechanics, mining, mine surveying, machine configuration, power system, economics, ecology and law, to carry out comprehensive evaluation in collaboration with scientific research forces of various professional disciplines.

A preliminary evaluation of the PSPSuM in the Yellow River basin was carried out by comprehensively considering the space size, spatial structure and surrounding rock stability of abandoned mines. The results show that, taking 100 MW as the minimum installed scale, 91 abandoned mines suitable for the construction of pumped storage power stations are screened out in the Yellow River basin, with a total installed capacity of 15,830 MW, saving 0.39 million tons of standard coal annually and reducing carbon dioxide emissions of about one million tons. The effect of reducing carbon emissions is very significant. Especially in Inner Mongolia, Gansu, Qinghai provinces where renewable energy is enriched and highly developed, there are abandoned mines that can be used to build PSPS. These potential PSPSuM provide a feasible solution to improve the efficiency of renewable energy utilization in the Northwest region of the Yellow River basin.

Data availability statement

The original contributions presented in the study are included in the article/Supplementary Material, further inquiries can be directed to the corresponding author.

Author contributions

FX: Conceptualization, methodology, data curation, formal analysis, writing-original draft, project administration. RY: Conceptualization, methodology, writing-review and editing. JS: Conceptualization, supervision, writing-review and editing. JZ: formal analysis, data curation, RW: methodology, writing-review and editing.

Funding

This research was funded by the National Natural Science Foundation of China (Grant Nos 42103079 and 41907402).

Conflict of interest

The authors declare that the research was conducted in the absence of any commercial or financial relationships that could be construed as a potential conflict of interest.

Publisher's note

All claims expressed in this article are solely those of the authors and do not necessarily represent those of their affiliated organizations, or those of the publisher, the editors and the reviewers. Any product that may be evaluated in this article, or claim that may be made by its manufacturer, is not guaranteed or endorsed by the publisher.

References

ANL, Acres American Incorporates for Argonne National Laboratory. (1976). Siting opportunities in the U.S. For compressed air and underground pumped hydro energy storage facilities.

Bian, Z. F., Zhou, Y. J., Zeng, C. L., et al. (2021). Exploration of the foundation problem of underground construction of pumped storage reservoir in abandoned mines. *J. China Coal Soc.* 46 (10), 3308–3318. doi:10.13225/j.cnki.jccs.yg21.0392

BMWI, Federal Ministry of Economics and Technology. (2014). Die Energie der Zukunft: Erster Fortschrittsbericht zur Energiewende.

Boust, M. (2012). Europa beschleunigt den Pumpspeicher-Ausbau. *Wasserwirtsch.* 102 (3), 42–44. doi:10.1365/s35147-012-0231-z

BP. (2021). BP statistical review of world energy 2021.

Busch, W., and Kaiser, F. (2013). *Unkonventionelle Pumpspeicher: Schlüsseltechnologie der zukünftigen Energielandschaft. Band 16 Goettingen.* Göttingen, Germany: Cuvillier Verlag.

Chang, G. C., Thompson, P. A., et al. (1980). *Pumped storage hydroelectric plants with underground lower reservoirs. Proceedings of the International Symposium (Rockstore 80).* Oxford: Pergamon Press, 579–585.

Chas, T. M. (1978). Underground hydroelectric pumped storage: An evaluation of the concept. *Boston Main.* 1, 399–404.

China Power Enterprise Management. (2021). Medium-and long-term development plan for pumped storage

CSG (2021). Council of state governments. The carbon peak action plan by 2030. Available at: https://www.mee.gov.cn/zcwj/gwywj/202110/t20211026_957879.shtml.

Electric Power Research Institute (1976). *An assessment of energy storage systems suitable for use by electric utilities.* Newark: Public Service Electric and Gas Company Newark.

Gao, Y. L., Zhang, J. X., and Cui, S. B. (2002). Chemical and nonferrous metal industry of the Yellow River Basin and the river water quality. *Yellow River* 24 (7), 21–23. doi:10.3969/j.issn.1000-1379.2002.07.011

HEC, Harza Engineering Company. (1977). Underground pumped hydro storage facilities and compressed air energy storage. An analysis of regional markets and development potential.

HPDGI (2022). *Hydropower planning and design general institute.* China: China's Renewable Energy Development Report.

Huang, S., Xi, F., Chen, Y., Gao, M., Pan, X., and Ren, C. (2021). Land use optimization and simulation of low-carbon-oriented—a case study of jinhua, China. *Land* 10 (10), 1020. doi:10.3390/land10101020

Huang, Z., and Xie, X. (2021). Energy change under the carbon-neutral vision. *Bull. Chin. Acad. Sci.* 36 (09), 1010–1018. doi:10.16418/j.issn.1000-3045.20210812001

IPCC (2018). *Special report on global warming of 1.5°C.* UK: Cambridge University Press.

IPCC (2021). The working group I report of the Sixth assessment report issued by the intergovernmental Panel on climate change. Available at https://unfccc.int/topics/science/workstreams/cooperation-with-the-ipcc/the-sixth-assessment-report-of-the- ipcc.

Jin, F. J. (2019). Coordinated promotion strategy of ecological protection and high-quality development in the Yellow River Basin. *Reform* 2019 (11), 33–39.

Li, J. Z., and Zhang, J. D. (2018). Investigation of mine geological environment in China. *Hydrogeology Eng. Geol.* 45 (04), 169–172. doi:10.16030/j.cnki.issn.1000-3665.2018.04.25

Liu, W. D., Tang, Z. P., Xia, M. Y., et al. (2019). Machine learning identification and evolution of the key impact factors of carbon strength in China. *Acta Geogr. Sin.* 74 (12), 2592–2603. doi:10.11821/dlxb201912012

Luo, K., Shi, W. H., Cao, F., et al. (2018). Preliminary exploration of the construction of pumped storage power station by using abandoned mines. *Energy China* 40 (10), 42–47. doi:10.3969/j.issn.1003-2355.2018.10.007

NASA. (1976). STI/Recon Technical Report. Underground pumped storage research priorities.

NEA. (2021). National energy administration. China energy statistical yearbook 2020.

NOAA (2021). National oceanic and atmospheric administration. Trends in atmospheric carbon dioxide. Available at : https://gml.noaa.gov/ccgg/trends/.

Peng, S. P., and Bi, Y. L. (2020). Key technology and strategic thinking of ecological environment restoration in Yellow River basin. *J. China Coal Soc.* 45 (04), 1211–1221. doi:10.13225/j.cnki.jccs.2020.0444

Schmidt, B., et al. (2011). *Windenergiespeicherung durch Nachnutzung stillgelegter Bergwerke. Schriftenreihe des Energie-Forschungszentrums Niedersachsen, Band 7.* Göttingen: Cuvillier Verlag.

Su, J., Liang, Y. B., Ding, L., Zhang, G., and Liu, H. (2021). Research on China's energy development strategy under carbon neutrality. *Bull. Chin. Acad. Sci.* 36 (9), 1001–1009. doi:10.16418/j.issn.1000-3045.20210727001

Tam, S. W., Blomquist, C. A., and Kartsounes, G. T. (1979). Underground pumped hydro storage-an overview. *Energy sources.* 4, 329–351. doi:10.1080/00908317908908068

UDE (2014). *Sachstand zur Machbarkeitsstudie einer Nachfolgenutzung der Anlagen des Steinkohlebergbaus im Ruhrgebiet als Pumpspeicherwerke.*

U.S. Patent. (1917). US1247520, fessenden R A. System of storing power.

Walia, M., and McCreath, D. R. (1976). Siting opportunities in the U.S. For compressed air and underground pumped hydro energy storage facilities. *Storage Excav. Rock Caverns Rockstore* 77, 117–123. doi:10.1016/B978-1-4832-8406-4.50025-7

Xi, F. R., Wang, R. P., Shi, J., Zhang, J., Yu, Y., Wang, N., et al. (2022). Spatio-temporal pattern and conflict identification of production–living–ecological space in the Yellow River basin. *Land* 11 (5), 744. doi:10.3390/land11050744

Xi, F. R., Zhang, J. D., Wang, Y. Y., et al. (2020). Technical points and feasibility analysis of underground pumped storage power station in China. *Sci. Technol. Rev.* 38 (11), 41–50. doi:10.3981/j.issn.1000-7857.2020.11.005

Xi, J. P. (2019). Speech at the Yellow River Basin ecological protection and high-quality development symposium. *Qiushi* 2019 (20), 1–5.

Xi, J. P. (2020). We will build on past achievements and forge ahead, and embark on a new global journey to tackle climate change- Speaking at the Climate Ambition Summit. *The People's Daily* 2020 (12), 9.

Xie, H. P., Hou, Z. M., Gao, F., et al. (2015). New technology of pumped storage power generation in underground coal mine: Principle, current situation and prospect. *J. China Coal Soc.* 40 (05), 965–972. doi:10.13225/j.cnki.jccs.2015.0690

Yuan, L. (2017). Scientific conception of accurate coal mining. *J. China Coal Soc.* 42 (1), 1–7. doi:10.13225/j.cnki.jccs.2016.1661

Zhang, H. M., Yuan, P. F., and Zhu, Z. S. (2022). Decoupling effects of carbon emissions and reduction path in the Yellow River Basin. *Resour. Sci.* 44 (01), 59–69. doi:10.18402/resci.2022.01.05

Zhang, J. D., and Xi, F. R. (2020). Research on ecological restoration of abandoned mines in China. *Acta Ecol. Sin.* 40 (21), 7921–7930. doi:10.5846/stxb201908301799

Zhang, Y. S., Lian, J. J., Zhang, J. L., et al. (2022). Research on the construction of unit multi-energy complementary energy base in the Yellow River basin. *Water Power* 48 (06), 6–11. doi:10.3969/j.issn.0559-9342.2022.06.002

frontiers | Frontiers in Environmental Science

ORIGINAL RESEARCH
published: 30 September 2022
doi: 10.3389/fenvs.2022.944708

Decoupling China's mining carbon emissions from economic development: Analysis of influencing factors

Wenjie Sun[1], *Shunli Ren*[1]*, *Kai Liu*[2]* *and Chaoyao Zan*[1]

[1]College of Geoscience and Surveying Engineering, China University of Mining & Technology, Beijing, China, [2]Chinese Academy of Geological Sciences, Beijing, China

Mining provides basic materials and energy for human life and supports economic and social prosperity and development. The decoupling of mining carbon emissions from economic development is an important way of achieving China's carbon peaking and carbon neutrality goals. This study uses the Tapio decoupling model to measure the relationship between China's economic development and carbon emissions from 2001 to 2018. It analyzes the overall industry as well as its subdivisions and identifies the factors driving carbon emissions with help from the improved Kaya identity and LMDI decomposition models. The results show that, except for the unstable situation in the oil and natural gas mining industry, the other mining divisions have attained strong decoupling and have become stable, showing a continuous positive trend. On the whole, the mining product smelting and processing industry has achieved a major transformation, moving from negative decoupling to weak decoupling, but there are great differences between different sub-sectors. The overall consumption of China's mining products, and the incremental carbon emissions have continued to decline, while economic development has shifted from inefficient expansion to high-quality economic development, although without reaching the ideal state. The economic factor and energy intensity effects are the key factors in increasing and restraining carbon emissions, respectively, and their influence should not be ignored. This study aims to provide a decision-making basis for China's mining industry, that it might carry out carbon emission reduction planning, and promote the clean and efficient construction of the industry and the green and high-quality development of the economy.

Keywords: carbon emissions, economic growth, mining, Tapio decoupling, LMDI decomposition

Edited by:
Jingying Fu, Institute of Geographic Sciences and Natural Resources Research (CAS), China

Reviewed by:
Xiaoyue Wang, Institute of Geographic Sciences and Natural Resources Research (CAS), China
Chizhong Wang, Renmin University of China, China

Correspondence:
Shunli Ren
rensl_wel@163.com
Kai Liu
acancer@163.com

Specialty section:
This article was submitted to Environmental Economics and Management, a section of the journal Frontiers in Environmental Science

Received: *15 May 2022*
Accepted: *22 June 2022*
Published: *30 September 2022*

Citation:
Sun W, Ren S, Liu K and Zan C (2022) Decoupling China's mining carbon emissions from economic development: Analysis of influencing factors. Front. Environ. Sci. 10:944708. doi: 10.3389/fenvs.2022.944708

INTRODUCTION

Global warming is an urgent problem faced by the whole world. In 2020, global greenhouse gas emissions continued to rise, with the global average temperature about 1.2°C higher than the pre-industrial level (World Meteorological Organization, 2020), and atmospheric CO_2 concentration exceeding 415ppm (Guo, 2019). As the world's largest CO_2 emitter, in response to climate change China announced in September 2020 that its CO_2 emissions would peak by 2030, and that it would strive to achieve carbon neutrality by 2060 (Xinhua Network, 2020). In March 2021, China included the goals of carbon peaking and carbon neutrality in the overall layout of its "ecological civilization" plan (Xinhua News Agency, 2021), and integrated ecological and environmental governance with ecological civilization construction, and produced a balanced development plan for an ecologically sustainable environment and high-quality economic growth.

As a pillar industry in China, the mining industry has caused serious damage to the ecological environment, while simultaneously promoting rapid economic growth. This is especially true of the coal-based mining industry, due to the massive scale of the mining, processing, and consuming of fossil fuels, resulting in the continuous and rapid growth of CO_2 emissions, which have in turn caused a series of environmental problems with a serious impact on the natural environment and the economic development of China (Blöcher et al., 2018; Liu et al., 2021a). In 2020, China's coal production was about 3.9 billion tons, with total annual energy consumption of about 4.98 billion tons of standard coal. Although China's total coal consumption control effect is obvious, and the total share of primary energy consumption continues to decline, in 2020 the proportion of primary energy consumption of coal, oil, and natural gas, were, in turn, 56.8%, 18.9%, and 8.3%, respectively. At the same time, the carbon emissions of these three sources accounted for 67.4%, 22.4%, and 5.4%, respectively (Zhang et al., 2022). Fossil energy dominated by coal still plays the main role in the structure of energy consumption. Energy structure adjustment is the first means of solving traditional energy exhaustion and environmental pollution (Deng et al., 2022). The mining industry supports more than 70% of China's national economy. Against the background of the new normal of economic development, China's economy is shifting from high-speed growth to high-quality development, and the mining industry needs to follow the principles of scientific and sustainable development, deepen structural reform on the supply side, and promote low-carbon and high-quality economic development in the process of achieving carbon peaking and carbon neutrality goals (Ju and Qiang, 2017; Wu and Tu, 2019; Hu and Xiao, 2020; Qiang et al., 2021).

Under the new normal, climate change and low-carbon economic development further produce new and higher requirements for mining. Various studies on economic growth and carbon emissions have recently been conducted. Gao and Ge (2020) pointed out the spatial and temporal characteristics of China's economic growth and energy carbon emissions, based on the evolutionary trends of decoupling China's economy and energy carbon emissions between 2001 and 2015. Han et al. (2021) described the regional differences in carbon emissions in China's provinces from 2005 to 2017 and showed the evolving trend of the decoupling index. Climent and Pardo (2007) analyzed the decoupling of Brazil's economic growth and energy-induced carbon emissions from 2004 to 2009 and conducted an exponential decomposition analysis on the variations in carbon emissions. Wu et al. (2019) studied the decoupling effect of China's provinces from 2001 to 2015 and pointed out that 30 provinces in China generally realized the transition from weak decoupling to strong decoupling. Based on a BP neural network model, Liu et al. (2005) studied the decoupling of carbon emissions and GDP growth in China's nonferrous metals industry from 1995 to 2010, providing a reference for the industry's low-carbon transition. Based on the decoupling model, Luo and Wu (2018) analyzed the carbon emissions from the energy consumption of the mining industry in China from 1994 to 2015, and the results show that the dominant status is weak decoupling. Ramachandra et al. (2017) analyzed the relationship between energy carbon emissions and economic gaps in Bangalore, India, indicating that the economic level is an important factor influencing energy consumption and greenhouse gas emissions in India. Sun and Zhou (2017) constructed a spatial measurement model of carbon emissions from 1996 to 2014, showing that energy intensity and economic development levels are the main factors influencing the decoupling index. Zhang et al. (2019) analyzed the factors affecting carbon emissions in Pakistan from 1971 to 2014, and their results showed that population, fossil energy, and GDP per capita are the main factors affecting carbon emissions in Pakistan.

As for the analysis of the decoupling state and the influencing factors of energy and the economy, most studies are carried out at a single level or in different spatial regions. Few studies have produced a multi-stage and deep analysis based on a long time series, combining the general and local aspects of the whole life cycle. The green, low-carbon, and sustainable development of the mining industry is the main driving force behind China's economic construction and high-quality development. Therefore, this study takes the whole life cycle of carbon emissions and economic growth of the mining industry as the research object; carries out research into the decoupling of carbon emissions and GDP; measures the decoupling effect of carbon emissions in each stage of the mining industry based on the Tapio decoupling model; explores the decoupling characteristics of carbon emission in each industry at each stage of the mining industry; and further adopts the LMDI decomposition model to systematically analyze the influencing factors of carbon emission. The innovation of this study is found in its decomposition of the carbon emission process over the whole life cycle of the mining industry from 2001 to 2018; in the way it carries out carbon emission characterization and analysis of each industry at different stages; and in the way it provides accurate and rapid solutions for pollution traceability. Based on a long time series, a combination of local and general approaches are used to carry out year-by-year and cumulative annual carbon emission driver analysis, which clearly shows the influence results of each factor in each time period. It is expected this work will provide references for understanding the intrinsic mechanism of carbon emission changes, for predicting the future trend of carbon emissions (Lv, 2019), for exploring the path of high-quality economic growth, for adjusting the energy structure, and for formulating and implementing differentiated carbon emission reduction policies in the mining industry.

TABLE 1 | Decoupling state classification.

Type	E(C, D)	△C	△D	Decoupling state
1	(-∞, 0)	<0	>0	Strong decoupling
2	[0, 0.8)	>0	>0	Weak decoupling
3	(1.2, ∞)	<0	<0	Recessive decoupling
4	[0.8, 1.2]	>0	>0	Expansive coupling
5	[0.8, 1.2]	<0	<0	Recessive coupling
6	(1.2, ∞)	>0	>0	Expansive negative
7	(-∞, 0)	>0	<0	Strong negative decoupling
8	[0, 0.8)	<0	<0	Weak negative decoupling

METHODS AND DATA SOURCES

Tapio decoupling model

The Tapio decoupling model is an elastic analysis, and the calculated results have strong stability (Song, 2021; Weng et al., 2021), The decoupling index between GDP growth and carbon emissions is calculated as **Eq (1)**:

$$E_{(C,D)} = \frac{\frac{\Delta C}{C}}{\frac{\Delta D}{D}} \quad (1)$$

where $E_{(C,\ D)}$ is the decoupling index, $\triangle C$ is the amount of change in carbon emissions from the mining industry, $\triangle D$ the amount of change in gross domestic product (GDP), and C and D are total carbon emissions and GDP. Decoupling indices and decoupling types are given in **Table 1**.

LMDI method

The modified Kaya constant equation (**Eq. 2**) and the LMDI (**Eq. 3**) decomposition method are chosen to analyze the influence factors behind carbon emissions from the mining industry, and the Kaya constant equation of carbon emissions from energy consumption is as follows:

$$C = \sum_n \frac{C_n}{E_n} \times \frac{E_n}{D} \times \frac{D}{M} \times \frac{M}{P} \times P = \sum_n f_n \times p_n \times \varphi \times \lambda \times \theta \quad (2)$$

where C is the total carbon emissions of the mining industry; C_n is the nth industrial energy consumption carbon emissions; E_n is the energy consumption of the nth industry; D is the total energy consumption; M is the GDP; P is the total population; f_n is the carbon emission factors; P_n is the energy structure; φ is the energy intensity; λ is the economic factor; and θ is the population size.

Decomposing the amount of carbon emission changes according to the additive form in the LMDI model, assuming that C_o and C_t are the total carbon emissions in the base year, and

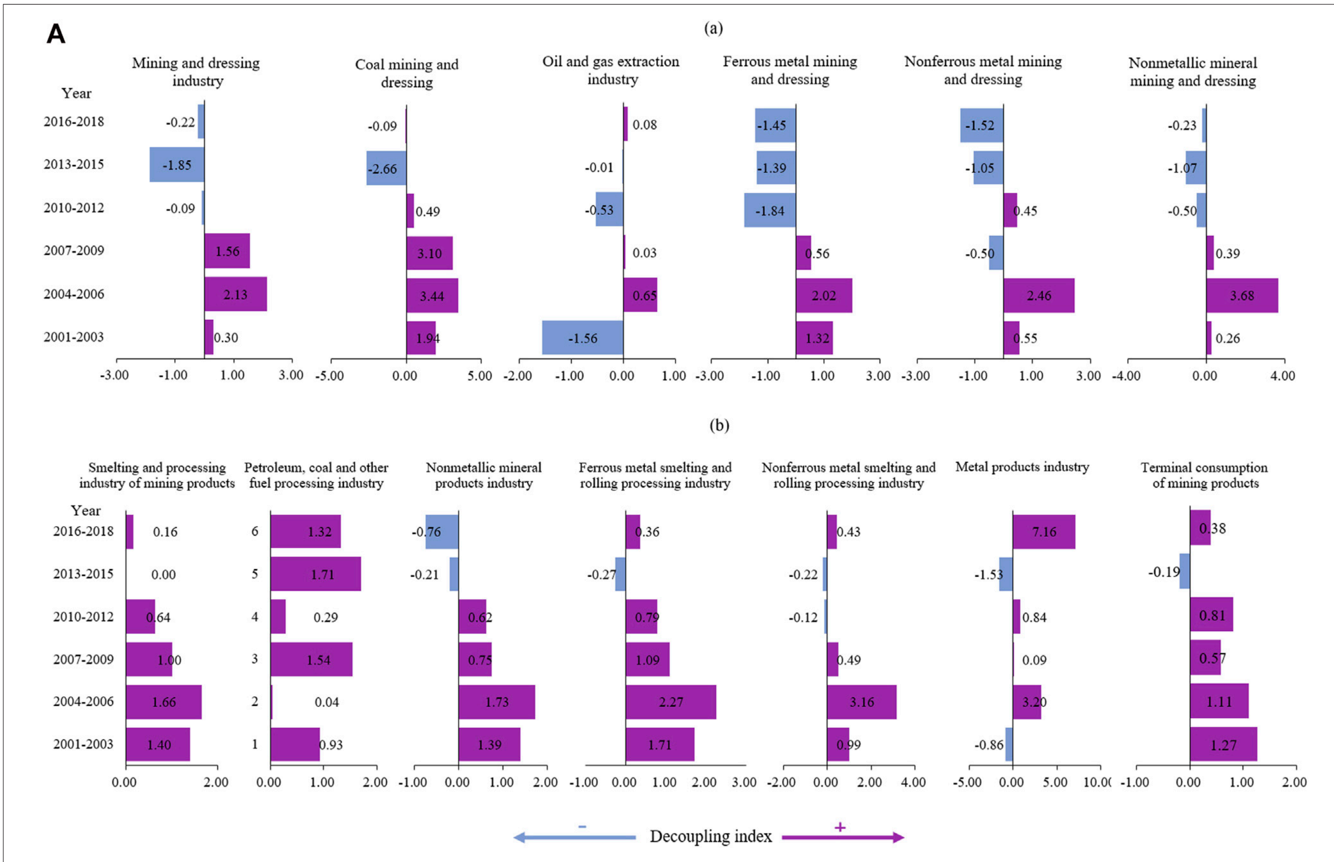

FIGURE 1 | (Continued).

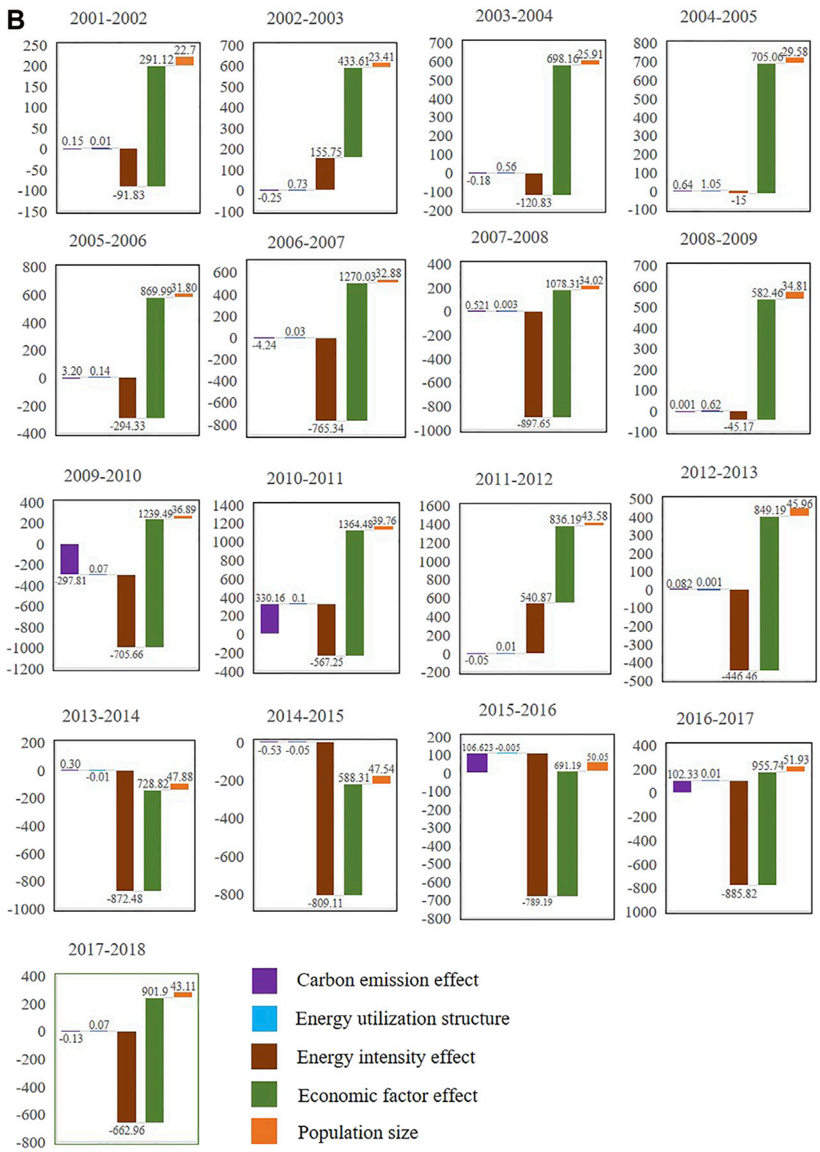

FIGURE 1 | (Continued). Decoupling index of various industries. **(Aa)** Changes in carbon emission decoupling trends in mining and dressing industry, 2001–2018. **(Ab)** Changes in carbon emission decoupling trends in the smelting and processing industry of mining products and in terminal consumption of mining products, 2001–2018. **(B)** Effects of five factors on carbon emissions of China's mining industry. Annual effects of various factors on mining carbon emissions, 2001–2018.

the total carbon emissions in the target year t, respectively, the equation is as follows:

$$\Delta C = C_t - C_o = \Delta C_f + \Delta C_p + \Delta C_\varphi + \Delta C_\lambda + \Delta C_\theta \qquad (3)$$

where $\Delta C_f + \Delta C_p + \Delta C_\varphi + \Delta C_\lambda + \Delta C_\theta$ indicate carbon emission intensity of the mining industry, energy utilization structure, energy intensity effect, economic effect, and population size. The calculation formula of each decomposition factor is as follows:

$$\Delta C_f = \sum_n \frac{C_n^T - C_n^o}{\ln C_n^T - \ln C_n^T} \times \left(\ln f_n^T - \ln f_n^o\right) \qquad (4)$$

$$\Delta C_p = \sum_n \frac{C_n^T - C_n^o}{\ln C_n^T - \ln C_n^T} \times \left(\ln P_n^T - \ln P_n^o\right) \qquad (5)$$

$$\Delta C_\varphi = \sum_n \frac{C_n^T - C_n^o}{\ln C_n^T - \ln C_n^T} \times \left(\ln \varphi_n^T - \ln \varphi_n^o\right) \qquad (6)$$

$$\Delta C_\lambda = \sum_n \frac{C_n^T - C_n^o}{\ln C_n^T - \ln C_n^T} \times \left(\ln \lambda_n^T - \ln \lambda_n^o\right) \qquad (7)$$

$$\Delta C_\theta = \sum_n \frac{C_n^T - C_n^o}{\ln C_n^T - \ln C_n^T} \times \left(\ln \theta_n^T - \ln \theta_n^o\right) \qquad (8)$$

Data resource

The data of GDP and the GDP index in this study are from the China Statistical Yearbook (after accounting). In order to ensure comparability, the GDP is treated at constant prices based on

2001. Carbon emissions from the mining industry are mainly divided into three aspects: the mining industry, the smelting and processing industry, and the terminal consumption of mining products. This study focuses on energy products, and the carbon emission data of each industry comes from the CEADS database and the National Bureau of Statistics.

RESULTS AND DISCUSSION

Decoupling analysis of carbon emissions from mining and dressing industry

The changing trend of the overall carbon emissions from the mining and dressing industry (**Figure 1Aa**) reflects a decoupling status and transformation from weak decoupling, to negative decoupling, and then to strong decoupling. During 2001–2009, carbon emissions and economic levels grew rapidly. Then, with the active promotion of China's green mining industry and circular economy, China's economy achieved rapid growth from 2010 to 2018, while the growth of carbon emissions from the mining and dressing industry gradually stabilized, and decreased year by year (Luo and Wu, 2018). In terms of the development status of each sub-sector, in 2010 and 2007, coal and ferrous metal mining and dressing industries reached a strong decoupling state, respectively, and have remained in a stable state, realizing the transformation from high carbon to low carbon development. The mining and dressing industries of nonferrous metals and nonmetallic minerals were in a weak decoupling state during 2001–2003, and in a negative decoupling state from 2004 to 2006, but then attained a strong decoupling state. The decoupling state of the oil and gas extraction industry has gone from strong decoupling to weak decoupling and is in an unstable state. Although the growth rate of carbon emissions is lower than the economic growth rate, this unstable development state is not conducive to the transition to low-carbon industry and brings potential pressure to high-quality economic development. The above results show that China's mining and extraction industry has achieved structural optimization as a whole, but the oil and natural gas extraction industry has room for improvement. Unit intensity control targets should therefore be strengthened to further reduce unit energy consumption (Tian and Xu, 2012). Continuing to promote green and low-carbon transformation is an inevitable direction for the sustainable development and healthy economic growth of China's mining and dressing industry (Liu et al., 2021a).

Decoupling analysis of carbon emissions from the mining product smelting and processing industry

As a whole, the mining product smelting and processing industry (**Figure 1Ab**) has realized the transformation from negative decoupling to weak decoupling, which has altered the traditional development mode to a large extent. However, the industry has been in a state of weak decoupling since 2010, and as an industry with high CO_2 emissions, there is still a large gap before low-carbon development will be realized. The development status of each sub-mining product in the smelting and processing industry reveals petroleum, coal, and other fuel processing is in a relatively poor condition, with the growth rate of CO_2 emissions at a high level, and the economic growth rate significantly lower. From 2001 to 2018, economic growth and carbon emissions were in a relative state, with a slight improvement in the middle, but with little effect, and there has been a lengthy negative decoupling state of expansion since 2013. The nonmetallic mineral products industry has achieved benign development by realizing the transition from negative decoupling of carbon emissions and economic development to weak decoupling, and then to strong decoupling. The ferrous and nonferrous metal smelting and rolling processing industries also showed a better development trend, with expansion of the negative decoupling state to weak and strong decoupling occurring, with carbon emissions still increasing, but by and large effectively controlled. As of 2018, the metal products industry had poor emission reduction and an unstable development status. The trend of decoupling carbon emissions and economic growth is unclear and there is an obvious alternation phenomenon. As the demand for metal products in society continues to expand, the metal products industry needs to actively comply with the low-carbon trend and enhance the strength and sustainability of carbon reduction.

The mining products smelting and processing industry is an important part of China's mining industry. China's mineral resources are gradually shifting from shallow to deep mines, while resource endowment, backward processing technology, low efficiency of production equipment, resource uncertainty and dynamics, etc. pose serious challenges to the low-carbon transformation of the industry. Therefore, as the backbone of the whole life cycle of the mining industry, we should strengthen digitalization, intelligence, and automation, and upgrade the industry in terms of safety, efficiency, the economy, and green and sustainable development (Liu et al., 2021b).

Decoupling analysis of carbon emissions from mining product end consumption

From **Figure 1Ab**, it can be seen that from 2001 to 2018, the incremental carbon emissions from the end consumption of mining products in China, which by and large are in a continuous downward trend, achieved a shift from negative decoupling to weak decoupling, indicating that with the development of the economy and the optimization and upgrading of the mining structure, the utilization efficiency of mineral products improved continuously, and the value creation capacity was increasingly enhanced. There was a brief rebound during 2010–2012, after which the low-carbon state was gradually restored and stabilized, but economic growth and carbon emissions did not achieve coordinated development, and the process of achieving high-quality economic growth needs further improvement.

Rational and efficient utilization of mineral resources is the basis of high-quality economic development. Currently, China is in the stage of rapid industrialization and urbanization. The

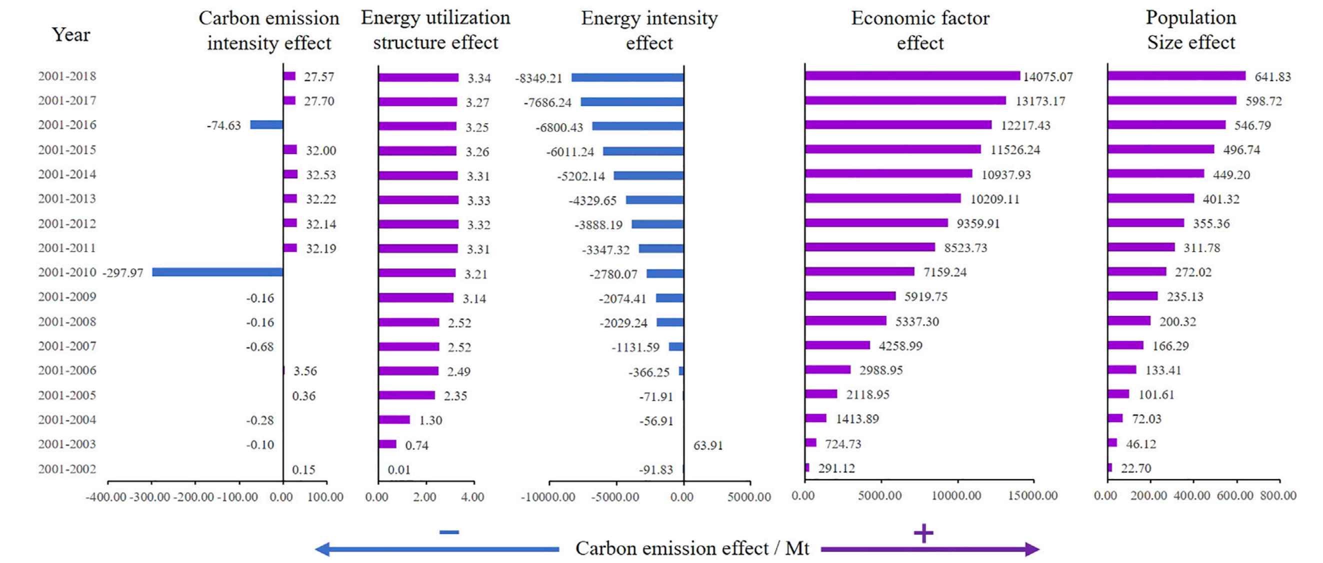

FIGURE 2 | Effects of five factors on carbon emissions of China's mining industry. Cumulative effects of various factors on mining carbon emissions, 2001–2018.

demand for mineral resources continues to grow, and promoting the comprehensive utilization and clean and efficient use of mineral resources has become a top priority (Shang et al., 2022). CO_2, generated by the consumption of energy products, accounts for more than 85% of total carbon emissions. Accelerating the adjustment of the energy consumption structure (Li et al., 2022), reducing the proportion of fossil energy with high carbon emissions, and continuously increasing the proportion of clean energy are important ways to realize the transition from weak decoupling of consumption carbon emissions and economic growth, to strong decoupling (Li, 2022).

Decomposition analysis of carbon emission drivers in the mining industry

The factors influencing carbon emissions from China's mining industry from 2001 to 2018 were decomposed by the LMDI model into a carbon intensity factor, an energy utilization structure factor, an energy intensity factor, an economic effect factor, and a population size factor. From the results of the year-by-year effect of the model's operation (**Figure 1B**), we can clearly see the driving or inhibiting effects of these five factors on carbon emissions in each part of the study period, and the different time changes in the same factors. The carbon intensity factor was consistently stable and mostly suppressed carbon emissions from the mining industry during the period 2001–2009, although there were two large fluctuations during the periods 2009–2012, and 2015–2018. Except for the period 2013–2016, the energy structure factors are positively correlated, and the other periods are relatively stable, with all of them showing the inhibition effect on carbon emissions. Energy intensity factors play a dominant role in inhibiting CO_2 growth, and only in 2002–2003 are they positively correlated with carbon emissions, being negatively correlated for the remainder of the period. Carbon emission reduction reached 8.9764 million tons during 2007–2008. The contribution of economic effects to carbon emissions was promoted from 2001 to 2018. Due to China's previous high-speed economic development model and its large share in the overall emission situation, there are higher requirements for carbon emission reduction. The population size factor continues to have a positive effect on carbon emissions, with a low share during the study period, and as the population size continues to increase, the consumption of resources also expands, thus leading to an increase in CO_2 emissions.

The trend of the cumulative effect of each factor on carbon emissions of energy consumption in China's mining industry from 2001 to 2018 can be seen in **Figure 2**. From an overall perspective, the cumulative effect of carbon intensity alternates positively and negatively during the study period, had a low impact on carbon emissions, and, most of the time, CO_2 emissions increased with a small positive value. During the analysis period, the cumulative effect of energy utilization continued to grow slowly with a positive value, reflecting that China's previous energy utilization structure was relatively unified, leading to an increase in CO_2 emissions. The cumulative effect of energy intensity is the greatest contributor to mining emissions reduction, showing a significant effect on curbing CO_2 emissions by a large amount each year. The effect of economic factors is positively correlated with the decomposition of carbon emissions from the mining industry, both year-by-year, and cumulatively, and contributes most significantly to the increase in carbon emissions throughout the study period. The cumulative effect of the population size factor also continues to stimulate the increase of CO_2 emissions at a faster rate. Although the cumulative effect of the population size factor now accounts for a smaller share in emissions, its influence should not be ignored given the rapid increase in population, the desire for a high quality of life, and increasing carbon emissions from personal energy consumption.

In conclusion, China's economic development transition is still occurring, and energy consumption per unit of GDP is still at a relatively high level, about 1.46 times the world average (Li, 2022). Energy utilization is mainly based on coal (Zhuang and Yan, 2017) and a relatively unified energy structure. China has a large population base, and with the development of a well-off society in an all-around way, and people's yearning for a better life, energy consumption will greatly increase, and the scale of carbon emission activities will gradually expand (Gao et al., 2021). The COVID-19 epidemic has also impacted China's economic development. Energy is the foundation of economic development, and economic recovery after the epidemic reveals a huge gap in energy supply. Therefore, it is of great significance to build a circular economic system decoupling economic growth from resource consumption (Meng et al., 2021), to expand the influence of energy intensity on carbon emission reduction, and to master the driving factors of carbon emissions for the green development of China's mining industry.

CONCLUSION

Based on data on China's economic development and mining carbon emissions from 2001 to 2018, and using the Tapio decoupling state analysis model and improved Kaya identity and LMDI decomposition model, this study explores the decoupling relationship between mining carbon emissions and economic development in China. Related factors affecting mining carbon emissions were decomposed and analyzed based on time patterns. The main conclusions are as follows:

(1) The overall development of China's mining and extraction industry has achieved a major shift, with the decoupling index dropping from 0.304 to −0.266, achieving and continuing to develop a strong decoupling state since 2010. The carbon emissions of coal mining and dressing, ferrous metal mining and dressing, nonmetallic mining and dressing, and nonferrous metal mining and dressing have been greatly controlled. The decoupling index decreased from 1.938, 1.318, 0.259, and 0.553 in the early stage to −0.088, −1.452, −0.226, and −1.525 in the later stage, respectively, reflecting the harmonious development of the mining and extraction industry and the economy. However, the development of the oil and natural gas mining industry is unstable, with the decoupling index alternating between positive and negative, showing a repeated situation of strong decoupling and weak negative decoupling. Therefore, this industry sector needs to strengthen carbon emission reduction actions and improve the space for green and low-carbon development.

(2) CO_2 emissions from the mining products smelting and processing industry were effectively controlled at the overall level, and the decoupling index changed from the previous 1.402 to the later 0.16, thus achieving a shift from negative decoupling to weak decoupling. This indicates that the overall industrial structure is optimized, and is gradually transforming from a high-energy consumption industry to a low-energy consumption industry. The nonmetallic mineral products industry, and nonferrous metal smelting and rolling processing industries, all achieved low-carbon development, with decoupling values ranging from-0.5 to 1.4, hence successively achieving a strong decoupling development state. The ferrous metal smelting and rolling processing industry also achieved better development, with the decoupling value between −0.3 and 1.8, showing a downward trend on the whole, and changing the state of inefficient expansion of the industry. The development of petroleum, coal, other fuel processing industries, and the metal products industry is not as positive, with the former decoupling index in 2007 remaining above 1.5, and the decoupling index of the latter alternating between positive and negative, with a wide floating range, and still a large gap before strong decoupling is achieved.

(3) China's energy end consumption has achieved a shift from high consumption and high carbon emissions to low carbon emissions and green economic development, with a decoupling index between −0.2 and 1.3, although it has not yet reached the ideal state. Based on the time pattern, China's energy carbon emissions are on a growth trend. As China's fossil energy consumption accounts for a relatively large proportion of emissions, it is difficult to achieve a rapid restructuring of the mining industry over a short period of time. Therefore, in order to achieve green and low-carbon development in China, increasing the proportion of clean energy, and adjusting the energy consumption structure are important ways forward.

(4) In the analysis of annual effect and annual cumulative effect, economic factors promoting CO_2 emission have the greatest impact on CO_2 emissions every year. Production reached a peak of 1,364.48 million tons (Mt) in 2011, which was the main factor in promoting carbon emission. While the effect of energy intensity fully shows the advantages of suppressing CO_2 emission, the restraining effect was small in 2001–2006. There was an obvious restraining effect from 2007, with the restraining amount reaching a peak of 885.82 Mt in 2017. Most of the time carbon intensity shows positive and negative alternation in a widely fluctuating range. At the same time, this will be an important aspect of carbon reduction and emission reduction in the future. The effect value of the population factor is positive year by year, and it keeps increasing at an annual growth rate of about 0.04%. The annual effect value of the energy utilization structure is -0.15~1.1 (Mt). Although this

accounts for a small proportion of the total, its impact should not be ignored.

DATA AVAILABILITY STATEMENT

The original contributions presented in the study are included in the article/supplementary material; further inquiries can be directed to the corresponding authors.

AUTHOR CONTRIBUTIONS

WS contributed to all aspects of this work; SR conducted data analysis; SR and KL wrote the manuscript text; CZ gave some useful suggestions and comments to this work. All authors reviewed the manuscript.

FUNDING

This study is funded by the National Natural Science Foundation of China (42172282), Shanxi Key Laboratory of Coalmine Water Hazard Control (2021SKMS01), Open Fund (KJZH2022K02, KJZH2022K03) of Hebei State Key Laboratory of Mine Disaster Prevention, North China Institute of Science and Technology, and Fundamental Research Funds for the Central Universities (2022YJSDC06, 2021YQMT01).

ACKNOWLEDGMENTS

We would like to thank the editors and reviewers for their helpful remarks.

REFERENCES

Blöcher, M., Zimmermann, G., Moeck, I., Brandt, W., Hassanzadegan, A., and Magri, F. (2018). Carbon emission decoupling and decomposition of energy consumption in mining industry of China. *Resour. Industries* 20 (01), 61–67. doi:10.13776/j.cnki.resourcesindustries.20180212.010

Climent, F., and Pardo, A. (2007). Decoupling factors on the energy–output linkage: The Spanish case. *Energy Policy* 35, 522–528. doi:10.1016/j.enpol.2005.12.022

Deng, M. J., Ming, B., Li, Y., Huang, Q., Li, P., and Wu, M. (2022). Pathways towards a cleaner energy system for Xinjiang under carbon peak and carbon neutrality goals. *J. Nat. Resour.* 37 (05), 1107–1122. doi:10.31497/zrzyxb.20220501

Gao, C. C., Ge, H. Q., Lu, Y. Y., Wang, W. J., and Zhang, Y. J. (2021). Decoupling of provincial energy-related CO_2 emissions from economic growth in China and its convergence from 1995 to 2017. *J. Clean. Prod.* 297, 126627. doi:10.1016/J.JCLEPRO.2021.126627

Gao, C., and Ge, H. (2020). Spatiotemporal characteristics of China's carbon emissions and driving forces: A five-year plan perspective from 2001 to 2015. *J. Clean. Prod.* 248, 119280–120127. doi:10.1016/j.jclepro.2019.119280

Guo, Y. N. (2019). Atmospheric CO_2 concentration reaches historic peak. *Ecol. Econ.* 35 (07), 5–8.

Han, M. Y., Liu, W. D., Xie, Y. T., and Jiang, W. B. (2021). Regional disparity and decoupling evolution of China's carbon emissions by province. *Resour. Sci.* 43 (04), 710–721.

Hu, Z. Q., and Xiao, W. (2020). Some thoughts on green development strategy of coal industry: From aspects of ecological restoration. *Coal Sci. Technol.* 48 (04), 35–42. doi:10.13199/j.cnki.cst.2020.04.002

Ju, J. H., and Qiang, H. Y. (2017). The trend and direction of green development of the mining industry in China. *China Min. Mag.* 26 (02), 7–12.

Li, H., Pang, B., Zhu, F. H., Sun, X. L., Xu, J. X., and Wang, S. (2022). *Comparative energy consumption structure and mode between China and major energy consuming countries under the background of carbon emission reduction*. Springer, 1–13. doi:10.13227/j.hjkx.202112065

Li, J. (2022). Research on the relationship and impact of energy consumption and high-quality economic development in China. *Mod. Econ. Res.* 2022 (04), 11–20+132. doi:10.13891/j.cnki.mer.2022.04.006

Liu, G. X., Jia, F. R., Yue, Q., Ma, D. Z., Pan, H. D., and Wu, M. (2005). Decoupling of nonferrous metal consumption from economic growth in China. *Environ. Dev. Sustain.* 18 (1), 221–235. doi:10.1007/s10668-015-9635-0

Liu, X. J., Hou, H. L., Sun, Y. X., and Zhou, P. (2021a). Thinking about the connotation and realization path for green mining in China. *Min. Res. Dev.* 41 (10), 180–186. doi:10.13827/j.cnki.kyyk.2021.10.031

Liu, X. J., Hou, H. L., Wu, Q., Tian, X., Wu, S. K., and Huang, J. (2021b). Spatial pattern of the green development of mining industry in the Yangtze river economic belt and its driving mechanism. *Min. Res. Dev.* 41 (04), 176–182. doi:10.13827/j.cnki.kyyk.2021.04.033

Luo, S. X., and Wu, X. (2018). Carbon Emission Decoupling and Decomposition of Energy Consumption in Mining Industry of China. *Resour. Ind.* 20 (1), 61–67. doi:10.13776/j.cnki.resourcesindustries.20180212.010

Lv, Q. (2019). *Study on spatiotemporal dynamic characteristics and reduction strategy of energy consumption carbon emissions in China*. Beijing: China University of Mining & Technology. [master's thesis].

Meng, X. Y., Wang, Y., and Zheng, X. Z. (2021). Circular economy strategy for the target of carbon neutralization: Management experience and enlightenment from turku. *Finl. Environ. Prot.* 49 (12), 76–80. doi:10.14026/j.cnki.0253-9705.2021.12.003

Qiang, H. Y., Gao, B., Guo, D. Y., and Wang, X. Y. (2021). Options for sustainable development of mining industry under the background of carbon neutrality. *Nat. Resour. Econ. China* 34 (04), 4–11. doi:10.19676/j.cnki.1672-6995.000603

Ramachandra, T. V., Bajpai, V., Kulkarni, G., Aithal, B. H., and Han, S. S. (2017). Economic disparity and CO2 emissions: The domestic energy sector in greater Bangalore, India. *Renew. Sustain. Energy Rev.* 67, 1331–1344. doi:10.1016/j.rser.2016.09.038

Shang, M., Wang, R. R., and Hu, Z. (2022). Study on spatial and temporal evolution and driving mechanism of carbon emissions from provincial energy consumption in China - the analysis based on the perspective of environmental regulation. *Environ. Pollut. Control* 44 (04), 529–534+551. doi:10.15985/j.cnki.1001-3865.2022.04.020

Song, Z. G. (2021). Economic growth and carbon emissions: Estimation of a panel threshold model for the transition process in China. *J. Clean. Prod.* 278, 123773. doi:10.1016/j.jclepro.2020.123773

Sun, Y. F., and Zhou, M. (2017). Decoupling and driving factors analysis between the energy carbon emissions and economic growth in China. *Rev. Econ. Manag.* 33 (06), 21–30. doi:10.13962/j.cnki.37-1486/f.2017.06.003

Tian, F., and Xu, X. F. (2012). Mechanism analysis about exploitation of oil and gas resources in China under low-carbon economy. *Future Dev.* 35 (01), 48–50+55.

Weng, G. M., Li, C. H., Pan, Y., and Li, J. P. (2021). Decoupling Effect and Influencing Factors of Carbon Emissions in China's Tourism Industry. *Geogr. Geo-Inf. Sci.* 37 (2), 114–120.

World Meteorological Organization (2020). *WMO state of the global climate 2020 (provisional report)*. Geneva: WMO.

Wu, Q., and Tu, K. (2019). Analysis on the dual constraints of energy and environment to the development of China and countermeasures. *Chin. Sci. Bull.* 64 (15), 1535–1544. doi:10.1360/n972018-01057

Wu, Y., Tam, V. W. Y., Shuai, C., Shen, L., Zhang, Y., and Liao, S. (2019). Decoupling China's economic growth from carbon emissions: Empirical studies from 30 Chinese provinces (2001–2015). *Sci. Total Environ.* 656, 576–588. doi:10.1016/j.scitotenv.2018.11.384

Xinhua Network (2020). President Xi Jinping delivered an important speech at the general debate of the 75th session of the UN General Assembly. Available at: https://www.mfa.gov.cn/ce/ceus/eng/zgyw/t1817766.htm.

Xinhua News Agency (2021). President xi jinping presided over the ninth meeting of the central finance and economics commission. *Budg. Manag. Account.* 1 (04), 4–5.

Zhang, K., Miao, M., and Zhang, L. Q. (2022). Carbon peaking and carbon neutrality goals and reflections on China's energy transition Part II——fossil energy in energy transition. *Sino-Global Energy* 27 (04), 1–7.

Zhang, Q. Y., Zhang, Y. L., and Pan, B. B. (2019). Influence factor to carbon emissions in Pakistan. *South Asian Stud. Q.* 2019 (02), 50–57+5. doi:10.13252/j.cnki.sasq.2019.02.07

Zhuang, Z. Q., and Yan, W. L. (2017). The contribution of technical innovation capability to optimize the structure of energy utilization in China: A theoretical and empirical analysis. *Nanjing J. Soc. Sci.* 2017, 24–31. doi:10.15937/j.cnki.issn1001-8263.2017.10.004

Conflict of Interest: The authors declare that the research was conducted in the absence of any commercial or financial relationships that could be construed as a potential conflict of interest.

Publisher's Note: All claims expressed in this article are solely those of the authors and do not necessarily represent those of their affiliated organizations, or those of the publisher, the editors, and the reviewers. Any product that may be evaluated in this article, or claim that may be made by its manufacturer, is not guaranteed or endorsed by the publisher.

frontiers | Frontiers in Environmental Science

TYPE Original Research
PUBLISHED 08 December 2022
DOI 10.3389/fenvs.2022.994543

Check for updates

OPEN ACCESS

EDITED BY
Usama Awan,
Inland Norway University of Applied Sciences, Norway

REVIEWED BY
Joanna Rosak-Szyrocka,
Częstochowa University of Technology, Poland
Mohamed A. Mohamed,
Minia University, Egypt

*CORRESPONDENCE
Jingying Fu,
fujy@igsnrr.ac.cn
Yitong Yin,
yyt0910@outlook.com

SPECIALTY SECTION
This article was submitted to Environmental Economics and Management, a section of the journal Frontiers in Environmental Science

RECEIVED 15 July 2022
ACCEPTED 28 November 2022
PUBLISHED 08 December 2022

CITATION
Lin G, Jiang D, Fu J and Yin Y (2022), Pathways for the carbon peak of resource-based cities under an energy-water coupling relationship: A case study of Taiyuan, Shanxi Province. *Front. Environ. Sci.* 10:994543.
doi: 10.3389/fenvs.2022.994543

Pathways for the carbon peak of resource-based cities under an energy-water coupling relationship: A case study of Taiyuan, Shanxi Province

Gang Lin[1], Dong Jiang[1,2,3], Jingying Fu[1]* and Yitong Yin[4]*

[1]Institute of Geographic Sciences and Natural Resources Research, Chinese Academy of Sciences, Beijing, China, [2]College of Resources and Environment, University of Chinese Academy of Sciences, Beijing, China, [3]Key Laboratory of Carrying Capacity Assessment for Resource and Environment, Ministry of Natural Resources, Beijing, China, [4]State Key Laboratory of Remote Sensing Science, College of Global Change and Earth System Science, Beijing Normal University, Beijing, China

The "dual carbon" goal proposes new requirements for urban development, and the contradiction between high-speed urban development and environmental problems is becoming increasingly critical. The path of green and low-carbon development urgently needs to be investigated. In this paper, a simulation system of urban carbon emission based on system dynamics is built from four perspectives of population, economy, water resources and energy, aiming at building a method system for carbon peak path that is universally applicable to resource-based cities from a systematic perspective. This paper designs five scenarios: business as unusual scenario (BAU), adjustment of industrial structure (CPA_1), adjustment of energy structure (CPA_2), reduce energy consumption per unit of GDP (CPA_3) and comprehensive management ($CPA_{comprehensive}$). Compared with the other four scenarios, the comprehensive scenario had the best coordination benefit for the coupling system, which took into account economic development, resource consumption and carbon emission reduction and could promote the realization of a carbon peak in Taiyuan city in 2029, and the comprehensive scenario will reduce CO_2 by 17.14 million tons, water consumption by 158 million m^3, energy consumption by 5.58 million tons of standard coal and economic growth by 175.21 billion yuan in 2029.

KEYWORDS

carbon peak, water-energy coupling system, system dynamics, resource-based city, Shanxi

1 Introduction

In 2014, the Fifth Assessment Report of the Intergovernmental Panel on Climate Change (IPCC) clearly pointed out that greenhouse gas emissions and other anthropogenic driving factors have been the main causes of climate warming since the mid-20th century. The continuous emission of greenhouse gases will cause further warming and lasting changes in all components of the climate system (IPCC Fifth Assessment Report, 2014). Global warming not only affects the economic and social development of all countries but also poses a threat to human survival (Li et al., 2018). Therefore, how to achieve greater economic output while continuously reducing greenhouse gas emissions is a great challenge for mankind to achieve sustainable development (Awan et al., 2020). Carbon peak and carbon neutralization are the new development strategies adopted by human society to cope with global warming (John et al., 2016). Authoritative reports issued by the International Renewable Energy Agency (IRENA) and others pointed out that to control global warming at 1.5°C, it is necessary to achieve global net zero emissions of greenhouse gases in the middle of the 21st century, that is, to achieve carbon neutrality (Marijn, et al., 2020; Corrado and Ilaria, 2021). The timing of net zero will depend on how many negative emission technologies (i.e., BECCS, DACCS, afforestation, etc.) are deployed by the end of the century, and peaking carbon emissions as early as possible could help avoid reliance on large-scale negative emissions towards the end of the century to meet the 2°C target. Presently, most developed countries in Europe and the United States have reached a carbon peak, and 130 countries and regions around the world have set a carbon neutral timetable. On 22 September 2020, at the general debate of the 75th Session of the United Nations General Assembly, China announced that it aims to achieve a peak in carbon dioxide emissions by 2030 and to achieve carbon neutrality by 2060 (Hereinafter referred to as the “dual carbon”). The 2020 Central Economic Work Conference listed “carbon peak and carbon neutral” as one of China’s eight key tasks in 2021. As a country with high energy consumption and carbon emissions, achieving a carbon peak and carbon neutrality is both a challenge and an opportunity. The process of realizing “dual carbon” will drive great transformation of China’s economy and society as well as great changes in a wide range of fields. In this context, relevant national ministries and commissions have taken the lead in formulating action plans for China to achieve the “dual carbon” goal. For example, the Global Energy Internet Development Cooperation Organization has released the Report on China’s Carbon Peak by 2030 and The Report on China’s Carbon Neutral by 2060, and the Chinese Academy of Sciences has released a roadmap for the “carbon neutral” framework. These authoritative reports point out that China needs to make concerted efforts in industrial structure (Zhu and Zhang, 2021), energy intensity (Xiu et al., 2020), energy consumption (Zhu and Shan, 2020) and other aspects to achieve the goal of “dual carbon”, simultaneously promote economic development and carbon reduction and emission reduction, and fulfill China’s commitment of carbon peak by 2030 and carbon neutral by 2060.

The concept of carbon reduction and emission reduction has promoted the development of relevant research on carbon emissions in the fields of economy (He et al., 2021; Awan and Sroufe, 2022; Abbasi and Tufail, 2021), population (Pan et al., 2021; Hussain et al., 2021), water resources (Lahlou et al., 2022), and energy (Jiu et al., 2021; Abbasi et al., 2021). At the international level, Noam Bergman explained that energy consumption is the main reason for the continuous increase in carbon emissions in the United Kingdom and believed that the development of the new energy industry can further promote the development of the low-carbon economy and reduce CO_2 emissions (Bergman and Eyre, 2011). Charles, Lin sue j investigated the *status quo* of the production structure and the basic situation of energy consumption and established a rating evaluation index system, including economic indicators, energy indicators and environmental quality indicators. They proposed adjusting and optimizing the industrial structure, changing the industrial development model, actively developing low-carbon industries, reducing high energy-intensive industries to reduce energy consumption and developing a low-carbon economy (Chang and Lin, 1999). Fahad Alsokhiry develops a typical framework of a home energy management system for Smart grids scenarios using newly limited and multi-limited planning approaches for domestic users. The simulation results advocate for the quality and high performance of the proposed model by minimizing the total cost and managing energy consumption economically (Alsokhiry et al., 2022). Loiy Al-Ghussain aims to investigate, for the first time, the use of Jordan’s previously planned hybrid renewable energy system in relation to the growing energy demand potential of electric vehicles (Al-Ghussain et al., 2022). At the domestic level, Zhao et al. studied carbon emissions from water system from the urban level through water-energy-carbon coupling relationship, and the results showed that water intake, water use and water transport would lead to increased energy consumption and carbon emissions from water system (Zhao et al., 2021). Li et al. studied the link between urban energy carbon emissions and water resources based on Leap model, and believed that energy consumption structure and technological optimization were the key to realizing low carbon and water saving (Zeng, 2019). Hong et al. (2022) proposed a distributionally robust dispatch model for the integrated rural energy system with broiler houses to improve the economic benefits. To sum up the above studies, domestic and foreign scholars have conducted in-depth explorations of carbon emission reduction paths from one or more dimensions (such as energy or energy-economic, economy-energy- water coupled) and have achieved good carbon reduction effects. However, there are few researches on carbon peak

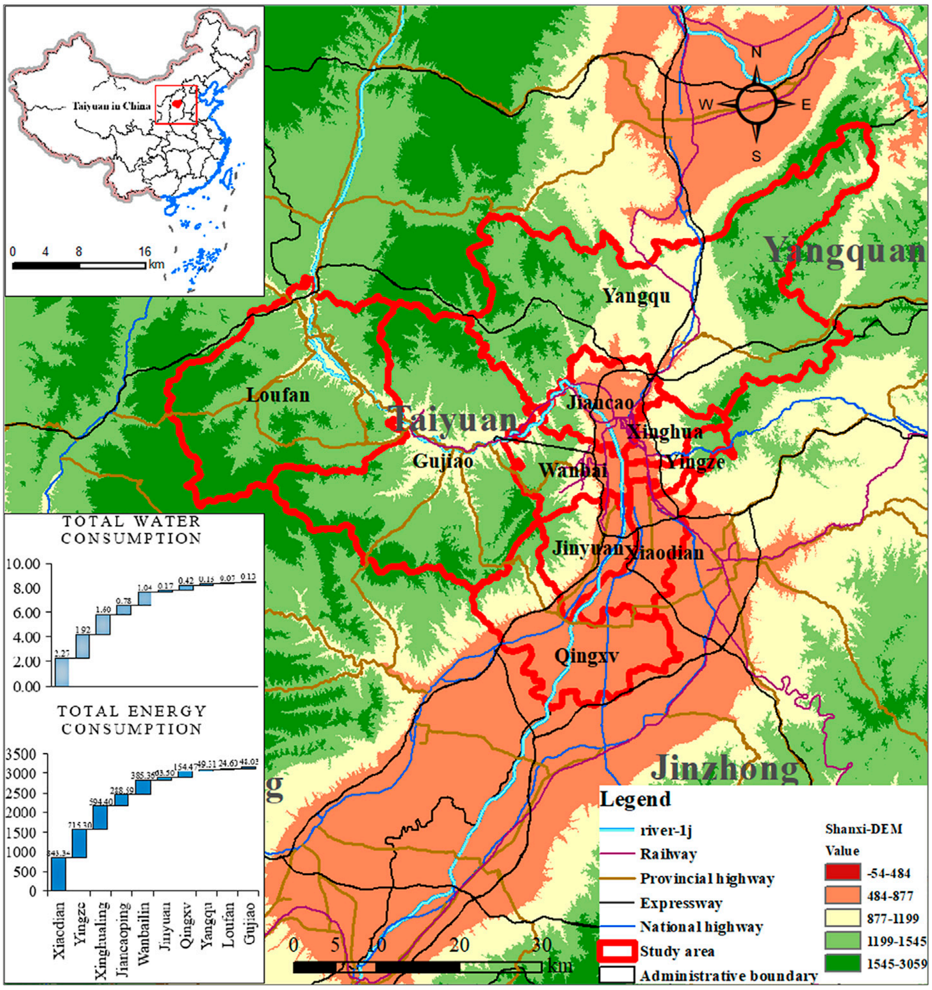

FIGURE 1
Location of study region in China (The unit of total water consumption is 100 million cubic meters, The unit of total energy consumption is 10,000 tons of standard coal, the unit of DEM base map is meter, and the unit of scale is kilometer).

pathways for resource-based cities and they lack universality, which are not enough to support the current "dual carbon" action. In addition, while top-down integrated assessment models have provided vital insights into identifying decarbonization pathways at the global and continental levels, their coarse spatial and temporal resolution and lack of detail means that complementary bottom-up analysis is needed to identify optimal strategies at the local level. Therefore, based on the energy-water coupling relationship, this paper analyzes the carbon emission driving-feedback mechanism of resource-based cities with the method of multi-system coupling, providing scientific support for the realization path of carbon peak, and analyzing the carbon peak path of resource-based cities. Therefore, this article selects the System Dynamic (SD) model (Li et al., 2021; Alam et al., 2022; Xiao et al., 2022) to study the coupling of carbon emission systems, which can not only integrate multiple subsystems but also simulate the carbon peak path and dynamic change under the comprehensive effect of future economic development, technological progress, and resource and energy consumption and has broad requirements on data availability and a long-term adjustable simulation time period. Integrates multiple subsystems of economy, population, water resources and energy; selects 116 built-in variables, and builds a connection bridge of a four-dimensional coupling system by using industrial output value, urban and rural population, water-related energy consumption and energy-related water consumption, using a causal feedback loop and the built-in function of the SD model to refine the logical and quantitative relationships of variables. Based on the carbon peak background (Mei, 2021), a comprehensive carbon emission historical data fitting, carbon peak path simulation and future carbon emission prediction are carried out. In particular, it can integrate multiple subsystems from a macro perspective, analyze and study the driving-feedback mechanism of each subsystem and the coupling system, so as to identify the key action paths and influencing factors. It is helpful to explore the coordinated development (Zhi, 2019) mode of economy, population, resources and energy (Li et al., 2019) and carbon emissions, to boost cities, provinces and the whole country to achieve the peak goal of carbon emissions as soon as possible, to provide a reference for China's low-carbon development direction after the peak year, and to help achieve China's "dual carbon" goal.

2 Materials and methods

2.1 Study area

Taiyuan (Figure 1) is located in the middle of Shanxi Province, with geographic coordinates of 111°30′E-113°09′E, 37°27′N-38°25′N, and with high terrain in the north and low terrain in the south, in the shape of a dustpan. The bat-shaped region has jurisdiction over six municipal districts, three counties and one county-level city. By 2020, the city had a permanent population of 5304100, covering an area of 6,988 km^2. Taiyuan is critically lacking water resources (Wu et al., 2021). The average total water resources of the city for many years comprise 660 million cubic meters, and the *per capita* water resources comprise 202 cubic meters, which is only 38.5% of the *per capita* water resources of Shanxi Province, 11.9% of the national *per capita* water resources and 1.7% of the global *per capita* water resources. Groundwater is the main water supply of Taiyuan, accounting for more than 75% of the total water supply, and the city's average annual overexploitation of groundwater resources is 112 million cubic meters. Atmospheric precipitation is the main supply source of Taiyuan, but precipitation and runoff change greatly and are unevenly distributed. In the continuous drought and years of the dry season, the shortage of water resources is becoming increasingly prominent. The shortage of water resources and the advancement of urbanization cause the agriculture of Taiyuan continue to develop in a low state. The *per capita* cultivated land of Taiyuan is 0.67 mu, which is the lowest among the 11 cities in Shanxi Province and lower than the minimum warning line of 0.795 mu set by the United Nations Food and Agriculture Organization. Shanxi is known as the "coal Sea" because of its abundant coal. Taiyuan is located in the middle of the "coal Sea", and the coal reserves in Taiyuan are referred to as "Taiyuan system coal" in geological terms, ranking seventh in the province. The coal resources in this area are not only abundant in quantity but also complete in variety.

As the only resource-based provincial capital city in China, Taiyuan is not only the political, economic, cultural and international exchange center of Shanxi Province but also one of the important energy and heavy industry bases in China, which is a typical representative among many resource-based cities in China. Presently, with the development of industry, reconstruction of villages inside cities, continuous expansion of the scope of cities and towns, and increasing urban population, the consumption of energy and water resources are also accumulating, which has caused a series of environmental problems (i.e., carbon emissions of energy consumption, carbon emission of domestic sewage and carbon emission of production wastewater, etc.) that directly or indirectly affect residents' lives and economic development. How to reduce energy and resource consumption while ensuring economic growth under the background of the carbon peak and achieving a balance between the growth of energy consumption and the reduction of carbon emissions are the challenges facing the future development of Taiyuan. This paper takes Taiyuan city as an example to put forward the path suitable for all resource-based cities in China to achieve carbon peak.

2.2 Research framework

Research on the carbon peak path with the energy-water coupling relationship is carried out through the following steps:

Step 1. Based on the statistical Yearbook of Shanxi Province, Taiyuan Water Resources Bulletin and Taiyuan Environmental Status Bulletin and using the IPCC carbon emission factor as the carbon emission coefficient of water resources and energy-related variables, a dataset of 116 variables from 2005 to 2021 was established.

Step 2. Integrate the four subsystems of economy, population, water resources and energy; explore the logical and functional relationships among variables; and establish an SD model to analyze the current situation of economic growth, resource consumption and carbon emissions in Taiyuan.

Step 3. With the carbon peak as the research objective, based on the water resources and energy consumption of Taiyuan from 2005 to 2021, the related parameters of the coupling system are adjusted to simulate the carbon peak path.

2.3 Data collection and analysis

The carbon emission coefficients of various energy sources refer to the General Principles for Calculation of Comprehensive Energy Consumption (GB/T 2589-2008) (http://tjsjnxh.com/uploads/) and the Guidelines for Compilation of Provincial Greenhouse Gas Inventories (http://www.cbcsd.org.cn/sjk/nengyuan/standard/home/). By sorting out the carbon emission coefficients of relevant variables and based on the principle of unit consistency, it is transformed into the carbon

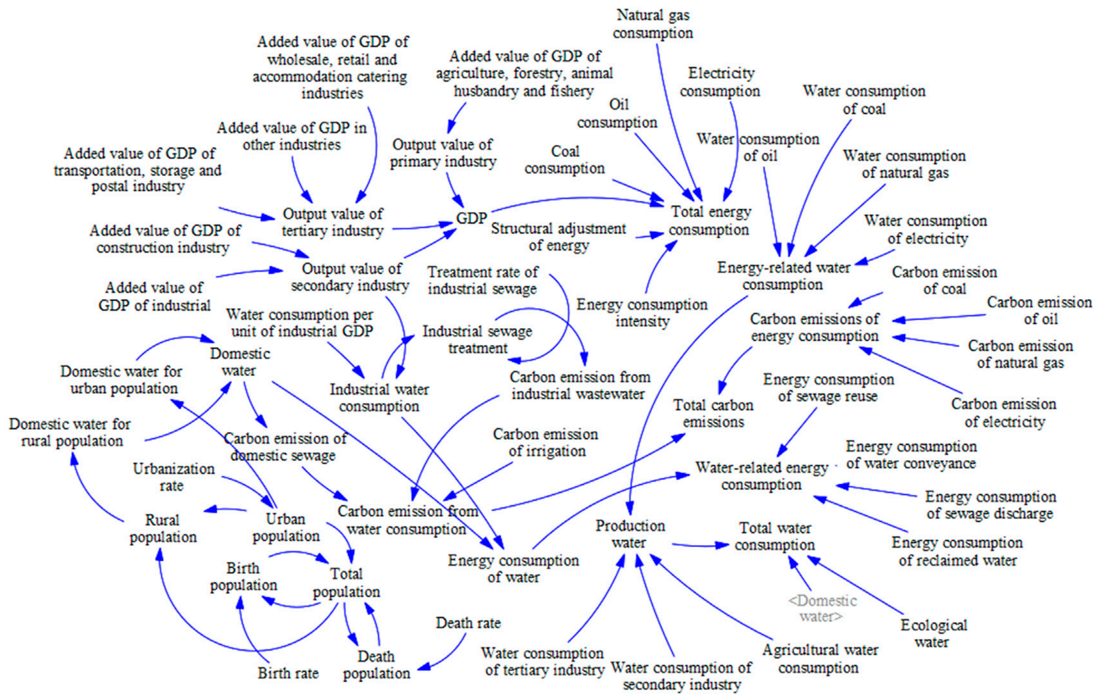

FIGURE 2
Causal loop diagram of the carbon emissions in Taiyuan.

emission factor consistent with the variable unit in the model to established a carbon emission dataset. The dataset of water resources and energy consumption in Taiyuan established according to the Taiyuan Water Resources Bulletin (http://swj.taiyuan.gov.cn/) and Taiyuan Environmental Status Bulletin (http://hbj.taiyuan.gov.cn/hjzl/tjnbgb/index.shtml) includes the water consumption and energy consumption of all links of the social water cycle, all industries and all kinds of energy. The dataset contains nearly 60 historical statistics from 2005 to 2021, almost all from the values reported in the official Yearbook. In this study, 900 exact statistical data of four subsystems in the dataset are employed in a coupling system analysis to ensure the reliability of the data prediction and path simulation.

2.4 Establishment of the System Dynamic model of carbon emissions

2.4.1 Construction of causal loop diagram

System dynamics can reflect the interaction among the elements in a system. Based on the close dependence between the system behavior and the internal mechanism, it is obtained through the process of establishing and operating the mathematical model, and gradually discover the cause and effect relationship that produces the change form. Modeling with computer software Vensim, the thinking process and research on complex problems can be displayed, which is suitable for analyzing and solving a series of non-linear, complex system problems (Yin et al., 2021). This paper selects the geospatial boundary of Taiyuan city, Shanxi Province, as the research system boundary. Carbon emissions comprise multidimensional, comprehensive, environmental effect research involving population, economy, water resources, and energy. Therefore, in this paper, the construction of the coupling system is divided into two first-level subsystems: water resource carbon emissions and energy carbon emissions. The water resource carbon emissions are divided into two second-level subsystems: living and production. The energy carbon emissions are divided into carbon emissions generated by the consumption of coal, oil, natural gas and electric power. The industrial output value, urban and rural population, water-related energy consumption and energy-related water consumption are considered as the connection bridges of the four-dimensional coupling system. According to the data availability and statistical results of past years, the causal loop diagram of energy-water carbon emissions in Taiyuan is established (Figure 2).

2.4.2 Establishment of variable equations

A coupled system is not a simple sum of independent subsystems. Building coupled systems using SD models

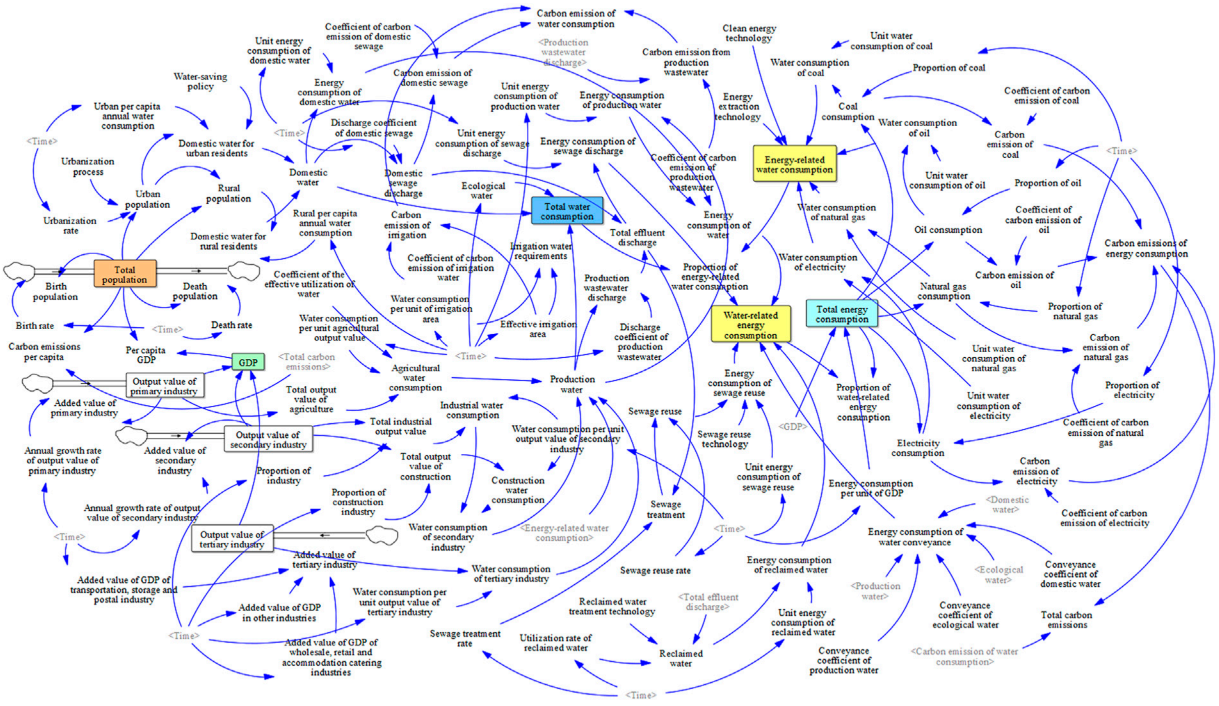

FIGURE 3
System dynamics model of carbon emission in Taiyuan under energy-water coupling relationship.

requires solving the following two problems: first, two independent subsystems must become an integrated system through one or more bridges or mediums (Yin et al., 2021). In this study, water resource carbon emissions and energy carbon emissions are related through total water consumption, total energy consumption, water-related energy consumption and energy-related water consumption. Second, the coupling system may produce overlapping effects, resulting in total carbon emissions greater than the actual value (Yin et al., 2021). To eliminate the overlapping effect, this paper divides total energy consumption into water-related energy consumption introduced by the social water cycle and other types of energy consumption other than water-related energy consumption. Total water consumption is divided into energy-related water consumption and other types of water consumption other than energy-related water consumption of each industry. The core variables and equations involved in the model are listed in Supplementary Table S1.

2.4.3 Construction of the System Dynamic model

The previously established function relationship is assigned to each transfer-feedback loop to establish a complete SD model of the resource-based, city carbon emission system with the energy-water coupling relationship (Figure 3).

2.4.4 Model validity check

Visual inspection. Through further analysis of the collected data, the unit consistency and the rationality of the structure are tested. In the process of building the model, a large number of documents are referenced, and the model structure is consistent with the structure of the actual system.

Historical test. The degree of fitting of the system behavior with historical data are determined. Selecting 2005 as the base year, the data from 2005 to 2020 are utilized to fit the variable equations. The total population, urban population and rural population are selected in the population subsystem; the total output value of the primary industry and the total output value of the secondary industry are selected in the economic subsystem; the domestic water, production water and total water consumption are selected in the water resources subsystem; and the total energy consumption is selected in the energy subsystem. The simulation errors of the model were verified by comparing the relative errors of the historical data and the simulation results. According to the following formula (Yin et al., 2021), the relative errors of the simulated values of nine variables from 2005 to 2020 were calculated. As shown in Supplementary Table S2, among the 9 variables, the relative errors of production water in 2018 are large (3.32%); the relative errors of total water consumption in 2013 and 2018 are 1.66% and 1.9%; and the relative errors in

TABLE 1 Variable selection and parameter setting for sensitivity analysis.

Variables for sensitivity analysis	Simulation value	The range of observations	Simulation times	Random seed	Target observed value
Urbanization process	0.7	0.5–0.9	200	1,2,3,4	Urban population
Water-saving policy	0.5	0.3–0.7	200	1,2,3,4	Domestic water for urban residents
Energy extraction technology	1	0.9–1.1	200	1,2,3,4	Energy-related water consumption
Clean energy technology	0.7	0.5–0.9	200	1,2,3,4	Energy-related water consumption

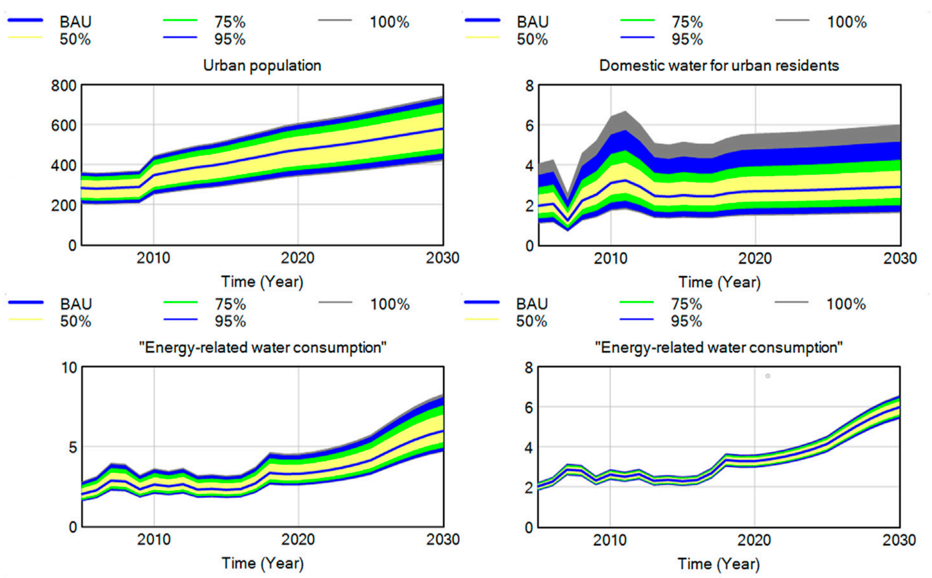

FIGURE 4
Sensitivity Response of urban population, domestic water for urban residents and energy-related water consumption.

other years are approximately 0.7%, indicating a good simulation effect. The simulation error of the economic and energy subsystems was within 0.1% in each year, and this simulation effect was the best. The relative error of the population subsystem was approximately 0.3% in each year. The values of each variable in 2021 are predicted by using the fitting data from 2005 to 2020, and the predicted results are compared with the actual values in 2021 to verify the prediction error of the model. As shown in Supplementary Table S2, the relative errors of the predicted data are approximately 2%, indicating that the model has high accuracy.

$$\delta = \frac{\varepsilon}{R} \times 100\%$$

$$\varepsilon = R - M$$

In the formula, δ is the relative error, ε is the absolute error, M is the simulated value, and R is the real value.

2.4.5 Sensitivity analysis

The key to testing the stability of the model is to study the sensitivity of the model behavior to the variation in the parameter values within a reasonable range and to observe whether the model behavior is changed due to the slight variation in some parameters. In this study, a Monte Carlo, random, uniform distribution is applied to analyze the sensitivity of the main constant numerical parameters (only one parameter value is adjusted at a time). The noise seed is applied to specify the starting value position of the long sequence of random numbers, and different noise seeds need to be established. To avoid using the same simulation data every time, 1,234 is usually employed

(Table 1). Figure 4 shows the sensitivity analysis diagram of SD model output.

According to the sensitivity response of each variable (Figure 4), the impacts of the urbanization process on population of urban residents, of the water-saving policy on urban residents' domestic water consumption, of the energy extraction technology and clean energy technology on energy-related water consumption cause the target observation value to fluctuate with the basic simulation data. Compared with clean energy technology, energy extraction technology has a greater impact on energy-related water consumption, but in general, the floating range is small, the numerical sensitivity is low, and the model is stable.

2.5 Scenario settings

Scenario analysis, as an important means of implementing management and assisting decision-making, has been widely applied in resources (Duinker et al., 2007), ecological environment and regional development (Zhang et al., 2019). According to the current situation of resource utilization, carbon emissions and the principle of coordinated development of Taiyuan city, this paper proposes two scenarios, namely, the "business as usual (BAU)" scenario and "carbon peak action (CPA)" scenario. The pressure Taiyuan faces to achieve a carbon peak and carbon neutrality is mainly derived from three aspects: first, the development is unbalanced, insufficient and uncoordinated; economic growth occurs in the period of high-speed and high-quality development; the energy demand is constantly increasing; and the carbon emissions are still in the rising stage. Second, the proportion of coal consumption is too large, and third, energy consumption per unit of Gross domestic product (GDP) is high. These challenges need to be addressed from multiple dimensions, such as transforming the economic development model, energy supply and consumption patterns. Based on the Action Plan for Carbon Peak before 2030 (http://www.gov.cn/zhengce/) issued by The State Council (Editorial Department, 2021) and the relevant policies (http://fgw.taiyuan.gov.cn/doc/2021/05/21/1089043.shtml) and plans for low-carbon energy development (http://fgw.taiyuan.gov.cn/doc/2021/05/24/1089523.shtml) and industrial structure transformation in Taiyuan (http://www.shanxi.gov.cn/; http://taiyuan.gov.cn/), this paper selects the BAU scenario to simulate the normal evolution of water resources, energy and carbon emissions driven by natural, economic and social factors, while the CPA scenario starts with industrial structure, energy structure, energy consumption intensity and comprehensive control to predict carbon emissions (The scenario setting here does not mean that the economy is decoupled from the energy, but only represents the comprehensive impact on the economy-water-energy-carbon coupling model when the force is separately applied to the energy, economy or some other subsystem). The specific control directions and measures are shown in Table 2.

3 Results and analysis

3.1 Analysis of carbon emission characteristics in taiyuan city

Figure 5 analyzes the changes in the economy, water resources, energy and carbon emissions from 2005 to 2021 from the perspective of industry. In general, from 2005 to 2021, the GDP, water consumption, energy consumption and carbon emission increased by 346.68 billion yuan, 315.78 million cubic meters, 7.98 million tons of standard coal and 23.34 million tons of CO_2 respectively, the GDP of all industries in Taiyuan continued to grow, and the consumption of water resources and energy continued to rise, which caused an increase in carbon emissions of water resources and energy. However, the simultaneous development of economic growth and reduction in resource consumption and carbon emissions has not yet been realized. From 2005 to 2021, the added value of agriculture in Taiyuan reached 1.43 billion yuan, which has reached a cooperation among economic growth and CO_2 emissions, water resources and energy consumption reduction, indicating that a series of major measures taken by the agricultural sector in Taiyuan in recent years (agricultural mechanization, promoting the modernization of agricultural machinery, land scale, accelerating the adjustment of industrial structure, etc.) have achieved good results. It is mainly attributed to the improvement of effective irrigation rate and the increase of water-saving irrigation area due to the optimization of agricultural technology. While the total output value of the industrial sector has increased, resources, energy and carbon emissions have continued to rise. Taiyuan's industry is the main component of Shanxi's industry. Taiyuan's industrial structure is dominated by heavy industry and energy industry, while coal consumption accounted for more than 80% of the total primary energy consumption. The continuous growth of energy consumption will inevitably cause an increase in carbon emissions. Taiyuan should actively optimize and upgrade its industrial structure, which will make low-carbon development as the top priority of industrial transformation in Taiyuan. In addition to the industrial sector, the CO_2 emissions and resource consumption of the construction industry, wholesale and retail industry and accommodation and catering industry continue to increase with economic growth. Among them, carbon emission reduction in the construction industry focuses on controlling the use of building materials, saving energy and reducing the energy consumption of existing buildings. With continuous advancement in the urbanization process, the increase in

TABLE 2 Direction and measures of situation setting.

Scene settings	Direction	Measures
BAU	natural evolution	—
CPA_1	adjustment of industrial structures	The proportion of tertiary industry increased by 10%
CPA_2	adjustment of energy structure	By 2025, the proportion of non-fossil fuels increased by 5% than that in 2020, and by 2030, the proportion of non-fossil fuels increased by 10% than that in 2020
CPA_3	reduce energy consumption per unit of GDP	By 2025, energy consumption per unit of GDP will be 13.5% lower than that in 2020, and by 2030, energy consumption per unit of GDP will be 25% lower than that in 2020
$CPA_{comprehensive}$	aggregate adjustment	The above measures will be implemented together

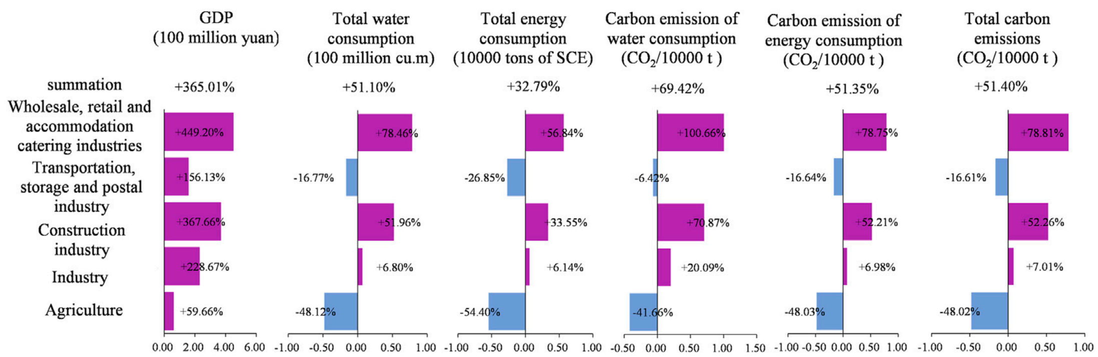

FIGURE 5
GDP, water resources, energy and carbon emissions of various industries in Taiyuan from 2005 to 2021.

urban populations will further contribute to the expansion of construction land and an increase in carbon emissions in the construction industry. The economic growth, CO_2 emissions and resource consumption of the wholesale and retail industry and accommodation and catering industry experienced the greatest increase, indicating that the tertiary industry in Taiyuan has developed rapidly in recent years but that the development process should not proceed at the cost of doubling resource consumption and carbon emissions. The carbon emission reduction in the transportation, storage, and postal industries is mainly derived from the elimination of old cars, improvement in emission standards and other terminal governance measures. While the GDP of the transportation, storage, and postal industries in Taiyuan increased by 11.77 billion yuan, water resources and energy consumption of the industry reduced by 16.77% and 26.85%, respectively, and carbon emissions reduced by 18.66%, indicating that Taiyuan has achieved good results in reducing carbon emissions by vigorously developing new energy vehicles while promoting the implementation of terminal governance. In general, the potential of carbon emission reduction of Taiyuan's energy, industrial and transportation structure adjustment needs to be further released. In the next step, low-carbon emission reduction measures should be actively promoted to realize the synergistic benefits of economic growth, resource consumption reduction and carbon emission reduction.

3.2 Scenario analysis of carbon peak in taiyuan city

3.2.1 Simulation results for different industries

Economic growth, resource consumption and carbon emissions show high heterogeneity within different industries (Figure 6). In the BAU scenario, agriculture contributes the least to economic growth and consumes the least amount of water resources, energy and carbon emissions. Under the scenario of adjusting the industrial structure, of energy structure and of reducing energy consumption per unit of GDP, this phenomenon still remains unchanged. As the traditional economic pillar industry of Taiyuan, the industrial sector is still a strong guarantee to drive economic growth. However, while promoting the obvious rise of GDP, water resources, energy consumption and carbon emissions are the largest. In the scenario of industrial structure adjustment, the

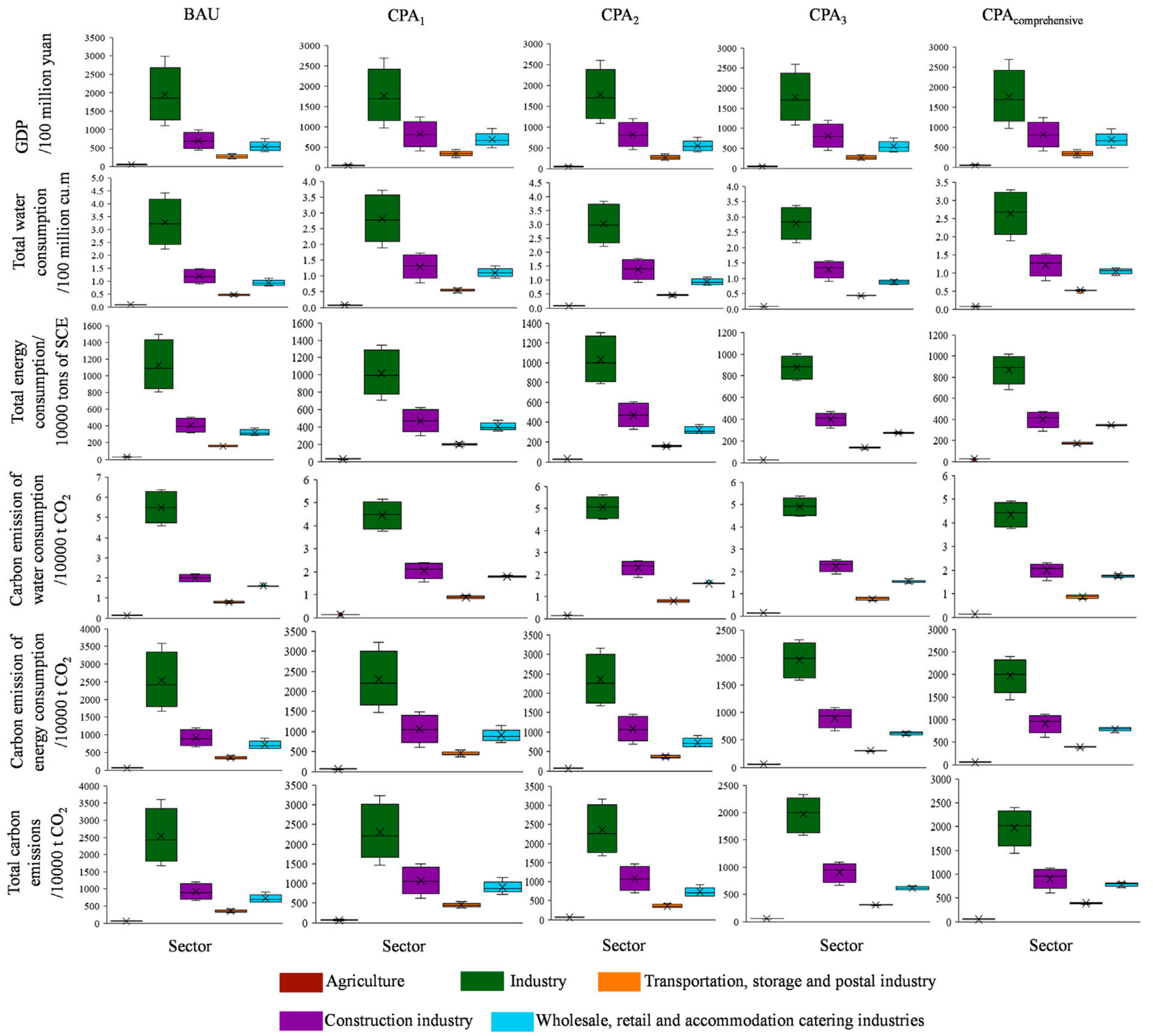

FIGURE 6
Comparison of the simulation results for different industries from 2022 to 2030 (The distance between the median and the upper (lower) quartile of the box chart is relatively narrow, indicating that the data within this distance is relatively concentrated. The upper (lower) edge of the box chart is relatively long, indicating that the data covers a wide range on the *X* axis. The range outside the upper and lower edges indicates abnormal values. Here, take GDP as an example. Specifically, the lower edge of the box in the figure represents the 25th percentile of all GDP values arranged from small to large; The top edge of the box in the figure represents the 75th percentile of all GDP values arranged from small to large; The middle horizontal line of the box represents the median of all GDP values, and the upper and lower exposed parts represent the minimum and maximum of all GDP values, so as to visually compare the average, minimum, maximum and abnormal GDP levels of various industries).

proportion of the tertiary industry increases, and the proportion of the primary industry and secondary industry decrease accordingly, resulting in the reduction of water and energy consumption and carbon emissions in the industrial sector. Compared with the scenario of the adjustment of industrial structure and of the adjustment of energy structure, the scenario of the reduction of energy consumption per unit of GDP has the greatest impact on all aspects of the industrial sector and the least impact on the agricultural sector, while the transportation, storage, and postal industries, wholesale and retail industry, and accommodation and catering industry have significantly reduced water resources, energy consumption and carbon emissions when the GDP change rate is very small. This finding shows that reducing energy consumption per unit of GDP has achieved a good carbon reduction effect while maintaining economic output. In the comprehensive scenario, the tertiary industry is increased by 10%, the proportion of non-fossil fuels is

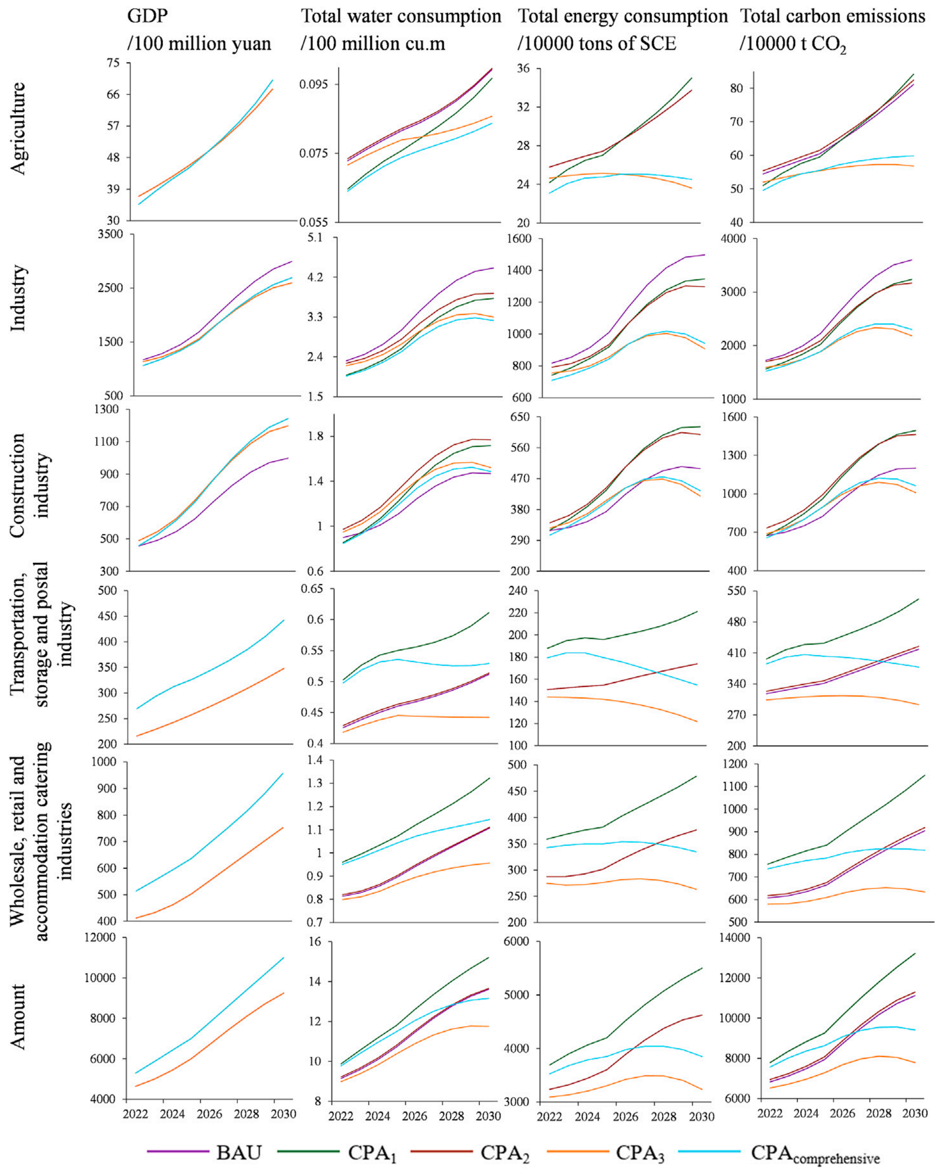

FIGURE 7
Comparison of the simulation results in different scenarios from 2022 to 2030.

increased by 10%, and the energy consumption per unit GDP is reduced by 25%. It can be seen that the economy, resource consumption and carbon emissions of the agricultural sector remain basically unchanged. When the GDP of the industrial and construction sectors decreases, the decrease in energy is greater than that in water resources, and carbon emissions are reduced simultaneously. The GDP of the transportation, storage, and postal industries, wholesale and retail industry, and accommodation and catering industry increased significantly, which also caused a significant increase in water consumption, energy consumption and carbon emissions in these two industries.

3.2.2 Simulation results in different scenarios

With the adjustment of industrial structure, Taiyuan cannot achieve a carbon peak before 2030 (Figure 7). Compared with the BAU scenario, the annual average change rates of GDP for the agriculture and industry during the simulated period are −1.53% and −9.36%, respectively, and the annual average change rates for the construction industry, transportation, storage, and postal industries, wholesale and retail industry, accommodation and catering industry are 13.61%, 25.41%, and 25.41%, respectively. The annual average change rate of GDP of the whole industry increased by 15.84%, indicating that increasing the proportion of tertiary industry can promote sustained and rapid economic growth and obtain a good economic output effect. The consumption of water resources for agriculture and industry decreases relatively in the simulation period. However, due to the development of agricultural modernization, the efficiency of using agricultural machinery is improved, and the consumption of electricity increases, resulting in an increase in agricultural energy consumption and carbon emissions relative to the BAU scenario since 2027. The amount of industrial carbon emissions also decreases with a reduction in resource consumption. The construction industry, transportation, storage, and postal industries, wholesale and retail industry, and accommodation and catering industry are similar with regard to the changes in water resources, energy consumption and carbon emissions, which all show "S-shaped" changes higher than BAU. None of the industries achieve a single industry carbon peak, and the annual average change rates of water resources, energy consumption and carbon emission in the whole industry have increased by 9.55%, 15.84%, and 15.81%, respectively.

With the adjustment of energy structure, Taiyuan cannot achieve a carbon peak before 2030 (Figure 7). Compared with the BAU scenario, with the exception that the annual average change rate of industrial GDP decreased by 7.79% and that of the construction GDP increased by 15.16%, other industries remained basically unchanged, and the annual average change rate of the GDP of the whole industry was almost zero, indicating that the adjustment of energy structure had an extremely small impact on GDP. The decrease in the proportion of coal, oil, natural gas and other fossil fuels generated a 7.79% decrease in the average annual change rate of energy consumption in the industrial sector, a 15.16% increase in the average annual change rate of energy consumption in the construction industry, a 1.39% increase in the average annual change rate in other industries, and a 1.9% increase in the average annual change rate in the whole industry. This finding shows that the alternative use of non-fossil fuels has a great impact on the construction industry, while the industrial sector is still dominated by fossil fuel consumption. Only by changing the energy consumption structure of the industrial sector as soon as possible can energy carbon emissions be effectively reduced. With a slight increase in total energy consumption, production water consumption is indirectly affected by energy-related water consumption, resulting in the annual change rate of water resource consumption of the whole industry increased by 0.64%, indicating that energy-related water consumption occupies a large share of the total water consumption. The annual average change rate of carbon emissions in the whole industry increased by 1.67%.

By reducing the energy intensity, Taiyuan can achieve a carbon peak in 2029 (Figure 7). The annual average change rate of GDP of all industries is basically the same as that of the adjusting energy structure. With the GDP growth of the construction industry, the water consumption of the construction industry increases. Regarding the changes in water consumption among all industries, except for the annual average change rate of the construction industry, which increases by 8.46%, other industries have decreased compared with the BAU scenario. The water consumption of the whole industry will reach a peak in 2029 with the water consumption of 148 million m^3 lower than the BAU scenario. Compared with the BAU scenario, the energy consumption of all industries is significantly reduced, and the energy consumption of the agriculture industry, construction industry, wholesale and retail industry, and accommodation and catering industry will peak in 2025, 2028, 2028, and 2027, respectively. The energy consumption of the transportation, storage and postal industries has exhibited a downward trend during the simulation period. The energy consumption of the whole industry reached its peak two years earlier than that of water consumption and achieved a carbon peak in 2028 with 20.69 million tons of CO_2 lower than the BAU scenario.

Under the comprehensive scenario, Taiyuan can achieve a carbon peak in 2029 (Figure 7). Compared with only adjusting the industrial structure, the annual average change rate of GDP of all industries is basically unchanged, and the annual average change rate of water consumption decreases by 9.54%. Compared with only reducing energy consumption per unit of GDP, there was no peak of water consumption in the simulation period. Compared with only adjusting the energy structure, the annual cumulative change in energy consumption saves 3.13 tons of standard coal and achieves the peak of energy in 2027. Compared with the BAU scenario, carbon emissions will decrease by 17.14 million tons of CO_2 and peak in 2029. In general, compared with other scenarios, economic output, resource and energy consumption and carbon emissions under the comprehensive scenario can achieve a relative balance (Figure 8), which can provide a valuable reference for Taiyuan to maintain coordinated and sustainable economic development and to explore the path of the carbon peak.

4 Discussion

China's "dual carbon" goal is to reach the carbon peak before 2030 and to achieve carbon neutrality before 2060, which will introduce a boom in China's urban agglomerations and economic belts to adjust the industrial structure and energy structure and to reduce carbon emissions. As a typical resource-based city in China, Taiyuan is facing unprecedented challenges, such as reforming its traditional energy consumption structure and upgrading its energy consumption system in a short time. As the forefront of low-carbon energy transformation on the Chinese mainland (Zhao et al., 2022), Taiyuan promised in its Energy Low-Carbon Development Forum that it would focus on promoting technological innovation, industrial innovation and business model innovation with green and low-carbon orientation; constantly improve the construction of scientific and technological innovation platform systems;

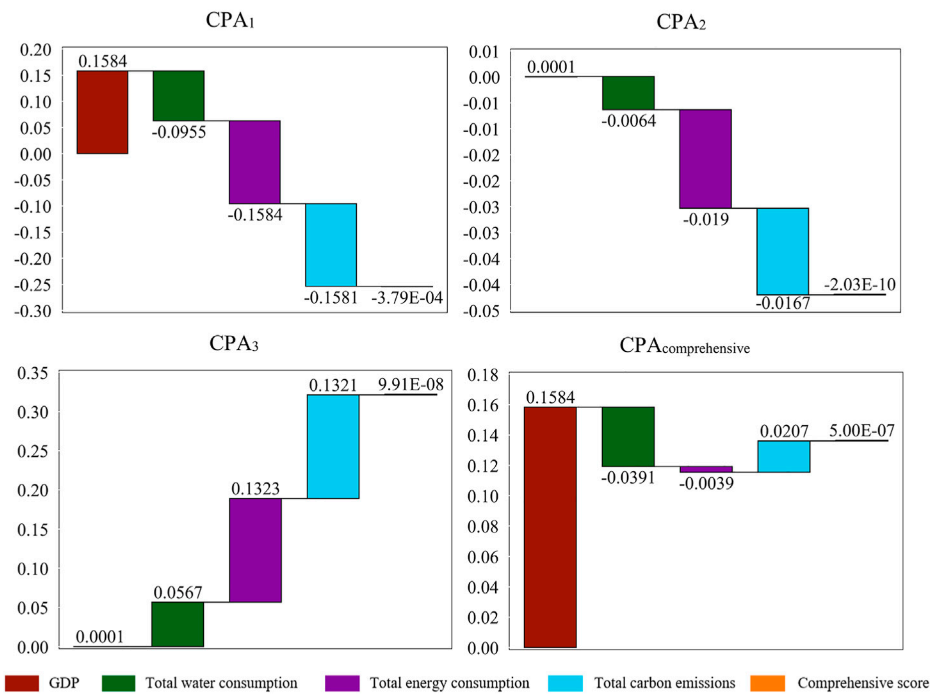

FIGURE 8
Annual average change rate and comprehensive score under different scenarios (Waterfall diagram adopts the combination of absolute value and relative value, which can not only reflect the amount of data, but also intuitively reflect the change process of data increase or decrease. The annual average change rate represents the increase or decrease rate of GDP, energy consumption, water consumption and carbon emission under different scenarios from 2022 to 2030. It not only shows an upward (downward) trend, but also indicates the amount of increase (decrease). The higher the comprehensive score is, the more coordinated of the economic development, resource consumption reduction and carbon emission of the city is).

strengthen research on cutting-edge, low-carbon technologies; promote and apply pollution and carbon reduction technologies; evaluate green and low-carbon technologies; adhere to improving the market economy system; fully utilize the role of the market in the allocation of green resources (Raza Abbasi et al., 2021); attach equal importance to economic development and environmental protection; and effectively promote the energy technology revolution to drive industrial upgrading (Ying et al., 2021). An appropriate energy development (Zhang et al., 2021) strategy is the key to accelerating the decarbonization (Shamsuzzaman et al. 2021) of Taiyuan's energy system in the next few years, which will help improve the overall carbon reduction level of Taiyuan and promote the smooth realization of the carbon peak goal of Taiyuan.

Coupling system can more comprehensively consider the influence of various variables on carbon emissions. Single-dimension and single-constraint conditions cannot fully consider the complex interaction and conflict mechanism among variables, which will increase the difficulty of achieving a carbon peak. It is necessary to integrate carbon emissions, economic growth and resource consumption into a unified framework, and the synergies among them and their relevance to socioeconomic and natural resource systems need to be fully considered through the development of coupled system models. The dynamic mechanism of carbon emission reduction is derived from the material flow and information flow of the internal structure and main variables of the coupling system. Among them, population, economy, water resources and energy are the key components. Water and energy carry resources through material flow. The CPA aims to achieve peak carbon emissions by 2030 through policy implementation across the subsystems of the system. In this process, the goal is to maintain the sustainability of the coupled system through a series of regulatory policies for each subsystem and to achieve the common interests of sustained economic growth and reduced consumption of resources and energy while reducing carbon emissions.

Shifting from fossil energy to renewable energy (Danish and Ulucak, 2021; Abbasi et al., 2021) is the most recognized strategy in energy system transformation. Taiyuan has unique geographical and natural conditions. Developing the clean utilization of fossil energy and improving the clean conversion efficiency of fossil energy can greatly reduce the energy carbon emissions of Taiyuan. This process needs an orderly withdrawal of traditional coal-fired power plants (Tramošljika et al., 2021) from the market with increased investment in energy infrastructure to expand the share of non-fossil energy in the market. In the long run, clean energy is likely to have higher total economic returns than fossil fuels (Hao et al., 2019). Therefore, Taiyuan should identify effective and economical ways to apply clean energy and renewable energy and fully utilize its advantages in service, technology, market resource allocation and the labor force. Presently, the total energy consumption per unit of GDP is still 40.98% higher than the national average energy consumption per unit of GDP. With the promotion and upgrading of energy-saving technologies and energy regulatory policies, Taiyuan's energy intensity is expected to decrease continuously in the future. In addition to reducing energy intensity, energy security (Sinha et al., 2022) should also be included in Taiyuan's energy system transformation. Taiyuan needs to establish a multilevel and all-around energy interconnection system between various industries and departments, and to guide the reduction of energy carbon emissions by improving the competitiveness of clean energy.

We encourage low-carbon optimization design of urban water system for energy conservation and carbon reduction. Based on the perspective of "water-energy" correlation and the goal of carbon peak, the energy saving transformation of water system should be strengthened to realize low carbon operation of water system. Focus on improving water-energy utilization efficiency in agriculture, industry and daily life. Strengthen the comprehensive management of resources and the collaborative emission reduction of different departments and industries, build an information platform for water-energy collaborative optimization and management, realize the real-time monitoring and intelligent management of the whole process of the water system, and further improve the incentive mechanism for water conservation and energy conservation from the aspects of policy orientation, regulatory constraints and economic means, so as to promote energy conservation and carbon emission reduction in the process of water consumption (Zhao et al., 2021).

Zhang et al. selected the SD model to study the green and low-carbon paths of Beijing-Tianjin-Hebei urban agglomeration, which is consistent with the conclusions of this paper: a comprehensive scenario can better promote the coordinated development of city's economy, resources and carbon emissions (Jing, et al., 2021). Yang et al. conducted a study on "near zero carbon emissions" in Taiyuan high-tech industry park by using the scenario analysis method, among them, low-carbon scenario optimization can reduce the carbon emission intensity of high-tech industrial parks in Taiyuan, which is consistent with the simulation trend of CPA_3 set in this paper (Jun et al., 2017). However, compared with existing studies, the innovation of this paper lies in, the fact that, with the help of the advantages of the SD model in the scenario simulations and macro driver performance, the transfer-feedback mechanism of the water–energy–carbon coupling system was obtained, and the two-way inference of "cause-effect" and of "effect-cause" was realized.

However, the SD method still has some limitations. First, SD cannot consider the spatial attributes of a region or a city; that is, it is impossible to analyze the spatial characteristics of a city's economy, population, water resources, energy, etc. It can only export the prediction results of the SD model and then carry out spatiotemporal analysis with the help of ARCGIS. Second, the lack of coupling of the physical mechanisms, such as crop growth and rainfall, can only be derived from the operational results of the SD and then analyzed using biophysical models. For the shortcomings of the above two points, in the next step, we hope to use the coupled spatial allocation model (He et al., 2017; Zhang et al., 2017; Liu et al., 2020; Song et al., 2020) and SD model to realize the combination of quantity structure and space allocation. For the coupling of the physical mechanism, we hope to optimize the physical mechanism by coupling the biophysical model (Yoon et al., 2021). However, this paper focused on combination of qualitative and quantitative analyses, and it emphasized the consideration of carbon peaking from the perspective of system coupling. It did not measure the exact value but grasped the change trend of the water, energy, and carbon emissions from an overall perspective. In future work, we will combine the above summary of the SD methods to enhance the accuracy of the numerical predictions.

5 Conclusion

As the only resource-based, provincial capital city in China (Dan, 2020), Taiyuan's economic development has depended on the coal industry for a long time, which renders the problems of a single economic structure and environmental pollution prominent. The proposal of the "dual carbon" goal creates opportunities and challenges to the green development of Taiyuan. On the one hand, the realization of the "dual carbon" goal is conducive to the optimization of the industrial structure and energy structure of Taiyuan; on the other hand, the realization of the "dual carbon" goal proposes higher requirements for the development of Taiyuan. Under this background, aiming at exploring the path of the carbon peak in Taiyuan, this paper combined the logical relationship between various elements of urban development and the present condition of resource consumption. Applying this combination as the chain of system simulation, this paper constructed a resource-based, urban carbon peak simulation system based on SD; verified the matching degree between the system simulation results and the actual results through historical data; performed multi-scene simulation; selected different influencing factors, including industrial structure adjustment, energy structure adjustment and energy consumption intensity; and simulated the economy, resources, energy and carbon emissions of Taiyuan in different scenarios. The specific conclusions are presented as follows:

(1) Based on the total carbon emissions and industrial carbon emissions in Taiyuan, it can be seen that the total carbon emissions of the whole industry in Taiyuan increased slightly every year from 2005 to 2021 and that the overall growth

trend is relatively stable. Although carbon emissions from the agriculture, transportation, storage and postal industries in Taiyuan have decreased, the total carbon emissions have not reduced. Taiyuan still needs to further strengthen its carbon emission reduction efforts and pay more attention to the carbon emissions of the industry, construction industry, wholesale and retail industry, and accommodation and catering industry.

(2) The change in a single influencing factor does not have a comprehensive impact on the coupling system. In particular, rapid economic growth alone will contribute to the sharp growth of carbon emissions, and it is difficult to achieve the carbon peak requirement before 2030. For example, the GDP in CPA_1 increased by 15.84%, but carbon emissions also increased by 15.81%. The comprehensive scenario simulation results show that through the balanced adjustment of various factors, even a small change will have a great impact on the economy, resources, energy and carbon emissions of the whole city. Meanwhile, the results indicate that system coupling can more comprehensively consider the impact of economic development and resource consumption on carbon emissions. By establishing different carbon peak scenarios, with the exception of the comprehensive scenario, the coordination effects of other scenarios in descending order are listed as follows: reduction of energy consumption per unit of GDP, adjustment of industrial structure, and adjustment of energy structure.

(3) In this paper, SD method is adopted to study the carbon peak path of resource-based cities, taking Taiyuan as an example. Considering the development characteristics of Taiyuan city and the natural growth of population, the proportion of tertiary industry will be increased by 10% compared with the natural development scenario. By 2025, the proportion of non-fossil fuels will be increased by 5% compared with 2020. The energy consumption per unit of GDP will be reduced by 13.5% compared with 2020. By 2030, the proportion of non-fossil fuels will be increased by 10% compared with 2020, The energy consumption per unit of GDP will be reduced by 25% compared with 2020. The above measures are an effective path for Taiyuan to achieve carbon peak before 2030 (Abbasi and Tufail, 2021).

Data availability statement

The original contributions presented in the study are included in the article/Supplementary Material, further inquiries can be directed to the corresponding authors.

Author contributions

GL and JF contributed to all aspects of this work; DJ conducted data analysis; YY wrote the main manuscript text. All authors reviewed the manuscript. All authors have read and agreed to the published version of the manuscript.

Funding

This work was supported by a grant National Natural Science Foundation of China (Grant No. 41971250 and 42202280), Youth Innovation Promotion Association (Grant No. 2018068), State Key Laboratory of Resources and Environmental Information System and Institute of Geographic Sciences and Natural Resources Research, Chinese Academy of Sciences (Grant No. E0V00112YZ).

Acknowledgments

We like to thank the editors and reviewers for their helpful remarks.

Conflict of interest

The authors declare that the research was conducted in the absence of any commercial or financial relationships that could be construed as a potential conflict of interest.

Publisher's note

All claims expressed in this article are solely those of the authors and do not necessarily represent those of their affiliated organizations, or those of the publisher, the editors and the reviewers. Any product that may be evaluated in this article, or claim that may be made by its manufacturer, is not guaranteed or endorsed by the publisher.

Supplementary material

The Supplementary Material for this article can be found online at: https://www.frontiersin.org/articles/10.3389/fenvs.2022.994543/full#supplementary-material

References

Abbasi, K. R., Adedoyin, F. F., and Hussain, K. (2021). The impact of energy depletion and renewable energy on CO_2 emissions in Thailand: Fresh evidence from the novel dynamic ARDL simulation. *Renew. Energy* 180, 1439–1450. doi:10.1016/j.renene.2021.08.078

Abbasi, K. R., and Tufail, M. (2021). Revisiting electricity consumption, price, and real GDP: A modified sectoral level analysis from Pakistan. *Energy Policy* 149, 112087. doi:10.1016/j.enpol.2020.112087

Al-Ghussain, L., Ahmad, A. D., Abubaker, A. M., Mohamed, M. A., Hassan, M. A., and Akafuah, N. K. (2022). Optimal sizing of country-scale renewable energy systems towards green transportation sector in developing countries. *Case Stud. Therm. Eng.* 39, 102442. doi:10.1016/j.csite.2022.102442

Alam, P., Sharholy, M., Khan, A. H., Ahmad, K., Alomayri, T., Radwan, N., et al. (2022). Energy generation and revenue potential from municipal solid waste using system dynamic approach. *Chemosphere* 299, 134351. doi:10.1016/J.CHEMOSPHERE.2022.134351

Alsokhiry, F., Siano, P., Annuk, A., and Mohamed, M. A. (2022). A novel time-of-use pricing based energy management system for Smart home appliances: Cost-effective method. *Sustainability* 14, 14556. doi:10.3390/su142114556

Awan, U., Kraslawski, A., Huiskonen, J., and Suleman, N. (2020). "Exploring the locus of social sustainability implementation: A south asian perspective on planning for sustainable development," in *Universities and sustainable communities: Meeting the goals of the agenda 2030*. Editors W. Leal Filho, U. Tortato, and F. Frankenberger (Cham: Springer International Publishing), 89–105.

Awan, U., and Sroufe, R. (2022). Sustainability in the circular economy: Insights and dynamics of designing circular business models. *Appl. Sci.* 12 (3), 1521. doi:10.3390/app12031521

Bergman, N., and Eyre, N. (2011). What role for microgeneration in a shift to a low carbon domestic energy sector in the UK? *Energy Effic.* 4, 335–353. doi:10.1007/s12053-011-9107-9

Chang, T. C., and Lin, S. J. (1999). Grey relation analysis of carbon dioxide emissions from industrial production and energy uses in Taiwan. *J. Environ. Manag.* 56, 247–257. doi:10.1006/jema.1999.0288

Corrado, S., and Ilaria, D. (2021). Renewable energy sources in local sustainable energy action PLANs (SEAPs): Analysis and outcomes. *Energy Policy* 156, 112475. doi:10.1016/J.ENPOL.2021.112475

Dan, Y. (2020). Research on low carbon economic development of Taiyuan city from the perspective of carbon emission. *Proc. 2020 Annu. Conf. Chin. Soc. Environ. Sci.* 4, 629–634. doi:10.26914c.cnkihy.2020.040069

Danish and Ulucak, R. (2021). Renewable energy, technological innovation and the environment: A novel dynamic auto-regressive distributive lag simulation. *Renew. Sustain. Energy Rev.* 150, 111433. doi:10.1016/J.RSER.2021.111433

Duinker, P. N., and Greig, L. A. (2007). Scenario analysis in environmental impact assessment: Improving explorations of the future. *Environ. Impact Assess. Rev.* 27 (3), 206–219. doi:10.1016/j.eiar.2006.11.001

Editorial Department (2021). Notice of the state Council on the issuance of an action plan for carbon peak by 2030. http://www.gov.cn/zhengce/zhengceku/2021-10/26/content_5644984.htm (Accessed March 15, 2022).

Hao, C., He, L., Chen, J., Yuan, B., Huang, T., and Cui, Q. (2019). Impacts of clean energy substitution for polluting fossil-fuels in terminal energy consumption on the economy and environment in China. *Sustainability* 11, 6419. doi:10.3390/su11226419

He, C. Y., Li, J., Zhang, X., Liu, Z., and Zhang, D. (2017). Will rapid urban expansion in, the drylands of northern China continue: A scenario analysis based on the land use scenario dynamics-urban model and the shared socioeconomic pathways. *J. Clean. Prod.* 165, 57–69. doi:10.1016/j.jclepro.2017.07.018

He, W., Zhang, B., Li, Y., and Chen, H. (2021). A performance analysis framework for carbon emission quota allocation schemes in China: Perspectives from economics and energy conservation. *J. Environ. Manag.* 296, 113165. doi:10.1016/J.JENVMAN.2021.113165

Hong, T., Yan, W., Ren, Z., Wang, Q., and Mohamed, M. A. (2022). Distributionally robust operation for integrated rural energy systems with broiler houses. *Energy* 254, 124398. doi:10.1016/j.energy.2022.124398

Hussain, T., Wei, Z., Ahmad, S., Xuehao, B., and Gaoli, Z. (2021). Impact of urban village disamenity on neighboring residential properties: Empirical evidence from nanjing through hedonic pricing model appraisal. *J. Urban Plann. Dev.* 147 (1), 04020055. doi:10.1061/(asce)up.1943-5444.0000645

IPCC Fifth Assessment Report (2014). Climate Change impacts are everywhere. *Chin. Environ. Sci.* 34, 1292. doi:10.3969/j.issn.1000-6923.2014.05.038

Jing, Z., Di, Y., Jin, Z., Zeng, S., Xiao, Y., et al. (2021). Study on green and low-carbon path of urban agglomeration from the perspective of system dynamics. *Technol. Industry* 21, 307–314. doi:10.3969/j.issn.1671-1807.2021.11.054

Jiu, Y., Ding, Q., and Fan, X. (2021). Direct and indirect contributions of energy consumption structure to carbon emission intensity. *Int. J. Energy Sect. Manag.* 15, 665–677. doi:10.1108/IJESM-08-2020-0009

John, C., Oreskes, N., Doran, P. T., Anderegg, W. R. L., Verheggen, B., Maibach, E. W., et al. (2016). Consensus on consensus: A synthesis of consensus estimates on human-caused global warming. *Environ. Res. Lett.* 11, 048002. doi:10.1088/1748-9326/11/4/048002

Jun, Y., Yan, P., Jian, C., and Yong, Z. (2017). Research on approaches to "Zero-carbon emission" high-tech industrial park-A case study of Taiyuan city. *Resour. Dev. Mark.* 33 (05), 559–563+583. doi:10.3969/j.issn.1005-8141.2017.05.010

Lahlou, F-Z., Mackey, H. R., and Al-Ansari, T. (2022). Role of wastewater in achieving carbon and water neutral agricultural production. *J. Clean. Prod.* 339, 130706. doi:10.1016/J.JCLEPRO.2022.130706

Li, J. F., Chen, Y. Q., Gan, T. Y., and Lau, N. C. (2018). Elevated increases in human-perceived temperature under climate warming. *Nature Climate Change*. doi:10.1038/s41558-017-0036-2

Li, F., Gu, A. L., Ma, Z. Y., Zhang, C. L., and Sun, Z. Q. (2019). Economic development, energy demand, and carbon emission prospects of China's provinces during the 14th Five-Year Plan period: Application of CMRCGE model. *Adv. Clim. Change Res.* 103, 165–173. doi:10.1016/j.accre.2019.09.003

Li, J., Yu, Y., Wang, X., and Zhou, Z. (2021). System dynamic relationship between service water and food: Case study at Jinghe River Basin. *J. Clean. Prod.* 330, 129794. doi:10.1016/j.jclepro.2021.129794

Liu, Z. F., He, C., Yang, Y., and Fang, Z. (2020). Planning sustainable urban landscape under the stress of climate change in the drylands of northern China: A scenario analysis based on LUSD-urban model. *J. Clean. Prod.* 244, 118709. doi:10.1016/j.jclepro.2019.118709

Marijn, P., Niles, M. T., Veraart, J. A., Werners, S. E., Korporaal, F. C., and Mulder, B. C. (2020). Communicating climate change risk: A content analysis of IPCC's summary for policymakers. *Sustainability* 12, 4861. doi:10.3390/su12124861

Mei, C. (2021). An analysis of the fiscal and taxation policies path of energy conservation and efficiency improvement in Shanxi province under the background of peak carbon dioxide emissions and achieve carbon neutrality. *Finance* 11, 392–398. doi:10.12677/FIN.2021.114044

Pan, C., Wang, H., Guo, H., and Pan, H. (2021). How do the population structure changes of China affect carbon emissions? An empirical study based on ridge regression analysis. *Sustainability* 13, 3319. doi:10.3390/SU13063319

Raza Abbasi, K., Hussain, K., Fatai Adedoyin, F., Ahmed Shaikh, P., Yousaf, H., Muhammad, F., et al. (2021). Analyzing the role of industrial sector's electricity consumption, prices, and GDP: A modified empirical evidence from Pakistan. *AIMS Energy* 9 (1), 29–49. doi:10.3934/energy.2021003

Shamsuzzaman, M., Shamsuzzoha, A., Maged, A., Haridy, S., Bashir, H., and Karim, A. (2021). Effective monitoring of carbon emissions from industrial sector using statistical process control. *Appl. Energy* 300, 117352. doi:10.1016/J.APENERGY.2021.117352

Sinha, S. K., Srikanth, R., and Mahalingam, S. (2022). Regulatory framework for India's energy security and sustainability. *Energy Policy* 162, 112815. doi:10.1016/J.ENPOL.2022.112815

Song, S. X., Liu, Z., He, C., and Lu, W. (2020). Evaluating the effects of urban expansion on natural habitat quality by coupling localized shared socioeconomic pathways and the land use scenario dynamics-urban model. *Ecol. Indic.* 112, 106071. doi:10.1016/j.ecolind.2020.106071

Tramošljika, B., Blecich, P., Bonefacic, I., and Glazar, V. (2021). Advanced ultra-supercritical coal-fired power plant with post-combustion carbon capture: Analysis of electricity penalty and CO2 emission reduction. *Sustainability* 13, 801. doi:10.3390/SU13020801

Wu, J., Wang, Z., and Dong, L. (2021). Prediction and analysis of water resources demand in Taiyuan City based on principal component analysis and BP neural network. *Ecosyst. Soc.* 708, 1272–1286. doi:10.2166/AQUA.2021.205

Xiao, S., Dong, H., Geng, Y., and Tian, X. (2022). Low carbon potential of urban symbiosis under different municipal solid waste sorting modes based on a system dynamic method. *Resour. Conservation Recycl.* 179, 106108. doi:10.1016/J.RESCONREC.2021.106108

Xiu, Z., Wang, R., and Du, Q. (2020). How does industrial restructuring influence carbon emissions: City-level evidence from China. *J. Environ. Manag.* 276, 111093. doi:10.1016/j.jenvman.2020.111093

Yin, Y., Jiang, D., Fu, J., and Dong, D. (2021). Multi-scenario simulation of a water–energy coupling system based on system dynamics: A case study of ningbo city. *Energies* 14, 5854. doi:10.3390/EN14185854

Ying, Z., Wei, T., Chen, S., Wang, S., and Qiu, R. (2021). Pathways to a more efficient and cleaner energy system in guangdong-Hong Kong-Macao greater bay area: A system-based simulation during 2015-2035. *Resour. Conservation Recycl.* 174, 105835. doi:10.1016/j.resconrec.2021.105835

Yoon, J., Klassert, C., Selby, P., Lachaut, T., Knox, S., Avisse, N., et al. (2021). A coupled human-natural system analysis of freshwater security under climate and population change. *Proc. Natl. Acad. Sci. U. S. A.* 118 (14), e2020431118. doi:10.1073/pnas.2020431118

Zeng, L. (2019). *The analysis of the relationship between energy carbon emissions and water resources in surrounded cities Beijing-Tianjin [D].* Beijing: China University of Mining & Technology. doi:10.27624/d.cnki.gzkbu.2019.000196

Zhang, D., Huang, Q., He, C., and Wu, J. (2017). Impacts of urban expansion on ecosystem services in the beijing-tianjin-hebei urban agglomeration, China: A scenario analysis based on the shared socioeconomic pathways. *Resour. Conservation Recycl.* 125, 115–130. doi:10.1016/j.resconrec.2017.06.003

Zhang, C., Su, B., Zhou, K., and Yang, S. (2019). Decomposition analysis of China's CO2 emissions (2000–2016) and scenario analysis of its carbon intensity targets in 2020 and 2030. *Sci. Total Environ.* 668, 432–442. doi:10.1016/j.scitotenv.2019.02.406

Zhang, M., Yang, Z., Liu, L., and Zhou, D. (2021). Impact of renewable energy investment on carbon emissions in China - an empirical study using a nonparametric additive regression model. *Sci. Total Environ.* 785, 147109. doi:10.1016/J.SCITOTENV.2021.147109

Zhao, R., Yu, J., Xiao, L., Sun, J., Luo, H., Yang, W., et al. (2021). Carbon emissions of urban water system based on water-energy-carbon nexus [J]. *J. Geogr.* 76 (12), 3119–3134. doi:10.11821/dlxb202112017

Zhao, X., Ma, X., Chen, B., Shang, Y., and Song, M. (2022). Challenges toward carbon neutrality in China: Strategies and countermeasures. *Resour. Conservation Recycl.* 176, 105959. doi:10.1016/j.resconrec.2021.105959

Zhi, L. (2019). Analysis on the coordinated development of industrial structure and carbon emission in zhenjiang city. *Sustain. Dev.* 09, 412–420. doi:10.12677/sd.2019.93050

Zhu, B., and Shan, H. (2020). Impacts of industrial structures reconstructing on carbon emission and energy consumption: A case of beijing. *J. Clean. Prod.* 245, 118916. doi:10.1016/j.jclepro.2019.118916

Zhu, B., and Zhang, T. (2021). The impact of cross-region industrial structure optimization on economy, carbon emissions and energy consumption: A case of the yangtze river delta. *Sci. Total Environ.* 778, 146089. doi:10.1016/J.SCITOTENV.2021.146089